Detection of therapeutic targets in human highly prevalent diseases through mathematical modelling of their molecular basis

Guido Santos

Director:
Dr. Néstor V. Torres

Tesis doctoral
2016

ULL | Universidad de La Laguna

Universidad de La Laguna

Departamento de Bioquímica, Microbiología y Genética

D. Néstor V. Torres Darias, Catedrático de Bioquímica y Biología Molecular del Departamento de Bioquímica, Microbiología, Biología Celular y Genética de la Universidad dela Laguna,

CERTIFICA

Que la presente memoria, titulada *"Detection of therapeutic targets in human highly prevalent diseases through mathematical modelling of their molecular basis"* presentada por D. Guido Santos Rosales como Tesis Doctoral en la modalidad de Compendio de Publicaciones, dentro del Programa de Doctorado en Ciencias Biomédicas de la Universidad de la Laguna, ha sido realizada en los laboratorios del Departamento de Bioquímica, Microbiología, Biología Celular y Genética bajo mi dirección, recogiendo fielmente los resultados.

En San Cristóbal de La Laguna, 3 de mayo de 2016.

Dr. Néstor Torres Darias

Este trabajo ha sido subvencionado por los siguientes proyectos: MICINN BIO2011-29233-C02-02; MINECO BIO2014-54411-C2-2-R; ACIISI PIL2071001, IMBRAIN ref. FP7-REGPOT-2012-CT2012-31637-IMRAIN

Detection of therapeutic targets in human highly prevalent diseases through mathematical modelling of their molecular basis

Guido Santos Rosales

Tesis doctoral

Director: Dr. Néstor V. Torres Darias
Catedrático de la Universidad de La Laguna

Departamento de Bioquímica, Microbiología, Biología Celular y Genética
Universidad de La Laguna

San Cristóbal de La Laguna, 2016

Agradecimientos

Con la culminación de esta tesis el trabajo ha dado sus frutos, pero los frutos necesitan de un ambiente óptimo para poder llevar a producirse, permítanme que dedique unas palabras a describir cuál fue el mío.

Mi ambiente familiar y mis amigos han sido el soporte vital de mi crecimiento profesional. El soporte vital y el apoyo emocional que he recibido durante toda mi vida han sido como los nutrientes, el agua y la luz del sol que toda planta necesita para desarrollarse. Mis padres, Marcos y Montse, que me han aguantado toda mi vida; mi hermano Dani, con sus ocurrencias que me desternillan y toda mi familia cercana, que resultaría muy largo nombrar uno a uno aquí, pero que ellos bien saben que forman parte de mi vida; mis amigos, Felipe, Iván, Yazmina, Cathy, Charly, Casandra, Nayra, Mela y Andre, la segunda familia. Y una mención especial a mi pareja María, sus constantes muestras de apoyo me han permitido superar las adversidades.

Ese ambiente ha garantizado mi crecimiento, pero una planta ha de ser cultivada para que los frutos sean productivos. Y yo he crecido en un ambiente profesional que ha retroalimentado mi productividad. El Grupo de Tecnología Bioquímica (nombre con el que recordaré siempre el laboratorio) ha sido un ecosistema óptimo para la interacción y el crecimiento profesional y personal. Muchas gracias a Carlos, del cual obtuve gran parte de mi pasión por las matemáticas y la naturaleza. A los visitantes del laboratorio que han enriquecido mi experiencia: Bettina 1 y Bettina 2, Michele, Hugo, Pastor y Daniel. A José, por ser mi mentor extraoficial y porque toda mi pasión por la física se la debo a él y a los interesantes debates que hemos compartido. A Semidán y Nakens, junto con los que formé el grupo de trabajo con el que más he congeniado, y porque ha trascendido a la amistad. Y finalmente a mi director de tesis Néstor. Creyó en mí inicialmente proporcionándome todos los medios para alcanzar mis objetivos. Ha sido como el jardinero que dirige el crecimiento hacia el lugar óptimo podando o reforzando mis ramas intelectuales.

Durante mi desarrollo profesional he tenido la oportunidad de conocer a antiguos miembros de mi laboratorio, los gigantes de cuyos hombros he podido mirar más lejos. Alberto ha sido un referente intelectual para mí, y en lo personal alguien con quien me divierto mucho. Julio, a quien admiro mucho, y además me ha dado la oportunidad de participar en su laboratorio de investigación en dos ocasiones. No dispongo de espacio suficiente para agradecer a Julio acorde a las oportunidades que me ha brindado. *I want to thank also the members of the Laboratory of Systems Tumor Immunology for making me feel very comfortable in Germany*. Cristina, María, Agustín y Mario han sido colaboradores con los que trabajar ha sido un placer. José María ha abierto mi visión escéptica y de él he aprendido la importancia de divulgar la ciencia. Finalmente, los miembros de JINTE, en especial a los que conformaron la primera Junta Directiva y las comisiones de trabajo. Siento no mencionarlos a todos aquí, pero no me cabe duda que sabrán sentirse aludidos al leer estas palabras.

A todos, pueden sentir que son parte de este trabajo que ahora culmino.

Corrigendum

Figures 2 and 3 of the chapter of VIH were switched in the present thesis respecting the actual publication. It was an edition mistake and it was corrected here manually.

Durante el desarrollo de la presente tesis se han realizado las siguientes comunicaciones, algunas de las cuales forman parte del compendio presentado

Artículos científicos

Santos G, Svetoslav Nikolov, Lai X, Eberhardt M, Dreyer FS, Paul S, Schuler G and Vera J (2016) Model-based genotype-phenotype mapping used to investigate gene signatures of immune sensitivity and resistance in melanoma micrometastasis. *Scientific Reports.* 6:24967. doi: 10.1038/srep24967

Santos G, Diaz ML and Torres NV (2016). Lipid raft size and lipid mobility in non-raft domains increase during aging and are exacerbated in APP/PS1 mice model of Alzheimer's disease. Predictions from an agent-based mathematical model. *Front. Physiol.* 7:90. doi: 10.3389/fphys.2016.00090

Torres NV and Santos G (2015) The (Mathematical) Modeling Process in Biosciences. *Frontiers in Genetics*. 6(354): 1-9. DOI: 10.3389/fgene.2015.00354

Santos G, Valenzuela-Fernández A and Torres NV (2014) Quantitative Analysis of the Processes and Signaling Events Involved in Early HIV-1 Infection of T Cells. *PLoS one*. 9 - 8, pp. e103845

Santos G and Torres NV (2014) Intra-host mathematical models of malaria. *CAB reviews.* 9 - 025, pp. 1 - 7

Santos G and Torres NV (2013) New Targets for Drug Discovery against Malaria. *World Biomedical Frontiers*. Disponible en Internet en: <http://biomedfrontiers.org/infection-2013-11-22/>. ISSN 2328-0166

Velasco-Bedrán H, Hormiga JA, Santos G and Torres NV (2013) Model-Based Analysis of a Phenol Bio-Oxidation Process by Adhered and Suspended Candida tropicalis*. Applied Mathematics.* pp. 1 - 9

Santos G and Torres NV. New Targets for Drug Discovery against Malaria. *PLoS one*. 8(3): - e59968

Santos G, Hormiga JA, Arense P, Cánovas M and Torres NV (2012) Modelling and Analysis of Central Metabolism Operating Regulatory Interactions in Salt Stress Conditions in a L-Carnitine Overproducing E. coli Strain. *PLoS one*. 7 - 4, pp. 34533

Comunicaciones a congresos

Mathematical modelling of the amyloidogenic pathway during Alzheimer's disease in the context of the lipid membrane

Guido Santos Rosales; Mario Díaz González; Néstor V. Torres Darias. Póster

Nombre del congreso: XXXVII Congreso de la Sociedad Española de Bioquímica y Biología

Molecular Ciudad de celebración: Granada, Andalucía, España

Fecha de celebración: 09/09/2014

Fecha de finalización: 12/09/2014

Entidad organizadora: Sociedad Española de Bioquímica y Biología Molecular

Mathematical modelling of the amyloidogenic pathway during Alzheimer's disease in the context of the lipid membrane
Guido Santos Rosales; Néstor V. Torres Darias; Mario Díaz González. Póster
Nombre del congreso: 9th European Conference on Mathematical and Theoretical Biology
Ciudad de celebración: Gotemburgo, Extra-Regio, Suecia
Fecha de celebración: 15/06/2014
Fecha de finalización: 19/06/2014
Entidad organizadora: *European Society of Mathematical and Theoretical Biology*

Integration and quantification of the main processes during the invasion of lymphocytes T by the HIV
Guido Santos Rosales; Agustín Valenzuela Fernández; Néstor V. Torres Darias. Ponencia oral
Nombre del congreso: XXXVI Congreso de la Sociedad Española de Bioquímica y Biología Molecular
Ciudad de celebración: Madrid, Comunidad de Madrid, España
Fecha de celebración: 06/09/2013
Fecha de finalización: 06/09/2013
Entidad organizadora: Sociedad Española de Bioquímica y Biología Molecular

HIV Infection: Connecting Cellular Events with the Dynamics of the HIV Host Population
Guido Santos Rosales; Agustín Valenzuela Fernández; Néstor V. Torres Darias. Póster
Nombre del congreso: *Frontiers in Systems and Synthetic Biology '13*
Ciudad de celebración: Atlanta, Estados Unidos de América
Fecha de celebración: 20/03/2013
Fecha de finalización: 24/03/2013
Entidad organizadora: *Georgia Tech. Integrative BioSystems Institute*

Quantitative analysis of the central metabolism regulatory interactions of E. coli in salt stress conditions
Guido Santos Rosales; José A. Hormiga Cerdeña; Paula Arense; Manuel Cánovas; Néstor V. Torres Darias. Póster
Nombre del congreso: *IUBMB-FEBS 2012. From Single Molecules to Systems Biology*
Ciudad de celebración: Sevilla, Andalucía, España
Fecha de celebración: 04/09/2012
Fecha de finalización: 09/09/2012
Entidad organizadora: IUBMB y FEBS

Systems biology approches for the interrogation of anti-malarial compounds
Guido Santos Rosales; Néstor V. Torres Darias. Póster
Nombre del congreso: *IUBMB-FEBS 2012. From Single Molecules to Systems Biology*
Ciudad de celebración: Sevilla, Andalucía, España
Fecha de celebración: 04/09/2012
Fecha de finalización: 09/09/2012
Entidad organizadora: IUBMB y FEBS

Modelling of E. coli metabolism in salt stress conditions. Application to the overproduction of succinate and L-carnitine
Guido Santos Rosales; José Hormiga Cerdeña; Carlos González Alcón; Paula Arense Parra; Vicente Bernal Salar; Hugo Velazco Bedrán; Manuel Cánovas Díaz; Néstor V. Torres Darias. Póster
Nombre del congreso: *XII International Congress on Molecular Systems Biology*
Ciudad de celebración: Lleida, Cataluña, España
Fecha de celebración: 09/05/2011
Fecha de finalización: 12/05/2011
Entidad organizadora: *Universitat de Lleida*

Application to the biosíntesis of succinate and L-carnitine in E. coli in salt stress conditions
Néstor V. Torres Darias; Manuel Cánovas Díaz; José A. Hormiga Cerdeña; Guido Santos Rosales. Póster
Nombre del congreso: *Advanced Lecture Course on Systems Biology: FEBS-SystemsX-SysBio2011*
Ciudad de celebración: Innsbruck, Austria
Fecha de celebración: 26/02/2011
Fecha de finalización: 04/03/2011
Entidad organizadora: *Federation of European Biochemical Societies*

Application to the biosíntesis of succinate and L-carnitine in E. coli in salt stress conditions
Néstor V. Torres Darias; Manuel Cánovas Díaz; José A. Hormiga Cerdeña; Guido Santos Rosales. Póster
Nombre del congreso: *6th Meeting of the Spanish Systems Biology Network*
Ciudad de celebración: Barcelona, Cataluña, España
Fecha de celebración: 09/12/2010
Fecha de finalización: 10/12/2010
Entidad organizadora: Red Española de Biología de Sistemas

Abstract

Diseases are due to a malfunctioning of the physiology of the organism. In order to understand the mechanisms of the diseases it has to be taken into account the structural complexity of the biological organisms, not only as the set of molecular interactions but also its dynamics. Since in many cases the disease is due to a dynamical imbalance of the system we need methods to induce the dynamics from the interacting network to find strategies to cure them. The approach which deals with this problem is systems biology; it makes use of mathematical modelling methodologies to deal with the structural and dynamical complexity of the biological organisms. First, the general considerations about mathematical modelling in biosciences are discussed, and then it is presented a review of mathematical modelling approaches in the topic of intra-host malaria infection. Four highly prevalent diseases are evaluated in this perspective to unravel the molecular and cellular complexity which explains their physiology. Malaria is highly prevalent in developing countries, and it is produced by the dynamical interaction of the parasite and the cells in the blood stream; HIV infection is firstly produced by the invasion of the T4 lymphocytes by the virus. This process is driven by many molecular pathways triggered by the virus inside the lymphocyte, these signaling pathways produce the opening of a small pore through the HIV enters; Alzheimer's disease is a neurodegenerative pathology without known cause, the main hypothesis relates the production of the neurotoxic peptide β-amyloid with certain lipid domains formed by differential lateral movement of the lipids in the membrane of the neurons; finally, melanoma is a very aggressive kind of cancer. After a metastasis, a microtumor originates in the bloodstream and it interacts with the immune system; the final outcome depends on this dynamical interaction. Potential therapeutic targets in which can be focused on the search of new drugs against these diseases are proposed by the models which reproduce the disease in certain conditions.

Resumen

Las enfermedades se producen por un mal funcionamiento del organismo. Con el fin de comprender los mecanismos de las enfermedades se debe tener en cuenta la complejidad de los organismos biológicos, no sólo como el conjunto de interacciones moleculares, sino también su dinámica. Las enfermedades se producen por un desequilibrio en la dinámica del sistema, ello implica que hacen falta métodos que permitan inducir la dinámica a partir de la red de interacciones de forma que sea posible encontrar nuevas estrategias para el tratamiento de las enfermedades. El enfoque que se ocupa de este inferir la dinámica a partir de las redes de interacciones es la biología de sistemas; esta hace uso de metodologías de modelización matemática para hacer frente a la complejidad estructural y dinámica de los organismos biológicos. En primer lugar se resumen y analizan las cuestiones generales sobre modelización matemática en biociencias, luego se presenta una revisión de aproximaciones mediante modelización matemática en el tema de infección por malaria dentro del hospedador. Cuatro enfermedades altamente prevalentes son evaluados bajo este enfoque desentrañando la complejidad molecular y celular que explica su fisiología. La malaria es altamente prevalente en los países en desarrollo, y es producida por la interacción dinámica del parásito y las células del sistema inmunológico en el torrente sanguíneo; la infección por VIH es producida en primer lugar por la invasión de los linfocitos T4 por el virus, este proceso está promovido por muchas rutas de señalización molecular desencadenadas por el virus en el interior del linfocito, que culminan con la apertura de un poro por el cual entra el VIH; la enfermedad de Alzheimer es una patología neurodegenerativa sin causa conocida, la hipótesis principal alude a la producción de un péptido neurotóxico, el β-amiloide, en ciertos dominios lipídicos formados por el movimiento lateral diferencial de los lípidos en la membrana de las neuronas; por último, el melanoma es un tipo de cáncer de melanocitos muy agresivo. Inicialmente, un microtumor crece en el torrente sanguíneo interactuando con el sistema inmune; la evolución de la

enfermedad depende de esta interacción dinámica. En cada caso se proponen potenciales dianas terapéuticas en las que puede centrarse la búsqueda de nuevos fármacos contra estas enfermedades haciendo uso de los modelos que reproducen la enfermedad en determinadas condiciones.

Contents

1. Introduction

Historical introduction

A disease is an abnormal condition of the organism physiology. Many classifications of the diseases can be made depending on the chosen criterion; we group them based on the causes. Some of the diseases are produced by external agents, as traumatisms, nutritional disorders or caused by toxins. These can be considered passive diseases as the agent is not able to reproduce. On the other hand, active external agents are microorganisms and parasites. The diseases which have an endogen origin can be caused by immune system malfunction, for example in allergic, inflammatory and autoimmune diseases; others are able to be inherited or caused congenitally and, finally, neoplastic and degenerative diseases are mostly caused during aging, although they can also be produced by acquired mutations. Some other diseases do not have any known cause, as Alzheimer's disease. There are two main strategies to deal with the treatment of the diseases: i) removing the external agent, when there is one; ii) restoring the physiology to its normal condition. Conceptually, the first strategy is easier because the objective is to destroy the physiology of the pathogen, but the second strategy requires restoring the patient physiology to its unique functional state. In practice, many situations can make the problem more complicated, for example the acquirement of resistance to the treatment by the pathogen. When the causes of the disease are well known the intuitive strategy is trying to reverse the malfunction without affecting any other relevant process in a way that the result of the treatment is not worse than the disease. We are saying that the target of the treatment is the same as the target of the disease. However many treatments are able to restore the organism physiology without reversing the affected process. Instead of that, they act on a different place in a way that they are able to compensate the malfunction in a whole. We can say that these are counterintuitive therapies, as there is no easy way to find them by intuition, considering the high complexity of the organism. These kinds of treatments are mostly found under extensive screening of substances, or even by chance. But as it will be discussed below, it is possible to find counterintuitive treatments in a directed way.

A biological organism is not a soup of elements, knowing its precise composition is not enough to understand its physiology. The individual functionality arises from the orchestrated interaction of all the elements in space and in time. Even knowing the complete genome of one cell it is not possible to predict its response to certain stimulus, because the genetic information has only sense in the context of the dynamic networks of molecules. This network has two main characteristics: i) all processes occur far from the thermodynamic equilibrium; ii) the interactions between elements are nonlinear (doubling the input does not duplicate the response). These two properties make the system admit very complicated dynamical behavior, as oscillations and chaos. It is frequent that for a proper functioning of the organisms this dynamics has to be conserved, in a way that losing oscillatory or even chaotic dynamics would produce a disease (Mackey and Glass, 1977). Then, it is crucial being able to infer the dynamical

response of the biological systems from the interaction network in order to understand the physiology of the diseases. As it was mentioned above, some counterintuitive responses under certain modifications are expected if we are not able to infer the dynamic response of the system. The approach which deals with the biological organisms in the presented way above is systems biology. As it was said it is not a methodology but an approach to study biological systems, it is the paradigm shift needed to understand the complexity of the biological organisms.

The history of systems biology begins out of biology. As many, if not all, of the scientific disciplines we can assume that it started with the publication of *Philosophiæ naturalis principia mathematica* by Isaac Newton, in England. In this precise moment the humanity was able to understand that there are mathematical principles which rule the Universe, but at the same time Isaac Newton also provides to the world a new tool to analyze and predict the dynamical behavior of the nature, differential calculus. The genius said to us where and how we can discover the secrets of the universe, and the era of the great scientific discoveries began. The study of the nature was mostly descriptive until then, however the ability to uncover the mathematical principles of the observed phenomena concludes with the establishment of universal laws. Mechanics was followed by thermodynamics and electrodynamics, and the scientists began to think they were able to predict any process in the universe, as it was manifested by one of the biggest scientists of the time, William Thomson, first Baron Kelvin: "there is nothing new to be discovered in physics now. All that remains is more and more precise measurement". However, since science cannot be stopped, Max Planck unravels another relevant mathematical principle on nature, quantum mechanics. It was the beginning of the second revolution in physics during the XX century, which ends with the two current big theories about the mathematical principles of nature, the Standard Model and the General Theory of Relativity.

The mathematical principles which rule the biological systems are the same as in the inert matter, but it was very late in the history of science when it could be known. The explicit differences between living organisms and the rest of phenomena established the vitalism, which assumes a conceptual difference between the living and non-living entities. It was considered that the laws of physics cannot be applied to biology, and hence the lack of interest in finding the mathematical principles of the biological systems. After the famous experiment of Friedrich Wöhler synthesizing the organic compound urea in laboratory the vitalism theory was called into question, and then it was admissible applying the laws of nature to living organisms. Although the application of the natural laws on the biological systems was not so obvious, some exercises in order to unravel the mathematical nature of biological systems were made at the beginnings of XX century. Alfred J. Lotka applied the mathematical law of the kinetics of chemical reactions, as autocatalysis and mass action law, into a set of ecological models in which species interact, culminating in 1920 with a mathematical model of predator-prey interaction in an ecosystem (Lotka, 1920); and during the same time, Vito Volterra derived the same equations to explain the observed oscillations on the number of marine individual (Volterra, 1927). Also during the first years of the XX century, sir Ronald Ross, using the same ideas from the mass action law, proposed the mathematical behavior of epidemic diseases (Ross, 1915). From these ideas it arose the current epidemiological models, the concept of basic reproduction number and the vaccination control of epidemics using mathematical concepts as the herd immunity. Also very remarkable, the foundations of enzyme kinetics were established by Leonor Michaelis and Maud Menten in 1913 (Johnson and Goody, 2011), based in chemical reaction mathematical principles as well. Nevertheless it had to be developed an emerging idea which was growing in parallel to this initial application of mathematical models to biology, the principles of the Systems Theory. It was the formalization of previous approaches to the complexity, as Control Theory which deals with dynamical systems and the effect of the output on the input of systems by feedback loops; Chaos Theory which

had its conceptual origins at the end of XIX century, or other discoveries of interest in biology as the self-reproducing systems founded by John von Neumann in his cellular automata model. Ludwig von Bertalanffy published the General Theory of Systems in 1969 (Bertalanffy, 1969), and it provided a mathematical structure for complexity, a set of interacting elements from which they emerge some common properties and behaviors which can be analyzed, referred as the system. After this great formalization for the study of systems other key contributions for the culmination of the mathematical analysis of biological systems were the concepts of dissipative structures as a way to apply the laws of thermodynamics on living structures, being them open systems far from the equilibrium. The dissipative structures were presented by Ilya Prigogine in 1961 (Prigogine, 1968). The first great application to systems theory on biology was the mathematical model of Alan Hodgkin and Andrew Huxley in 1952 (Hodgkin and Huxley, 1952), in this work they were able to reproduce the dynamical behavior of the initiation and propagation of the action potential in axons. This model proposed the ionic mechanisms under the process which was verified later by molecular experiments.

The next revolution on the field of systems biology was in technology, the development of personal computers gave a very potent tool to analyze mathematical models. As it was introduced before, the interactions occurring between elements in biological systems are nonlinear, which produce mathematical equations which are very difficult or even impossible to analyze by hand. The use of computational power made possible the application of mathematical tools for numerical analysis which require a lot of simple calculations. With the theories and mathematical tools available the attention was drawn to the study of metabolism during the seventies. Metabolic pathway were well known since the molecular biology and enzyme assays studies, but the knowledge were based on analyzing individual reactions *in vitro*, and the inference of the dynamical behavior of the whole network is not an easy task. There was no any method which took into account the nonlinear nature of those biochemical systems. Trying to deal with this lack, two mathematical approaches appeared on this decade, Metabolic Control Analysis (Fell, 1996; Heinrich and Rapoport, 1974; Kacser and Burns, 1973) and Biochemical Systems Theory (Savageau, 1969, 2010), converging both in the main ideas behind the mathematical principles of biochemical systems. The first approach tried to solve the conceptual problem of limiting reaction, as it cannot be predicted from *in vitro* studies. It is because the limiting reaction of a pathway is an emerging property of the whole pathway, depending on the connectivity and kinetics of the network. This approach gives some mathematical properties of the biochemical networks which are conserved, in a way that it is possible to predict from the network which reactions are able to mostly control the velocity of the whole pathway, based on control coefficients which inform about the amount of control on the system that each reaction has. On the other hand, Biochemical Systems Theory introduced a canonical mathematical formalization to analyze the dynamics of biochemical pathways; it assumes a linear relationship between reactants and reaction rate under a double log representation. This assumption has proved to deal with the main nonlinearities on biological dynamic behavior (saturability, synergy, oscillations, etc.) and also this assumption let to easily formulate and analyze biochemical pathways. From this formulation it can be derived the sensitivities of the system response under changes in biochemical parameters, which has a very close relationship with the control coefficients of Metabolic Control Analysis (Savageau et al., 1987). The application of those approaches to metabolism has provided the understanding of many responses coming from metabolic systems (Voit, 2013), and it also uncovered the design principles on metabolic pathways which explain the observed phenomena (Savageau, 2011).

The last revolution on systems biology started after the development of methodologies to obtain high throughput data, also called omics. It began with the Human Genome Project, for the first time the whole genetic information of one human was available. At that moment it was a very

complicated challenge in which there was involved an international consortium of many countries during one decade. Advances in sequencing technology provide now the opportunity for almost every laboratory in the world to be able to sequence the entire genome of an organism in days. The next challenges came by increasing the amount of data, as the 1000 Genomes Project (1000 Genomes Project Consortium et al., 2010) or the ENCODE Project (ENCODE Project Consortium, 2004). It is also available high throughput data for any kind of biological information, the expression level of all genes, the amount of proteins of a cell, the metabolites concentration and the epigenetic marks are just some examples of the emerging technologies to obtain data from the whole organism. The data collected from the omics technologies need to be analyzed to obtain useful information from it, which makes bioinformatics and data analysis very useful and trending disciplines nowadays. This is the first round of analysis which can be made from this kind of data, but further steps must be done in order to really understand the biological systems from the data. If we only perform statistical analysis on data we are losing the information that the data give about the network of interactions of molecules.

Network theory has its origins on mathematics. It was Leonhard Euler the first to solve a problem using graphs as mathematical objects, in the famous problem of the Seven Bridges of Königsberg. Out of mathematics it was mostly applied on information theory and social sciences, but with the emergence of omics and high throughput data it was possible to contrast biological networks with sufficient data measured from one organism. With this methodology it was possible to construct the whole biochemical and genetic network of biological organisms and analyzing its properties. Proposing new therapies for diseases based on biological networks inferred from high throughput data is one of the most recent methodologies which deal with the problem of finding counterintuitive therapies based on the network properties (Pérez-Nueno, 2015).

Although network analysis is a very informative and potent methodology to uncover the complexity of biological systems it is not the last step for the comprehension of the function of them. The physiology of an organism is not static, it changes during time. The knowledge of the actual network of interactions of an organism does not give information about the dynamical response after certain stimuli, as the response varies during time. The ultimate step for a genuine understanding of the physiology of an organism comes from inferring its dynamical response from the network. To deal with this challenge it is necessary the use of mathematical tools which explicitly incorporate the time dimension. Although this methodology is the best approach to understand the biological physiology, it is yet under improvement. The reason is that for constructing dynamical networks experimental data taken during time are needed, which is not so available yet. Furthermore, dynamic mathematical models are much more computationally expensive than the static ones, so they use to be constructed in a smaller scale of detail. However, as the available data and the computing power increase exponentially it is expected that the size and resolution of dynamical models keep increasing. Even under the current situation about dynamical networks, there exist multiple applications of them to unravel the molecular complexity of the diseases and proposing new directed and counterintuitive therapies based on the dynamical response of small networks. Its utility and validation has been proven as they are able to reproduce the dynamical networks which exist at different scaling levels.

Examples of dynamical mathematical models in biomedicine

The application of the principles of systems biology to biomedicine provides a new approach to uncover the molecular mechanisms of the diseases, systems biomedicine (Antony et al., 2012; Zou et al., 2013). This approach allows to propose therapies based on the dynamical structure of the organisms, opening a new field of discoveries which was hidden under the reductionist approach alone. Now, it is

accepted that the study of the isolated elements of the system in conjunction with the holistic vision which provides systems biomedicine is the most promising strategy to deal with the diseases. In this section it will be presented a small selection of works on the topic of systems biomedicine to illustrate the utility of the approach. It will be focused on mathematical models which explicitly include time, so the diseases are studied as dynamical networks.

Neurodegenerative diseases are complex pathologies which ultimately affect neurons. The causes are, in the best cases, partially known. In the case of Alzheimer's disease (AD) the cause for the most frequent kind, sporadic AD, is not known. The currently accepted hypothesis is based on the aberrant production and accumulation of β-amyloid polymers on the extracellular region of the brain, which produces the death of the neurons (Gouras et al., 2014). Based on this hypothesis, mathematical models can provide useful information for the diagnosis of the evolution of the disease. A compartmental mathematical model was used to evaluate the dynamics on the distribution of the β-amyloid peptides through brain regions, as the cerebrospinal fluid, plasma and the brain (Craft et al., 2002). It concluded that decreasing the production/elongation of peptides reduces the burden of β-amyloid in all compartments, but increasing the clearance of the polymers only decreases the β-amyloid burden in the brain, and it can even increase its amount on cerebrospinal fluid and plasma. This is a notable consideration, as it would modify the interpretation of biomarkers based on the β-amyloid burden on plasma. The intracellular accumulation of Tau protein is also considered as a key driver of AD, as this accumulation would affect the proper structure of the cytoskeleton of neurons (Giacobini and Gold, 2013). The cytoskeleton is a complex dynamic structure, and it makes very difficult to figure out what is the actual effect of Tau on its physiology. In order to understand the structural changes on microtubules in the neurons promoted by Tau, it was implemented a three-dimensional mathematical model which considered the microtubule spatial dynamics (Buxton et al., 2010). It was able to predict the changes observed by Tau accumulation, providing a dynamic mechanism which could prevent the aberrant structure observed. If during the depolymerization of microtubules a new process of polymerization occurs faster than the hydrolyzation of the terminal GTP the catastrophic depolymerization can be terminated. It points at molecular targets for drug design based in a dynamical view of the disease. The problem can also be considered in a wider scale, including the relationship between the different cells on the brain. One mathematical model includes the crosstalk between microglia, astroglia, neurons and β-amyloid (Puri and Li, 2010). Using this scale it was possible to establish that the inflammatory activation of microglia is a relevant process for the evolution of the disease, being an interesting target for drug design. Parkinson's disease (PD) consists on a selective death of dopaminergic neurons in the *substantia nigra* of the brain; the main driver considered is the accumulation of α-synuclein (Dehay et al., 2015). The current main therapeutic strategy consists on the increase of the accumulation of dopamine to compensate the reduction of dopaminergic neurons. But, as metabolic pathways for dopamine production are very complex, and some other undesirable effects as oxidative stress are involved, finding a proper therapy is not easy using exclusively reductionist approaches. Two mathematical models which reproduce the metabolism of dopamine were able to propose molecular therapies combined in a way that increase dopamine and decrease oxidative stress (Qi et al., 2008; Sass et al., 2009).

Infectious diseases are driven by pathogens which colonize the organism, so we need to understand the relationship between the microorganism and the host. Most of the infectious microorganisms invade the cells to reproduce inside them. HIV infection is a relevant example. HIV infects T4 lymphocytes and appropriates the cell machinery, then the virus becomes dormant during many years, until it eventually produces AIDS (Marsden and Zack, 2013). Knowing the dynamics of the disease is very convenient to control it, and it was analyzed using a mathematical model in 1996

(Perelson et al., 1996). It was predicted the average life-span of infected cells, the mean production of virus and the HIV life cycle *in vivo*. In another study of the same year it was predicted that the observed reduction on the viremia during the acute phase of the HIV can be produced without any increase on the rate of removal of free virions or virus-infected cells (Phillips, 1996), which pointed to the fact that the decrease in viremia of the acute phase was not produced by the HIV-specific immune response to control the virus replication. More recently, a mathematical analysis established that the liver damage previously associated to HIV/HBV coinfection can be caused by a HIV monoinfection (Nampala et al., 2013). Equally recent is another mathematical model of HIV, but concerning the virus maturation (Könnyű et al., 2013). It focuses on the Cag-Pol polyproteins processing by the viral protease, which is needed for its infectivity. This quantitative analysis allowed to identify rate limiting step on the process as well as the main points to modify which would block the maturation. This is a promising strategy to focus on for the search of potential molecular target and new antiviral drugs. Finally, it is given an example of another infectious disease, tuberculosis. A very prevalent infectious disease, affecting initially lungs but with potential to extend to other tissues (Oliwa et al., 2015). There is a very recent mathematical analysis of the latency of tuberculosis, responsible of drug and immune resistance (Magombedze and Mulder, 2013). It combined a bioinformatics approach to analyze microarray gene expression data with mathematical modelling techniques to propose certain genes responsible to entry in latency. Targeting these genes is a promising strategy to increase the effectiveness of new therapies against this pathogen.

Colorectal cancer is one of the most prevalent neoplasms. It occurs as an abnormal growth in the crypts of the colon (Susman et al., 2012). This tissue has a very high regenerative ability; all the cells of the crypt are renewed after one week. In order to maintain the equilibrium the number of cells has to be controlled by a continuous cell death. Increasing the growth rate of the stem cells of the crypt can promote abnormal growth which can culminate in malignant tumors. A simple mathematical model which includes the basic processes for cell growth, differentiation and death was able to predict the observed evolution of the disease, from stable benign tumors to malignant uncontrolled growth (Johnston et al., 2007). It was formulated as a set of cumulative mutations which increase the growth rate of cells. A second example on colorectal cancer studied the drug resistance by KRAS mutation (Sameen et al., 2015). They were able to predict that a small initial population of KRAS mutated cells has the ability of making all the tumor refractory to the treatment. Also, it was analyzed the effectiveness of the combination of monoclonal antibody (cetuximab) and chemotherapy (irinotecan) in patients with KRAS mutations. They predicted that only in patients with high immune strengths it would be recommended as first-line therapy.

The last examples are going to be on the topic of immune and metabolic diseases. Immune diseases are produced by the malfunction of the immune system. Chronic inflammation and autoimmune disease are examples of malfunctions in which immune system increases its activity above its physiological level. Inflammation is related with the onset of atherosclerosis, by shear stress in the epithelium (Bryan et al., 2014). A mathematical model of the signaling pathway triggered under shear stress in endothelial cells was able to predict the biochemical observations (Yin et al., 2010). It was used to propose the crucial role of the Bone Morphogenic Protein 4 and $p47^{phox}$-dependent NADPH oxidases in the inflammation of the endothelium. As an example on autoimmune disease, a mathematical analysis of the multiple sclerosis was made recently (Broome and Coleman, 2011). This is a neurodegenerative disorder in which immune systems is thought to attack myelin of neurons. It was studied the role of reactive oxygen and nitrogen species, the permeability transition pore, apoptotic factors and cell death of oligodendrocytes. The most promising therapy predicted by the model was preventing the opening of the permeability transition pore. Concerning metabolic diseases, several

approaches have been made to elucidate the complexity of metabolism and its malfunction. The general methodology to deal with the malfunctioning of one enzyme using systemic methodologies is explained in the study Vera et al., 2007. It consists on integrating the main metabolic pathways in which this enzyme is enrolled into a model, and then some mathematical methods, as optimization, point to promising metabolic processes which would reverse the normal physiology and minimizing the effect on other processes. This methodology was applied in this work to propose therapies for hyperuricemia. The results predicted six different therapies involving dietary modifications, one of them coinciding with the conventional treatment. Finally, another study concerning metabolic abnormalities focused on purine metabolism and gout (Curto et al., 1998). Gout is a metabolic disease produced by the abnormal accumulation of uric acid on the blood stream which causes arthritis. In order to uncover the mechanisms leading gout this mathematical modelling of the metabolism of purines allows to understand that the accumulation of two substrates of the enzyme adenylosuccinate lyase is enough to predict the metabolic imbalance observed in the disease.

2. Methodology

The present work is based on the principles of systems biology; specifically it is focused on the study of the diseases as dynamical networks. The main workflow consists on the following sequence: i) proposing an objective for the study; ii) integrating the information concerning a disease; iii) selecting the main elements and processes which intervene in the disease and constructing a conceptual model for the relationship between elements and processes (network); iv) formalizing the conceptual model into a mathematical framework which considers the time dimension explicitly; v) use dynamical experimental information from bibliography to calibrate the model; vi) validating the predictions of the model using new experimental information not used during the calibration; vii) using the mathematical model to make predictions and answering the objective. Each of these steps is described in detail below.

Proposing an objective for the study

Based on the knowledge about a biological problem it is proposed an objective which can be answered with the available knowledge and experimental measurement on the disease. It is formulated in a way that it can provide quantitative and dynamical new knowledge of the disease. The objective will be focused on understanding the molecular and cellular mechanisms which drive the disease and proposing new therapies based on dynamical and integrative knowledge.

Integrating the information concerning a disease

When you are looking for all the systematic information about any disease on the bibliography, you have to deal with dispersed and contradictory information. Although some opposite results can be due to errors, most of the time the reason is that the experiments to obtain the information were displayed in very specific conditions where the interesting process was isolated. Then, incorporating knowledge into a unique conceptual framework is a hard task in which it is important to reduce the importance of the details and focusing on the main characteristics of the disease.

From the systematic review of the knowledge about the disease it is understood what the established hypotheses and the open questions are. It is common that the understanding of the physiology of the diseases is based on static explanations of the molecular and cellular processes, which makes the quantitative and dynamical analysis appropriate to deal with very interesting open questions and for proposing new therapies.

Selecting the main elements and processes which intervene in the disease and constructing a conceptual model

Simplifying is one of the main concepts in science, especially in biology. Biological organisms are "noisy" and very complicated, which makes essential to focus on the main elements that play a relevant role on the phenomena of interest. Simplifying is basically a problem concerning scaling. There are some processes which are mostly disconnected from others because they occur at different time scale, or because they are differentially compartmentalized. Also, it is possible that the network of interactions makes some elements being virtually independent of each other under certain circumstances, or simply that under specific conditions some processes simply do not occur. When the scaling is not useful any more to reduce the complexity of the system a second strategy is based on grouping elements or processes. Under certain circumstances, and focusing on specific phenomena, it is admissible to group elements and using a representative element of this group, or even to consider the mean value within the group. Finally, it will be obtained a simplified representation of the real system which would be able to predict the dynamics at the scale of interest for answering the proposed objective.

Based on the collected information and after the subsequent simplification of the interaction network it is built a conceptual model. It consists on a structuration of the ideas of the relevant processes of the disease of interest focused on the proposed objective. This conceptualization, by itself, is a fundamental piece of knowledge and it is common that in this step many of the previous ideas have to be reformulated. The next step is to provide to the model a quantitative and dynamical meaning based on biological measurements, but to do this the conceptual model has to be formalized into a mathematical framework which explicitly includes the time dimension.

Formalizing the conceptual model into a mathematical framework which considers the time dimension explicitly

The selection of a proper mathematical formalism to formalize the conceptual model depends on the objective proposed, the knowledge about the disease and the experimental data available. For a description of mathematical formalisms used on biology and their main characteristics see the following review (Machado et al., 2011).

The most extended mathematical formalism for dynamical quantification of biological systems is based on ordinary differential equations (ODE). These equations explicitly consider the time as the derivatives are with respect to time. The predictions of the models based on ODE are trajectories of the changes during time of the elements of the model. ODE models are useful when the biological system contains a lot of elements, so the random noise can be neglected. ODE equations are deterministic and they provide the same output for the same conditions, which is almost true in systems with many elements (Gustafsson and Sternad, 2013). Another important condition to be satisfied is the spatial homogeneity. This is never true, but can be assumed depending on the spatial scale considered, and sometimes it can be solved assuming discrete spatial compartments between which the mass is interchanged (Bielecki et al., 2008).

These equations can be analyzed for finding special biological situations, for example searching for stationary solutions. This is crucial because many elements of the biological organisms remain constant, based on the principles of homeostasis. The mathematically procedure consists on doing the derivatives respecting time to zero, so we are saying that the evolution with respect to time is null for the elements of our model. In practice this methodology cannot be always applied for two reasons: i) many biological processes are dynamically active, which means that they are changing during time. For

example oscillations, signals, etc. ii) Nonlinearities on the dynamics usually makes very difficult to obtain a solution for the equations. Instead of searching for stationary behaviors we can focus on the dynamics. To do that it is needed another mathematical tool to obtain the dynamics from the model. It is numerical analysis. The derivatives of the model are solved approximately using numerical calculus which provides the evolution during time of the elements of our model.

Another interesting mathematical method which ODE models provide is sensitivity analysis (Savageau, 1971). It is used to measure the robustness on the response of the system under changes on the parameters of the model. Biological systems are robust because they are exposed to continuous environmental changes and noise and they can keep the internal homeostasis. Because of that, sensitivity analysis on the mathematical model is a quality measurement which gives information of the robustness of the model, if the model responds changing a lot after small changes it means that it is not biologically realistic. But this methodology can also be used for proposing interesting targeting points for drug design, as the most sensitive processes in the model are the ones which are the most easy to manipulate to change the output of the system.

Different equations can be used to represent a specific dynamical process depending on the assumptions and observations on the phenomena. In this review (Voit, 2013) it is presented the most used mathematical formalisms for ODE models in biology. Here the attention will only be focused on two forms: i) mass actions; ii) power-law.

Mass action was originally developed in chemistry (Waage and Gulberg, 1986), it considers that the velocity of the processes are proportional to the elements intervening in it raised to the corresponding kinetic order, which in a chemical reaction coincides with the stoichiometric index. Basically it assumes that the velocities are linear dependent on concentration of elements on monosubstrate processes. This assumption is a good option because of simplicity, and it is commonly used on the first modelling approaches. Even when the processes involved are non-linearly related we can assume linearity in some region around certain condition. However, this formalism cannot be able to reproduce all dynamical behavior of the biological systems, which makes necessary to change to a more complex formalism when it starts failing.

Power-law formalism is based on the Biochemical Systems Analysis explained above (Voit, 2013). It assumes that the relationship between velocities and elements are linear in a double log representation. This is equivalent to assume that the elements intervening in one process are raised to an exponent, which can be a real number, instead of an integer as in mass action formalism. It began as a way to simulate biochemical reactions using a canonical mathematical representation, which does not depend on the enzymatic mechanism (Savageau, 2010), as it happens in Michaelis-Menten formulation. Then it has proved to be useful in many other biological systems out of metabolism (Boykin and Ogle, 2010; Liu et al., 2008; Renton et al., 2005; Smith, 1975; Vera et al., 2008). This is because even being a linearizable formalism it is able to reproduce most of the non-linear behaviors observed in biological organisms. It also provides an easy way of making stationary and sensitivity analysis of the models.

Another mathematical formalization different from ODE models is agent based modelling (ABM) (Marchi and Page, 2014). The main difference is that instead of being based on equations, the elements are particles which can move and interact with other elements and with the environment. It is defined creating a framework in which the particles can move, assigning the number and characteristics of the particles and finally defining a set of rules to be followed by the particles. The advantages are that this formulation has a resolution of individuals and it considers the spatial dimension. However, due to the individual definition it is not appropriate to simulate biological systems with many elements. It is a good

option when it is needed to focus the attention on a specific mechanism produced by the interaction of few elements, in which is difficult to induce general rules at higher scale.

Use dynamical experimental information from bibliography to calibrate the model

Experimental data is the obliged reference of mathematical models in science, and specifically in biological systems. Calibration of a mathematical model consists on giving values to the free parameters of the equations of the model in a way that they are able to reproduce the observed phenomena.

The first step for calibration is looking for experimental data measured during time (for dynamical models) (Voit and Chou, 2010). It is relevant to consider the quality of the data, not only concerning the lack of errors, but the fact that data is measured in the proper conditions in which the model was defined. Frequently data has to be processed and compared with data taken in similar or even in different conditions. Normalization is a common post-processing task when it is integrated data from many different works; usually experimental observations are divided by the mean value of the data set, or even expressed between 0 and 1.

Once the data is formatted to the model, many different mathematical tools can be used to obtain the value of the free parameters from the data. It can be applied linear or non-linear regression and optimization techniques. In case we need to obtain the value of many parameters of non-linear equations it can be used optimization algorithms which can find solutions of the model which predict data by an extensive and directed way. The objective is that the model is able to predict the dynamical behavior of the data.

Another option, usually combined with the previous one, is finding kinetic parameters from bibliography which can be used as parameters of the model. One example is taking measurements of the half-live ($t_{1/2}$) of molecules in the organisms which can be transformed into kinetic parameters (k) by the following expression:

$$k = \frac{\ln(0.5)}{t_{1/2}}$$

Other kinetic parameters like Michaelis constant or the maximum velocity can also be used in the model.

At the end the model will be able to predict the dynamical response of the biological system of interest under certain condition. Before using it to answer the objective proposed it is necessary to test the validity of the mathematical model.

Validating the predictions of the model using new experimental information not used during the calibration

A mathematical model is basically a hypothesis of the dynamical mechanism of the biological system of interest. This hypothesis must be validated before using it to obtain new knowledge. In order to test the validity of the model is needed new experimental data taken in slightly different conditions that the data used for the calibration. The idea is evaluating the ability of the model of predict conditions out of its “comfort zone”, that is the condition in which it is able to properly predict the observed phenomena. Insofar as it is able to predict different conditions it would mean that the

mathematical model is a good representative of the actual system under the conditions for answering the objective.

The classical way to verify the model is starting from a set of data which was measured in the same organism but changing some of the biological conditions. Under this optimal situation a subset of the data is used for the calibration and the rest serves for validation. But, as not always is possible to dispose these kinds of data it is necessarily to look for new experimental data from other studies taken in the same, or very similar, organisms but using different experimental conditions. Finally, a very interesting approach to verify the model is the following: first a prediction from the model by changing the conditions is obtained, and then it is designed an experiment which matches the new conditions of the model and comparing the prediction made by the model with the data from the experiment. This constitutes verification *a posteriori*, because the experimental measurement comes later.

Using the mathematical model to make predictions and answering the objective

Once the mathematical model is able to predict different conditions of our biological system it is ready to be used to answer the objective of the work. One advantage of mathematical models is that is it very easy, cheap and fast performing experiments in them. This makes mathematical modelling very attractive to test preliminary experiments before performing them in a wet laboratory.

If we are interested in understanding the behavior of the system in a different condition we only have to simulate with the model this condition, but it is usually more interesting looking for a specific condition which would give the output of interest, for example a therapy for a disease. As it was mentioned before, sensitivity analysis can serve as a preliminary study to propose promising therapies, as it is pointing to the change in the system which makes the higher change in the response. However a systematic perturbation of the model is usually performed to find new therapies. It is interesting to evaluate combinations of few modifications which could be more effective than the sum of the perturbations alone, based on the synergy of the system. The result of this kind of analysis is a set of proposals for drug target searching which can be then tested in the laboratory.

The strength of this methodology is that it is able to integrate the disperse information about one disease in a mathematical framework which can consider the temporal dimension of the problem. Real understanding of the biological systems comes by the fact that all the processes and their dynamics are analyzed simultaneously. Based on this approach the therapeutic strategies are proposed considering the dynamical and complex nature of the organisms. It opens the possibility of finding new targets which cannot be conceived by reductionist approach alone.

3. References

1000 Genomes Project Consortium, Abecasis, G.R., Altshuler, D., Auton, A., Brooks, L.D., Durbin, R.M., Gibbs, R.A., Hurles, M.E., and McVean, G.A. (2010). A map of human genome variation from population-scale sequencing. Nature *467*, 1061–1073.

Antony, P.M.A., Balling, R., and Vlassis, N. (2012). From systems biology to systems biomedicine. Curr. Opin. Biotechnol. *23*, 604–608.

Bertalanffy, L.V. (1969). General System Theory: Foundations, Development, Applications (George Braziller Inc.).

Bielecki, A., Kalita, P., Lewandowski, M., and Skomorowski, M. (2008). Compartment model of neuropeptide synaptic transport with impulse control. Biol. Cybern. *99*, 443–458.

Boykin, E.R., and Ogle, W.O. (2010). Using heterogeneous data sources in a systems biology approach to modeling the Sonic Hedgehog signaling pathway. Mol. Biosyst. *6*, 1993–2003.

Broome, T.M., and Coleman, R.A. (2011). A mathematical model of cell death in multiple sclerosis. J. Neurosci. Methods *201*, 420–425.

Bryan, M.T., Duckles, H., Feng, S., Hsiao, S.T., Kim, H.R., Serbanovic-Canic, J., and Evans, P.C. (2014). Mechanoresponsive networks controlling vascular inflammation. Arterioscler. Thromb. Vasc. Biol. *34*, 2199–2205.

Buxton, G.A., Siedlak, S.L., Perry, G., and Smith, M.A. (2010). Mathematical modeling of microtubule dynamics: insights into physiology and disease. Prog. Neurobiol. *92*, 478–483.

Craft, D.L., Wein, L.M., and Selkoe, D.J. (2002). A mathematical model of the impact of novel treatments on the A beta burden in the Alzheimer's brain, CSF and plasma. Bull. Math. Biol. *64*, 1011–1031.

Curto, R., Voit, E.O., and Cascante, M. (1998). Analysis of abnormalities in purine metabolism leading to gout and to neurological dysfunctions in man. Biochem. J. *329 (Pt 3)*, 477–487.

Dehay, B., Bourdenx, M., Gorry, P., Przedborski, S., Vila, M., Hunot, S., Singleton, A., Olanow, C.W., Merchant, K.M., Bezard, E., et al. (2015). Targeting α-synuclein for treatment of Parkinson's disease: mechanistic and therapeutic considerations. Lancet Neurol. *14*, 855–866.

ENCODE Project Consortium (2004). The ENCODE (ENCyclopedia Of DNA Elements) Project. Science *306*, 636–640.

Fell, D. (1996). Understanding the Control of Metabolism (Portland Pr).

Giacobini, E., and Gold, G. (2013). Alzheimer disease therapy--moving from amyloid-β to tau. Nat. Rev. Neurol. *9*, 677–686.

Gouras, G.K., Willén, K., and Faideau, M. (2014). The inside-out amyloid hypothesis and synapse pathology in Alzheimer's disease. Neurodegener. Dis. *13*, 142–146.

Gustafsson, L., and Sternad, M. (2013). When can a deterministic model of a population system reveal what will happen on average? Math. Biosci. *243*, 28–45.

Heinrich, R., and Rapoport, T.A. (1974). A linear steady-state treatment of enzymatic chains. General properties, control and effector strength. Eur. J. Biochem. FEBS *42*, 89–95.

Hodgkin, A.L., and Huxley, A.F. (1952). A quantitative description of membrane current and its application to conduction and excitation in nerve. J. Physiol. *117*, 500–544.

Johnson, K.A., and Goody, R.S. (2011). The Original Michaelis Constant: Translation of the 1913 Michaelis-Menten Paper. Biochemistry (Mosc.) *50*, 8264–8269.

Johnston, M.D., Edwards, C.M., Bodmer, W.F., Maini, P.K., and Chapman, S.J. (2007). Mathematical modeling of cell population dynamics in the colonic crypt and in colorectal cancer. Proc. Natl. Acad. Sci. U. S. A. *104*, 4008–4013.

Kacser, H., and Burns, J. (1973). The control of flux. Symp Soc Exp Biol *27*, 65–104.

Könnyű, B., Sadiq, S.K., Turányi, T., Hírmondó, R., Müller, B., Kräusslich, H.-G., Coveney, P.V., and Müller, V. (2013). Gag-Pol processing during HIV-1 virion maturation: a systems biology approach. PLoS Comput. Biol. *9*, e1003103.

Liu, Y.-W., Chen, C.-K., and Lin, C.-L. (2008). Signal Transduction Networks in Biological Systems Based on Michaelis-Menten Equation and S-system. In Proceedings of the 7th WSEAS International Conference on Computational Intelligence, Man-Machine Systems and Cybernetics, (Stevens Point, Wisconsin, USA: World Scientific and Engineering Academy and Society (WSEAS)), pp. 25–28.

Lotka, A.J. (1920). Analytical Note on Certain Rhythmic Relations in Organic Systems. Proc. Natl. Acad. Sci. U. S. A. *6*, 410–415.

Machado, D., Costa, R.S., Rocha, M., Ferreira, E.C., Tidor, B., and Rocha, I. (2011). Modeling formalisms in Systems Biology. AMB Express *1*, 45.

Mackey, M.C., and Glass, L. (1977). Oscillation and chaos in physiological control systems. Science *197*, 287–289.

Magombedze, G., and Mulder, N. (2013). Understanding TB latency using computational and dynamic modelling procedures. Infect. Genet. Evol. J. Mol. Epidemiol. Evol. Genet. Infect. Dis. *13*, 267–283.

Marchi, S. de, and Page, S.E. (2014). Agent-Based Models. Annu. Rev. Polit. Sci. *17*, 1–20.

Marsden, M.D., and Zack, J.A. (2013). HIV/AIDS eradication. Bioorg. Med. Chem. Lett. *23*, 4003–4010.

Nampala, H., Luboobi, L.S., Mugisha, J.Y.T., and Obua, C. (2013). Mathematical modeling of liver enzyme elevation in HIV mono-infection. Math. Biosci. *242*, 77–85.

Oliwa, J.N., Karumbi, J.M., Marais, B.J., Madhi, S.A., and Graham, S.M. (2015). Tuberculosis as a cause or comorbidity of childhood pneumonia in tuberculosis-endemic areas: a systematic review. Lancet Respir. Med. *3*, 235–243.

Perelson, A.S., Neumann, A.U., Markowitz, M., Leonard, J.M., and Ho, D.D. (1996). HIV-1 dynamics in vivo: virion clearance rate, infected cell life-span, and viral generation time. Science *271*, 1582–1586.

Pérez-Nueno, V.I. (2015). Using quantitative systems pharmacology for novel drug discovery. Expert Opin. Drug Discov. *10*, 1315–1331.

Phillips, A.N. (1996). Reduction of HIV concentration during acute infection: independence from a specific immune response. Science *271*, 497–499.

Prigogine, I. (1968). Introduction to Thermodynamics of Irreversible Processes (John Wiley & Sons Inc).

Puri, I.K., and Li, L. (2010). Mathematical modeling for the pathogenesis of Alzheimer's disease. PloS One *5*, e15176.

Qi, Z., Miller, G.W., and Voit, E.O. (2008). Computational systems analysis of dopamine metabolism. PloS One *3*, e2444.

Renton, M., Hanan, J., and Burrage, K. (2005). Using the canonical modelling approach to simplify the simulation of function in functional-structural plant models. New Phytol. *166*, 845–857.

Ross, R. (1915). Some a priori pathometric equations. Br. Med. J. *1*, 546–547.

Sameen, S., Barbuti, R., Milazzo, P., Cerone, A., Del Re, M., and Danesi, R. (2015). Mathematical modeling of drug resistance due to KRAS mutation in colorectal cancer. J. Theor. Biol. *389*, 263–273.

Sass, M.B., Lorenz, A.N., Green, R.L., and Coleman, R.A. (2009). A pragmatic approach to biochemical systems theory applied to an alpha-synuclein-based model of Parkinson's disease. J. Neurosci. Methods *178*, 366–377.

Savageau, M.A. (1969). Biochemical systems analysis. J. Theor. Biol. *25*, 365–369.

Savageau, M.A. (1971). Parameter sensitivity as a criterion for evaluating and comparing the performance of biochemical systems. Nature *229*, 542–544.

Savageau, M.A. (2010). Biochemical Systems Analysis: A Study of Function and Design in Molecular Biology (Reading, Mass.: CreateSpace Independent Publishing Platform).

Savageau, M.A. (2011). Biomedical engineering strategies in system design space. Ann. Biomed. Eng. *39*, 1278–1295.

Savageau, M.A., Voit, E.O., and Irvine, D.H. (1987). Biochemical systems theory and metabolic control theory: 1. fundamental similarities and differences. Math. Biosci. *86*, 127–145.

Smith, D.F. (1975). Quantitative analysis of the functional relationships existing between ecosystem components. Oecologia *21*, 17–29.

Susman, S., Tomuleasa, C., Soritau, O., Mihu, C., Rus-Ciuca, D., Sabourin, J.-C., Bibeau, F., Irimie, A., and Buiga, R. (2012). The colorectal cancer stem-like cell hypothesis: a pathologist's point of view. J. BUON Off. J. Balk. Union Oncol. *17*, 230–236.

Vera, J., Curto, R., Cascante, M., and Torres, N.V. (2007). Detection of potential enzyme targets by metabolic modelling and optimization: application to a simple enzymopathy. Bioinforma. Oxf. Engl. *23*, 2281–2289.

Vera, J., Bachmann, J., Pfeifer, A.C., Becker, V., Hormiga, J.A., Darias, N.V.T., Timmer, J., Klingmüller, U., and Wolkenhauer, O. (2008). A systems biology approach to analyse amplification in the JAK2-STAT5 signalling pathway. BMC Syst. Biol. *2*, 38.

Voit, E.O. (2013). Biochemical Systems Theory: A Review. Int. Sch. Res. Not. Int. Sch. Res. Not. *2013*, e897658.

Voit, E., and Chou, I. (2010). Parameter estimation in canonical biological systems models. Int. J. Syst. Synth. Biol. *1*, 1–19.

Volterra, V. (1927). Variazioni e fluttuazioni del numero d'individui in specie animali conviventi (Memoria della Reale Accademia Nazionale dei Lincei).

Waage, P., and Gulberg, C.M. (1986). Studies concerning affinity. J. Chem. Educ. *63*, 1044.

Yin, W., Jo, H., and Voit, E.O. (2010). Systems analysis of the role of bone morphogenic protein 4 in endothelial inflammation. Ann. Biomed. Eng. *38*, 291–307.

Zou, J., Zheng, M.-W., Li, G., and Su, Z.-G. (2013). Advanced systems biology methods in drug discovery and translational biomedicine. BioMed Res. Int. *2013*, 742835.

4. Objective

The objective of the present work is to increase the comprehension of the physiology under some diseases with high prevalence making use of mathematical analysis which integrates all the information available about a specific process of interest in a single interaction network and incorporating the dynamical aspect of the disease. Based on the mathematical modelling concepts it will be proposed some potential therapeutic strategies on prevalent diseases which would have been difficult to find by classical reductionist approaches, because they are considered counterintuitive. The four diseases to be analyzed are malaria, HIV infection, Alzheimer's disease and melanoma. These four works are based on the main four publications which constitutes the present thesis. But in this thesis two first articles are presented as an introduction of mathematical modelling in biosciences. The first one discuss a general approach of mathematical modelling in biosciences, and the second one presents a review of mathematical models developed in the topic of malaria infection, focused on modelling the process occurring inside the human host.

The work about malaria is a mathematical model using ODE equations based on the power-law formalism. It is focused on the intra-host interactions between the parasite and the immune system of the patient. The objective is to propose new targets in which the antimalarial drug process to search can be focused on.

The one about HIV simulates the first steps of the invasion of T4 lymphocytes by HIV; this is an important process to be controlled to prevent the disease. It is developed a mathematical model on ODE equations using the mass actions formalism. The objective is to understand the relative importance of all molecular pathways playing a role during the virus entry and pointing to some molecules which would be interesting to modify to impede the access of the virus inside T4 lymphocytes.

Another one is about Alzheimer's disease and it will be focused on the relationship between the neuron cell membrane lipids composition and dynamics and the production of β-amyloid in the brain. The objective is to understand the effect of the change in physical properties of lipid domains (lipid rafts) in the membrane on the evolution of the disease. It will also be proposed dietary therapeutic strategies to slow the evolutions of Alzheimer's disease.

One additional article includes the work obtained during the stay in the Laboratory of Systems Tumor Immunology at *FAU Universität Nürnberg-Erlangen* in Germany. The study was focused on the improvement of an immunotherapy as treatment for melanoma patients. It is based on the analysis of an ODE mathematical model and numerical analysis. It is used to propose co-adjuvant therapy in combination with the vaccine to improve the efficacy of the vaccine in patients in which this vaccine has not effect.

5. Modelling in Biosciences - *Frontiers in Genetics*

DOI: 10.3389/fgene.2015.00354

frontiers in Genetics

REVIEW
published: 22 December 2015
doi: 10.3389/fgene.2015.00354

The (Mathematical) Modeling Process in Biosciences

Néstor V. Torres[1,2]* *and Guido Santos*[1,2]

[1] *Systems Biology and Mathematical Modelling Group, Departamento de Bioquímica, Microbiología, Biología Celular y Genética, Sección de Biología de la Facultad de Ciencias, Universidad de La Laguna, San Cristóbal de La Laguna, Spain,*
[2] *Instituto de Tecnología Biomédica, CIBICAN, San Cristóbal de La Laguna, Spain*

In this communication, we introduce a general framework and discussion on the role of models and the modeling process in the field of biosciences. The objective is to sum up the common procedures during the formalization and analysis of a biological problem from the perspective of Systems Biology, which approaches the study of biological systems as a whole. We begin by presenting the definitions of (biological) system and model. Particular attention is given to the meaning of mathematical model within the context of biology. Then, we present the process of modeling and analysis of biological systems. Three stages are described in detail: conceptualization of the biological system into a model, mathematical formalization of the previous conceptual model and optimization and system management derived from the analysis of the mathematical model. All along this work the main features and shortcomings of the process are analyzed and a set of rules that could help in the task of modeling any biological system are presented. Special regard is given to the formative requirements and the interdisciplinary nature of this approach. We conclude with some general considerations on the challenges that modeling is posing to current biology.

Keywords: biosciences, biological system, model, mathematical model, systems biology

OPEN ACCESS

Edited by:
Rui Alves,
Universitat de Lleida, Spain

Reviewed by:
Miguel Ángel Medina,
University of Málaga, Spain
Ester Vilaprinyo,
University of Lleida – Institut de Recerca Biomèdica de Lleida, Spain

***Correspondence:**
Néstor V. Torres
ntorres@ull.edu.es

Specialty section:
This article was submitted to Systems Biology, a section of the journal Frontiers in Genetics

Received: *23 September 2015*
Accepted: *07 December 2015*
Published: *22 December 2015*

Citation:
Torres NV and Santos G (2015) The (Mathematical) Modeling Process in Biosciences. Front. Genet. 6:354. doi: 10.3389/fgene.2015.00354

INTRODUCTION

A theory has only the alternative of being right or wrong. A model has a third possibility: it may be right, but irrelevant.

Manfred Eigen. The Origins of Biological Information.

There are many definitions of science (Popper, 1935; Kuhn, 1962, 1965; Lakatos, 1970), but all of them refer to a body of knowledge obtained through a particular method based on the observation of the physical world, linked to systematically structured reasoning, strategies by which general principles and laws are deduced. That particular method is the "Scientific Method", defined by the Oxford English Dictionary as "*. . .the procedure. . ., consisting in systematic observation, measurement, and experiment, and the formulation, testing, and modification of hypotheses.*" In the above statements there are two core ideas which are relevant here and that derive directly from what science is: the first one is that any scientific activity requires measurements and thus, quantification of real magnitudes. The second is that any scientific activity makes sense only if it allows us to gain "knowledge"; that is understanding, predicting and control. In science these goals are achieved through the building of models and theories. Both serve, with different degrees of generality, to explain the observed facts and predict with high probability the evolution and behavior of natural systems.

Biological Systems and Models

Before describing the modeling process, it is advisable to clarify the meaning of two key concepts, "biological system" and "model" that we assume are inextricably linked.

Any biological system is composed of a set of elements, physical objects, usually numerous and diverse, that influence each other (i.e., they interact) and that are physically and functionally separated from their environment. The physical separation is a frontier, which can be real (e.g., a membrane) or imaginary, which is permeable to matter, and energy (i.e., an open system). The functional separation is a consequence of the fact that biological systems are far from thermodynamic equilibrium, in contrast with the environment. The interchange of matter and energy with the environment is indeed a necessary requisite to sustain the chemical–physical processes that occur far from equilibrium. Thus defined, a living system involves a reference to the environment in which it is located and with which it interacts. It is worth noting here that when we focus solely on the elements, disregarding the interactions between them and with the environment, the system disappears, because a set of entities devoid of interaction is a mere aggregation of elements. This is the essence of "system", a holistic approach to research as opposite to a reductionist view.

For our purposes here, a model is a conceptual or mathematical representation of a system that serves to understand and quantify it. The difference between conceptual and mathematical resides only on the way the representation is formulated. A model is always a simplified representation of the reference system, which the scientist wishes to understand and quantify. It ultimately serves as a means of systematizing the available knowledge and understanding of a given phenomenon and the facts concerning it.

A first step in any model-building attempt is the simple verbalization of statements about the biological system. Soon this phase leads to a more productive one, where observations and hypothesis transform the observations and data into an organized core, the so-called "conceptual" model. Conceptual models constitute, thus, a first level of qualitative integration of the information on the system under scrutiny. Conceptual models are so ingrained in our everyday life that we usually do not make a distinction between models and the real thing. Very often, they come as diagrams, words or physical structures, which deal with either the structure and/or the function of the real system. The causal diagrams are examples of suitable tools that help in dealing with the conceptual models (Voit, 1992; Minegishi and Thiel, 2000; Allender et al., 2015).

A key feature of the conceptual models is that they only make a qualitative description of the real system. Examples of such conceptual models in biology range from the typical plant or animal cell diagram (one that integrates many observations of multiple types of cells obtained through a great variety of techniques) to the models about enzyme action and metabolic pathways. The enzyme action model describes how the substrate attaches to the active site of the enzyme, and how the enzyme structure changes in different molecular environments. Another ubiquitous conceptual model is that of metabolic pathways; they represent the coordinated and sequential activities and regulatory features of many enzymes. The main value of the conceptual models is that, as the result of the (tough) complex process involved in its development, it allows the integration of disperse information obtained from different sources. However, their origin renders them imprecise, and conceptual models can be interpreted differently by different people.

A further refinement in the process of system understanding is given by the translation of the conceptual model into a form subject to a quantitative description, evaluation and validation. This form is the mathematical model. A mathematical model is the formalized description of the system derived from a previous conceptual model. Mathematical models may be very diverse in nature. Dynamical models consider changes in the elements with time, and can be categorized into deterministic and stochastic. In the deterministic ones, the velocities only depend on the concentration of the elements and the parameters of the model. The opposite are the stochastic ones, in which the velocities also depend on the random noise of the system, due to the uncertainty present in systems containing statistically non-abundant elements. On the other hand, static models try to understand the structure of the interconnection of the elements, which remains constant during time under specific conditions (Voit, 2012).

The mathematical models not only help us to understand the system, but also are instrumental to yield insight into the complex processes involved in biological systems by extracting the essential meaning of the hypotheses (Wimsatt, 1987; Bedau, 1999; Schank, 2008) and allows to study the effects of changes in its components and/or environmental conditions on the system's behavior; that is, they allow the control and optimization of the system.

Mathematical Models in Biology

The usefulness of mathematical models in physics and technology is well documented; in fact they can be traced back to the very origins of physics. Since the days of Galileo, Kepler and Newton scientists have striven to develop their models by means of mathematical formalism. What we want to present and develop here is the tenet that modeling in general, but specifically mathematical modeling, particularly in biology –as well as in science in general- is the only way to attain such quantitative understanding and control. Mathematical modeling should thus be an essential and inseparable part of any scientific endeavor in the realm of XXI century bioscience.

It has been claimed that the maturity of a scientific field correlates positively with how often mathematical models are developed and used to understand and control the real system (Weidlich, 2003; Medio, 2006; Brauer and Castillo-Chavez, 2010; Gunawardena, 2011). In this regard, it has not been until recently that dynamic mathematical models in biology have become a common feature. Besides the well-known cases of the Michaelis–Menten model to describe the dynamics of the enzyme-catalyzed reactions (Michaelis and Menten, 1913) and its subsequent development for the case of allosteric enzymes (Monod et al., 1965), the Hodgkin–Huxley model of the action potentials in

neurons (Hodkin and Huxley, 1952), the Lotka–Volterra model about the interaction of species (Lotka, 1920; Volterra, 1926) and the epidemiological models of epidemics (Ross, 1915; MacDonald et al., 1968), the emergence and widespread recognition of the role and importance of mathematical models in biology is a recent phenomenon.

It is easy to understand why only until very late in scientific research mathematical modeling of biological systems has been put in use. Biological systems, by their nature, are refractory to precise quantitative and mathematical description. They are composed by many elements closely interconnected by processes and interactions that take place at different levels of organization (molecular, cellular, in tissue, whole animals and ecological). At the same time, these processes occur in an open system as a result of the existence of multiple gradients far from the thermodynamic equilibrium, which in the end produce very complicated non-linear dynamics between the elements of the system (Prigogine, 1961). This situation has impaired the quantitative and dynamic approach to the understanding of biological systems through the use of mathematical models.

However, two technological advancements that have made feasible the construction and resolution of mathematical models for biological systems have been developed in the last decades. There is a general accessibility and almost universal ubiquity of the computational power required for the management of information and the calculation of large systems. On the other hand, the development of the high throughput techniques and the emergence of the "omics" sciences (genomics, transcriptomics, proteomics, signalomics, and metabolomics) have generated a great deal of dynamic information on the structure and behavior of the biological systems. This information has become easier and cheaper to acquire, process and store than ever before.

All the above have been instrumental to the arrival of Systems Biology, as the XXI century approach to the quantitative and interdisciplinary study of the complex interactions and the collective behavior of a cell, an organism or an ecosystem. The distinctive feature of Systems Biology is the concern with the organization and biological function. This approach goes beyond the classical reductionist approach, where the researcher seeks to understand the systems by breaking them down into their constituent elements and analyzing them separately or, in a novel version of the old paradigm facilitated by the high throughput techniques, by collecting every piece of accessible information. In the Systems Biology approach, research is focussed not on the parts considered individually, but on the relationships that exist between the structural components of biological systems and their function, and on the characteristics of the interactions that occur between different sub-systems. This method allows the detection of emerging higher levels of structural and functional organization. In contrast with the reductionist approach, Systems Biology deals with the reconstructive and integrative task upon the available biological information. And it is here where models and modeling becomes a central tenet in Systems Biology.

In the following section we will develop a general framework where the role of models and the modeling process within the scientific activity in biosciences is highlighted. Also, a set of rules that help the modeling activity is presented together with some general considerations on the challenges that modeling currently poses.

A MODEL OF THE MODELING PROCESS IN BIOSCIENCES

The purpose of models is not to fit the data but to sharpen the questions.

Samuel Karlin

The **Figure 1** summarizes the set of activities and elements involved in the development of models, as organized following the Scientific Method.

I. Conceptualization

The first stage of the scientific modeling process is the conceptualization phase. In any research process all activities are organized around the Real System, which is the compulsory, continuous reference in the whole process. This central position is represented in **Figure 1** as a circle.

The first step in the conceptualization stage is to formulate, from the very first observations of the phenomenon (Observation; see **Figure 1**), generally made in an unsystematic form, an explanatory hypothesis of it: the first version of the conceptual model. This is a critical task where it is necessary to coordinate, to contrast and discuss many issues with the aim of making the best decisions. Some of the questions that should be addressed at this stage are: what aspects of the real system should be incorporated into the model? What features should/can be ignored? Or, what hypotheses can support the observations/information rendered by the system?

Given that any model is an instrument designed for a purpose, the very first question that should be posed at this stage is: what is the model for? That is, the objective of the model. No model makes sense or is justified for its own sake. Thus, what first defines a model is the specific question that it is going to answer.

Trying to develop a model to explain all aspects of a biological phenomenon will be practically impossible, a very complex and highly unmanageable task. However, a model with a limited purpose will be feasible, and easier to be analyzed and managed. At this stage of modeling, our thinking process uses the categories of space, time, substance (namely, material components, and elements), quality, quantity, and relationship. These categories help us to bring order to the perceived complexity of the real world. Nevertheless, this act of classification and identification differ considerably from one scientific discipline to another.

The meaning and significance of the modeling process is rooted in the core of the scientific process: from the observation of some part of the biological world some questions arise, the model being the tool that eventually would serve to provide an answer. As can be seen, any modeling exercise forces, from the very beginning, to define and make explicit the focus of our research and to keep, all along the way, our attention on the main objective.

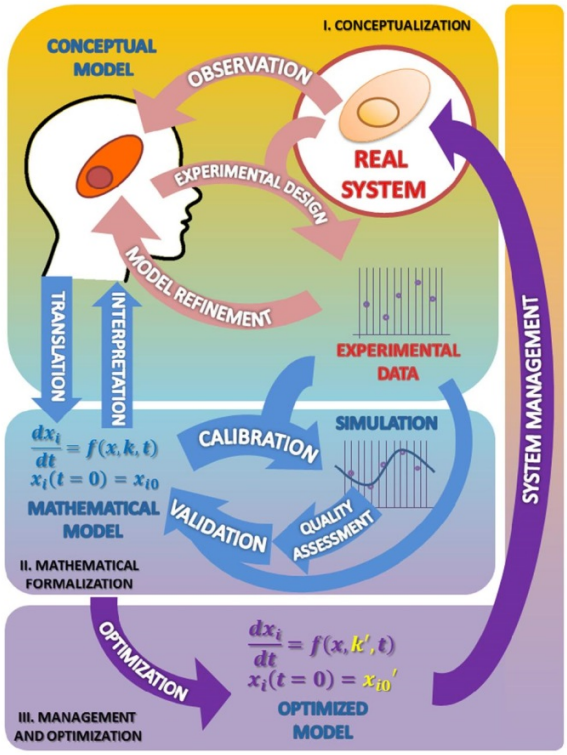

FIGURE 1 | The modeling process in biosciences. The main activities involved in this procedure are observation followed by mathematical modeling; simulation, analysis, optimization and back to observation. In this cycle the mathematical model occupies, just after the real system, the center position. **I. Conceptualization**. Having chosen the subject of research and after some initial observations are made, the biologist should reflect on the model to be built. From the information available and a set of well-founded hypothesis, it will build a first version of the model that presents a first selection of variables, processes and interactions considered relevant (conceptual model). The iteration of this process constitutes the classical version of the scientific method (light pink arrows). **II. Mathematical formalization.** From this proposal the first mathematical formulation of the model is derived (Mathematical model). Getting to this point has required an exercise of integration of hypotheses and information that yields a new, deeper degree of knowledge about the system not reached before (light blue arrows). **III. Management and optimization.** As a result of these two phases the information needed to validate the model becomes evident, which in turn suggests new experimental designs that propitiate a new round of improvement cycle (purple arrows). As can be seen the process of building a model, itself determines the path to a greater and coherent understanding of the system that makes feasible its rational control and management. See text for more information.

The conceptualization stage is where modeling becomes very often an art, a subjective task. The choice of the essential attributes of the real system and the omission of irrelevant ones requires a selective perception that you cannot specify through an algorithm. There is some dosage of freedom and arbitrariness at this stage since different researchers equally well informed can define different models. As we are educated in a specific biological scientific discipline, we are trained to observe the real world in the light of a certain conceptual framework.

In some instances, the discussion of contrasting opinions addressed to demarcate the border between the system and its environment, or to discriminate between different possible scenarios or to evaluate the importance of the experimental error associated with the observed values, leads to different versions of the model. Based on the final selection of hypotheses, the next step is to carry out experiments (Experimental design; see **Figure 1**) devised to obtain experimental data to test the chosen hypothesis. From the analysis of the experimental results, the hypothesis can be reformulated or discarded (Model refinement; see **Figure 1**), thereby initiating a virtuous cycle (pink arrows) that leads to an improved conceptual model. Eventually, this refined model version is expected to answer, though qualitatively, the questions initially raised. At this stage, the need to change the initial hypothesis, far from being a failure, should be understood as progress toward a better understanding of the behavior of the system. This allows to rule out some proposals, which will be replaced by new ones that might be more effective in the building process of the conceptual model.

The above sequence illustrates the fact that observation and science are not the same thing. The aim of the scientific method is not to describe but to explain the observed, to understand and interpret the observations. It is here where the collaboration between the modeling part and the field experts becomes essential. And it is at this stage where interdisciplinarity occurs. The best version of the modeling task results when it is a team effort, where the competences and expertise of different specialists blend. Those with the best knowledge on the particular subject should be able to communicate with the modeler. They must be able to understand each other; the expert presenting the whole picture and selecting from it the elements, interactions, processes, and values that are deemed relevant in the light of the model's objective. At this point the modeler should translate this selection into a conceptual representation that usually takes de form of a mechanistic picture where the elements and their relations are represented. To be useful, this picture should be explicit enough to be translated into a series of elementary steps representing the individual mechanisms. The modeler here is instrumental in defining which are the magnitudes considered as variables and which are not; this is a critical distinction that determines to a great extent the model's output.

The development of the modeling approach has at this point one of its great challenges, because it requires that the different specialists share a common language. There is a need, on the side of the modeler, to become acquainted with the features and nuances of the system under scrutiny, and to speak in terms easy to understand by the non-modeler party. On the other side, the specialist should adopt an integrative way of thinking and be able to make explicit his knowledge and express it in the most precise terms.

More often than not, it is necessary to repeat the conceptualization stage of discussion and analysis several times, before the proposed model becomes able to respond

successfully to all the objections that could be raised by the experts who come in contact with the model. Once you have reached an acceptable version you will be able to consider the next stage: the mathematical formalization.

At this phase of the model building process it could happen that the modeler may be tempted by the challenge of building a wholly comprehensive model system, that is, one that takes into account, if not all, most of the characteristics of the real system. Besides the misunderstanding of the modeling process that this shows, this attitude has additional costs, because if two models serve to give the desired answers, the simpler one is better. A modeler intending to include all variables and parameters described would also be faced with the task of analyzing the influence of all the parameters on all the variables. This in turn would require an additional, usually non-negligible effort for its interpretation, making the model more difficult to understand. In modeling, more and harder is not necessarily better. In fact it sometimes happens that the largest and most complicated model may be the poorest in attaining its objectives or expressing necessary or meaningful details of the reality. A nice illustration of this point is the very simple model of the signaling pathway of NF-κβ, in which with only three elements it is reproduced the main dynamical behavior of the original system (Krishna et al., 2006). In other words, we should try to make the complex as uncomplicated as possible. Despite this, the discussion of its results can enrich the conceptual model building when considering the traits and characteristics that were not initially included.

Related with this is the fact that the developments of the conceptual model force the analysis and the systematic review of available knowledge about the system and its behavior. As a result of this exercise of verbalization of the knowledge -often unconscious- that experts have about the system, a new light is shed on the phenomenon, which very often contributes to a better understanding of the system.

It may happen that some gaps of information about interactions or relevant parts that had hitherto gone unnoticed become evident. This usually suggests new avenues of exploration and ultimately contributes to a better understanding of the observed reality. Also, the discussions on the variables or the processes involved help to change previous assumptions or facilitates a new view and understanding of some facts that previously remained without an explanation. As an example, Cheong et al. (2008) review the contributions of mathematical modeling on the understanding of the NF-κβ pathway. It is also very common to become aware of contradictions in the understanding of biological mechanisms. Most of the knowledge or information about an issue may pass through several authors undisputed, but when all this is mathematically formalized, problems to join all in a single framework emerge. Mathematical thinking forces to reconsider every piece of knowledge.

Finally, there is a modeling principle that should be commented here: "If the hypotheses of the model are erroneous, the conclusions raised from it will be wrong too." As obvious as it may be, this principle is not less important. This principle should be taken into account all along the model-building process, particularly in the mathematical formalization that follows, because the resulting model should be faithful to the proposed hypothesis.

II. The Mathematical Formalization

Mathematical Translation

The first question to be addressed in this new phase is about which mathematical formalism is best suited to represent the system (Translation; see **Figure 1**). There are many formal modeling approaches, based on differential equations, Bayesian equations, stochastic systems, agent-based modeling, etc. (for a review, see ElKalaawy and Wassal, 2015). Each of these has unique strengths and limitations. The choice heavily depends on the nature of the model. It often happens that a research group ends up enslaved by the modeling techniques which it dominates or prefers. For example, a team with experience in modeling using differential equations may tend to approach every problem from the standpoint of this technique, when in fact not all biological problems are deterministic. It is natural to preferentially use the methods that are best known and previously proven fruitful. But the ideal attitude is to adapt the specific modeling technique to the nature of the problem.

The task of developing a model is a process of approximation due to the simplifications that must be introduced. These simplifications should make sense in terms of the physical–chemical processes being studied, but must also be valid form a mathematical point of view. The general approach to the mathematical formulation usually involves the definition of the key variables and the expression of their functional relationship with the other variables of the system. Equations are then derived establishing the actual mathematical relationship among the variables. This derivation can be done empirically (data-driven), through the use of statistical methods (curve fitting) analytically o numerically, or by deriving the equations from theoretical considerations (model-driven). A classic example of model-driven is given by Michaelis and Menten (1913) kinetics. Other common techniques of data-driven modeling are shown in Janes and Yaffe (2006). In the model we should make clear the differences among the variables (concentrations of biochemical compounds of the investigated network: metabolites, proteins, messenger RNAs, etc.) and the parameters. Variables can be dependent, being the elements which vary over time according to the state of the system (also called states); and independent, being the ones that can be controlled during the experiment (light, pH, etc.). The parameters set internal and external constraints on the system. The specific numerical values for the parameters are determined using prior biological knowledge, such as information about the basal steady states of the system (Voit, 2000), or experimental data from dynamical perturbations (Vera et al., 2007, 2008). Usually the models integrate kinetic data and other available information about the elements of the process, as well as fluxes obtained from experimental observations.

It often happens that an existing model is used to describe another system. This strategy, although tempting, should be used with caution. Each new system should be studied in their specific conditions of environment and structure. It is also necessary to consider that a model not only depends on the system that it

represents and the techniques used for its construction, but also from the motivations and objectives of their creators. Therefore one must always beware from attributing the motivations and objectives of others to our own model.

The process of developing a mathematical formulation of the conceptual model forces the investigator to describe the system in simple terms. At this stage the research team must take into account details about the system which might otherwise go unnoticed, which contribute to the improvement of the model. Also, a healthy consequence of the formalization process is that the explanations of the initial, sometimes unexamined assumptions reveal processes and features that remained unrecognized under the less precise conceptual formulations.

The interpretation and understanding of the system has an additional resource in the mathematical expression of it (see **Figure 1**). The set of equations of the mathematical model is likely to be discussed with the plethora of techniques and mathematical tools that allow the description and analysis of the complex interrelated processes that occur in the real system; these techniques can help to elucidate the structure, properties, and dynamic behavior of the system. These analyses can reveal details about the behavior of a model such as the occurrence of oscillations or other complex behaviors that are often the motivating force for studying these systems.

Parameter Estimation and Quality Assessment

Once the conceptual model has been translated to its mathematical form, the model should be provided with the values of its parameters. Parameter estimation or model calibration is a recurrent issue in the model building process; it deals with the finding of the numerical values which characterize the mathematical representation of a given system from experimental data (Park et al., 1997). A key feature of these experimental measurements is that they must come from variables representing their main features both at a given particular time, as well as along its evolution over time (Polisety and Voit, 2006; van Riel, 2006; Ashyraliyev et al., 2008; Banga, 2008). In addition, the quality of the model should be tested through some numerical quality assessments. The quality assessment of the model includes the evaluation of aspects such as the stability of steady states, a prerequisite for any model describing actual biological systems; and the robustness of the model, a test to evaluate whether the model is able to tolerate small structural changes (Savageau, 1971; Hsiung et al., 2008) and the dynamic features that characterize the transient responses to temporary perturbations or permanent alterations (Wu et al., 2008). These analyses often pinpoint problems of consistency and reliability of the mathematical representation (Okamoto and Savageau, 1984, 1986; Ni and Savageau, 1996a,b); this constitutes by itself a further cycle of model refinement (**Figure 1**, light blue cycle). These changes result in improvements of the initial conceptual model. The conceptual model so improved will in turn suggest further experimentation leading to a new refined version that is enriched from the formalization phase.

At all instances it should be borne in mind that both the parameters and the structure of real systems change over time. Therefore, a given model, which can be satisfactory at one time or certain conditions, may lose its effectiveness at another time or in other conditions. But the equations by themselves do not contribute much to the understanding of the system. It is necessary to solve the equations for some representative values of the parameters. Accordingly, the model is submitted to the simulation and validation processes.

Simulation and Prediction

The mathematical model should be programmed in the computer. The computer program is the translation of the mathematical model to another language useful for computing purposes. There are many computer languages and platforms to deal with this task; advances in computer numerical analysis have made the solution of complicated systems fast and accurate. It is at this point where computation becomes critical, since the equations describing biological processes nearly always involve control and regulatory mechanisms that have non-linear components. In contrast with linear differential equations that often can be solved analytically, non-linearities make it generally impossible. But through the use of numerical methods implemented on computers we can obtain good estimates and model predicted data.

Model Validation

Validation stands here as the correspondence between the real system and the mathematical model. A model can be considered good and useful only if its predictions in a given scenario agree with the experimental observations made on the actual system setting. As it is shown in the **Figure 1**, we can accept the model as a plausible representation of the system under scrutiny only when the comparison of the predicted outputs with the real ones yields similar results (and when this occurs in a significant number of situations).

The validation process can only be based on comparative observations of the output values and trajectories of the model and the real system, under certain given experimental conditions. As it is shown in the **Figure 1**, for validation purposes, a first cycle of calibration and quality assessment is needed, and then a second one, with new experimental data from a different condition. As a result, the model might require some modification in order to minimize the observed discrepancies.

There are several ways to perform the validation process. One is to compare the evolution of the variables from some, other initial conditions; with data obtained by different, other research groups in similar systems. Another way is to use all available data in some given conditions, not for the development of our own model, but to use these data for the comparison with our model's predictions instead (Santos and Torres, 2013). In some cases, a useful technique is to vary some model's parameters within the range of biologically plausible values, and observe how the system responds in relation to its actual behavior (Segre et al., 2002). Finally, a technique that can be used in some instances involves subjecting the model to extreme conditions, deliberately looking for their failures. The logic behind this is that, if a model represents the system well in extreme conditions, so it will under normal conditions. In any instance the observed discrepancies indicate errors in the assumptions used in the building of the

mathematical and/or the conceptual model. The discrepancies may be large enough as to require the revision and change of the hypothesis of the conceptual model, or the introduction of only slight modifications in the parameters of the mathematical version.

It should be recalled that the quality of a model depends directly on the quality of the information on which it is based. This statement is just the translation to the modeling context of the classical motto: "garbage in, garbage out". A mathematical model logically processes the information with which it has been built; it cannot recognize or correct errors in the definitions or the input information. The model predictions are the result of the assumptions used, hence the extreme importance of caring for the conceptualization phase and the quality of the initial information.

Very often the most important results of this phase are negative: a well-crafted model would serve to discard a particular mechanism as the explanation for experimental observations. After sufficient validation, we will eventually arrive to a mathematical version of the model that can be used to perform experiments in much the same manner as in the real system. A model is considered valid in this respect when the decisions made using the mathematical model are "similar" to those that would have been made by physically experimenting with the real system.

This model version and its computer counterpart allow testing conditions that may be difficult to attain in the laboratory, or that have not yet been examined in actual experiments. Each numerical solution of the model provides a simulation of a real or potential experiment carried out on the Real System. As an example of mathematical simulations which were useful to understand the dynamics of the cell membrane, a biological process elusive under laboratory experiments see Marrink and Tieleman (2013).

In this phase, starting from a first version of the mathematical model we come to an improved, validated version, through a new virtuous cycle (light blue arrows) that sum up to the first one (light pink arrows). Repeated excursion through this research loop can result in further improvements in both the mathematical and the conceptual model that provides an unbiased test of the hypothesis involved in the conceptual model. This type of feedback loops, which are an essential part of the process of developing a model (and indeed of the scientific method), must, however, stop at some point. The validation phase often leads to a situation in which a slight increase in the trust of the model requires a huge effort. In these cases, it is advisable to stop the process at this point.

Model Refinement and Interpretation

Once we have reached a sound mathematical version of the real system we can advance in its interpretation and understanding. At this stage, there is an opportunity to debate and criticize the validity of the consequences and results of the model. The ultimate aim should be to achieve plausible associations between the model and the real system. At this point it should be clear that, if the conceptualization process was successful, the logical conclusions are as valid as rigorous the mathematical techniques employed, given that the model's results are a direct consequence of the hypotheses and concepts defined in the conceptualization phase.

III. Management and Optimization

A model fulfills its objective if it is useful and fruitful for the purpose for which it was developed. The availability of such a model has then additional benefits: it allows informed management of the system and its optimization. In this vein, mathematical modeling can be combined with operations research in order to support bio-scientists in the improvement of bioprocesses with technological or biomedical purposes (Torres and Voit, 2002; Vera and Torres, 2003; Vera et al., 2010). These type of questions can be rationally answered using mathematical modeling in combination with data mining and operations research, that have been shown to be a promising approach in fields such as drug discovery (Vera et al., 2007) and operations research (Vera et al., 2010).

The optimized model, as any candidate model, should be evaluated in terms of its numerical quality in the same terms as presented above, to be a proven suitable representation of a real system (see the Parameter estimation and quality assessment section). And, as usual in these cases (see the parameter estimation and quality assessment section above) these analyses contribute to the refinement of the model through another iterative virtuous cycle (purple arrows) that superimposes to the previous one, leading to a further improved conceptual model.

CONCLUDING REMARKS

Mathematical modeling was made possible as early as the 17th century, but it is with today's techniques that it has become available to natural (and even social) scientists. There is already an ample evidence of the value and usefulness of the modeling approach in solving relevant problems in biosciences (Hübner et al., 2011; Lanza et al., 2012; Visser et al., 2014). However, in order to place modeling at the core of biological research it is necessary for the new generations of bio-scientists to be prepared to be able to build models. Currently, there are two conditions that must be met for this trend to accelerate. First, it is a matter of fact that the ecumenical nature of the training required by the modeling task in biosciences has impaired this desired evolution. The paradigm shift that involves the incorporation of the integrative approach requires shaping and expanding the training base of the new bioscience graduates with elements that include a broad and solid background in mathematics, thermodynamics, and scientific computing, among other new disciplines, in addition to the classic as chemistry, genetics and bioinformatics. Mathematical modeling of bioprocesses also has severe limitations for development and generalization because of the lack of training in math observed in many bioscience postgraduates (Watters and Watters, 2006; Koenig, 2011). It is our view that the best way to overcome this flaw is through the inclusion of two elements that are, at least not well developed in the curricula of the biosciences graduates, if not absent. One is the appropriate, and properly adapted mathematical contents, which could deal with the normally underdeveloped mathematical

thinking of the students. There is some discussion as to what contents and to what extent the biosciences students should be exposed to (Voit and Kemp, 2009). But what seems unavoidable is the fact that the biological scientist of the XXI century should be fluent not only in mathematics (in statistics and also in other mathematical concepts such as ordinary differential equations) but also in modeling techniques. Fortunately, there is an increasing awareness in this regard and some material is already available to fill this gap (Voit, 2012; Torres, 2013).

The understanding of the system through the use of the mathematical tools that allow the description and analysis of the complex systems can help to deepen the knowledge of the structure, properties and dynamic behavior of the system. However, the collaboration with experienced mathematicians is required for analyses such as the choice of the proper numerical methods, and the selection of the valid simplifications of complicated models. This is the area where most of the typical modeling projects develop: the fertile interface among established disciplines such as cellular biology, biochemistry, genetics and mathematics, and others. In this task all parties are benefited from valuable insight from the interdisciplinary experience. Modeling implies the definition of the model's objectives, and the curation of the available information. It facilitates not only the finding of previously unsuspected areas of exploration, but the proposition of new questions that were not at all evident from the reductionist approach. The systematic practice of modeling in this context also naturally facilitates the fusion of scientific disciplines; this unifying tension is felt not only among biological specialties (e.g., biochemistry, cell biology, microbiology, and genetics) but also with other (seemingly) distant ones, as operational research, computer science and mathematical analysis.

Most of the modelers are well between two extreme positions. On one side lie the idealistic ones who consider model building as a mental process in which the inductive dimension is not valued. For them the mathematical structure obtained represents reality. Opposed to this is the one with a pragmatic view, for whom the goal is to adjust the model to the actual data but without paying attention to a better understanding of reality. The right position would be that in which the model is adjusted to the data, but reaching an understanding of the observed reality is always the aim. The optimum position of a good modeler is halfway between the most pragmatic and utilitarian view of an engineer and the more general outlook of the philosopher.

Finally, it should be noted that although the most common approach in the current biological research is the study of the design of living organisms by observing examples available in nature, there is an inductive, subsequent task that should not be forgotten. We refer to the derivation of general principles from these examples. Efforts are being carried out to gain insight into what is possible in biological design (Savageau, 1976; Alon, 2006; Salvado et al., 2011; Wolkenhauer and Green, 2013) that may lead to practical techniques for generating designs for biological systems intended to carry out particular tasks.

AUTHOR CONTRIBUTIONS

ND has contributed to the conception and design of the work and the analysis and interpretation of the relevant information and the drafting and revision of it's content. Also gave the final approval of the version to be published.

GS has contributed to the conception and design of the work and the analysis and interpretation of the relevant information and the drafting and revision of it's content. Also gave the final approval of the version to be published.

FUNDING

This work was funded by research grants from MINECO, Project BIO2014-54411-C2-2-R and the IMBRAIN project, REF. FP7-REGPOT-2012-CT2012-31637-IMBRAIN.

ACKNOWLEDGMENT

The authors acknowledge discussions with Dr. Daniel Guebel and Dr. Catalina Feledi for her valuable collaboration.

REFERENCES

Allender, S., Brynle, O., Kuhlberg, J., Lowe, J., Nagorcka-Smith, P., Whelan, J., et al. (2015). Community based systems diagram of obesity causes. *PLoS ONE* 10:e0129683. doi: 10.1371/journal.pone.0129683

Alon, U. (2006). *An Introduction to Systems Biology: Design Principles of Biological Circuits*. London: Chapman and Hall Publisher.

Ashyraliyev, M., Fomekong-Nanfack, Y., Kaandorp, J. A., and Blom, J. G. (2008). Systems biology: parameter estimation for biochemical model. *FEBS J.* 276, 886–902. doi: 10.1111/j.1742-4658.2008.06844.x

Banga, J. R. (2008). Optimization in computational systems biology. *BMC Syst. Biol.* 2:4. doi: 10.1186/1752-0509-2-47

Bedau, M. A. (1999). "Can unrealistic computer models illuminate theoretical biology?," in *Proceedings of the 1999 Genetic and Evolutionary Computation Conference Workshop*, ed. A. Wu (Orlando, FL: GECC), 20–23.

Brauer, F., and Castillo-Chavez, C. (2010). *Mathematical Models in Population Biology and Epidemiology*. New York, NY: Springer.

Cheong, R., Hoffmann, H., and Levchenko, A. (2008). Understanding NF-κB signaling via mathematical modelling. *Mol. Syst. Biol.* 4, 1–11. doi: 10.1038/msb.2008.30

ElKalaawy, N., and Wassal, A. (2015). Methodologies for the modeling and simulation of biochemical networks, illustrated for signal transduction pathways: a primer. *BioSystems* 129, 1–18. doi: 10.1016/j.biosystems.2015.01.008

Gunawardena, J. (2011). Some lessons about models from michaelis and menten. *MBoC Perspect.* 23, 517–519. doi: 10.1091/mbc.E11-07-0643

Hodkin, A. L., and Huxley, A. F. (1952). A quantitative description of membrane current and its application to conduction and excitation in nerve. *J. Physiol.* 117, 500–544. doi: 10.1113/jphysiol.1952.sp004764

Hsiung, W., Feng, W., Wang, S., and Chang, M. S. (2008). Dynamic sensitivity analysis of biological systems. *BMC Bioinformatics* 9:S17. doi: 10.1186/1471-2105-9-S12-S17

Hübner, K., Sahle, S., and Kummer, U. (2011). Applications and trends in systems biology in biochemistry. *FEBS J.* 278, 2767–2857. doi: 10.1111/j.1742-4658.2011.08217.x

Janes, K. A., and Yaffe, M. B. (2006). Data-driven modelling of signal-transduction networks. *Nat. Rev. Mol. Cell Biol.* 7, 820–828. doi: 10.1038/nrm2041

Koenig, J. (2011). A Survey of the Mathematics Landscape within Bioscience Undergraduate and Postgraduate UK Higher Education. UK Centre for Bioscience, Higher Education Academy.

Krishna, S., Jensen, M. H., and Sneppen, K. (2006). Minimal model of spiky oscillations in NF-κB signalling. *Proc. Natl. Acad. Sci. U.S.A.* 103, 10840–10845. doi: 10.1073/pnas.0604085103

Kuhn, T. S. (1962). *The Structure of Scientific Revolutions*. Chicago: University of Chicago Press.

Kuhn, T. S. (1965). Logic of discovery or psychology of research. *Crit. Growth Knowl.* 1970, 1–23.

Lakatos, I. (1970). Falsification and the methodology of scientific research programs. *Crit. Growth Knowl.* 1970, 91–95.

Lanza, A. M., Crook, N. C., and Alper, H. S. (2012). Innovation at the intersection of synthetic and systems biology. *Curr. Opin. Biotechnol.* 23, 712–717. doi: 10.1016/j.copbio.2011.12.026

Lotka, A. L. (1920). Analytical note on certain rhythmic relations in organic systems. *Proc. Natl. Acad. Sci. U.S.A.* 6, 410–415. doi: 10.1073/pnas.6.7.410

MacDonald, G., Cuellar, C. B., and Foll, C. V. (1968). The dynamics of malaria. *Bull. World Health Organ.* 38, 743–755.

Marrink, S. J., and Tieleman, D. P. (2013). Perspective on the Martini model. *Chem. Soc. Rev.* 2013:6801. doi: 10.1039/c3cs60093a

Medio, A. (2006). *Mathematical Models in Economy: Mathematical Models*, Vol. 3. Paris: Encyclopedia of Life Support Systems, 1–3.

Michaelis, L., and Menten, M. L. (1913). Die Kinetik der Invertinwirkung. *Biochem. Z.* 49, 333–369.

Minegishi, S., and Thiel, D. (2000). System dynamics modelling and simulation of a particular food supply chain. *Simul. Pract. Theory* 8, 321–339. doi: 10.1016/S0928-4869(00)00026-4

Monod, J., Wyman, J., and Changeux, J. (1965). On the nature of allosteric transitions: a plausible model. *J. Mol. Biol.* 12, 88–118. doi: 10.1016/S0022-2836(65)80285-6

Ni, T. C., and Savageau, M. A. (1996a). Application of biochemical systems theory to metabolism in human red blood cells. Signal propagation and accuracy of representation. *J. Biol. Chem.* 271, 7927–7941. doi: 10.1074/jbc.271.14.7927

Ni, T. C., and Savageau, M. A. (1996b). Model assessment and refinement using strategies from biochemical systems theory: application to metabolism in human red blood cells. *J. Theor. Biol.* 179, 329–368. doi: 10.1006/jtbi.1996.0072

Okamoto, M., and Savageau, M. (1984). Integrated function of a kinetic proofreading mechanism: steady-state analysis testing internal consistency of data obtained in vivo and in vitro and predicting parameter values. *Biochemistry* 23, 1701–1709. doi: 10.1021/bi00303a019

Okamoto, M., and Savageau, M. (1986). Integrated function of a kinetic proofreading mechanisms: double-stage proofreading by isoleucyl-tRNA synthetase. *Biochemistry* 25, 1969–1975. doi: 10.1021/bi00356a020

Park, L. J., Park, C. H., Park, C., and Lee, T. (1997). Application of genetic algorithms to parameter estimation of bioprocesses. *Med. Biol. Eng. Comput.* 35, 47–49. doi: 10.1007/BF02510391

Polisety, P. K., and Voit, E. O. (2006). Identification of metabolic system parameters using global optimization methods. *Theor. Biol. Med. Modell.* 3:4. doi: 10.1186/1742-4682-3-4

Popper, K. (1935). *The Logic of Scientific Discovery*. Vienna: Verlag von Julius Springer.

Prigogine, I. (1961). *Introduction to Thermodynamics of Irreversible Processes*. New York, NY: Interscience Publisher.

Ross, R. (1915). Some a priori pathometric equations. *Br. Med. J.* 1, 546–547. doi: 10.1136/bmj.1.2830.546

Salvado, B., Karathia, H., Chimenos, A. U., Vilaprinyo, E., Omholt, S., Sorribas, A., et al. (2011). Methods for and results from the study of design principles in molecular systems. *Math. Biosci.* 231, 3–18. doi: 10.1016/j.mbs.2011.02.005

Santos, G., and Torres, N. V. (2013). New Targets for Drug Discovery against Malaria. *PLoS ONE* 8:e59968. doi: 10.1371/journal.pone.0059968

Savageau, M. A. (1971). Parameter sensitivity as a criterion for evaluating and comparing the performance of biochemical systems. *Nature* 229, 542–544. doi: 10.1038/229542a0

Savageau, M. A. (1976). *Biochemical Systems Analysis: A Study of Function and Design in Molecular Biology*. Boston, MA: Addison-Wesley.

Schank, J. C. (2008). The development of locomotor kinematics in neonatal rats: an agent-based modelling analysis in group and individual contexts. *J. Theor. Biol.* 254, 826–842. doi: 10.1016/j.jtbi.2008.07.024

Segre, D., Vitkup, D., and Church, G. M. (2002). Analysis of optimality in natural and perturbed metabolic networks. *Proc. Natl. Acad. Sci. U.S.A.* 99, 15112–15117. doi: 10.1073/pnas.232349399

Torres, N. V. (2013). Introducing systems biology to bioscience students through mathematical modelling. a practical module. *Biosci. Educ.* 21, 54–63. doi: 10.11120/beej.2013.00012

Torres, N. V., and Voit, E. O. (2002). *Pathway Analysis and Optimization in Metabolic Engineering*. Cambridge: Cambridge University Press.

van Riel, N. A. W. (2006). Dynamic modelling and analysis of biochemical networks: mechanism-based models and model-based experiments. *Brief. Bioinform.* 7, 364–374. doi: 10.1093/bib/bbl040

Vera, J., Bachmann, J., Pfeifer, A. C., Becker, V., Hormiga, J. A., and Torres Darias, N. V. (2008). A systems biology approach to analyse amplification in the JAK2-STAT5 signalling pathway. *BMC Syst. Biol.* 2:38. doi: 10.1186/1752-0509-2-38

Vera, J., Curto, R., Cascante, M., and Torres, N. V. (2007). Detection of potential enzyme targets by metabolic modelling and optimization. *Appl. Simple Enzymopathy Bioinform.* 23, 2281–2289. doi: 10.1093/bioinformatics/btm326

Vera, J., González-Alcón, C., Marín-Sanguino, A., and Torres, N. V. (2010). Optimization of biochemical systems through mathematical programming: methods and applications. *Comput. Operat. Res.* 37, 1427–1438. doi: 10.1016/j.cor.2009.02.021

Vera, J., and Torres, N. V. (2003). MetMAP: an integrated MatlabTM package for analysis and optimization of metabolic systems. *In Silico Biol.* 4:10. doi: 10.1016/j.mechrescom.2011.03.011

Visser, S. A. G., Alwis, D. P., Kerbusch, T., Stone, J. A., and Allerheiligen, S. R. B. (2014). Implementation of quantitative and systems pharmacology in large pharma. *CPT Pharm. Syst. Pharmacol.* 3:e142. doi: 10.1038/psp.2014.40

Voit, E. (1992). Optimization in integrated biochemical systems. *Biotechnol. Bioeng.* 40, 572–582. doi: 10.1002/bit.260400504

Voit, E. O. (2000). *Computational Analysis of Biochemical Systems. A Practical Guide for Biochemists, and Molecular Biologist*. Cambridge: Cambridge University Press.

Voit, E. O. (2012). *A First Course in Systems Biology*. New York, NY: Garland Science.

Voit, E. O., and Kemp, M. L. (2009). So, you want to be a systems biologist? Determinants for creating graduate curricula in systems biology. *IET Syst. Biol.* 5, 70–79. doi: 10.1049/iet-syb.2009.0071

Volterra, V. (1926). Variazioni e Fluttuazioni del Numero d'Individui in Specie Animali Conventi. *Mem. Acad. Lincei Roma.* 2, 31–113.

Watters, D. J., and Watters, J. J. (2006). Student understandind of pH. "I Don't know what the log actually is, I only know where the button is on my calculator". *Biochem. Mol. Biol. Educ.* 34, 278–284. doi: 10.1002/bmb.2006.494034042628

Weidlich, W. (2003). Sociodynamics-a systematic approach to mathematical modelling in the social sciences. *Chaos Solitons Fract.* 18, 431–437. doi: 10.1142/S0219477503001294

Wimsatt, W. C. (1987). "Re-Engineering philosophy for limited beings," in *Neutral Models in Biology*, eds M. H. Nitecki and A. Hoffman (New York, NY: Oxford University Press), 23–55.

Wolkenhauer, O., and Green, S. (2013). The search for organizing principles as a cure against reductionism in systems medicine. *FEBS J.* 280, 5938–5948. doi: 10.1111/febs.12311

Wu, W. H., Wang, F. S., and Chang, M. S. (2008). Dynamic sensitivity analysis of biological systems. *BMC Bioinform.* 9:S17. doi: 10.1186/1471-2105-9-S12-S17

Conflict of Interest Statement: The authors declare that the research was conducted in the absence of any commercial or financial relationships that could be construed as a potential conflict of interest.

The reviewer Ester Vilaprinyo and handling Editor Rui Alves declare that despite their previous collaborations the review process was conducted objectively.

6. Review of Models in Malaria - *CAB Reviews*

DOI: 10.1079/PAVSNNR20149025

Intra-host mathematical models of malaria

Guido Santos[1,2] **and Néstor V. Torres**[1,2]*

Address: [1] Mathematical Modeling and Systems Biology Group, Department of Biochemistry, Microbiology, Cellular Biology and Genetics, University of La Laguna, La Laguna 38071, Spain. [2] Instituto de Tecnología Biomédica, CIBICAN, University of La Laguna, La Laguna 38071, Spain.

***Correspondence:** Néstor V. Torres. Email: ntorres@ull.edu.es

Received: 7 June 2014
Accepted: 9 July 2014

doi: 10.1079/PAVSNNR20149025

The electronic version of this article is the definitive one. It is located here: http://www.cabi.org/cabreviews

Abstract

Mathematical modelling of intra-host malaria is a relatively recent topic. Although the first mathematical model related to malaria was proposed by Sir Ronald Ross in 1915, the first attempt to model the parasite–host interactions was as recent as 1989. Since then, a moderate but steadily growing number of articles dealing with this topic have been published, including a couple of reviews. In this review, we aim to sum up the knowledge that this particular mathematical modelling approach has provided with respect to the role played by *Plasmodium* in infection mechanisms.

Keywords: Malaria, mathematical modeling, intra-host models, antigenic variants, species competition, erythropoiesis, drug therapy

Introduction

Malaria is one of the most prevalent infectious diseases worldwide, with about 500 million people affected annually and almost 1 million deaths per year [1]. There are five parasite species of malaria affecting humans, *Plasmodium falciparum* being the most harmful as it can evolve into the almost lethal cerebral malaria. A higher prevalence is seen in the continent of Africa while in some regions of South East Asia, strains of the parasite resistant to current drug therapies (artemisinin-combined therapies) are emerging [2]. Furthermore, there is no effective vaccine. Since the discovery of the infectious agent of malaria at the beginning of the twentieth century by Sir Ronald Ross, a lot of work has been done aiming to understand the infection mechanism of *Plasmodium* with the ultimate goal being control and eventually eradication of the disease.

The malaria life cycle is complex, with many stages taking place inside the human host. When the mosquito bites, it introduces parasites in the host in the sporozoite stage. They migrate to the liver where they reproduce asexually for 2 weeks. Then, they leave the liver having entered another stage of the parasite life cycle, the merozoite, which can invade the blood's erythrocytes. Merozoites asexually divide inside the red blood cells, producing about 16 new merozoites per erythrocyte, which are then released into the blood stream after breaking the erythrocyte. This merozoite division process is itself a complex one, where the merozoite evolves through different stages. The most characteristic of them is the ring stage, in which the merozoite adopts an erythrocyte shape. Within the red blood cells, some of the merozoites differentiate to a sexual stage, the gametocyte. The gametocyte remains in the human host's red blood cells. Eventually, another mosquito would take them, thus closing the parasite life cycle after fecundation in the gut of the mosquito. From the above, it can be seen that while the merozoites are responsible for the severity of the disease, the gametocytes parasite phase stage leads to the transmission of the disease. One important feature of the dynamics of the parasitaemia is the optimal very good synchronization of the merozoites, which lets to oscillations in the parasitaemia. These oscillations lead to recurrent fevers, one of the characteristic symptoms of malaria.

Mathematical modelling

Mathematical modelling is becoming one of the most relevant methodologies to design rational therapeutic

strategies in biomedical problems. Its increasing prevalence in this field comes from the fact that this approach allows the integration of the interactions between the components of systems as complex as diseases in quantitative frameworks. It has also the advantage that it can benefit from the amount of information already available in literature and data bases and that, since *in silico* testing bench is cheaper and easier to control than animal and *in vitro* models, it facilitates the rational explorations of new therapeutic approaches.

Interestingly enough, Sir Ronald Ross not only discovered the infectious agent of malaria but he was also the first one to carry out a mathematical analysis of the epidemiology of malaria [3]. Although since that seminal paper many other epidemiological models have been presented [4], the truly first mathematical model of the intra-host mechanism of infection is dated 21 years later [5]. This contribution signals the beginning of the use of mathematical modelling in this field, and it was in 1999 when the first review on this topic was published [6]. The most recent reported reviews were published in 2008 [7, 8].

In this work, taking reviews in the field as the starting point, we present an up-to-date panorama of the developments in this area and an evaluation of the knowledge that the mathematical modelling approach has been able to provide on parasite–host interactions and malaria infection mechanisms.

Antecedents and Precursors

Among the previous reviews on the mathematical modelling of intra-host malaria approaches, the most significant are that by Molineaux and Dietz, published in 1999 [5] and, more recently, the works by Mideo and Day and published in 2008 [9].

In the paper by Molineaux and Dietz, the authors present the first systematic review of intra-host mathematical models of malaria in a moment when this specific topic was in its early stages. The work is a presentation of the approach and was instrumental in supporting it up to the point that it covered not only malaria models, but also modelling approaches in related diseases like trypanosomiasis. They separate malaria models into three categories. The first one comprises models based on the precursor of malaria intra-host models ([7], p. 5). This first attempt was formulated in ordinary differential equations. A more extended version of the model [10, 11] considers the invasion of uninfected red blood cells by merozoites and simulates the dynamics of uninfected, parasite red blood cells and merozoites, including the immune response. The authors used the model to evaluate the effectiveness of the immune response to the parasite infection and the effect of parasite infection on anaemia. They observed that the antigenic variation may not be the only mechanism responsible for the recrudescence and that in the presence of immunity, two clones of parasite can coexist. Finally, they explore some considerations about the pharmacokinetics and pharmacodynamics of some drugs aiming to optimize the prophylactic and therapeutic drug regimens to reduce the emergence of resistance. Here, we can see how, owing to its very nature, the model approach leads naturally to the design of new therapeutic strategies, all based on the model analysis and thus, leaving behind the classical 'trial and error' methodology.

A second family of modelling approaches is represented by the Kwiatkowski [12, 13] proposal. These are, essentially, discontinuous models of intra-host malaria. They use finite difference equations and the population of parasite erythrocytes is categorized by age group. The main results were the unravelling of some features of the control of parasitaemia by toxic feedback, as experienced in the fever response.

The third kind of model within this group was started by McKenzie and Bossert [10, 11]. Their approach is very similar to that of Anderson *et al.* [7], but the objective was to analyse the gametocytogenesis. They consider the parasite erythrocytes, gametocyte population and immune effectors and they established that the gametocyte production rate is negatively correlated with the asexual parasitaemia.

The second contribution to the subject that we would like to refer to here is that by Mideo and Day ([9], p. 7). These authors review the outcome of 20 years of mathematical modelling on intra-host malaria. They classify the factors affecting the dynamics of the disease in two categories; the resource-mediated and the immune-mediated factors. In another paper, Mideo and Day [9] illustrate how the availability of erythrocytes (resource-mediated factors) controls parasitaemia, while in Dietz [14], it is shown how the immune system leads to the control of the disease (immune-mediated factors).

The main insights obtained from these modelling studies correlate well with the evolution and changing focus of interest in malaria research. In this regard, a first relevant observation raised by these authors refers to the immune system as a target for treatments. They concluded that the immune system is more effective against the parasite erythrocytes than against free merozoites. Also, they observed that the innate immune response controls the primary peak of parasitaemia but not the long-term dynamics. Another relevant finding refers to the clone interactions. They compiled evidence showing that inferior clones could overcome superior ones by arriving first and that the low gametocytaemia then observed can be explained in terms of competition for the same immune response. It was also observed that gametocytogenesis changes during infection. They found that the dynamics and clinical observation between *Plasmodium* species are the result of the varying erythrocyte affinity associated to blood-cell age. Finally, they discredited the idea of the erythropoiesis suppression

during malaria infection, by showing that in fact it increases.

As stated before, one of the immediate outputs coming from these early mathematical modelling exercises is the rational evaluation of the efficacy of diseases interventions. Thus, some of these preliminary approaches in the realm of vaccination strategies concluded that the optimal vaccination programme is strongly host-dependent. Furthermore, nested models, which combine intra-host and epidemiologic mechanisms, lead to the proposal of some mechanistic interventions with effects on the infected population level.

A third line of mathematical model proposals are the type presented by Crooks [8]. This author claims that continuous modelling on intra-host malaria is a bad choice for describing the actual system dynamics. It is argued that, since parasite replication occurs in discrete steps of about 48 h, any continuous growth model is not suitable to adequately reproduce its dynamics. To support this statement, a comparative analysis of the results of three kinds of continuous models that include the asexual multiplication factor (number of merozoites after one cycle of division) and the gametocyte production were considered, and the dynamics of the first peak of parasitaemia compared with those obtained from a discrete model. Of the three type of continuous models, one group is composed by those where only a single equation describing the dynamics of the asexual stage of the parasites is considered; a second one is that of models in which the merozoite dynamics (intra- and extra-erythrocytes) are described. A last group is composed by the models where the parasite population is divided into different age groups.

Group one models showed to provide the most accurate description of the dynamic after a reduction of the asexual rupture rate, while group two models were the best after reducing the invasion rate of erythrocytes by merozoites. But it was the third group that showed the best performance. Since increasing the number of age compartments resembles the discrete situation, the author concluded that any age compartment model is the best-suited, continuous mode strategy.

Intra-host mathematical models about malaria

Antigenic variants of pathogen

More recently, a new sort of intra-host model has been presented where the issue of the mechanism and dynamics of antigenic variants of parasite inside the host have been addressed. The interest in this issue comes from the fact that the evolution of malaria parasites inside the host has accelerated owing to the high variability of the external receptor. And, although it has been established that the antigenic variations might not be the only factor explaining the recrudescence [15], it is, however, clear that it is a mechanism that plays a significant role.

Recker *et al.* in 2004 [16] presented the first model for antigenic variation of parasite and its relationship with the immune response. This work was, in some sense, the precursor of a line of developments presented in a series of papers [17–20, 24, 25] that discuss and extend some various mathematical features of that model. In particular, Blyuss and Gupta [19] carry out a stability and bifurcations analysis of the antigenic variation in malaria while Mitchell and Carr [20] show how it model is able to describe the observed oscillations in an intra-host model of *Plasmodium falciparum* in terms of the cross-reactive immune response.

In 2005, Dodin and Levoir [17], using a model on differential equations proposed that the high rate of *Plasmodium* evolution can be associated to the low-complexity genome region changes. Furthermore, this model predicted that cross-reactive immune response is a main cause for the recrudescence of the disease. Accordingly, they suggested that the best parasite evolutionary strategy is to change only one antigen.

In 2007, Adda *et al.* [18] published a differential equations model of the host–parasite interaction. They considered the interaction of two strains and concluded that the principle of exclusion operates between them.

Blyuss and Gupta published in 2009 [19] presented a model with multiple epitopes. The subsequent stability analysis showed that when the long-lasting specific immune response does not decay, the system has two parameter domains with different stability. This observation correlates well with the observed divergence on the parasitaemia phase of different parasite variants. But when the specific response does not decay, the system exhibits a large number of fixed points and undergoes the Hopf bifurcation.

Mitchell and Carr, in 2010 [20], following the proposal by Recker *et al.*, 2004 [16] and using a simplified version of its model were able to carry out a linear stability analysis. They concluded that for very small values of the variant-specific decay rate, there is still a possibility for oscillations in parasitaemia not to occur. However, if the cross-reactive immune response is much slower than the variant-specific immune response, then oscillations will occur.

A set of more recent models deal with different issues of the infection with different approaches. This is the case of the work by Blyuss and Kyrychko in 2012 [23]. These authors make use of bifurcation theory on delay differential equations to evaluate the effect of a time delay of the immune response on variants' dynamics. They conclude that enhancing the cross-reactive immune response reduces the critical value of the time delay at the Hopf bifurcation. A new agent-based approach on antigenic variants of *Plasmodium* was presented in 2012 [24] and more recently in 2012 [25] a hybrid, discrete-continuous model, dealing with very same topic was published. This last model represents the infection

duration, the antigenic profile and the immune response and serves to conclude that the pre-existing immunity can both increase or decrease the duration of the infection. What the final effect would be depended on the profile of variants and the strength of immunity.

A reverse approach on differential equations using malaria cohort data dealing with antigenic variations was presented in 2012 [21]. It shows that the observed reduction of asymptomatic parasitaemia in older groups can be attributed to a reduction of the parasite growth at the blood stage because of immunity. In 2013, two models relating to the antigenic variants were published [22, 26]. One of them [22], very much in this line, reaches general conclusions that are applicable to other systems on immune escape. The other one represents an antigenic variation on a discrete immune response delay model. The Hopf bifurcation analysis shows that the disease-free equilibrium could be stable [26]. However, this result proved to be controversial because Blyuss and Kyrychko claimed that these kinds of systems never undergo a Hopf bifurcation for the disease-free steady state [27]. Their model on differential equations about antigenic variations concluded that when variant-specific immunity is higher than cross-reactive immunity, the system develops asynchronous oscillations, this asynchrony being enhanced by even a small delay in immune response.

Species competition

Another important topic of interest in the field of malaria infection is the inter-specific competition between *Plasmodium* species and intra-specific competition between merozoites and gametocytes.

In 2006, Gurarie and McKenzie [28] studied the competition between resistant and sensitive to treatment strains. The differential equations model considers different treatment inoculation frequency, in absence or presence of further inoculation of parasites. The results lead the authors to claim that linear pharmacokinetic models are not adequate to deal with the competition between malaria strains. In the same year, another differential equations model [29] was used to study the competition for red blood cells between *P. falciparum* and *Plasmodium vivax*. The conclusion was that the two-species dynamics differ from that showed by each species individually considered. Thus, while in some cases one species eliminates the other, in other conditions they can coexist. In 2010, a model able to simulate the interaction between HIV and malaria was presented; a common case of co-infection in many countries in Africa [30]. The interest of this study lies in the fact that each infectious agent has the opposite effect on the host: malaria stimulates the immune response, whereas HIV infection suppresses the immunity. The differential equation model showed that the outcomes are strongly dependent on the individual. The relevant conclusion here was that any control strategy in this regard should be evaluated through modelling. In 2011, a model using a Michaelis–Menten–Monod formulation [31] was used to study the interaction between the immune cells, the infected red blood cells and the merozoites. It was concluded that there are two kinds of infection equilibria, with and without the specific immune response. In 2014, an age-structured model [32] was presented where the regular oscillations synchronization between parasites was observed. The Hopf bifurcation analysis showed that the regular oscillations are attained as the growth rate increases.

Tewa *et al.* [33], in a differential equation model, found that the immune response increases as the disease persists, being more effective against parasite red blood cells than against free merozoites. In 2013, Xiao and Zou [34] presented a differential equation model to study the coexistence of two species. They presented different findings from those in [29], but concluded that it is possible for different species to coexist only in a region, not in an individual. In the same vein, an age-structured model, presented in terms of a partial differential equation dealing with the multi-strain interactions [35] was presented. In this work, the principle of exclusion where only the strongest variant survives was established. Finally, in 2014, a work by Santhanam *et al.* [36] analysed the competition between the virulent and a non-virulent strains in a time-discrete, Bayesian inference model. The conclusion was that the ratio between the background loss rate of merozoites and invasion rate of mature erythrocytes should be clone-specific in order to predict the competence between these strains.

Erythropoiesis

Erythropoiesis is another important issue on malaria that has been studied with modelling techniques. As the infected persons develop severe anaemia, the effects of the malaria parasite on erythropoiesis and the control of erythropoiesis become critical.

A compartmentalized differential equation model dealing with this matter was published in 2008 [37]. The authors considered the different stages of erythrocytes to evaluate the effect of dyserythropoiesis on parasitaemia. It was seen that dyserythropoiesis decreases parasitaemia and increases anaemia but in contrast, compensatory erythropoiesis improves anaemia but increases parasitaemia. The model was also used to compare the evading capacity of *P. falciparum* and *P. vivax*. *Plasmodium falciparum* was shown to be better than *P. vivax* in evading immune response. In the same line, Cromer *et al.* [38] presented an adaptation of a mouse model to humans and concluded that increasing erythropoiesis does not alleviate the disease severity, but increases anaemia and parasitaemia. These topics were later addressed in two papers published in 2010. The first one, based on partial differential equations, evaluated the effect of malaria on erythropoiesis [39] and considered the effect of haemozoine on the precursor population. The authors observed that removing the haemozoine helps in recovering healthy levels of erythropoiesis in later stages. The other work is

a Bayesian differential equation model that is fitted to mice data [40]. It is proposed that the immune response controls the initial parasitaemia peak by acting against the parasite red blood cells and the healthy red blood cells. It is also established that the immune system is acting against healthy red blood cells on anaemia. Finally, in 2013, Ackleh *et al.* [41] proposed a finite-difference equation model in partial differential equations to analyse a malaria scenario with erythropoiesis. As a result, they proposed some model-based treatments for malaria: to decrease the infection rate; to increase the death rate of the parasite and to decrease the number of the parasite released.

Drug therapy

The ultimate aim of any mathematical model on malaria is to be an effective contribution in the search of drugs and strategies to control or to eradicate malaria. In this regard, as the available information grows and more knowledge on the processes involved is generated, modelling approaches become more apt for providing novel, rational and promising strategies, and recent publications support this view.

In 2008, Chiyaka *et al.* [42], based on a previous model proposal by Anderson *et al.* [7] presented a differential equation model to analyse the effect of a therapy against malaria. They concluded that any drug action based on inhibiting parasite production is better than those based on inhibiting merozoite invasion of red blood cells. In 2010, Saralamba *et al.* [43] presented a finite difference equations model analysing the resistance against artemisinin. The main finding was that the increase in resistance occurs in the ring stage of the parasite. A partial differential equations model published in 2011 by Thibodeaux and Schlittenhardt [44] proposed an optimal treatment for malaria infection consisting on a periodic drug administration in synchronization with the burst of parasites from the erythrocytes. A stochastic model, based on difference equations [45], was proposed as a testing bench to find treatments to decrease the transmission of the disease. Another optimized artemisinin combined treatment was designed based on a model presented in 2014 [46]. Using this model, a protocol was proposed to eradicate malaria from regions of South East Asia. Finally, in 2013, Santos and Torres [47] presented a differential equations model that was able to identify new targets against malaria. Following a previously presented optimization methodologies [48, 49] these authors were able to identify five targets for minimizing the parasite load; four of them never having been taken into account in drug design. The identified targets included increasing the death rate of the gametocytes, which is already used in current therapies. But also it was found that decreasing the invasion rate of the red blood cells by the merozoites, increasing the transformation of merozoites into gametocytes, decreasing the activation of the immune system by the gametocytes and combining the previously-identified target with decreasing the recycling rate of the red blood cells were also effective in eliminating the disease.

Concluding Remarks

There are already a significant number of mathematical models in the field of intra-host dynamics of malaria infection, although this number is still relatively scarce when compared with the use of this approach in other fields. Since the first model presented in 1989 [5], a great deal of somewhat diverse information on many aspects of the infection process has been integrated in models of different kinds. In these models, where the specific mechanisms are well-known, it is possible to set up precise mechanistic models. However, in many instances, as is particularly the case with the role of the immune response, such a precise mechanistic representation remains to be done. In these circumstances, a plausible strategy is the so-called phenomenological approach. In this approach, although we are explicitly ignoring the exact mechanisms, the simplification so attained facilitates the integration of the available information and thus the proposal of control strategies.

It is our view that the modelling of the processes involved in the intra-host interactions in malaria as well as other related infectious diseases is already contributing to the understanding of these processes. Through the understanding so gained and the further integration of the new information in new model, we will be in a position to find new target processes, drugs and control strategies.

Acknowledgements

The authors would like to thank Dr Carlos González Alcón and Nakens Núñez Martín for helpful observations during the seminars. This work was funded by research grants from the Spanish MICINN, Ref. no. BIO2011-29233-C02-02 and the Agencia Canaria de Investigación, Innovación y Sociedad de la Información, Ref. no. PIL2071001.

References

1. World Health Organization. World Malaria Report; 2012. ISBN: 978 92 4 156453 3. Available from: URL: http://www.who.int/malaria/publications/world_malaria_report_2012/report/en/
2. Parija SC. Drug resistance in malaria. Indian Journal of Medical Microbiology 2011;29:243–8.
3. Ross R. Some *a priori* pathometric equations. British Medical Journal 1915;1:546–7.
4. Macdonald G. The dynamics of malaria. Bulletin of World Health Organization 1968;38:743–55.
5. Molineaux L, Dietz K. Review of intra-host models of malaria. Parassitologia 1999;41:221–31.

6. Mideo N. Modeling malaria pathogenesis. Cellular Microbiology 2008;10:1947–55.
7. Anderson RM, May RM, Gupta S. Non-linear phenomena in host-parasite interactions. Parasitology 1989;99:S59–79.
8. Crooks L. Problems with continuous-time malaria models in describing gametocytogenesis. Parasitology 2008;135:881–96.
9. Mideo NM, Day T. On the evolution of reproductive restraint in malaria. Proceedings – Royal Society. Biological Sciences 2008;275:1217–24.
10. McKenzie FEM, Bossert W. The dynamics of Plasmodium falciparum Blood-stage infection. Journal of Theoretical Biology 1997;188:127–40.
11. McKenzie F. A target for intervention in plasmodium falciparum infections. American Journal of Tropical Medicine and Hygiene 1998;58:763–7.
12. Kwiatkowski D. Periodic and chaotic host-parasite interactions in human malaria. Proceedings of the National Academy of Sciences of the United States of America 1991;88:5111–3.
13. Gravenor M. An analysis of the temperature effects of fever on the intra-host population dynamics of plasmodium falciparum. Parasitology 1998;117:97–105.
14. Dietz K. Mathematical model of the first wave of plasmodium falciparum asexual parasitemia in non-immune and vaccinated individuals. American Journal of Tropical Medicine and Hygiene 2006;75:46–55.
15. Hetzel C, Anderson RM. The within-host dynamics of bloodstage malaria: theoretical and experimental studies. Parasitology 1996;113:25–38.
16. Recker M, Nee S, Bull P, Kinyanjui S, Marsh K, Newbold C, *et al.* Transient cross-reactive immune responses can orchestrate antigenic variation in malaria. Nature 2004;429:555–8.
17. Dodin GD, Levoir P. Replication slippage and the dynamics of the immune response in malaria: a formal model for immunity. Parasitology 2005;131:727–35.
18. Adda P, Dimi JL, Iggidr A, Kamgang JC, Sallet G, Tewa JJ. General models of host-parasite systems. Global analysis. Discrete and Continuous Dynamical Systems-Series B 2007;8:1–17.
19. Blyuss KB, Gupta S. Stability and bifurcations in a model of antigenic variation in malaria. Journal of Mathematical Biology 2009;58:923–37.
20. Mitchell JL, Carr TW. Oscillations in an intra-host model of *Plasmodium falciparum* malaria due to cross-reactive immune response. Bulletin of Mathematical Biology 2010;72:590–610.
21. Pinkevych M, Petravic J, Chelimo K, Kazura J, Moormann A, Davenport M. The dynamics of naturally acquired immunity to plasmodium falciparum infection. PLoS Computational Biology 2012;8:e1002729.
22. Blyuss K. The effects of symmetry on the dynamics of antigenic variation. Journal of Mathematical Biology 2013;66:115–37.
23. Blyuss KB, Kyrychko Y. Symmetry breaking in a model of antigenic variation with immune delay. Bulletin of Mathematical Biology 2012;74:2488–509.
24. Gurarie DG, Karl S, Zimmerman P, King C, Davis T, Edward R. Mathematical modeling of malaria infection with innate and adaptive immunity in individuals and agent-based communities. PLoS ONE 2012;7:e34040.
25. Eckhoff PE. *P. falciparum* infection durations and infectiousness are shaped by antigenic variation and innate and adaptive host immunity in a mathematical model. PLoS ONE 2012;7:e44950.
26. Ncube I. Absolute stability and Hopf bifurcation in a *Plasmodium falciparum* malaria model incorporating discrete immune response delay. Mathematical Biosciences 2013;243:131–5.
27. Blyuss KB, Kyrychko YN. Instability of disease-free equilibrium in a model of malaria with immune delay. Mathematical Biosciences 2014;248:54–6.
28. Gurarie D, McKenzie FE. Dynamics of immune response and drug resistance in malaria infection. Malaria Journal 2006;5.
29. McQueen PG, McKenzie FE. Competition for red blood cells can enhance *Plasmodium vivax* parasitemia in mixed-species malaria infections. American Journal of Tropical Medicine and Hygiene 2006;75:112–25.
30. Xiao DM, Bossert WH. An intra-host mathematical model on interaction between HIV and malaria. Bulletin of Mathematical Biology 2010;72:1892–911.
31. Li Y. The within-host dynamics of malaria infection with immune response. Mathematical Biosciences and Engineering 2011;8:999–1018.
32. Su Y, Ruan SG, Wei JJ. Periodicity and synchronization in blood-stage malaria infection. Journal of Mathematical Biology 2011;63:557–74.
33. Tewa JJ, Fokouop R, Mewoli B, Bowong S. Mathematical analysis of a general class of ordinary differential equations coming from within-hosts models of malaria with immune effectors. Applied Mathematics and Computation 2012;218:7347–61.
34. Xiao YY, Zou XF. Can multiple malaria species co-persist? SIAM Journal of Applied Mathematics 2013;73:351–73.
35. Demasse RD, Ducrot A. An age-structured within-host model for multistrain malaria infections. SIAM Journal of Applied Mathematics 2013;73:572–93.
36. Santhanam J, Råberg L, Read AF, Savill NJ. Immune-mediated competition in rodent malaria is most likely caused by induced changes in innate immune clearance of merozoites (immune-mediated competition in rodent malaria). PLoS Computational Biology 2014;10:e1003416.
37. McQueen PG, McKenzie FE. Host control of malaria infections: constraints on immune and erythropoeitic response kinetics. PLoS Computational Biology 2008;4(8):e1000149.
38. Cromer D, Stark J, Davenport MP. Low red cell production may protect against severe anemia during a malaria infection – insights from modeling. Journal of Theoretical Biology 2009;257:533.
39. Thibodeaux JJ. Modeling erythropoiesis subject to malaria infection. Mathematical Biosciences 2010;225:59–67.
40. Miller MR, Raberg L, Read AF, Savill NJ. Quantitative analysis of immune response and erythropoiesis during rodent malarial infection. PLoS Computational Biology 2010;6(8):e1000946.
41. Ackleh AS, Ma BL, Thibodeaux JJ. A second-order high resolution finite difference scheme for a structured erythropoiesis model subject to malaria infection. Mathematical Biosciences 2013;245:2–11.

42. Chiyaka C, Garira W, Dube S. Modeling immune response and drug therapy in human malaria infection. Computational and Mathematical Methods in Medicine 2008;9:143–63.

43. Saralamba S, Pan-Ngum W, Maude RJ, Lee SJ, Tarning J, Lindegårdh N, *et al*. Intrahost modeling of artemisinin resistance in *Plasmodium falciparum*. Proceedings of the National Academy of Sciences of the United States of America 2011;108:397–402.

44. Thibodeaux JJ, Schlittenhardt TP. Optimal treatment strategies for malaria infection. Bulletin of Mathematical Biology 2011;73:2791–808.

45. Johnston GL, Smith DL, Fidock DA. Malaria's missing number: calculating the human component of R0 by a within-host mechanistic model of *Plasmodium falciparum* infection and transmission. PLoS Computational Biology 2013;9:e1003025.

46. Johnston GL, Gething PW, Hay SI, Smith DL, Fidock DA. Modeling within-host effects of drugs on plasmodium falciparum transmission and prospects for malaria elimination (modeling transmission blocking and malaria elimination). PLoS Computational Biology 2014;10:e1003434.

47. Santos G, Torres NV. New targets for drug discovery against malaria. PLoS ONE 2013;8(3):59968.

48. Länger BM, Pou-Barreto C, González-Alcón C, Valladares B, Wimmer B, Torres NV. Modeling of Leishmaniasis infection dynamics: novel application to the design of effective therapies. BMC Systems Biology 2012;6:1.

49. Vera J, González-Alcón C, Marín-Sanguino A, Torres NV. Optimization of biochemical systems through mathematical programming: methods and applications. Computers & Operations Research 2010;37:1427–38.

7. Malaria - *PLoS one*

DOI: 10.1371/journal.pone.0059968

OPEN ACCESS Freely available online

PLOS ONE

New Targets for Drug Discovery against Malaria

Guido Santos[1], **Néstor V. Torres**[1,2]*

1 Departamento de Bioquímica y Biología Molecular, Universidad de La Laguna, San Cristóbal de La Laguna, Tenerife, Spain, **2** Instituto Universitario de Enfermedades Tropicales y Salud Pública de Canarias, Universidad de La Laguna, San Cristóbal de La Laguna. Tenerife, Spain

Abstract

A mathematical model which predicts the intraerythrocytic stages of *Plasmodium falciparum* infection was developed using data from malaria-infected mice. Variables selected accounted for levels of healthy red blood cells, merozoite (*Plasmodium* asexual phase) infected red blood cells, gametocyte (*Plasmodium* sexual phase) infected red blood cells and a phenomenological variable which accounts for the mean activity of the immune system of the host. The model built was able to reproduce the behavior of three different scenarios of malaria. It predicts the later dynamics of malaria-infected humans well after the first peak of parasitemia, the qualitative response of malaria-infected monkeys to vaccination and the changes observed in malaria-infected mice when they are treated with antimalarial drugs. The mathematical model was used to identify new targets to be focused on drug design. Optimization methodologies were applied to identify five targets for minimizing the parasite load; four of the targets thus identified have never before been taken into account in drug design. The potential targets include: 1) increasing the death rate of the gametocytes, 2) decreasing the invasion rate of the red blood cells by the merozoites, 3) increasing the transformation of merozoites into gametocytes, 4) decreasing the activation of the immune system by the gametocytes, and finally 5) a combination of the previous target with decreasing the recycling rate of the red blood cells. The first target is already used in current therapies, whereas the remainders are proposals for potential new targets. Furthermore, the combined target (the simultaneous decrease of the activation of IS by gRBC and the decrease of the influence of IS on the recycling of hRBC) is interesting, since this combination does not affect the parasite directly. Thus, it is not expected to generate selective pressure on the parasites, which means that it would not produce resistance in *Plasmodium*.

Citation: Santos G, Torres NV (2013) New Targets for Drug Discovery against Malaria. PLoS ONE 8(3): e59968. doi:10.1371/journal.pone.0059968

Editor: Claudio Romero Farias Marinho, Instituto de Ciências Biomédicas/Universidade de São Paulo - USP, Brazil

Received November 6, 2012; **Accepted** February 20, 2013; **Published** March 28, 2013

Funding: This work was co-funded by research grants from Spanish MICINN, Ref. No. BIO2011-29233-C02-02 and ACIISI Project PIL2070901. The funders had no role in study design, data collection and analysis, decision to publish, or preparation of the manuscript.

Competing Interests: Co-author Nestor Torres is a PLOS ONE Editorial Board member. This fact does not alter the authors' adherence to all the PLOS ONE policies on sharing data and materials.

* E-mail: ntorres@ull.edu.es

Introduction

According to the World Health Organization [1], malaria affects more than 500 million people worldwide, killing between 1 and 2.5 million people annually, most of whom are children under the age of five. It is caused by *Plasmodium* genus parasites (*Plasmodium vivax*, *P. ovale*, *P. malariae*, *P. knowlesi* and *P. falciparum*), *P. falciparum* being the most lethal. The parasites multiply inside human erythrocytes, killing the cells in the process, and are transmitted by female *Anopheles* mosquitoes. The area most affected by malaria is sub-Saharan Africa.

There is currently no effective vaccine against malaria. Some promising preliminary results have been seen, but no solution to this issue is expected over the next few years [2]. To make the situation even worse, the efficacy of transmission control by means of insecticide-treated nets and indoor residual spraying is dropping, because resistance to insecticides is increasing among mosquitoes in Africa [3]. Because of that malaria control is becoming totally dependent on pharmacological treatments.

There are several classes of drugs used to treat malaria. All share the feature of targeting the merozoites [4,5], while some target gametocytes as well. These drugs include quinolines, antifolates and artemisinin, administered alone or in combination. Quinolines are thought to affect the polymerization of hemozoin, which is toxic to the parasite. Antifolates inhibit the synthesis of folic acid by blocking the dihydrofolate reductase and dihydropteroate synthetase enzymes of the parasite. Although the mechanism of action of artemisinin is not known, the most accepted one is interference with the plasmodial sarcoplasmic/endoplasmic calcium ATPase [4]. Resistance to all these antimalarial drugs has been widely reported [5], even in the case of what the World Health Organization has identified as the most effective treatments, the artemisinin combined therapies. In particular, some resistance to the artemisinin combined therapies has been detected in South-East Asia. This poses a potentially dangerous and severe scenario, if the resistance spreads to endemic areas in Africa [6,7] since, to our knowledge, no other effective antimalarial treatments are in sight.

This situation can be attributed, at least in part, to the classical, reductionist pharmacological approach to finding new drugs. This approach is mainly based on reducing the disease to a small set of defined targets for which new drugs can be sought. In the case of malaria, it is evident that this approach has shown little success, a trend also observed in other complex diseases [8].

Wells 2010 divides all current drug discovery strategies into two groups: "whole parasite screening" and "rational design approaches" [9]. Whole parasite screening strategies are based on testing compounds *in vitro* and selecting those which affect a *Plasmodium* culture. The rational design approach strategies try to inhibit specific pathways of the parasite. Screening approaches

have the limitation that they are non-directed; there are a huge number of possible compounds to test and the entire screening process is conducted with the parasite isolated from the host system in *in vitro* conditions. Rational design is directed, but it depends on the knowledge of the mechanisms of the parasite [9] and is thus very reductionist in focus. Furthermore, none of these methods can deal with the existing pharmacological targets which only work *in vivo*.

While due credit must be given to these reductionist approaches for their contribution to the development of the drugs currently available, it is not equally clear that this strategy has proven sufficiently effective in providing a number of relevant drug solutions [10].

Accordingly, a third line of approach has been proposed to direct drug discovery [11]. This strategy, known as quantitative and systems pharmacology, aims to understand how drugs influence cellular networks in space and time and determine how they affect human pathophysiology. This approach follows the tenets of systems biology, and is based on the development of mathematical models that incorporate data at several temporal and spatial scales and are able to predict the dynamic behavior of the main variables involved in the parasite infection and the therapeutic effects of drugs. The principles of system biology thus provide the methodological framework and perspective needed for modeling system behavior *in vivo*, establishing the basis for a genuinely rational target identification and drug design. In this context, the defining feature of system biology is the combined use of mathematical and computable models and quantitative experimental data as a means to unravel the network-based (''emergent'') properties which cannot be deduced in any way from the knowledge of their components [12].

Such models, which lead to an educated and informed hypothesis, can then be used to identify the most sensitive processes of the system with a view to reducing the parasitemia (see Länger et al, 2012; [13]). The present work is in line with this approach, and with the current view that in order to identify new and better targets for antimalarial drug-based treatments, a model-based approach is needed [11].

In the present case, a model system constructed in this way will represent *Plasmodium* infection *in vivo*, and thus it is to be expected that well-selected interventions in some of these processes in the real system will lead to a recovery in the patient. The results thus obtained will be correlated and compared with current therapies against malaria.

Results

In order to analyze the dynamics of the infection process by *Plasmodium* and to propose new targets with potential for drug discovery against malaria, an ordinary differential equations mathematical model was developed (see Material and Methods). In the present study, we used the General Mass Action within the Power Law formalism [14]. This formalism has been used as the framework for modeling other infectious diseases [13]. Regarding other diseases, the range of pathologies that have been addressed using the Power Law formalism, either in the GMA or in the S-system version, goes from the analysis of the purine metabolism in human [15,16] to inflammation and preconditioning [17,18], mental disorders [19] and cancer [20].

The model so constructed is a phenomenological one, where some aspects of the physiological processes are lumped together and represented by a single process. The proposed model is focused on a critical phase of the *Plasmodium falciparum* life cycle within the host, namely the processes involved after the release of liver cell merozoites into the bloodstream.

As is well known, once they are in the bloodstream, the merozoites infect red blood cells, which in turn produce further merozoites. Subsequently, sexual forms (gametocytes) are produced which eventually, if taken up by a mosquito, will infect the insect and will continue the parasite life cycle. Figure 1 shows the simplified representation of these processes. The selected variables include the healthy erythrocyte population (hRBC) and the merozoite-parasitized erythrocyte cell density (mRBC). This latter variable represents all red blood cells infected at whatever stage of the asexual cycle of the merozoite. Another variable is the gametocyte-parasitized erythrocytes (gRBC), which represents all red blood cells containing a *Plasmodium* gametocyte. These three variables are all expressed as units per volume of blood (μL). A final variable accounts for the overall activity of the immune system (IS). The IS is a phenomenological variable measuring the mean response of the immune system against *Plasmodium* infection. The mouse IgG1 (immunoglobulin G1) measured in absorbance units is taken to represent the activity status of the immune system.

In the figure, black continuous arrows represent processes actually occurring during this stage of the infection, while blue dashed arrows stand for positive regulatory influences of the variables on different processes. In our model, the different stages of the intraerythrocytic cycle of parasite are represented by (mRBC; merozoites) and (gRBC; gametocytes). The processes represented in the model include the synthesis of hRBC by the host (V1), balanced by a rate that integrates the natural processes leading to erythrocyte decay (V2); the immune system (IS) has an influence on this rate [21]. Healthy erythrocytes are infected by *Plasmodium* merozoites, a process that is stimulated by the growing population of infected erythrocytes (mRBC) (V3) [22]. The transformation of mRBC into gRBC is also considered (V5). This process is assumed to be influenced by the IS (a representative component of the parasite stress in the model; see Material and Methods section), as has been shown [23]. The elimination of the infected red blood cells (mRBC and gRBC) is included (V4 and V6, respectively); this elimination is promoted by the IS. The model integrates all processes related to the activation of the immune components controlling the malaria parasite inside the host through the activation of the variable IS (V7). Finally, the inactivation of the IS is included (V8). In the model, we assume that the process leading to the growth of the free parasite population inside the liver does not affect its dynamics at the intraerythrocytic level.

Model Validation

Figure 2 shows the comparison between the model's fitting and the experimental data. Experimental measures were taken from the bibliography [24,25] and consist of measures from *Plasmodium chabaudi*-infected mice of different malaria-related components (healthy red blood cells, merozoite and gametocyte-infected red blood cells and IgG1). The initial conditions for the variables hRBC and IS, since they should represent the system condition before infection, were taken from the first experimental values in Figure 2. For all validations the values of the parameters were kept fixed.

Before the model is utilized for our intended purposes, it should be diagnosed for internal robustness. Accordingly, we identified and evaluated the stability of the initial and final steady states and carried out the sensitivity analysis (see Figure S1). Moreover, given the dynamic nature of the process, we calculated the dynamic sensitivities that serve to assess how changes in initial values affect the transient responses of a system (see Figure S2). Furthermore,

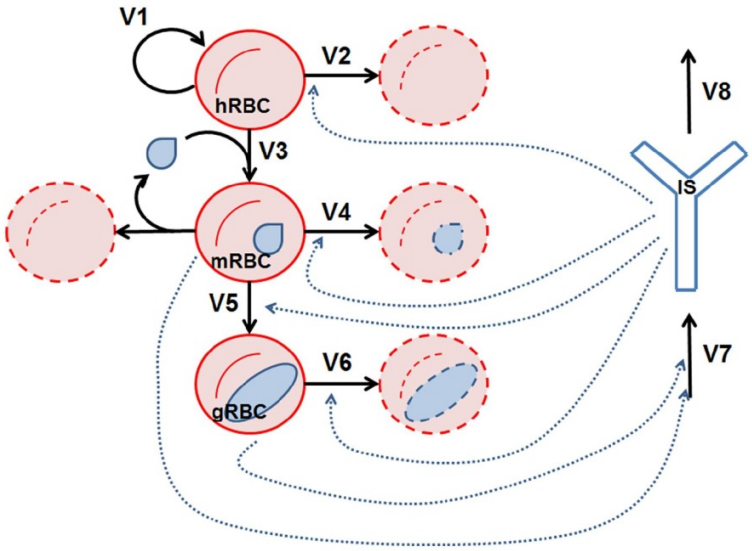

Figure 1. Erythrocyte infection model representation. In the picture, red circles represent the red blood cells, blue drops represent merozoites, blue ovals represent gametocytes and the blue "Y" represents the immune system. The variable acronyms are the healthy red blood cells (hRBC), the merozoite-infected red blood cells (mRBC), the gametocyte-infected red blood cells (gRBC) and the immune system (IS). Black continuous arrows represent processes while blue dashed arrows represent regulatory influences of the variables on processes.
doi:10.1371/journal.pone.0059968.g001

for a model to be reliable and useful, its predictions should be validated against the performance of the actual system in different experimental conditions. For this purpose, we used three different sets of experimental data obtained in diverse experimental settings and conditions. First, we compared the model's predictions with data on the dynamics of *Plasmodium falciparum* parasitemia in human hosts; secondly, experimental time series data of *Plasmodium falciparum* parasitemia in vaccinated and non-vaccinated monkeys

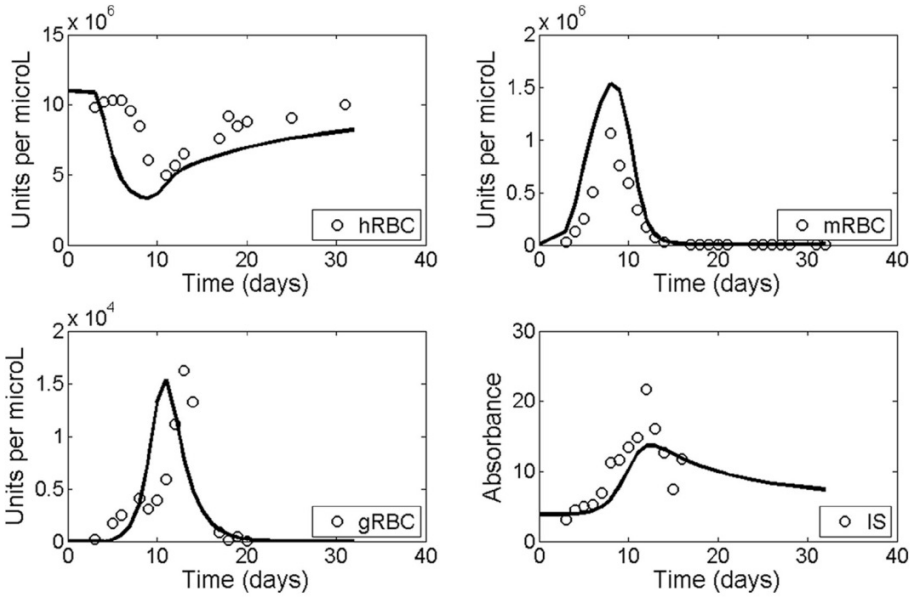

Figure 2. Model fitting. In all panels, continuous lines represent the model's prediction while dots represent the experimental data obtained from *Plasmodium chabaudi* [24,25]. Variable values are normalized.
doi:10.1371/journal.pone.0059968.g002

were evaluated against the model's predictions in correlative *in silico* scenarios; and thirdly, the observed dynamics of *Plasmodium chabaudi* in groups of drug-treated mice were contrasted with the model's expectations. It should be stressed that in all cases, the experimental data used were obtained in different conditions and settings from those used when constructing the model.

Dynamics of Plasmodium falciparum in human host. The first line of model validation was obtained from the comparison of the model's predictions with the experimental data obtained by Diebner et al. 2000 [26]. These authors measured the dynamics of the concentration of *P. falciparum* merozoites and gametocytes in infected, non-treated humans. We compared their results with the model's predictions (see Figure 3). From the observation of Panels A and B in Figure 3, a number of features emerge that merit further comment. The first observation is that the oscillating dynamics of the experimental parasitemia are reproduced by the model. More specifically, it should be noted that, although the experimental system (*P. falciparum* in infected, non-treated humans) differs from the one used to construct the model (*Plasmodium chabaudi* infection in mice), the model's prediction of the merozoite and gametocyte population dynamics correlates well with the experimental measures in terms of both the magnitude of the period and the relative amplitude of the oscillations. Moreover, the model reproduces the later attenuation of the parasitemia. It can be observed, however, that although the first peaks of merozoites and gametocytes are reproduced well by the model, the second peak of merozoites occurs between the gametocyte peaks, which are not the case in the model predictions. Regarding this point, we should stress here that since our model is a phenomenological one, we do not expect to see a quantitative reproduction of the data. On the contrary, we should take into account the fact that, in spite of the fact that the model is based on observations made in mice infected with *P. chabaudi*, it is able to qualitatively reproduce the dynamics observed in a different host (human) infected with a different pathogen (*P. falciparum*). Since the kinetics of the life cycle differs in the new conditions, we consider that the dynamic qualitative pattern reproduction was good enough for our objective.

2. Response to vaccination. Additional evidence of the model's quality comes from the comparison of the model's predictions with experimental time series data obtained in a study carried out in vaccinated and non-vaccinated monkeys (Makobongo et al. [27]). Figure 4 compares the model's predictions with the data on parasitemia dynamics obtained from non-vaccinated and vaccinated monkeys. Panel A shows the changes observed experimentally in parasitemia (merozoites) after vaccination, reflecting a delay in the maximum peak of parasitemia. In Panel B, the vaccinated condition was represented in the model by increasing the initial value of the variable IS, thus mimicking an improved immunological status**.** It can be seen that in spite of the fact that we are using a model based on the observed infection by *P. chabaudi* in CBA to predict the *P. falciparum* parasitemia dynamic in monkeys, the model is still able to reproduce both the general trend observed in the actual data and the specific features of the observed dynamics, such as the delay in the onset of the parasites and the time course of the parasitemia towards zero after 23 days. The difference in the % of parasitemia between Panels A and B can thus be attributed to the different experimental set-ups and to the well-known differences in the life cycle lengths of the parasite in monkeys and mice.

Taken together, these observations, based on different experimental set-ups and host types, lend support to the reliability of the model for its use as a testing bench in the search for effective antimalarial targets.

Model Extension: Effect of Different Modes of Drug Administration

The model presented above can be extended in order to give a better interpretation of how the different modes of administration of a current drug affect the infection dynamics. The case is illustrated by the comparison of the model's predictions with the course observed following certain antimalarial treatments. Chimanuka et al. [28] published the parasitemia time data series obtained following treatment of infected mice with the antimalarial drug β-artemether, which is known to enhance the death rate of the merozoites (mRBC). They studied the time course under two conditions: direct injection of the drug into the bloodstream and also when liposomes were used as a means for slowing drug delivery, which has been shown to yield better results measured as longer elimination half-lives.

Equations 5 in the Material and Methods section shows the model changes made to represent the two drug delivery systems used by Chimanuka et al. [28] (see Figure 5). It is considered that β-artemether concentration linearly eliminates the parasite at the level of mRBC, through a process represented by V_9. It can be argued that β-artemether would also affect V_4. In fact, we explored this mechanism of action, but the best correlation with the experimental data by Chimanuka (data not shown) was obtained instead when a different process (V_9) was assumed. This finding constitutes in itself a model prediction and suggests that the drug acts by eliminating the mRCB through a process different from its natural decay.

The comparison with the model's parasitemia predictions is shown in Figure 6. Panel A shows the results of the simulation of the direct, free drug inoculation into the mouse's bloodstream (right panel) compared with the experimental data (left panel). Panel B shows the simulation corresponding to drug delivery through the inoculation of liposomes carrying the drug into the bloodstream (right panel) compared with the experimental measures (left panel). In both cases the non-treated situation is shown in black. The temporal differences from Figures 6B with respect 6A are due to the different drug inoculation methods used in each case. Since the liposome drug release to the blood stream is slower, the dynamics takes more time.

In this figure it can be seen that the model's predictions of the pattern dynamics of the infection correlate well with all three sets of experimental data. In the non-treated mice, the model reproduces, for the two conditions assayed (panels A and B) the experimentally observed initial peak of parasitemia. Also, the model reproduces the experimental observations of a low and delayed peak of parasitemia when the mice are treated by direct inoculation of the drug (panel A). Finally, the model's prediction in conditions of intra-liposome drug inoculation (panel B) shows, in agreement with the experimental observations, a reduced initial peak of parasitemia followed by another, lower peak. In all cases, the model shows the oscillatory behavior as well as the relative decrease in the amplitude of the oscillations and the temporal delay between each. However, some discrepancies relative to the magnitude of the parasitemia in both panels, and the time scale in the Panel B are also evident. These differences can nevertheless be attributed to the fact that we are using a model based on the observed infection by *P. chabaudi adami* DK, a slow-growing strain [24] compared with the *P. chabaudi chabaudi* strain used for the verification data.

Model-guided Search for New Drug Action Targets

Using this model as a basis, we applied various search routines (see Material and Methods) to identify antimalarial targets for the minimization of parasite load and response time after infection

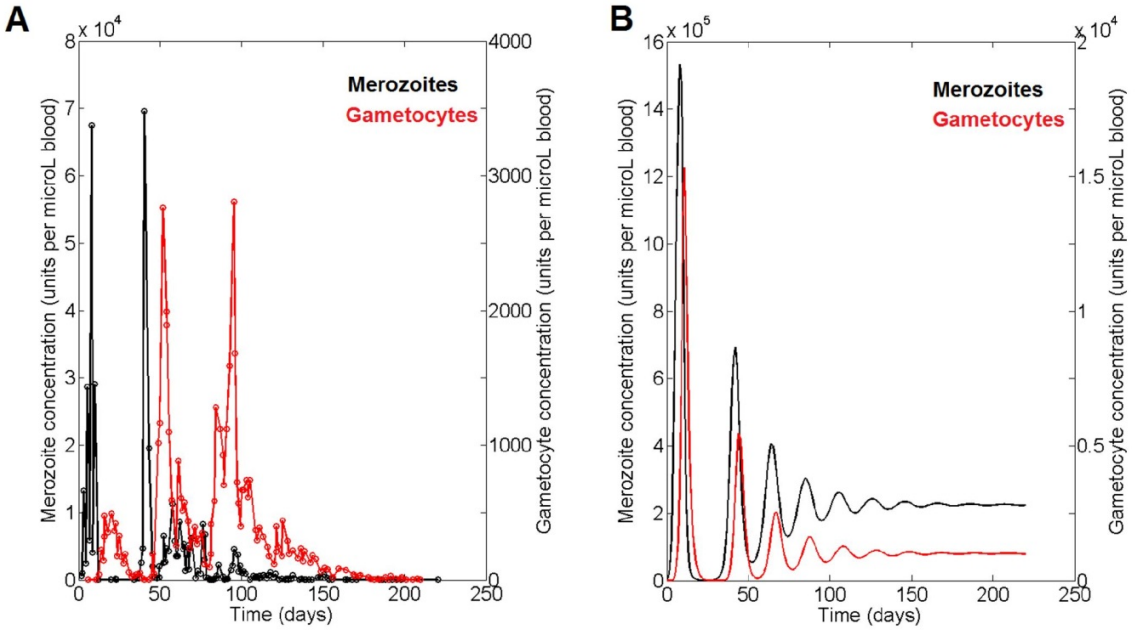

Figure 3. Dynamic prediction. A. Dynamics of the merozoites (black line) and gametocytes (red line) of *P. falciparum* measured in humans as described by Diebner et al. 2000 [26]. **B.** Prediction of the model on the dynamics of the merozoites (mRBC; black line) and gametocytes (gRBC; red line); variable values were normalized.
doi:10.1371/journal.pone.0059968.g003

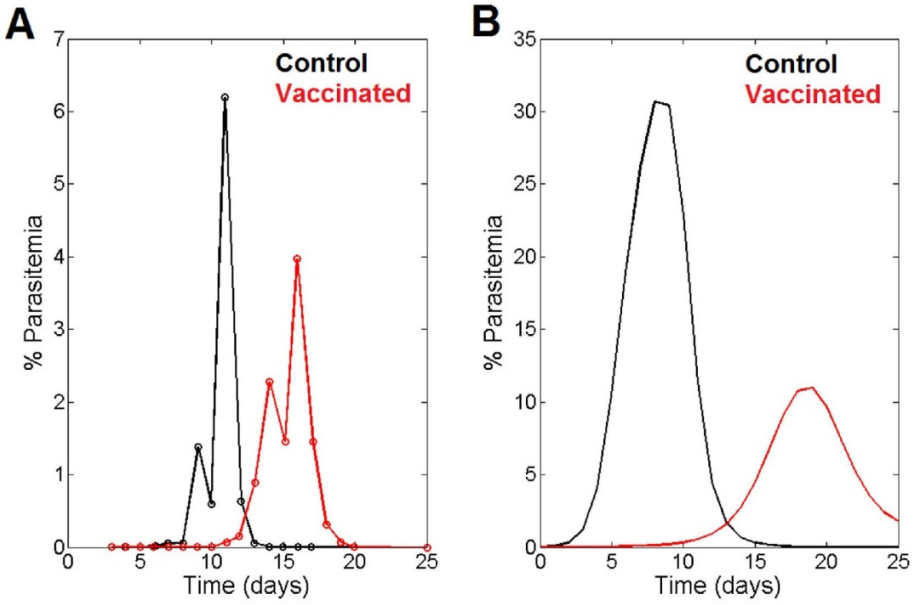

Figure 4. Experimental verification of the response to vaccination. A. Dynamics of the merozoites in non-vaccinated monkeys (black line) and in vaccinated monkeys (red line) of *P. falciparum* as measured by Makobongo et al. 2006 [27]. **B.** Prediction of the model on the effect of vaccination. Black line, control situation; red line, vaccinated condition. The vaccinated condition was represented in the model by increasing the initial value of the variable IS, thus mimicking an improved immunological status.
doi:10.1371/journal.pone.0059968.g004

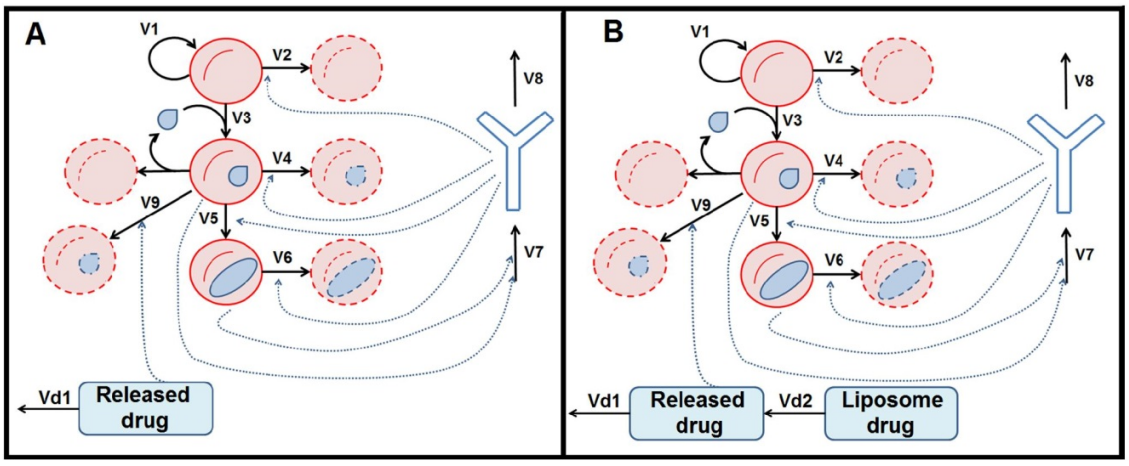

Figure 5. Model adaptation to treatment with antimalarial drug according with Chimanuka et al. [28]**. A.** The antimalarial drug is inoculated directly into the bloodstream. **B.** The drug is inoculated inside liposomes, which delays release into the bloodstream.
doi:10.1371/journal.pone.0059968.g005

[29]. We carried out this search in two phases. We searched for "single-target solutions" first, and then for combinations of "two-target solutions". The former aim at single targets, or processes that after modulation of their rate (either positively or negatively) by any means (e.g. by a drug) will cause the desired effect of reducing the parasite load and/or system response time. The latter target the same effects, but with consideration for the simultaneous modulation of two processes.

The results obtained are summarized in Figure 7. It can be seen that there are four single-target processes (Panel A) and only one combination of two-target processes (Panel B) where modifications through the action of any drug or other agent can achieve a significant reduction in the parasitemia of the host.

In Panel A, we see a first (single) target, which consists of decreasing on the invasion rate of the red blood cells by merozoitos. The invasion of red blood cells involves the participation of a moving junction formed between the erythrocyte and the parasite membranes [30,31]. The predicted effective intervention leading to a parasitemia reduction should be a reduction of this process. The other single targets detected involve the increase of the transformation rate of the merozoites into gametocytes (transformation of mRBC), the increase of the elimination of the gametocytes (death of gRBC) and the reduction of the influence of gametocytes on the synthesis and activation of the immune system (activation of IS by gRBC). In Panel B, we see the combined target predicted by the model, which consists of reducing the influence of gametocytes on the activation of the immune system (activation of IS by gRBC) while at the same time decreasing the elimination of healthy red blood cells by the immune system (recycling of hRBC).

The results of the above interventions are summarized in Figure 8. Figure 8A shows the effects of reducing the invasion of hRBC (dividing by 25 the basal, reference value of γ_3), thus mimicking the action of an antimalarial drug. It can be seen that the host variables hRBC and IS recover quickly and completely to healthy values, while mRBC and gRBC disappear quickly. There is already some experimental evidence of this prediction from the model [32,33]. In 1991, Beuria & Das [32] studied the therapeutic effect of dextran sulfate on the dynamics of parasitemia in mice. Dextran sulfate is a molecule that acts by inhibiting the erythrocyte infection rate of the merozoites without killing the parasites [34]. The authors demonstrated a significant reduction of the parasitemia and better survival rates when infected mice were treated with this chemical. Although dextran sulfate cannot be used to treat human infection due to its high toxicity [32], this result supports the inhibition of the invasion of hRBC as an antimalarial target, strongly suggesting that if another substance could be identified with this effect on erythrocyte infection, but with fewer or no side effects, it could prove to be an effective antimalarial drug. Even more interestingly, Vulliez-Le Normand et al. [33] recently suggested that any therapeutic strategies aimed at inhibiting the invasion mechanism should be effective in treating malaria. These author's findings support the idea that the interruption of the Apical Membrane Antigen 1 association with its receptor, the Rhoptry Neck Protein 2, is a target for the design and development of inhibitors. Their observations are further supported by the observation that the invasion-inhibitory peptide R1 [35,36] blocks the interaction between the Apical Membrane Antigen 1 and the Rhoptry Neck Protein complex in *P. falciparum* [37].

The effect of increasing the death rate of gRBC, V_6 (dividing by three the basal, reference value of γ_6) is shown also in Figure 8 (Panel B). As a result of this intervention, it is observed that the gametocytemia is reduced and that the oscillations disappear, albeit at the expense of a small increase in merozoite load.

Figure 8C shows the result of an intervention on the third single effective target: the decrease of the activation of IS by gRBC (twofold decrease in g_{73}). The aim of this intervention is to impair the stimulus exerted by the gametocytes on the immune system activation. This intervention causes a small decrease in both parasite forms (mRBC, gRBC) and an almost negligible effect on the host response (hRBC and IS).

Figure 8D shows the dynamics observed after an increase of the rate of transformation of the merozoites into gametocytes, V_5. This was simulated through an 80-fold increase in γ_5. What is observed are decays in mRBC and gRBC, and also a significant recovery of hRBC and IS.

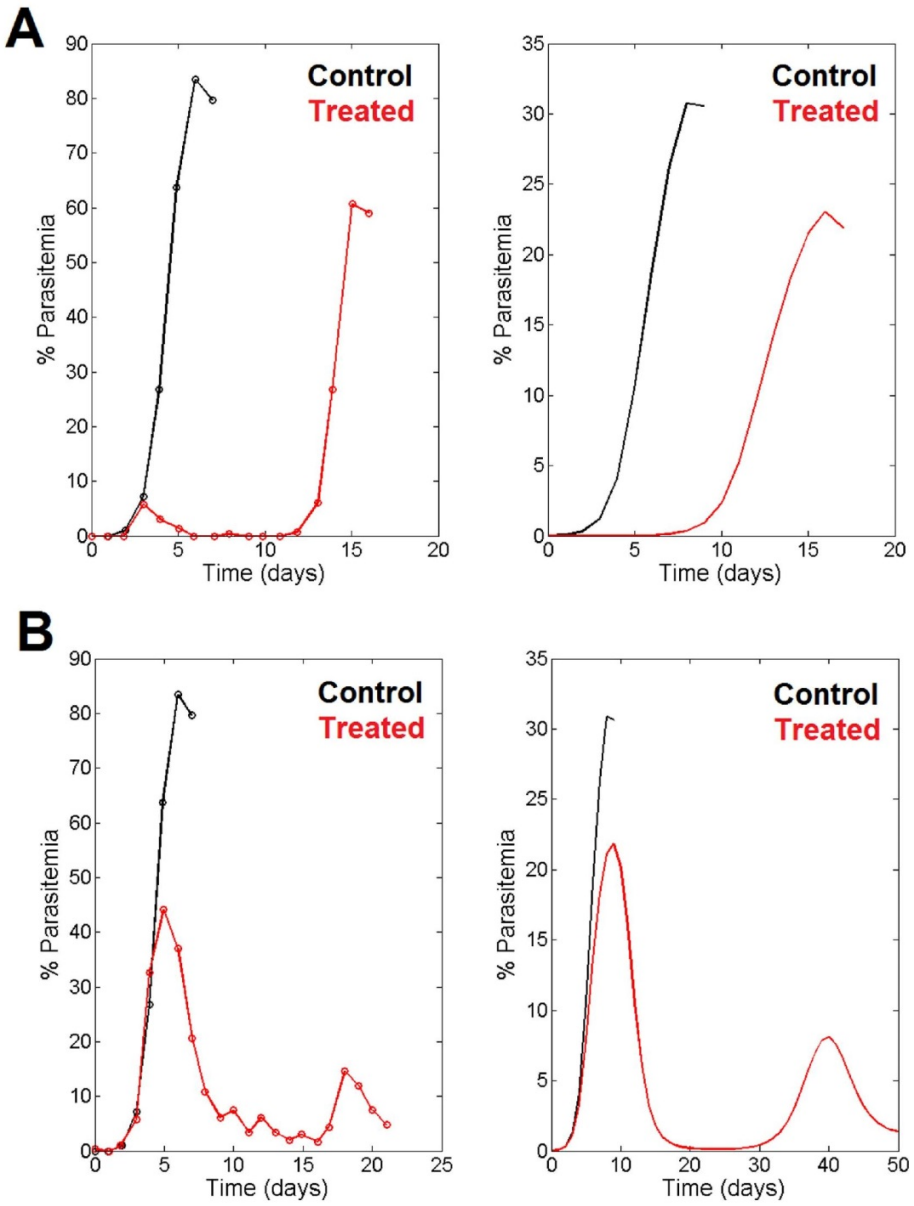

Figure 6. Experimental comparison of the model adaptation to treatment with antimalarial drug. A. When the antimalarial drug is inoculated directly into the bloodstream (Figure 5A), the left panel shows the experimental measure of merozoite parasitemia while the right panel shows the prediction of the merozoite parasitemia. Black line, parasitemia without treatment; red line, parasitemia under drug inoculation. **B.** When the drug is inoculated inside liposomes, the left panel shows the experimental measure of merozoite parasitemia while the right panel shows the prediction of the merozoite parasitemia. Black line, parasitemia without treatment; red line, parasitemia under drug inoculation. Data from Chimanuka et al. [28].
doi:10.1371/journal.pone.0059968.g006

Finally, Figure 8E presents the effects of the only double, simultaneous target intervention found that yielded a general improvement of the infection status. This combination involves the simultaneous decrease of the activation (dividing by two the basal, reference value of g_{73}) of the rate synthesis of IS by gRBC (V_7; the exponential effect of gRBC on IS) and the decrease (dividing by 200 the basal, reference value of g_{24}) of the effect of IS over hRBC (V_2) of the influence of IS on the recycling of hRBC. It is interesting to note that the final output is quantitatively rather similar to that observed with the single target "decreasing

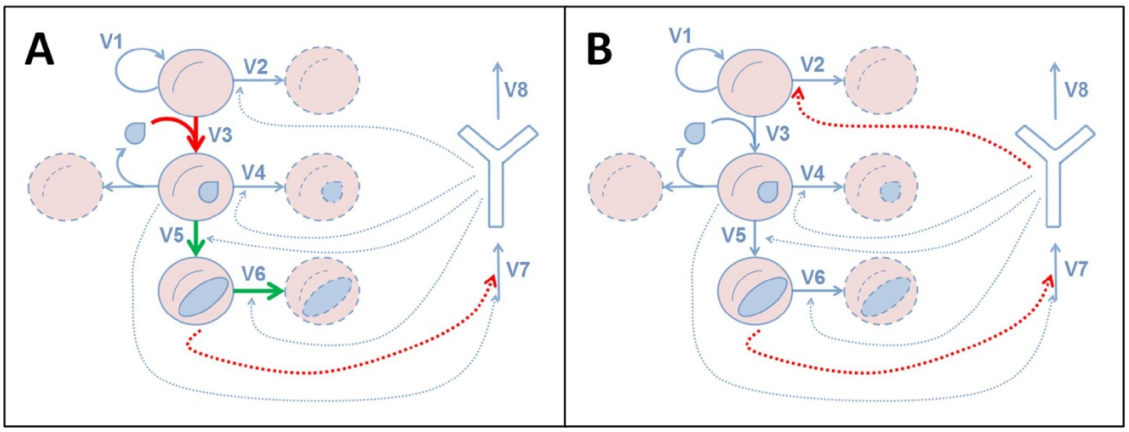

Figure 7. Single and combined targets for antimalarial drugs. A. Single targets (from top to bottom): decreasing invasion of hRBC (thick red arrow); increasing transformation of mRBC (thick green arrow); increasing death of gRBC (thick green arrow) and decreasing activation of IS by gRBC (dashed red arrow). **B.** Combined target: decreasing activation of IS by gRBC combined with decreasing recycling of hRBC (dashed red arrows).
doi:10.1371/journal.pone.0059968.g007

activation of IS by gRBC" (Panel C) but showing different dynamics.

Discussion

The objective of this study was to identify new targets with potential for drug discovery against malaria. Since malaria is a complex disease with plenty of host–parasite interactions, the disease's dynamics and symptoms (the system emergent properties) can only be understood through an integrated view of parasite infection and host responses. By acting on these targets, including those that only work *in vivo*, we aim to reduce the parasitemia of the two species of the parasite inside the host.

The proposed model focuses on the modeling of the underlying processes within the host-parasite dynamics of *Plasmodium* invasion of red blood cells. Its main objective is to allow for the systematic search, by means of an optimization approach**,** for the most interesting targets for drug research. Given the high number of processes involved and the model's inherent complexity, we opted for a phenomenological representation that is simple enough to permit the proposed search but at the same time rich enough to provide valuable insight into suitable targets. Based on the results of this search, we would set up the necessary conditions to find, or help to define, therapeutic strategies, including some which are counter-intuitive. These strategies will not necessarily impede infection but will reduce parasitemia and the risk of severe symptoms as well as diminish the risk of drug resistance and selective pressure for resistant *Plasmodium* strains. The model considered a set of relevant components, processes and interactions. Variables selected for the model were the two phases of the parasite inside the host erythrocytes (mRBC, merozoites, and gRBC, gametocytes), the healthy erythrocytes of the host, hRBC, and the immune activity of the host against the parasite, IS (see Figure 1). All the variables of the model were measured in terms of their concentration inside the bloodstream. The values of the variable IS are given by the concentration of IgG1, which serves as the representative component of the mean immune response against the parasite.

We are aware of the fact that we are extrapolating the *P. chabaudi* model dynamics built from mouse data to the same process with *P. falciparum* in monkeys and humans and that *Plasmodium* life cycle lengths differ between hosts and within the erythrocyte between *Plasmodium* species. But since our approach is phenomenological, we were able to obtain a qualitative verification of the observed general pattern of behavior in monkeys and humans. The approach serves to provide information about the basic mechanism that operates in this type of infection as well as some guidance for new targets for therapeutic drugs.

The proposed model is able to describe the dynamics of the infection by *Plasmodium chabaudi* in mice. In addition, the model's predictions were successfully compared with different experimental scenarios (Figures 3, 4 and 5). Figure 3 shows how the model reproduces the dynamics of the infection in humans after the first peak of parasitemia, predicting the attenuated oscillations and the delay observed between the phases; it also reproduces the final maintenance of the parasite load. The model's results also correlate well with the observed response to the infection of a vaccinated host (Figure 4). The model shows the observed retardation and maximum value of the first peak of parasitemia when the host is vaccinated. Since the model is able to reproduce the disease in a third host, it can be concluded that it has captured the essentials of the host–parasite interactions. A further confirmation of the model's reliability was obtained by comparing its predictions with the experimental measures of merozoite parasitemia in β-artemether treatment of mice infected with *Plasmodium chabaudi* [28] (Figure 5) using two different methods of inoculation of the drug. When β-artemether was injected directly into the bloodstream, the observed delayed and lower peak of parasitemia was predicted by the model (Figure 6A). Also, when the drug was inoculated through liposomes, the observed early, reduced peak of parasitemia followed by a second, lower peak was also forecast by the model (Figure 6B). Thus, the ability of the model to reproduce very different malaria infection scenarios (involving different species of *Plasmodium* as well as distinct hosts and various treatment methods) makes us confident enough to use it as a reliable tool in the search for effective pharmacological targets.

A set of such targets (single or combined) are presented in the Results section (see Figure 7). A first target would consist on decreasing the invasion rate of the erythrocytes by the merozoites; such an intervention would lead to the full recovery of the host (Figure 8A). Decreasing this rate means that free merozoites are

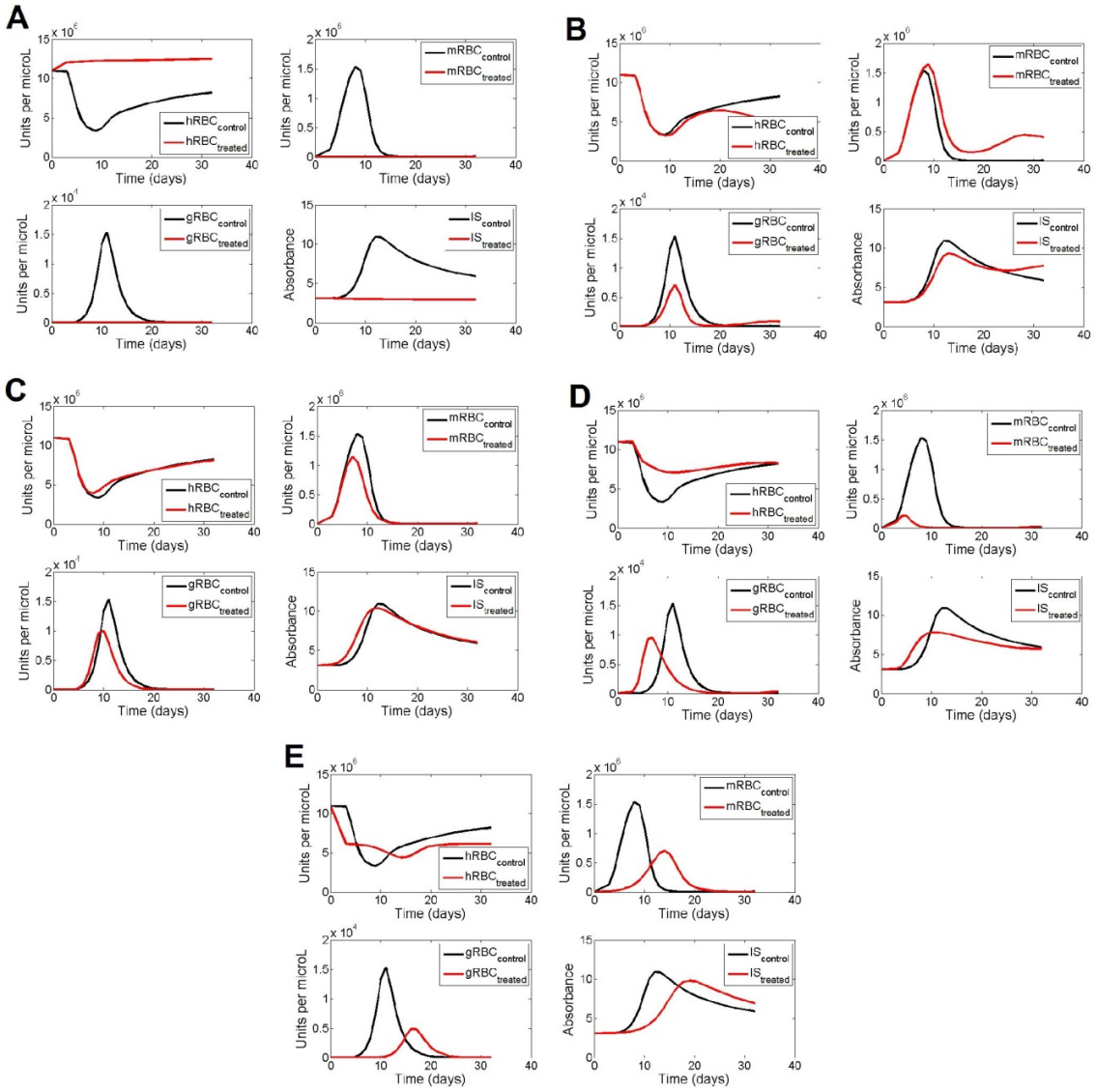

Figure 8. Model-based time course of the system variables after intervention on the selected target rate process. A. After a decrease of V_3 (γ_3, 25 times the initial, reference steady state value). **B.** After an increase of V_6 (γ_6, 3 times). **C.** Decrease of the influence of gRBC on V_7 (g_{73}, 2 times). **D.** Increase of V_5 (γ_5, 80 times). **E.** Simultaneous decrease of the influence of gRBC on V_7 (g_{73}, 2 times) and of the influence of IS on V_2 (g_{24}, 200 times). Continuous lines represent the prediction of the model in control conditions (no intervention on the target rate processes), while red continuous lines represent the prediction of the model after the corresponding interventions.
doi:10.1371/journal.pone.0059968.g008

less effective in invading red blood cells; thus they will be more exposed to the immune system [38]. Although this strategy has already been partially evaluated as a vaccination strategy [2, see also 33], our results suggest that it could also be effective as a pharmacological treatment. In fact, such an approach has been tested through the treatment of infected mice with dextran sulfate [32], a molecule that impairs the invasion of red blood cells by merozoites [34]. These authors [32] showed the effects of this substance on reducing the parasitemia and the parallel increase in the survival rate of the mice. More recently, Vulliez et al. [33] showed, through the use of structural methods, that impairment of the malaria parasite moving junction complex (decreasing the invasion rate of merozoites) is effective as antimalarial treatment. To sum up, our results indicate that decreasing the invasion rate of the red blood cells by merozoites is a target where some drug treatments can be effective against malaria.

The second single target proposed by the model works by increasing the death rate of the gametocytes. This intervention produces a decrease in gametocyte load but an increase in merozoite load, although the maximum peak will be attenuated

(Figure 8B). A treatment along these lines will reduce the transmission rate during the initial stages of the disease and can be combined with traditional treatments targeting the asexual phase. Such a strategy has been already used (artemisinin combined treatments, [39]), with the predicted effects of a lower transmission rate for the disease.

A third target was to decrease the ability of the gametocytes to activate the immune system. Its effect is to reduce the maximum peaks of both parasite species (Figure 8C), and so it is expected that it would alleviate the symptoms of non-complicated malaria and reduce the transmission rate during the initial stages of the infection. This target also has additional convenient characteristics. Since it does not directly affect the parasites, there is no selective pressure on them and thus the emergence of drug resistance is avoided. Also, if combined with traditional treatments, the doses could be reduced, thereby also reducing the emergence of drug resistance (see [40]). Since this target refers to a parasite-host interaction, the only chance to observe its effects would be in *in vivo* conditions. Of equal importance is the fact that it is a very counterintuitive solution. All this could explain why this strategy has never been explored. In addition, we are aware of the technical difficulties involved in the design and implementation of such a strategy, where the sensitivity of the immune system towards the presence of one of the parasite forms is to be impaired.

The last single target identified operates by increasing the transformation rate of merozoites into envisaged gametocytes. The effect of this increase is to produce a significant decrease in merozoite load and also a decrease in gametocyte load (see Figure 8D). Although it is not surprising that increasing the merozoite transformation rate would produce a decrease in merozoite load, what is not so intuitive is the model's prediction of a decrease in the gametocyte load. This is a good illustration of how the integration into a mathematical representation of the many non-linear interactions among the variables involved in the relevant processes can lead to the emergence of certain counterintuitive conclusions that cannot be derived from the consideration of the local changes only. This type of intervention has been shown to relax the symptomatology of non-complicated malaria [41] and reduce transmission during the initial stages of the infection [42]. It is interesting to observe that the activation of the transformation of merozoites into gametocytes has the effect of impairing the pathogen load. A higher gametocyte growth rate yields an initial increase in its population, but this is followed by a greater decrease in such a way that, as a whole, more parasites are eliminated earlier. This behavior has been observed in other parasitic diseases [13] and can be explained by stating that a pathogen that proliferates rapidly is more likely to be detected by the immune system. Increasing the gametocytogenesis is a strategy that has never been evaluated by structural drug design methods, and our results propose this target as a promising process where these techniques can be applied for drug design.

Our exploration of the effective combinations of two targets showed that reducing the influence of gametocytes on the activation of the immune system while at the same time decreasing the effect of the immune system on the death rate of the red blood cells (see Figure 7B) would cause a reduction in both of the parasite forms (Figure 8E). The latter action can be interpreted as making the immune system less efficient in removing old erythrocytes, thus enhancing their half-life. This therapeutic strategy is optimal in order to prevent the emergence of drug resistance in the parasite. These two proposed targets have never been evaluated by structural methods. There should be great interest in examining these two processes in order to design new drugs, because affecting these processes does not generate selective pressure on the parasites; thus, effective drugs will have a low probability of leading to the emergence of resistance, thereby extending their life span. Here we can see again how the systemic approach might shed new light on a well-studied process and help propose a novel combination of targets, none of which aims to directly kill the parasites, but which could reduce the parasitemia. In all these explorations, the magnitudes of target-related parameter changes, although related with the corresponding processes, do not have a direct translation into a particular process. Accordingly, they have to be interpreted as an indication of the magnitude and sense of the intervention that would lead to the desired effect.

The new, potential antimalarial targets proposed here were identified through the use of a mathematical model that reliably reproduces the infection dynamics under different *in vivo* scenarios of the disease. This model-based strategy can be of assistance in key phases of the drug discovery process, such as the identification of the right targets, since these targets allow us to guide drug design at the molecular level through the systematic use of other means such as structural methods (molecular docking) or data-mining of inhibitor databases. A best-case illustration is provided by the proposed target consisting of decreasing the invasion of red blood cells by merozoites, which relates to the interruption of the interaction between the Apical Membrane Antigen 1 associations with its receptor, the Rhoptry Neck Protein 2. In fact, the structural details of the specific Apical Membrane Antigen 1 with the Rhoptry Neck Protein 2 interaction involved in the invasion mechanism enables the design of molecules with optimal inhibitory properties to treat malarial infection. However, due to the phenomenological character of the model, the proposed targets do not have a direct translation into a concrete, well-defined process. On the contrary, it should be stressed that the contribution of this work is to propose certain processes of the intraerythrocytic cycle of *Plasmodium* as targets for a more detailed analysis that would eventually lead to the determination of a set of concrete processes where the activity of some drugs will cause the desired global effect. This second iteration would be the natural next step in this project.

Our results suggest that the invasion of erythrocytes by merozoites is a key point where any impairment intervention would cause a decrease in parasitemia. In this case, some work has already been done with respect to structural methods of drug design [33]. Furthermore, comparison of the effect on a known drug target (β-artemether administration through liposomes; Figure 5) with the new drug target of increasing gametocytogenesis (Figure 8D) shows that both reduce the peak of parasitemia (Figure 6, panel B). When β-artemether is inoculated directly, the same peak of parasitemia is observed, but with several days' delay (Figure 6, panel A). Chimanuka et al. [28] showed that the liposome inoculation allowed the mice to survive, in contrast with the direct inoculation. We can thus conclude that a drug which increases gametocytogenesis would produce the same effects on parasitemia (which permit survival in mice) as the β-artemether administration through liposomes.

We conclude that focusing on cellular function as a system rather than on the level of the single process or molecule will facilitate the discovery of novel classes of drugs. Through the integration into a model of the *in vivo* host–pathogen interactions, we can achieve an integrated view of parasite infection and host responses that will allow for an understanding of the host–parasite–drug interactions and the selection of drug combination strategies of therapeutic value, and for controlling the transmission of malaria by anopheline mosquitoes. In addition, the insight obtained from this work already suggests future extensions and refinements. In particular, models with a greater resolution in

terms of the mechanisms involved in the novel targets such as those represented by the V_6 (γ_6, elimination of gRBC), V_5, (γ_5, gametocytogenesis), V_7 (g_{73}, activation of the immune system by the gametocytes) or V_2 (g_{24}, recycling of the erythrocytes) would lead to more mechanistically detailed versions of the model that would suggest more precise targets for drug action. We are aware of the difficulties of translating the proposed targets into precise therapies; the aim of this work is to propose targets that would direct the drug search toward certain processes of the intraerythrocytic cycle of *Plasmodium*.

Moreover, since the systemic approach used here is a general methodology, it can be used in the selection of strategies for controlling a plethora of parasitic diseases. In each case, the specific processes and their corresponding variables and parameters should be considered, but the application of the model to other forms of parasitemia would benefit from the fact that there are many common features shared by all.

Materials and Methods

Experimental Data

The parameters of the model were fitted using published experimental data from non-treated animal model individuals. The modelization task refers to the initial stages of the infection dynamics.

Data for the variables hRBC, mRBC and gRBC were taken from [24]. In this work, CBA/Ca mice were inoculated with 10^6 parasitized red blood cells (*Plasmodium chabaudi*) and during the first 32 days after infection, measures were taken of the erythrocyte titer (units per µL of blood) and the parasitemia (mRBC and gRBC per µL). Data for the IS variable were taken from [25]. In this case, CBA/Ca mice were inoculated with $5{\cdot}10^4$ parasitized red blood cells (*Plasmodium chabaudi*); the parasitemia dynamics of this study were compared to the parasitemia measured in [24] in order to ensure the same infection dynamics (data not shown). IgG1 from infected mice was measured during the first 17 days post infection (absorbance units). Since the dynamics of the initial stages of the variables IgG1 and IgG2A (immunoglobulin G1 and G2A) in these infected mice were almost the same (see Mota et al. 98 [25]), the IgG1 data were used to infer the mean response of the immune system against *Plasmodium*.

Model Design

The dynamics of the infection process by *Plasmodium* were represented as a mathematical model in ordinary differential equations in the power-law formalism. In this formalism [14], which allows for non-integer kinetic orders, the processes that conforms the networks are modelled using power-law expansions in the variables of the system and are then included in non-linear ordinary differential equations with the following structure, called Generalized Mass Action (GMA):

$$\frac{dX_i}{dt} = \sum_{q=1}^{Q_i} (\pm V_q) \qquad i = 1,2,\ldots,N$$
$$V_q = \gamma_q \cdot \prod_{r=1}^{R_i} (X_r^{g_{q,r}}) \qquad (1)$$

In the above expression, X_i (for i equals 1 to N) represents the variables of the model. V_q represents each of the processes affecting the variation of X_i, while X_r represents the variables which influence the corresponding process V_q. γ_q and $g_{q,r}$ are the parameters of the model. γ_q is the rate constant related to the process V_q. $g_{q,r}$ is the kinetic order which quantifies the effect of the variable X_r on the process V_q. Q_i and R_i are the total number of fluxes and variables, respectively.

Model Equations

The model derived from the scheme in Figure 1 is given by:

$$\begin{aligned} \frac{dhRBC}{dt} &= V_1 - V_2 - V_3 \\ \frac{dmRBC}{dt} &= V_3 - V_4 - V_5 \\ \frac{dgRBC}{dt} &= V_5 - V_6 \\ \frac{dIS}{dt} &= V_7 - V_8 \end{aligned} \qquad (2)$$

where the corresponding rate equations in power law form corresponding to the different fluxes are:

$$\begin{aligned} V_1 &= \gamma_1 \\ V_2 &= \gamma_2 \cdot hRBC^{g_{21}} \cdot IS^{g_{24}} \\ V_3 &= \gamma_3 \cdot hRBC^{g_{31}} \cdot mRBC^{g_{32}} \\ V_4 &= \gamma_4 \cdot mRBC^{g_{42}} \cdot IS^{g_{44}} \\ V_5 &= \gamma_5 \cdot mRBC^{g_{52}} \cdot IS^{g_{54}} \\ V_6 &= \gamma_6 \cdot gRBC^{g_{63}} \cdot IS^{g_{64}} \\ V_7 &= \gamma_7 \cdot mRBC^{g_{72}} \cdot gRBC^{g_{73}} \\ V_8 &= \gamma_8 \cdot IS^{g_{84}} \end{aligned} \qquad (3)$$

Table 1 shows the values of the model parameters: This set of value corresponds to the only solution which fitted the data and verifies new experimental conditions (see results). Figure 2 presents the corresponding model data fitting.

Parameter Estimation and Model Fitting

Model parameters were determined by fitting the model to experimental data from infected mice during the first month of the disease after infection [24,25] (see Figure 2). The fitting was attained through the use of a heuristic optimization algorithm (Modified Genetic Algorithm) previously used and presented by us

Table 1. Model parameter values.

Rate constants		Kinetic orders			
Name	**Value**	**Name**	**Value**	**Name**	**Value**
γ_1	0.97	g_{21}	3.00	g_{63}	0.84
γ_2	0.94	g_{24}	1.73	g_{64}	0.83
γ_3	0.51	g_{31}	1.52	g_{72}	0.22
γ_4	0.73	g_{32}	1.01	g_{73}	0.63
γ_5	0.26	g_{42}	0.84	g_{84}	4.29
γ_6	0.49	g_{44}	2.98		
γ_7	0.15	g_{52}	1.80		
γ_8	0.09	g_{54}	2.98		

doi:10.1371/journal.pone.0059968.t001

elsewhere [43]. The objective function (*Fobj*) is minimized in the process:

$$Fobj = \frac{\sum_{i=1}^{N}\left[\sum_{h=0}^{Tm}\left[\frac{\left(X_i(t=h)-\overline{X_i}(t=h)\right)^2}{\overline{X_i}(t=h)}\right]\right]}{N\cdot Tm} \quad (4)$$

In this equation, $X_i(t=h)$ is the X_i variable value at the time point h and $\overline{X_i}(t=h)$ is the corresponding experimental value at the same time point h. The stopping criterion is the maximum number of iterations of the algorithm (1000), which in this model satisfy the convergence of the majority of the solutions. The best minimum reached is expected to reproduce the qualitative dynamic behavior of the measured data. Table 2 shows the value of the objective function of all the solutions presented. Values much higher than one (in days units) for γ parameters in a cellular scale would correspond to an excessive fast processes, furthermore values of g's higher than 3 represent strong sensitivities of the processes by the variables. Because of that, the parameter search boundaries were [0, 1] for the γ's, [0, 3] for the g's and [0, 6] for g_{84}. In this last case, this was due to the fact that g_{84} represents the combined influence on V_8 of IS as substrate and effector.

Model Validation

Any useful model is expected to reproduce the observed responses against different experimental scenarios and treatments. To do so here, we used other experimental data obtained in conditions of pharmacological treatment or from vaccinated individuals.

The first model validation comes from the comparison of the model dynamics of the parasite variables with the corresponding experimental values in malaria-affected humans [26]. A second set of comparisons was obtained from data taken from vaccinated and non-vaccinated infected monkeys [27]. In this case, the parasitemia course observed after the vaccination was used to verify the model response under a simulated vaccination. This last condition was performed in the model by increasing the initial value of the IS variable. The last verification test was realized by comparing the model's results against experimental data obtained from treated and non-treated mice infected with *Plasmodium* [28]. Two different forms of drug administration were considered: direct drug injection (*Free drug*) and administration through liposomes (*Liposome drug*). Equation 5 presents the model equations corresponding to these two modes of drug administration (see Figures 6A and 6B).

Table 2. Objective functions.

$Fopt_{both}$				$Fopt_g$	
Sol_{ori}	0.408	$Sol_{\gamma 5}$	0.202	Sol_{ori}	0.490
$Sol_{\gamma 3}$	0.023	Sol_{g73}	0.289	$Sol_{g73/g24}$	0.202
$Sol_{\gamma 6}$	0.271				

So_{ori} is the value of the objective function of the solution represented in Figure 2. $Sol_{\gamma 3}$, $Sol_{\gamma 5}$, $Sol_{\gamma 6}$, Sol_{g73}, *and* $Solu_{g73/g24}$ are the values of the objective functions for the solutions corresponding to the pharmacological treatment in γ_3, γ_5, γ_6, g_{73} and the combination of g_{73} and g_{24} respectively (see Figure 7). $Fobj_{both}$ and $Fobj_g$ are described in Material and Methods (equations 6).

doi:10.1371/journal.pone.0059968.t002

Direct drug injection

$$\begin{aligned} \tfrac{dmRBC}{dt} &= V_3 - V_4 - V_5 - V_9 \\ \tfrac{dFd}{dt} &= -V_{d1} \\ V_{d1} &= K_{d1}\cdot Fd \\ V_9 &= K_9\cdot mRBC\cdot Fd \\ K_9 &= 1 \\ K_{d1} &= 0.1 \end{aligned}$$

Liposome drug administration.

$$\begin{aligned} \tfrac{dmRBC}{dt} &= V_3 - V_4 - V_5 - V_9 \\ \tfrac{dFd}{dt} &= V_{d2} - V_{d1} \\ \tfrac{dLd}{dt} &= -V_{d2} \\ V_{d1} &= K_{d1}\cdot Fd \\ V_{d2} &= K_{d2}\cdot Ld \\ V_9 &= K_9\cdot mRBC\cdot Fd \\ K_9 &= 1 \\ K_{d1} &= 0.1 \\ K_{d2} &= 0.02 \end{aligned} \quad (5)$$

In these equations, *Fd* represents the variable Free drug (drug in the bloodstream), *Ld* represents the variable Liposome drug (drug inside liposomes), and V_{d1} is the drug clearance from the body in both the free drug and liposome drug administration models. K_{d1} and K_{d2} are the corresponding rate constants and V_{d2} is the drug diffusion from the liposomes. The parameter values K_9, K_{d1} and K_{d2} were estimated in order to fit the time scale and the relative decrease of the peak of parasitemia.

Search for Pharmacological Targets

In order to select the targets, each model parameter linked to a potential target was changed either one at a time or in combination with another, in an attempt to identify solutions showing reduced objective function. The objective function considers the relative difference of the mean healthy red blood cells with respect to the initial non-infected condition and the relative increase in the maximum parasite peak and the mean parasite load with respect to the initial value of parasites. So the search consists of looking for solutions with low values of objective function, which will be closer to the healthy situation. This set of parameter values was selected as the proposed target. For the combined targets, we chose those which were better than the worst of the single targets. The objective functions used during the search are displayed in Equation 6.

$$\begin{aligned} Fopt_{\text{both}} &= \frac{1}{5}\cdot\left(\left(\frac{\overline{hRBC}-hRBC(t=0)}{hRBC(t=0)}\right)^2+\left(\frac{\max(mRBC)}{\max(mRBC_0)}\right)^2+\right. \\ &\left.\left(\frac{\max(gRBC)}{\max(gRBC_0)}\right)^2+\left(\frac{\overline{mRBC}}{\overline{mRBC_0}}\right)^2+\left(\frac{\overline{gRBC}}{\overline{gRBC_0}}\right)^2\right) \\ Fopt_g &= \frac{1}{3}\cdot\left(\left(\frac{\overline{hRBC}-hRBC(t=0)}{hRBC(t=0)}\right)^2+\left(\frac{\max(gRBC)}{\max(gRBC_0)}\right)^2+\right. \\ &\left.\left(\frac{\overline{gRBC}}{\overline{gRBC_0}}\right)^2\right) \end{aligned} \quad (6)$$

$Fopt_{both}$ is the objective function used to select solutions having low levels in both forms of the parasite and healthy levels of erythrocytemia. The first term of this equation represents the relative squared difference between the mean value of the hRBC variable ($\overline{hRBC}$) of the solution and the value of this variable under healthy conditions ($hRBC(t=0)$), which has to be minimized for obtaining solutions with healthy levels of non-infected red blood cells. The second and third terms represent the relative value of the maximum level of parasitemia with respect to the initial value of the parasitemia; minimizing these allows us to obtain solutions with attenuated peaks of parasitemia. Finally, the

fourth and fifth terms represent the relative value of the mean level of parasitemia during the infection with respect to the initial value of parasitemia; minimizing these allows us to obtain solutions with low levels of parasitemia. $Fopt_g$ was used to find solutions with low gametocytemia. As can be seen in this equation, the three terms used correspond to those terms of the previous equations that are related to the gRBC species, because this objective function only considers the minimization of the gametocyte. Overlined variables represent the mean value of the corresponding variables over time; the subscript 0 represent the initial value, before the optimization. In both cases, the sum is divided by the number of summands (5 and 3 respectively) in order to compare the values of the objective function. Table 2 shows the value of the objective function for all the proposed targets.

Supporting Information

Figure S1 Absolute values of the steady state sensitivities at the healthy condition.
(TIF)

Figure S2 Absolute values of the dynamic sensitivities.
(TIF)

Information S1 Steady State Stability and Sensitivity Analysis.
(DOCX)

Acknowledgments

The authors gratefully thank Dr. Basilio Valladares, Dr. Carlos González-Alcon, Julio Vera González, Dr. Cristina Pou and Dr. María Ángeles Santana Morales for their helpful observations. Also the authors want to acknowledge the excellent work carried out by three independent and anonymous reviewers that have contributed significantly to improving the work.

Author Contributions

Conceived and designed the experiments: GS NVT. Performed the experiments: GS NVT. Analyzed the data: GS NVT. Contributed reagents/materials/analysis tools: GS NVT. Wrote the paper: GS NVT.

References

1. World Malaria Report (2012) WHO Library Cataloguing-in-Publication Data ISBN 978 92 4 156453 3.
2. Schwartz L, Brown GV, Genton B, Moorthy VS (2012) A review of malaria vaccine clinical projects based on the WHO rainbow table. Malaria J 11: 11.
3. Ranson H, N'Guessan R, Lines J, Moiroux N, Nkuni Z (2011) Pyrethroid resistance in african anopheline mosquitoes: What are the implications for malaria control? Trends Parasitol 27(2): 91–98.
4. Golenser J, Waknine JH, Krugliak M, Hunt HN, Grau GE (2006) Current perspectives on the mechanism of action of artemisinins. International Journal for Parasitology 36: 1427–1441.
5. Parija SC (2011) Drug resistance in malaria. Indian Journal of Medical Microbiology 29(3): 243–248.
6. Porter-Kelley JM (2010) Acquired resistance of malarial parasites against artemisinin-based drugs: Social and economic impacts. Infection and Drug Resistance 3: 87–94.
7. Aung PP (2012) Emergence of artemisinin-resistant malaria on the western border of Thailand: A longitudinal study. Lancet 379(9830): 1960–1966.
8. Swinney DC (2011). How were new medicines discovered? Nature Reviews Drug Discovery 10(7): 507–519.
9. Wells TNC (2010) Is the tide turning for new malaria medicines? Science 329(5996): 1153–1154.
10. Paul SM (2010) How to improve R&D productivity: The pharmaceutical industry's grand challenge. Nature Reviews Drug Discovery 9(3): 203–214.
11. Ward R (2011) Quantitative and systems pharmacology in the post-genomic era: New approaches to discovering drugs and understanding therapeutic mechanisms. An NIH white paper by the QSP workshop group.
12. Bhalla US (1999) Emergent properties of networks of biological signaling pathways. Science 283(5400): 381.
13. Langer BM (2012) Modeling of leishmaniasis infection dynamics: Novel application to the design of effective therapies. BMC Systems Biology 6: 1.
14. Voit EO (2000) Computational Analysis of Biochemical Systems. A Practical Guide for Biochemists and Molecular Biologists xii +530 pp., Cambridge University Press, Cambridge, UK.
15. Curto R, Voit EO, Cascante M (1998) Analysis of abnormalities in purine metabolism leading to gout and to neurological dysfunctions in ma. Biochemistry Journal 329: 777–487.
16. Vera-González J, Cascante M, Curto R, Torres NV (2007) Identification of Enzymatic Targets In Metabolic Diseases by Modelling and Optimisation. The Case of Hyperuricemia in Humans. Bioinformatics 23(17): 2281–2289.
17. Voit EO (2008) A systems-theoretical framework for health and disease. Mathematical Biosciences 217: 11–18.
18. Vodovotz Y, Constantine G, Rubin J, Csete M, Voit EO, An G (2009) Mechanistic simulations of inflammation: Current state and future prospects. Mathematical Biosciences 217: 1–10.
19. Qi Z, Miller GW, Voit EO (2011) Mathematical Models in Schizophrenia. Chapter 14 in Volume I of: M.S. Ritsner (Ed.): Textbook of Schizophrenia Spectrum Disorders. Springer Verlag, New York.
20. Marin-Sanguino A, Gupta SK, Voit EO, Vera J (2010) Biochemical pathway modeling tools for drug target detection in cancer and other complex diseases. Methods in Enzymology 487: 321–372.
21. Khandelwal S (2008) A role of phosphatidylserine externalization in clearance of erythrocytes exposed to stress but not in eliminating aging populations of erythrocyte in mice. Experimental Gerontology 43(8): 764–770.
22. Gaur D (2004) Parasite ligand-host receptor interactions during invasion of erythrocytes by plasmodium merozoites. International Journal for Parasitology 34(13–14): 1413–29.
23. Baker DA (2010) Malaria gametocytogenesis. Molecular & Biochemical Parasitology 172(2): 57–65.
24. Gadsby N (2009) A study on pathogenicity and mosquito transmission success in the rodent malaria parasite plasmodium chabaudi adami. International Journal for Parasitology 39(3): 347–354.
25. Mota MM (1998) Acute plasmodium chabaudi chabaudi malaria infection induces antibodies which bind to the surfaces of parasitized erythrocytes and promote their phagocytosis by macrophages in vitro. Infection and Immunity 66(9): 4080–6.
26. Diebner HH (2000) Modelling the transition of asexual blood stages of plasmodium falciparum to gametocytes. Journal of Theoretical Biology 202(2): 113–27.
27. Makobongo MO (2006) Immunization of aotus monkeys with recombinant cysteine-rich interdomain region 1α protects against severe disease during plasmodium falciparum reinfection. Journal of Infectious Diseases 193(5): 731–740.
28. Chimanuka B (2002) Preparation of β-artemether liposomes, their HPLC-UV evaluation and relevance for clearing recrudescent parasitaemia in plasmodium chabaudi malaria-infected mice. Journal of Pharmaceutical & Biomedical Analysis 28(1): 13.
29. Vera J, Curto R, Cascante M, Torres NV (2007) Detection of potential enzyme targets by metabolic modelling and optimization: Application to a simple enzymopathy. Bioinformatics 23(17): 2281.
30. Aikawa M (1978) Erythrocyte entry by malarial parasites. A moving junction between erythrocyte and parasite. The Journal of Cell Biology 77(1): 72–82.
31. Baum J (2006) Regulation of apicomplexan actin-based motility. Nature Reviews Microbiology 4(8): 621–628.
32. Beuria MK (1991) Dextran sulfate induced suppression of plasmodium berghei parasitaemia. Indian Journal of Experimental Biology 29(3): 284–5.
33. Vulliez-Le Normand B (2012) Structural and functional insights into the malaria parasite moving junction complex. PLoS Pathogens 8(6): 1–14.
34. Xiao L (1996) Sulfated polyanions inhibit invasion of erythrocytes by plasmodial merozoites and cytoadherence of endothelial cells to parasitized erythrocytes. Infection and Immunity 64(4): 1373–8.
35. Harris KS (2005) Binding hot spot for invasion inhibitory molecules on plasmodium falciparum apical membrane antigen 1. Infection and Immunity 73(10): 6981–9.
36. Harris KS (2009) Rapid optimization of a peptide inhibitor of malaria parasite invasion by comprehensive N-methyl scanning. Journal of Biological Chemistry 284(14): 9361–9371.
37. Richard D (2010) Interaction between plasmodium falciparum apical membrane antigen 1 and the rhoptry neck protein complex defines a key step in the erythrocyte invasion process of malaria parasites. Journal of Biological Chemistry 285(19): 14815–14822.
38. Beeson JG (2008) Recent insights into humoral and cellular immune responses against malaria. Trends in Parasitology 24(12): 578–584.
39. Murambiwa P (2011) Anti-malarial drug formulations and novel delivery systems: A review. Acta Tropica 118(2): 71–79.
40. Nosten F (2007) Artemisinin-based combination treatment of falciparum malaria. The American Journal of Tropical Medicine and Hygiene 77(6): 181–92.

41. Olliaro P (2008) Risk associated with asymptomatic parasitaemia occurring post-antimalarial treatment. Tropical Medicine & International Health 13(1): 83–90.
42. Okell LC (2008) Reduction of transmission from malaria patients by artemisinin combination therapies: A pooled analysis of six randomized trials. Malaria Journal 1–13.
43. Hormiga J (2010) Quantitative analysis of the dynamic signaling pathway involved in the cAMP mediated induction of l-carnitine biosynthesis in E. coli cultures. Molecular Biosystems 6(4): 699–710.

8. Malaria – Supplementary Material

Information S1. Steady State Stability and Sensitivity Analysis.

Any mathematical model of a biological system has to be stable and robust if it is to be considered a reliable representation of the real system. The model was thus submitted to a stability and sensitivity analysis. We determined that the healthy host steady state is stable (see Supporting Information, Section 3). At the same time, in order to check the model's robustness, we evaluated two types of system sensitivities: the steady state sensitivities, which refer to the normal, healthy steady state, and the dynamic system sensitivities parameters, which identify the parameters with major influence on the transient dynamics (see Supporting Information, Section 4). From this analysis we concluded that the model is robust enough to represent the biological system.

Stability Analysis

The stability of the healthy, reference steady state can be found in the model shown in Equations S1 that corresponds to the not infected, healthy host steady state through the evaluation of eigenvalues of the corresponding jacobian matrix:

$$\frac{dhRBC}{dt} = V_1 - V_2$$
$$\frac{dIS}{dt} = V_{IS} - V_8$$
$$V_1 = \gamma_1$$
$$V_2 = \gamma_2 \cdot hRBC^{g_{21}} \cdot IS^{g_{24}}$$
$$V_8 = \gamma_8 \cdot IS^{g_{84}}$$
$$V_{IS} \approx 0$$

Equations S1

where hRBC and IS are the same as in the original model (Equations 2 and 3 in the article), and V_{IS} is the rate associated with the host variable IS in the absence of infection.

Sensitivity Analysis

Sensitivity analysis enables the identification of parameters that exert a major influence on system response. Since we depart from and aim to reach a steady state where the variable values are stable at normal, healthy values, we should evaluate the robustness of this reference steady state. But our model is a dynamic one, too; therefore, it is also necessary to identify the parameters with a major influence on the transient dynamics.

Steady state sensitivities. Steady state sensitivities were calculated at the healthy, not infected steady state (Voit, E.O., 2000; Siljak, D.D., 1969; Frank, P.M., 1978). Steady state sensitivities measure the relative change to the value of variables with respect to an infinitesimal change in the parameters (kinetic orders and rate constants) or in the initial conditions. These sensitivities were calculated in accordance with Equation S2.

$$SS(X_i, P_k) = \frac{\log(s\hat{X}_i) - \log(sX_i)}{\log(s\hat{P}_k) - \log(sP_k)} \qquad i = 1,2,\ldots,N; k = 1,2,\ldots,M$$

$$SS(X_i, X_j(t=0)) = \frac{\log(s\hat{X}_i) - \log(sX_i)}{\log(\hat{X}_j(t=0)) - \log(X_j(t=0))} \qquad i, j = 1,2,\ldots,N$$

Equations S2

In the above expressions, $SS(X_i,P_k)$ and $SS(X_i,X_j(t=0))$ are the sensitivities of the variable X_i with respect to changes in parameter P_k and initial condition $X_j(t=0)$, respectively; sX_i is the steady state value of the variable X_i; $X_j(t=0)$ is the initial condition value of the variable X_j and P_k is the value of the parameter k. Carets are displayed over the variables and parameters which correspond to the perturbed situation. Figure S1 shows the values of the steady state sensitivity at the healthy condition when the variables mRBC and gRBC are not present. In all cases, the maximum absolute value of sensitivities is about 1.2.

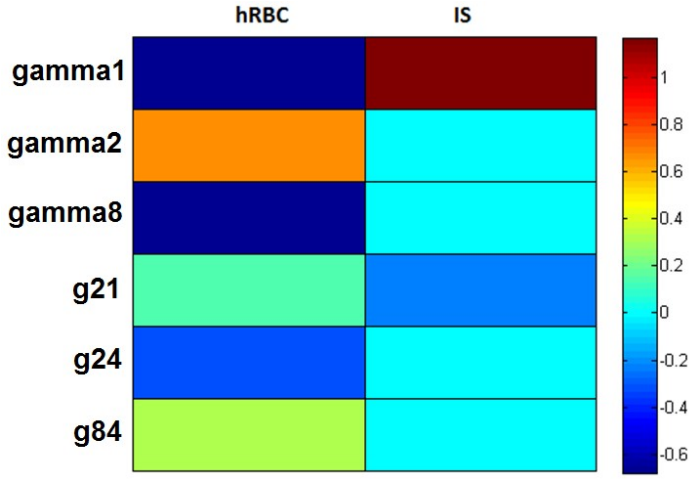

Figure S1. Dynamic sensitivities 1. Dynamic sensitivities measure the relative change on the value of the area under the curve of all the variables with respect to an infinitesimal change in the parameters (kinetic orders and rate constants) or in the initial conditions (see Hormiga, J., 2010). For this purpose we used the following equations:

$$DS(X_i, P_k) = \frac{\log(\int_{t=0}^{Tm} \hat{X}_i dt) - \log(\int_{t=0}^{Tm} X_i dt)}{\log(\hat{P}_k) - \log(P_k)} \qquad i = 1,2,\ldots,N; k = 1,2,\ldots,M$$

$$DS(X_i, X_j(t=0)) = \frac{\log(\int_{t=0}^{Tm} \hat{X}_i dt) - \log(\int_{t=0}^{Tm} X_i dt)}{\log(\hat{X}_j(t=0)) - \log(X_j(t=0))} \qquad i = 1,2,\ldots,N; k = 1,2,\ldots,M$$

Equations S3

In the above expressions, $DS(X_i,P_k)$ and $DS(X_i,X_j(t=0))$ are the dynamic sensitivities of the variable X_i with respect to changes in parameter P_k and initial condition $X_j(t=0)$, respectively; $\int_{t=0}^{Tm} X_i dt$ represents the area under the curve of the variable X_i during the time between 0 and final time Tm. Carets are displayed over the variables and parameters which correspond to the perturbed situation. Figure S2

shows the values of the dynamic sensitivities. In all cases the maximum absolute value of sensitivities is about 1.2.

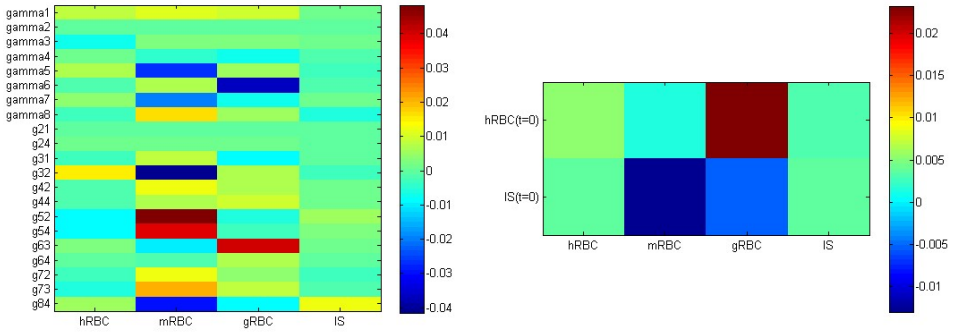

Figure S2. Dynamic sensitivities 2. Dynamic sensitivities measure the relative change on the value of the area under the curve of all the variables with respect to an infinitesimal change in the parameters (kinetic orders and rate constants) or in the initial conditions (see Hormiga, J., 2010). For this purpose we used the following equations:

References

Voit, E.O. (2000) Computational analysis of biochemical systems. Cambridge University Press.

Siljak, D.D. (1969) Nonlinear system: The parameter analysis and design. New York: Wiley.

Frank PM (1978) Introduction to systems sensitivity theory. New York: Academic Press.

Hormiga, J. (2010) Quantitative analysis of the dynamic signaling pathway involved in the cAMP mediated induction of L-carnitine biosynthesis in E. coli cultures. Molecular Biosystems *6*(4): 699-710.

9. VIH - *PLoS ONE*

DOI: 10.1371/JOURNAL.PONE.0103845

OPEN ACCESS Freely available online

PLOS ONE

Quantitative Analysis of the Processes and Signaling Events Involved in Early HIV-1 Infection of T Cells

Guido Santos[1,3], **Agustín Valenzuela-Fernández**[2]*, **Néstor V. Torres**[1,3]*

1 Grupo de Biología de Sistemas y Modelización Matemática, Departamento de Bioquímica, Microbiología, Biología Celular y Genética, Facultad de Biología, Universidad de La Laguna, San Cristóbal de La Laguna, Tenerife, España, **2** Laboratorio de Inmunología Celular y Viral, Departamento de Medicina Física y Farmacología, Facultad de Medicina, Universidad de La Laguna, San Cristóbal de La Laguna, Tenerife, España, **3** Instituto de Tecnología Biomédica, Universidad de La Laguna, San Cristóbal de La Laguna, Tenerife, Spain

Abstract

Lymphocyte invasion by HIV-1 is a complex, highly regulated process involving many different types of molecules that is prompted by the virus's association with viral receptors located at the cell-surface membrane that culminates in the formation of a fusion pore through which the virus enters the cell. A great deal of work has been done to identify the key actors in the process and determine the regulatory interactions; however, there have been no reports to date of attempts being made to fully understand the system dynamics through a systemic, quantitative modeling approach. In this paper, we introduce a dynamic mathematical model that integrates the available information on the molecular events involved in lymphocyte invasion. Our model shows that moesin activation is induced by virus signaling, while filamin-A is mobilized by the receptor capping. Actin disaggregation from the cap is facilitated by cofilin. Cofilin is inactivated by HIV-1 signaling in activated lymphocytes, while in resting lymphocytes another signal is required to activate cofilin in the later stages in order to accelerate the decay of the aggregated actin as a restriction factor for the viral entry. Furthermore, stopping the activation signaling of moesin is sufficient to liberate the actin filaments from the cap. The model also shows the positive effect of gelsolin on actin capping by means of the nucleation effect. These findings allow us to propose novel approaches in the search for new therapeutic strategies. In particular, gelsolin inhibition is seen as a promising target for preventing HIV-1 entry into lymphocytes, due to its role in facilitating the capping needed for the invasion. Also it is shown that HIV-1 should overcome the cortical actin barrier during early infection and predicts the different susceptibility of CD4+ T cells to be infected in terms of actin cytoskeleton dynamics driven by associated cellular factors.

Citation: Santos G, Valenzuela-Fernández A, Torres NV (2014) Quantitative Analysis of the Processes and Signaling Events Involved in Early HIV-1 Infection of T Cells. PLoS ONE 9(8): e103845. doi:10.1371/journal.pone.0103845

Editor: Yuntao Wu, George Mason University, United States of America

Received April 6, 2014; **Accepted** July 2, 2014; **Published** August 8, 2014

Data Availability: The authors confirm that all data underlying the findings are fully available without restriction. All data are included within the manuscript or in published materials.

Funding: This work was funded by research grants from the Spanish MICINN, Ref. No. BIO2011-29233-C02-02 and the Agencia Canaria de Investigación, Innovación y Sociedad de la Información, Ref. No. PIL2071001. AV-F is supported by the European Regional Development Fund, SAF2011-24671 (Ministerio de Ciencia e Innovación, Spain), 24-0740-09 (Fundación para la Investigación y la Prevención del SIDA en España (FIPSE), Spain), ProID20100020 (Agencia Canaria de Investigación, Innovación y Sociedad de la Información, Canary Island Government, Spain), and RIS-RETIC (Red Nacional de Investigación en SIDA, ISCIII, Spain) associated RD12/0017/0034 grants. The funders had no role in study design, data collection and analysis, decision to publish, or preparation of the manuscript.

Competing Interests: Co-author Nestor Torres is a PLOS ONE Editorial Board member. This fact does not alter the authors' adherence to all the PLOS ONE policies on sharing data and materials.

* Email: avalenzu@ull.edu.es (AV-F); ntorres@ull.edu.es (NVT)

Introduction

The invasion and infection of CD4+ T lymphocytes by human immunodeficiency virus type 1 (HIV-1) is a complex process involving many cellular events that have been the subject of many studies [1]. The accumulated evidence indicates that the actin mobilization that occurs before the formation of the fusion pore plays a central role in this process. In fact, the actin cytoskeleton is deeply involved in the capping of cell-surface receptors for viral infection, which facilitates the interaction with the viral envelope (Env) complex and the subsequent fusion pore formation. However, this is not the only cellular component of importance in the viral infection process. Another main character in this plot is the HIV-1 Env-gp120 viral-surface protein. This element, located in the virus's outer coat, docks with high affinity at the lymphocyte's surface CD4 receptor. As a consequence of this interaction, HIV-1 Env-gp120 changes its conformation, exposing other regions of the viral protein responsible for its binding to a second co-receptor, either CCR5 or CXCR4. These bindings trigger a signaling pathway inside the lymphocyte that culminates with the formation of an actin cap in a pole of the cell (hereinafter 'cap'), driving CD4 and co-receptor co-localization and direct interaction, in an actin-dependent manner. These HIV-1 Env-gp120/CD4-mediated actin and receptor reorganization and capping events have been shown to correlate with the infectivity of the virus [2]. This fact will be a central issue the present study, since we will choose a cap indicator as a measure of HIV-1 infectivity.

Another observed fact is that activated CD4+ T lymphocytes, due to its active cell cycling, are continuously remodeling their actin cytoskeleton. There is ample evidence that the inhibition of the signal transduction or the removal of the intracellular signaling domain of CXCR4/CCR5, did not affect HIV infection [3–6]. However, in resting CD4+ T lymphocytes such inhibition

diminishes HIV infection [7]. In the same vein it has been shown that resting T cells are more sensitive to actin inhibitors than transformed T cells [8]. All these evidences point out to the fact that while the viral requirement for actin dynamics are universal, the HIV-mediated signaling pathways to the actin activity are cell-line dependent. These facts have been taken into account in this modelling exercise.

The actin mobilization required for cap formation is in turn influenced by other elements. This is the case of moesin, for example, an HIV-1-activated protein that acts as a reversible link between the lymphocyte membrane and the actin filaments [9]. HIV-1-triggered moesin activation promotes the reorganization of cortical F-actin and its subsequent anchoring to the membrane at HIV-1-cell contact points [10]; through this interaction, it facilitates the receptor/co-receptor direct interaction and co-localization. Furthermore, moesin also promotes the polymerization of actin filaments as a nucleation factor [10–12]. Moreover, experimental results show that increasing the total moesin available at the lymphocyte enhances HIV-1 infectivity, while a decrease in the activity of moesin negatively affects the invasion process [10]. During fusion pore formation, moesin has to be deactivated to allow F-actin depolymerization and viral entry [13].

Other key players in these processes are gelsolin, filamin-A and cofilin. Gelsolin is an actin-binding protein with a severing activity on actin filaments, which thus also has an effect on actin mobilization. It is assumed that this severing activity is what underlies the protein's observed influence on virus infectivity, by driving HIV-1-mediated cortical actin reorganization [14]. Gelsolin acts as a basal restrictive barrier for HIV-1 infection by severing actin to control the appropriate amount of cortical actin to be reorganized together with CD4-CXCR4/CCR5 redistribution to one pole of the cell. Both events are required for limiting early viral infection [14]. In the case of filamin-A, this protein participates in the invasion by linking membrane receptors to the actin cytoskeleton [15]. It has been shown too, that changes in filamin-A activity affects the invasion process of HIV-1 [15].

Finally, the last element to be considered is the actin-severing factor cofilin. This protein is regulated by virus signaling through the CXCR4 co-receptor and LIMK activation that leads to cofilin phosphorylation and inactivation [7,16], thus assuring an intact actin cortex before fusion pore formation. However, the mechanism involved in the activation of cofilin, just at the instant where the fusion pore is formed to allow cortical actin destruction and viral capsid entry, is not well understood. It has been observed that increasing the activity of cofilin enhances the infectivity of HIV-1 on resting lymphocytes, but that this does not have any effect on active lymphocytes [7]. In order to explain these observations, it has been hypothesized that cofilin facilitates cortical actin remodeling after fusion pore formation in resting lymphocytes only; this effect is caused by the impairment of the viral restriction factor at the static cortical actin in resting cells at later stages of the invasion [7,17].

Furthermore, the complexity of this scenario is growing, as recently other actin-associated factors appear to alter early HIV-1 infection. Hence, RNA silencing of debrin decreases F-actin polymerization allowing HIV-1 infection [18], while syntenin-1 depolymerises F-actin in a post-fusion step [19]. Although the HIV-1 Env-mediated signaling that activates LIMK-cofilin appears to be more clear after the involvement of PAK1/2 and the role of LIMK in viral-induced actin capping, the factors that lies upstream the RhoA/Rac1-PAK1/2-LIMK-cofilin and syntenin-1 pathways remain poorly understood [19–23]. Similarly, the identity of the kinase that phosphorylates moesin in the ERM-F-actin/receptor complex is unknown [10]. The cap itself, together with the processes described above that lead to its formation, emerges in many studies [1,2,7,10,14,15,24] as one of the main system responses prompted by the HIV-1 signaling.

From this observation it can naturally be derived that any insight into this fairly complex dynamic phenomenon is of foremost interest. Consequently, a great deal of information has been accumulated on the factors influencing the cap formation [7,10,14,15]. The approach followed when gathering the bulk of this information has been determined by the need to isolate the influence of each element considered relevant from that of the others participating in the process. In our view, these attempts to understand cap formation can be complemented by taking an integrated approach, where the activities of most of the key factors already described are simultaneously considered in a quantitative and dynamic framework. This integrated approach is not new in the field, since it has been used to unravel different aspects of HIV-1 infection [25–28]. However, to our knowledge, the present work is the first integrated exercise on the invasion of lymphocytes by HIV-1 during the first stages of the viral cycle.

Following this line of reasoning, the aim of this work is to integrate all available information on the molecules, mechanisms and regulatory features involved in the early lymphocyte invasion process into a dynamic mathematical model. By means of this approach, we aim to achieve a better understanding of the dynamics of the process and the role played by the various molecular components. The model is based on a plethora of experimental observations already made on the functional role of a number of cytoskeleton elements (receptors, enzymes, proteins, etc.) that participate in cytoskeleton reorganization and plasma membrane dynamics. It is this systemic approach that will allow us to model and evaluate the dynamics of the plasma membrane, as well as the role and relative importance of the different cortical structures and signal transduction through the CD4 receptor and CXCR4 or CCR5 co-receptors, which are the viral receptors involved in the generation of the membrane fluidity to promote fusion pore formation, entry and infection.

Results and Discussion

The signaling structure involved in the actin mobilization observed throughout the first stages of lymphocyte invasion by HIV-1 has recently been elucidated in great detail (see Liu et al. 2009, [1]). Key actors in these series of events are the CD4 and CXCR4 (or CCR5) membrane receptors, filamin-A and the ERM protein moesin, actin and the severing factor cofilin, as well as gelsolin, another actin-severing factor. In order to unravel the role of each one of these molecules in the process, they have been studied separately [7,10,14,15]. As a result, we have a considerable body of information offering a great deal of insight into the series of coordinated events involved in lymphocyte invasion by HIV-1.

However, the existing descriptions and interpretations are in many cases "element biased", since there is currently no integrated picture of the process where all the system components are simultaneously considered in a dynamic and quantitative way. In this work, we have tried to fill this gap by proposing a mathematical model where a great deal of the available information about the elements and the interactions among them is organized and integrated in a dynamic fashion (Figure 1).

The model thus obtained has been shown to be a robust and reliable representation of the system under consideration (see Material and Methods). Based on this model and on its subsequent analysis, we have been able to quantify the relative importance of each component for the system.

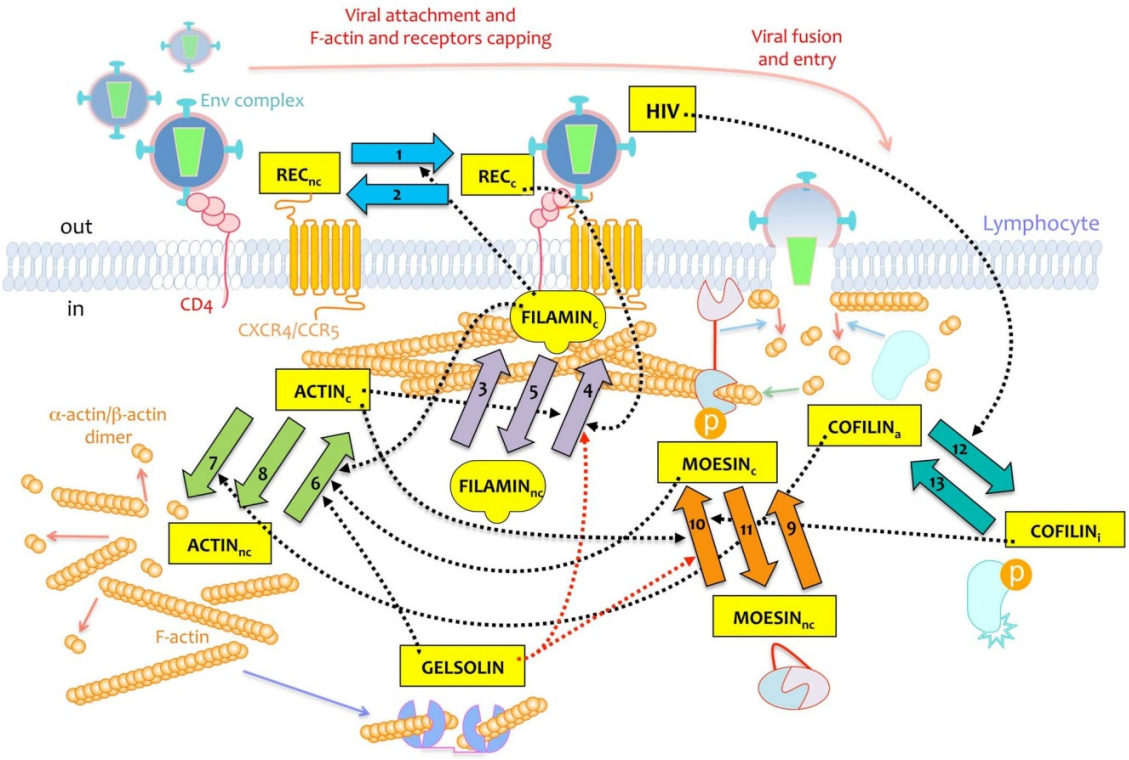

Figure 1. Representation of the molecular events simulated in the mathematical model. Molecules included in the model as variables are the following: HIV, REC (CD4 and CXCR4 or CCR5 receptors for HIV-1 infection on lymphocyte cell-surface), FILAMIN, MOESIN (phosphorylated and active; dephosphorylated and non-active), COFILIN (a, active; i, inactive), and ACTIN. Molecules recruited at the HIV-1-triggered capping regions are indicated by the c subscript, while non-capped molecules outside this region are indicated by the nc subscript. As it is assumed that gelsolin remains constant during the whole process, it is not incorporated as a variable in the model. Numbered arrows (from 1 to 13) are the processes included in the model, and dashed arrows are the interactions from the molecules to the processes (black are positive, red are negative). Gelsolin acts by remodeling the amount and size of actin filaments, so the total amount of actin and its reorganization is reduced by higher expression of gelsolin (negative influence of GELSOLIN on processes 4 and 10, see Material and Methods for details); furthermore, appropriate levels of gelsolin facilitate, through the orchestrated severing and remodeling of actin filaments, the capping of actin filaments at viral entry regions (positive effect of GELSOLIN on process 6). Continuous arrows serve as an additional explanation of molecular events taking place during the invasion. Thus, red arrows represent depolymerization of actin filaments, blue arrows represent components which assist the depolymerization of actin filaments (e.g., active cofilin and inactivation of moesin in fusion pore formation), the green arrow indicates actin monomer incorporation to the growing actin filaments, and the purple arrow represents the actin severing and remodeling by gelsolin, thereby controlling the size of actin filaments and the amount of filaments reorganized to the viral entry regions on the plasma membrane of target cells.
doi:10.1371/journal.pone.0103845.g001

Relevant processes

Valuable information can be obtained from the values of the processes' rate constants (K_n). Their values tell us about the relative velocity of the processes. In Figure 2 it can be seen that the values of the constants for processes 3, 5, 8, 9, and 13 are almost negligible. This implies that the system dynamics is virtually independent of them.

Processes 3 and 5 represent the spontaneous aggregation and disaggregation, respectively, of filamin to the cap. It thus seems that the dynamics of filamin comes mostly from the induced effect of the receptor capping (process 4).

Process 8 represents the spontaneous disaggregation of actin from the cap. We must therefore conclude that the disaggregation of the cap is due only to the positive signaling from the HIV-1-induced molecules. This model prediction is supported by the observations of Yoder et al. 2008 [7], where they established the influence of cofilin as being determinant of subsequent stages of the invasion process.

Another process which would appear to be of little, if any, relevance is process 9, which describes the activation of moesin by causes other than the HIV-1 induction. Instead, it is the HIV-1-induced activation of moesin which is of foremost importance, as stated by Barrero-Villar et al. 2009 [10].

The last of the processes that would appear to bear little relevance to the system dynamics is the activation of cofilin (process 13). The conclusion to be drawn here is that HIV-1 infection is not due to the activation of cofilin, but rather to the induced inactivation of cofilin (process 12). It should be noted that this is the situation observed in the active lymphocytes. The importance of this process in resting lymphocytes will be analyzed below.

The value of the rate constant of process 11 (the inactivation of moesin) deserves some attention. This constant has the larger of

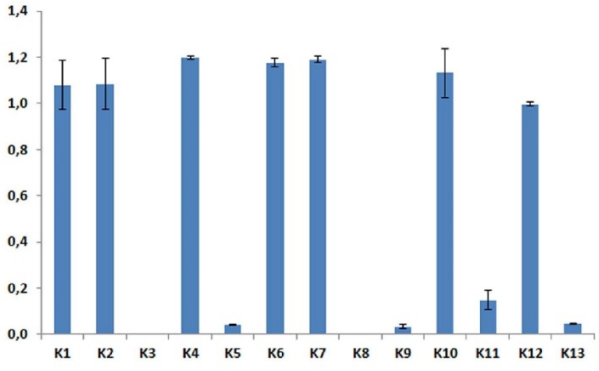

Figure 2. Rate constant values of the model processes. Rate constants from 1 to 13 correspond to the processes named from 1 to 13 in Figure 1. Mean values for the 12 selected solutions (see Material and Methods) are represented by the bars; standard deviation measures are included.
doi:10.1371/journal.pone.0103845.g002

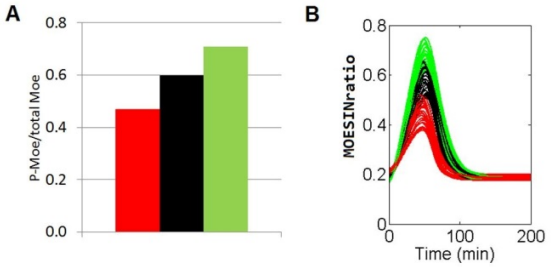

Figure 4. Model verification of the moesin role on the HIV-1 viral entry process. Panel A shows the total amount of functional moesin on the peak of activated moesin (at 90 minutes after infection) as determined by Barrero-Villar et al. 2009 [10]. Panel B shows the result of the MOESINratio value obtained from the model by modifying the parameter rate K_6 (related with the total amount of moesin). The red color refers to N-Moe (a dominant negative N-terminal fragment of the protein which impedes the physiological function of the intact moesin); the black refers to the control conditions and the green to the FL-Moe (an intact form of the protein which increases the total amount of moesin inside the lymphocyte).
doi:10.1371/journal.pone.0103845.g004

the low values (see Figure 2) of the rate constant. Some authors have claimed that the inactivation of moesin is necessary for the relaxation of the tension in the cap, which allows the virus to enter [10]. Our result shows that intense moesin inactivation is not a requisite for virus entry. Instead, stopping the moesin activation signaling is enough to lead to the disassembling of the actin cap (see Figure 3).

Moesin

The actin mobilization that occurs after activation is mediated by moesin, which activates the association of actin filaments to the lymphocyte membrane at the point of the HIV-1 infection. It has been shown that this process is of foremost importance [10].

Our model was able to reproduce the observation made by Barrero-Villar et al. 2009 [10] regarding the role of moesin during the invasion. This work evaluates the effect of changing the total amount of functional moesin (or overexpressing a dominant negative mutant of moesin) on the peak of activated moesin. As stated above [see the Mathematical Model section], these experiments can be simulated in our model by proportionally modifying the corresponding rate parameter K_6, which gives the

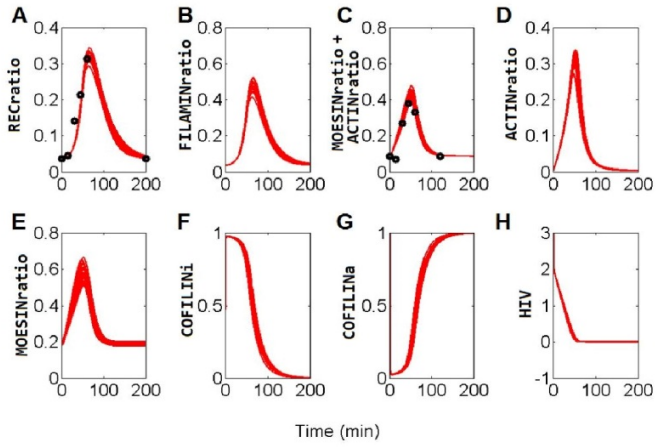

Figure 3. Model fitting and parameter estimation. These panels represent the 12 solutions - one for each of the predicted dynamics - which best predict the experimental ratio between total actin and total moesin as measured by Barrero-Villar et al. 2009 [10] (black solid circles). REC_{ratio}: receptor ratio inside the cap; FILAMIN $_{ratio}$: filamin-A ratio inside the cap; MOESIN $_{ratio}$+ACTIN $_{ratio}$: ratio of moesin within the cap over the total amount of actin and moesin, plus ratio of actin within the cap over the total amount of actin and moesin; ACTIN $_{ratio}$: proportion of actin in the cap; MOESIN $_{ratio}$: proportion of moesin in the cap; $COFILIN_i$: inactive cofilin ratio with respect to the total amount of cofilin; $COFILIN_a$: proportion of active cofilin over the total amount of cofilin; HIV: virus units per lymphocyte. The HIV variable correlates with the intensity of the signal inside the lymphocyte triggered by the virus.
doi:10.1371/journal.pone.0103845.g003

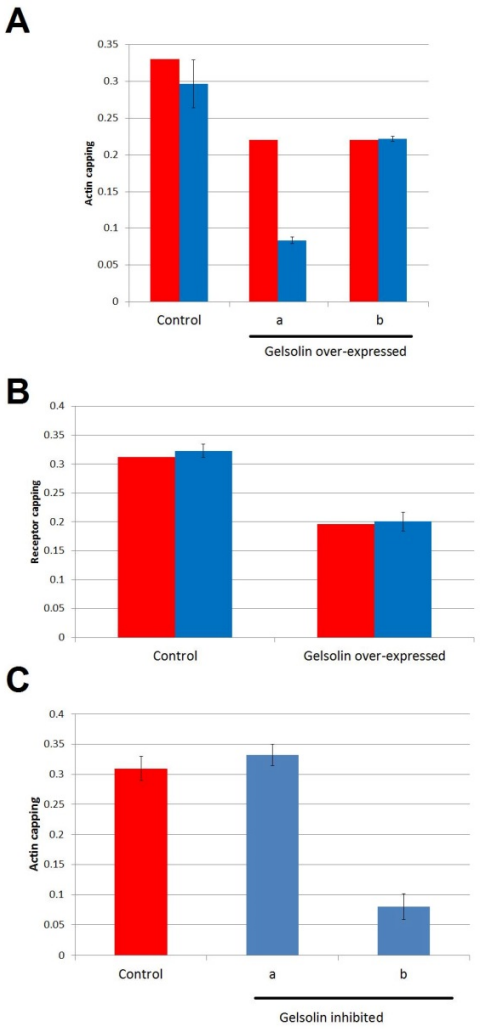

Figure 5. Comparison of the model predictions for two alternative roles of gelsolin in the cap formation. Red bars represent the experimental measurements of actin capping in a control situation or after over-expressing gelsolin. Blue bars represent the model prediction with the standard deviation of all solutions selected (see Material and Methods). **A.** A set of scenarios is evaluated in the model assuming different actin capping influences of gelsolin. In "a" K_7 was increased by 50%, assuming that gelsolin has a negative effect on actin capping. In "b", K_6 was increased to mimic a gelsolin activation on the actin capping by increasing the actin remodeling dynamics. **B.** Model verification of scenario "b" shown in panel A. The measured and the predicted maximum peak of the capping of receptors on the gelsolin over-expressed cell lines are shown. **C.** In "a" K_6, the parameter that models gelsolin stimulation of actin capping, takes the value of 0.75 times the value in Control; in "b" this figure is 0.5 times.
doi:10.1371/journal.pone.0103845.g005

total amount of functional moesin (see Supporting Information). The agreement of the model predictions regarding the moesin ratio value (Figure 4B) with the experimental maximum of the peak of activated moesin [Figure 4A] supports the reliability of our model as an integrated representation of the role of moesin in the process. We are thus provided with a suitable framework to assess the relative importance of the components of the system under different conditions.

Gelsolin

Gelsolin, an actin-severing protein related to actin cytoskeleton reorganization, plays a role in the cortical actin reorganization during HIV-1 invasion of lymphocytes.

Although gelsolin is not explicitly represented in the model, it is possible to use the model to predict how changes in gelsolin activity will affect the dynamics of the system. This can be achieved by translating the modified values of gelsolin into the kinetic rate parameter values and observing the predicted system behavior.

To do so, two types of changes should be made simultaneously in the model. First, we should increase the amount of gelsolin. It has been proposed that gelsolin has an actin-severing activity [29], and so this increase can be mimicked in our model by increasing the kinetic rate parameter of the actin disaggregation process 7 (K_7; see Figure 1). As an alternative to this proposed role of gelsolin, we also explored another mechanism proposed by García-Expósito et al. [14], which attributes to gelsolin a positive influence on the aggregation rate of actin to the cap. This was represented by an increase in K_6.

At the same time, based on the observations by García-Expósito et al. [14], where it is shown that the over-expression of gelsolin decreases the total actin expression by 30%, we changed the total actin activity in the model by reducing by 30% the rate constants of processes 4 and 10, which are the processes activated by actin (see the Mathematical Model section).

In Figure 5, the red bars show the actin capping measurements [14], while the blue bars correspond to the model predictions. Figure 5A shows the results obtained in K_7, K_6, K_4 and K_{10} following the changes described above.

The "control" condition shows that the model prediction is well within the observed range of values. In scenario "a" the values of K_4 and K_{10} have been lowered by 30% and at the same time K_7 has been raised by 50%. In scenario "b" K_4 and K_{10} have been lowered by 30% as before, but in this case, instead of K_7, the other simultaneous change was in K_6, which was increased by 27%. What can easily be observed is that there is a poor correlation between the experimental data and the data predicted by the model in scenario "a", but that both sets of results match in scenario "b". From these observations it can be concluded that our model supports the proposed role of gelsolin as an activator of the actin capping [14,29]. Accordingly, it also supports the actin-severing activity of gelsolin as instrumental in facilitating the aggregation of actin by producing actin filaments of optimum sizes and the appropriate amount of these filaments to be co-localized at virus-cell contact and entry regions.

In the same vein, other evidence provided in García-Expósito et al [14] offers additional support for the model's insights into the proposed role for gelsolin. It measures the maximum peak of the capping of receptors on the gelsolin over-expressed cell lines. When the experimental data (Figure 5B) are compared with the model predictions as described above (scenario "b" of Figure 5A), a good correlation between the experimental and model results can be observed. This model verification lends additional support to the proposed effect of gelsolin on the actin capping. As a whole, we can conclude from our model that gelsolin has two direct effects on actin: one by decreasing the total amount of actin in the lymphocyte and another through promoting the aggregation of actin in the cap.

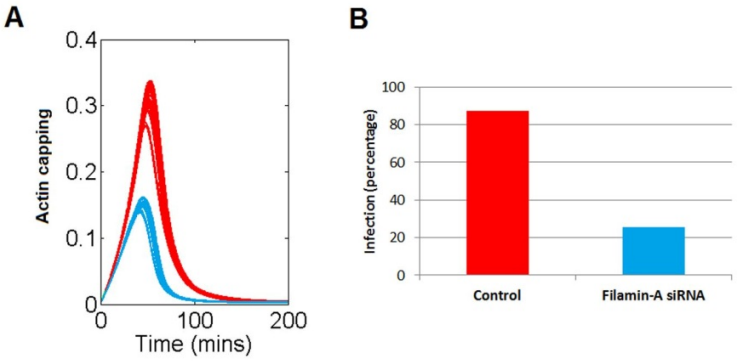

Figure 6. Model evaluation of the role of filamin on virus infectivity. Red curves and bars refer to the control situation, while the blue ones represent the predicted response after a decrease in the total amount of filamin-A. **A.** Virus-induced actin aggregation time course. **B.** Virus infectivity in control and filamin down-regulated conditions according to Jiménez-Baranda et al. 2007 [15].
doi:10.1371/journal.pone.0103845.g006

In the same work [14], it is reported that the inhibition of gelsolin negatively affects the efficiency of the virus-lymphocyte contact, and consequently impedes viral invasion. At the same time, it has been established that the amount of actin present in the cap correlates positively with infectivity [2]. In the following, we will use the actin in the cap as an indicator of the infectivity of the virus to evaluate the effect of inhibiting gelsolin in the model. As in the previous analysis, we will translate a decrease in gelsolin onto the parameters of the model in order to predict the impact of these changes on the actin capping.

Based in our previous conclusion, we can assume that a decrease in gelsolin activity will increase total actin expression (parameters K_4 and K_{10}) and reduce the rate of aggregation of actin filaments to the cap (process 6; Figure 1). In García-Expósito et al. 2013 [14], it is shown that specific knockdown of endogenous gelsolin (represented in our model as an inhibition of gelsolin function) increases the total actin expression by about 30%. Accordingly, we increased parameters K_4 and K_{10} by 30%. Figure 5C shows the actin capping prediction after these changes. The "control" bar is the predicted actin capping level before parameter changes. In scenario "a" we see the actin capping prediction when K_4 and K_{10} are raised by 30% and K_6 is lowered by 25%, while in scenario "b" K_4 and K_{10} remain the same as in "a" but K_6 is lowered by 50%. It can be interpreted that when the effect of gelsolin inhibition on the velocity of aggregation of actin (process 6) is above 25%, the infectivity is lower than in the physiological reference conditions, a finding that correlates well with observations [14].

Filamin-A

Filamin-A is an actin-crosslinking protein that binds to the CD4 and CXCR4 receptors after being induced by the signaling triggered by the association of the virus [15]. Interesting for the objectives of this study is the observation that the down-regulation of filamin impairs the infectivity of the virus (Jiménez-Baranda et al. 2007 [15]). Our model provides us with a tool to explore and explain this observation; for this purpose we will use, as before, the actin capping as an indicator of the infectivity. It is straightforward to simulate a decrease of the total amount of filamin-A ($FILAMIN_c$) in our model. This can be done through a simultaneous decrease in the rate constants of processes 1 and 6 (K_1 and K_6 respectively), which are regulated by $FILAMIN_c$ (see Figure 1).

Figure 6 shows the model prediction after simultaneous reduction in the values of K_1 and K_6. Figure 6A shows a decrease in the actin capping that correlates fairly well with the experimental observations (Figure 6B).

These facts constitute a mechanistic explanation, through the regulatory interactions measured by K_1 and K_6, of the observed reduction in the infectivity. This observation points to these regulatory interactions as potential therapeutic targets.

Cofilin

Cofilin is another of the key players in the HIV-1 infection process. This protein initially appears in its active form ($COFILIN_a$). $COFILIN_a$ stimulates the disaggregation of the actin from the cap through process 7 [see Figure 1] [7,16], thus contributing to the clearance of the cortical actin cap [7,16]. It is only after the pore formation that the inactive [phosphorylated] form is activated (dephosphorylated) ($COFILIN_i$) [7]. The inactivation of cofilin by the LIMK1 signaling pathway is represented in our model by a signal coming from HIV (process 12; Figure 1), but since this interaction has a limited temporal span, cofilin will be back in its active form at the later stages of the invasion (see panel G in Figure 3).

The model prediction on the behavior of the cofilin during the virus invasion can give us some insight into the role of this protein in the pore formation and the enhancement of HIV-1 infectivity.

Vorster et al. 2011 [22] have studied the LIMK1 signaling pathway leading to an early inactivation of cofilin, which promotes actin polymerization (see Figure 1). In the Figure 3G is represented the model predicted dynamics of the active cofilin. It can be seen the early inactivation of cofilin that rapidly falls from 1 to close to zero; behavior that tightly correlates with the sudden increase of the inactive of cofilin (Figure 3F).

Another work showed that knockdown of this LIMK1 signaling pathway decreased actin cap [23]. Again our model was able to reproduce this effect. Figure 7A and 7B displays the dynamics of the active cofilin and actin, respectively, before (black line) and after (red line) a 50% decrease in the strength of the LIMK1 signaling pathway. The model predicts a very slight decrease in the inactivation of cofilin, which, however, is enough to cause a decrease the actin cap to a third of the previous value. This prediction correlates very well with the results of Xu et al. 2012 [23] since it reproduces not only the observed fall in the peak of

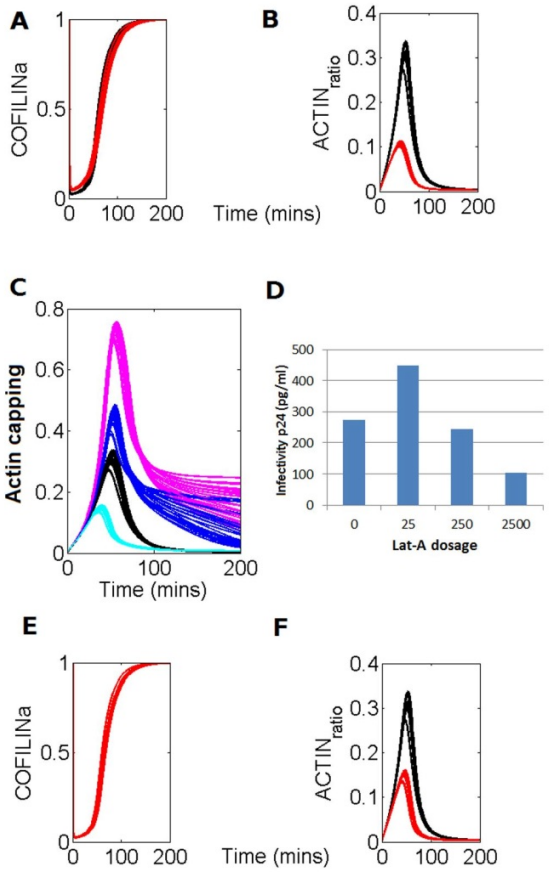

Figure 7. Model prediction and experimental verification of the LIMK1 signaling pathway knockdown and the actin polymerization inhibitor Lat-A on the virus infectivity. A. Black line displays the original solution showed in Figure 1 while the red line represents the model prediction of the COFILINa variable after inhibition of the LIMK signaling pathway by a 50%. **B.** Black line displays the original solution showed in Figure 1; red line represents the model prediction of the ACTIN variable after inhibition of the LIMK signaling pathway by a 50%. **C.** The black lines (control condition where cofilin is active before infection) show the model's predicted dynamics of the actin capping. Pink lines show the solutions obtained when the initial state of cofilin, just before infection, was inactive. Dark blue lines represent the predicted dynamics of the actin capping after the activation of virus signaling on the cofilin. Light blue lines represent an increase of the intensity of the activation signaling of cofilin by the virus **D.** Experimental measurements of infectivity of the virus in increased initial concentrations of the actin-severing factor Lat-A (Yoder et al. 2008, [7]). **E.** Black line displays the original solution showed in Figure 1 while the red line represents the model prediction of the COFILINa variable after inhibition of the WAVE2 signaling pathway by a 50%. **F.** Black line displays the original solution showed in Figure 1; red line represents the model prediction of the ACTIN variable after inhibition of the WAVE2 signaling pathway by a 50%.
doi:10.1371/journal.pone.0103845.g007

actin cap but also the observation of the almost negligible change in the ratio of activation of cofilin.

Yoder et al. 2008 [7], working with resting infected lymphocytes, have shown that there is a virus signaling triggered by the co-receptor that activates cofilin (process 13 in Figure 1). The same authors claim that this interaction is not present in active infected lymphocytes. In order to explain these observations, the same authors have proposed that the resting lymphocyte has a far more static cortical actin shell than the active lymphocyte [7]. Accordingly, this would be the cause of the impairment of the virus infectivity, since this cortical rigidity would impede the entry of the virus in the later stages of the invasion. In order to test this hypothesis in our model, which was built using information from experiments carried out with active infected lymphocytes [10], we have simulated a scenario in which the cortical actin situation mimics that of the resting lymphocyte. In the current model of the activated lymphocyte, it is assumed that all cofilin remains active, which also implies a very low rate of process 13. Thus, in order to test the hypothesis of Yoder et al. 2008 [7] in our model, we have to change the initial state of cofilin from active to inactive and, at the same time, to introduce a process allowing for the inactivation of cofilin in the absence of the virus. After making these changes (see Introducing an inactivation of cofilin process in Text S1), we set the rate of the new process to be 2% of the initial rate of activation of cofilin (process 13) in the activated lymphocytes in response to the virus signal. This value yields an initial inactivated cofilin of about 55% of the total actin.

Figure 7 shows the results of this exploration. In Figure 7C we see dynamics predicted by the model of the actin capping in different initial activation states of cofilin. It is observed that in conditions where cofilin remains inactive, thereby simulating a situation closer to that of a resting lymphocyte (pink curves in Figure 7C), the maximum peak of the actin present in the cap is higher than in the activated lymphocytes (black curves in Figure 7C). Also, the trend of the decay of this peak is slower when the cofilin is initially inactive as compared with the activated lymphocytes. There is additional evidence [17] that indicates that the virus invasion is less effective in resting lymphocytes than in active ones. Altogether these observations allow us to conclude that in spite of the higher peak of actin in the cap, it is the slower decay in the later stages of the invasion that serves as the restriction factor for the entry of the virus. This constitutes an "*a posteriori*", pragmatic experimental verification of the model.

Based on the above, we made additional explorations of the effects of the co-receptor signaling on the activation of cofilin. We included in the model the activation signal on the cofilin in the case of resting lymphocytes and subsequently evaluated the effects on the dynamics of the cap of increasing values of the rate constant K_{13} (rate constant of the activation of cofilin; see Figure 1). It was observed (Figure 7C) that the delay in the actin capping decay becomes less pronounced, thus making the virus invasion more effective (dark blue lines in Figure 7C).

This observation supports the hypothesis presented by different authors [7,22] about the role of co-receptor signaling and serves to clarify and quantify the role and importance of this signal. Also these model results correlate well with the above commented observations about the different actin dynamics and cortical F-actin amounts between non-cycling resting and cycling cell lines [8,14,30,31]. In this concern, chemokine-induced actin cytoskeleton reorganization has been associated to the establishment of HIV-1 latency in infected resting CD4+ T cells [32]. An observation reinforced by the fact that inhibition of chemokine receptor-associated ability to promote intracellular signals diminishes HIV-1 infection of resting CD4+ T cells [7].

The predicted effect of actin polymerization and/or the co-receptor signals on HIV-1 infection could be verified experimentally using related published data. For example, analyzing the effect of the actin-severing activity factor latrunculin A (Lat-A) on the virus infectivity. These results, which are shown in Figure 7D

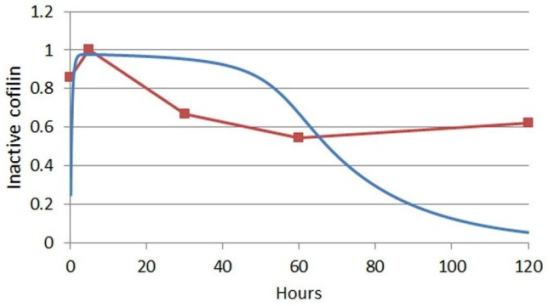

Figure 8. Model verification of the cofilin activity decay. Red dots and line represent the dynamics of the active cofilin during the invasion of HIV-1 as determined by Yoder et al. 2008 [7]. These observations are compared with the predicted dynamics (blue line) of the same model variable (Cof_a).
doi:10.1371/journal.pone.0103845.g008

(taken from Yoder et al. 2008, [7]), indicate that, in conditions of increasing dosages of the Lat-A factor, the infectivity of the virus increases after a later decay. This trend is in agreement with that predicted by our model (Figure 7C), since the increasing signal implemented in the model correlates with the increasing dosages of Lat-A: the initial increase in infectivity after a slight increase of the signal strength corresponds to a lesser delay of the actin cap. However, when the signaling intensity increases further, the model predicts a steeper decay of the actin in the cap (see light blue curves in Figure 7C), which negatively affects the invasion process and thus makes the virus infection less effective.

Considering the role of actin cytoskeleton, later after viral fusion and entry, it has been recently described that HIV-1 anchoring to CD4/CXCR4 or/CCR5 promotes transient actin polymerization in a WAVE2-Arp2/3-dependent manner, thereby favoring intracellular viral migration to the nucleus and therefore HIV-1 infection [33–35]. Hence, RNA interference of endogenous Arp2/3 perturbs actin nucleation and filament branching thereby diminishing viral intracellular trafficking to the nucleus and HIV-1 infection [21,35]. These events related to Arp2/3-mediated actin dynamics on HIV-1 infection occurs later after viral entry, and merit to be analyzed in a different piece of work that could be of relevance to engage with a recently reported work that highlights the importance of the intracellular traveling of intact viral capsides for HIV-1 infection and immune escape [36]. However, it is possible with the current modelling approach, to simulate the effect on the HIV infection of the inhibition of the WAVE2 signaling. As previously indicated process 12 represents the LIMK signaling that inactivates cofilin. In fact, the WAVE2 signal bifurcates from the LIMK one, although the WAVE2 signaling activates Arp2/3 instead [35]. Process 10 is activated from the same inputs as process 12 but can also be independently activated without inactivating cofilin. On the other hand, this same process 10 activates moesin and thus, induces the aggregation of actin filaments. Since this is a similar effect that the caused by Arp2/3 we could assume that the WAVE2 signaling is represented by this process. Figure 7F shows the model prediction of the effect of reducing the WAVE2 signaling by a 50%. It can be seen that this inhibition causes a reduction of the actin aggregation, an indicator in our model of the HIV infectivity. Furthermore, Figure 7A also shows that the inactive cofilin is not altered by the WAVE2 inhibition. This result constitutes a further validation of the model reliability. We are aware that these are preliminary results which are based on assumed suppositions. Future modeling exercises on this field through the use of new data not currently available will provide further insight of the role and importance of the WAVE2 signaling.

Finally, we compared the model predictions regarding the dynamics of the inactive cofilin with the experimental observations provided by Yoder et al. 2008 [7]. In Figure 8 it can be seen that there is a decay of this protein as the invasion progresses. Here, the model prediction is close to the experimental data only in the very first moments, after which it deviates significantly. Soon after the first 10 hours the predicted cofilin is above the experimental measurements. But it turns out that, in the light of the model hypothesis, these discrepancies help us gain a better comprehension of the role of the cellular factors that are operating in the invasion process. In our simplified model, it was assumed that cofilin is the only actin-severing factor which is regulated by HIV. However, it has been proposed that another actin-severing factor such as gelsolin might play a significant role in this process [14]. It is thus suggested that the observed discrepancies could be attributed to the role that these, somewhat neglected, actin-severing HIV-1 regulated factors play during invasion.

Our results and model integrate, and also appear to predict some reported evidences that indicate that the virus invasion is less effective in resting lymphocytes than in active ones [7,8,17]. Moreover and considering resting lymphocytes, memory CD4+ T cells appear to be more susceptible to be infected by HIV-1 compared to naïve cells [19,37–41]. Resting CD4+ T cells represent a major reservoir of HIV-1 [39,40], being responsible for viremia when antiretroviral therapy is stopped [40]. All these data could be explained in terms of actin dynamics and cortical F-actin amount, which is different between non-cycling resting and active primary cells or cycling cell lines, with a less or a highly dynamic actin cytoskeleton, respectively [14,30,31]. Therefore, HIV-1-triggered actin signaling seems critical for the infection of primary CD4+ T cells.

Altogether these data and our results prompted us to propose that the our model integrates and quantifies the processes and signaling events involved in early HIV-1 infection of T cells, and supports the role and importance of HIV-1 to overcome the cortical actin barrier for efficiently fuse and infect target cells. The model also predicts the observed different susceptibility of CD4+ T cells to be infected by HIV-1 in terms of their actin cytoskeleton dynamics and the amount of cortical actin reorganized.

Materials and Methods

Model Design

We used the findings and observations on the processes involved in early viral entry referred to above to construct a mathematical model of these processes. This representation integrates most of the available information on the components, pathways and regulatory interactions involved in the actin rearrangements and movements during lymphocyte invasion by HIV-1. Figure 1 shows, in a schematic form, the selection of variables, processes and signaling features used.

Regarding the variables, we distinguish between those components that are integrated within the cap (denoted with subscript c) and those that are outside the cap (subscript nc). The data for the HIV variable (from now HIV without the number 1 refers to the variable of the model) have been taken from cultures of lymphocytes [10]; accordingly, this variable is expressed in units of multiplicity of infection (MOI). It should be noted that the HIV is measured as the decay of the effective virus density; thus, this variable represents the intensity of the virus signaling in a lymphocyte culture. Accordingly, the model represents the

invasion at population level. Another relevant observation refers to cofilin. This protein, present in either its active or inactive form ($COFILIN_a$ and $COFILIN_i$, respectively), is measured in our model as the ratio of each form with respect to the total amount of cofilin present ($COFILIN_a$ and $COFILIN_i$).

In Figure 1, the wide arrows (numbered from 1 to 13) represent processes, while the black dashed arrows represent the referenced interactions, all of which are positive, among variables and processes.

The aggregation and disaggregation of the different forms of receptors and co-receptors (REC_{nc} and REC_c) during the HIV-1 junction is represented by processes 1 and 2, respectively. Aggregation process 1 is activated by the cap-aggregated filamin-A ($FILAMIN_c$) [15]. Processes 3 and 4 represent two different mobilization mechanisms of filamin-A to the cap. The former represents the non-regulated aggregation of filamin-A into the receptors assumed to be important, while the latter represents the aggregation of filamin-A influenced by the clustered receptors [15]. It has been shown [2,15] that the actin form ($ACTIN_c$) enhances aggregation process 4, through the interaction of filamin-A with the actin filaments. Process 5 represents the disaggregation of filamin-A from the cap.

The actin aggregation in the cap (process 6) is stimulated by filamin-A ($FILAMIN_c$) [15] and moesin [10]. We assume that the inverse process, the disaggregation of the actin from the cap, can occur either spontaneously (process 8) or be promoted by active cofilin ($cofilin_a$) through process 7 [7]. The spontaneous processes of association/disassociation of moesin with actin [10] are represented by processes 9 and 11. The activation of moesin by HIV-1 allows the actin to reorganize into the cell pole where the virus-cell contacts occur. This is where moesin anchors actin to the plasma membrane (this process is referred to as aggregation of moesin). In doing so, it facilitates the reorganization of CD4/CXCR4 or CCR5 receptors and the generation of the membrane tension needed for the virus-cell contacts and the fusion pore formation. During the formation of the fusion pore, moesin is inactivated, which relaxes the interaction of actin with the membrane and allows for the entry of the viral capsid. Process 10 represents the induced activation of moesin ($MOESIN_{nc}$) with actin to become $MOESIN_c$. This process is subject to two influences. One is the well-known effect of the virus on the activation process of the moesin to the cap [10]. This is represented through the interaction originating from the variable $COFILIN_i$, which in turn is activated by the HIV signaling. Although this interaction has not been reported at the intracellular level, it has been observed [7,10] that the accumulation of inactive cofilin in a culture occurs earlier than the accumulation of activated moesin. In addition, through this interaction the model is able to represent the observed time delay from the inactivation of cofilin to the activation of moesin.

On the other hand, it has been observed that, as the aggregated actin accumulates, its interaction with $MOESIN_c$ intensifies, thus exerting a positive influence on the moesin association [2,10].

Process 12 has a more complex meaning. It serves to represent the changes in the virus signaling (measured as a decay of the HIV) as well as the inactivation of COFILINa by the LIMK signaling pathway. We have chosen this form of representation since we want to illustrate the transmission of the signaling from the HIV-1 to the lymphocyte, represented as the inactivation of cofilin. Finally, process 13 represents the spontaneous transformation of the inactive cofilin ($COFILIN_i$) into its active form ($COFILIN_a$) [7].

The Mathematical Model

The dynamics of the invasion process of lymphocytes by HIV-1 was represented as a set of General Mass Action [42] ordinary differential equations in a mathematical model developed within the Power Law formalism [43]. This formalism allows for non-integer kinetic orders [42,43], but all rates were assumed to be linear. This assumption gives the formulation a mass action shape. A description of how the model equation was derived can be found in the Supporting Information (see equations S1 and S2 in Text S1).

Each of the processes described above (Figure 1; 1 to 13) has a rate kinetic constant parameter; these have been named K_1 to K_{13}. Figure 3 shows the corresponding values of the selected solutions for the model equations (mean value and standard deviation).

The regulatory interactions of a given variable on a given process (the red, dashed lines in Figure 1) are implemented in the model as having a linear effect on the corresponding rate process (see Text S1); that is, any change in the variable's value will translate proportionately to the rate of the regulated process. Accordingly, the effect of a change in the total amount of a given component in the model will be simulated in the model by changing the corresponding rate constants of the processes involved.

Experimental Data

The modeling task refers to the initial stages of the infection dynamics just before the virus capsid is introduced inside the lymphocyte. In a culture of lymphocytes this process lasts, on average, 90 minutes [10]. However, it should be noted that the entire process can be completed in just a few seconds in an isolated lymphocyte [10]; thus the rates here have to be interpreted as population rates.

The experimental data were drawn from the work done by Barrero-Villar et al. 2009 [10]. These authors used human activated CD4+/CXCR4+ T cells to be infected by HIV-1. They collected a series of temporal data of co-localization measurements of the CD4 and CXCR4 receptors, actin and moesin. Data of the CD4 and CXCR4 receptors were used to fit the REC_c variable of the model, while those of actin and the ERM proteins were used to fit the sum of the variables $ACTIN_c$ and $MOESIN_c$. In this calculation it is assumed that moesin is a representative component of the ERM proteins [9,10] (see Figure 3).

Parameter Estimation

As indicated above, the model parameters were determined by fitting the model to the experimental data drawn from Barrero-Villar et al. 2009 [10] (see Figure 3). Parameters were estimated using a heuristic evolutionary optimization algorithm (Modified Genetic Algorithm), run in Matlab, previously used and presented by us elsewhere [44–47]. Once the maximum allowed difference between data and simulation was determined (see Parameter estimation in Text S1), a set of 12 solutions that best predicted the experimental ratio between total actin and total moesin [10] were chosen (see Figure 3). The means of the parameter values for the 12 solutions are presented in Figure 3.

Sensitivity Analysis

Sensitivities represent the quantitative response of the model to small perturbations of physiological parameters; thus, sensitivity analysis is a powerful tool that provides a valuable indication of the robustness of a given model of system mathematical representation [48,49]. Robustness is a general property of biological systems. Since any actual biological system is permanently exposed to

perturbations from the environment, well-adapted systems should be able to conserve homeostasis. Accordingly, any useful biological model has to exhibit this property. A rule of thumb is that any sensitivity value under 1 means that the response of the system to perturbations is adequately controlled and biologically acceptable.

The sensitivity analysis yielded mean values below 0.1 for the sensitivities (see Sensitivity analysis in Text S1), which means that the model is robust enough to be considered an acceptable representation of the system.

Conclusions

The present work is, to our knowledge, the first attempt to model and quantify the complex molecular mechanisms and the dynamics of the key variables involved in early HIV-1 infection of lymphocytes. The model, based on recent findings about these mechanisms, integrates different experimental measurements into a mathematical framework that is able to compress all considered processes simultaneously. The model's reliability was tested against new sets of experimental data not used for its calibration and parameter estimation and was submitted to sensitivity analysis for assessment of its robustness.

In spite of the data limitations, the verifications carried out on some of the model's predictions allow us to answer some key questions about the infection process and the role of the interactions involved. The results of the model confirm the important role of moesin in mobilizing and concentrating actin filaments to the contact region of the virus, by linking them to the membrane in response to virus signaling. This means that stopping moesin activation signaling is sufficient for the release of the actin filaments from the cap. Moreover, the model confirms the hypothesis proposed by García-Expósito et al. 2013 [14] by which gelsolin, as an actin-severing factor, can improve the co-localization of actin during the invasion process, thus identifying gelsolin as a promising target to impede the invasion. We also confirmed the role of filamin-A in the actin capping by linking it to the receptors influenced by the receptor capping. It is also proposed that later cofilin activation by virus signaling facilitates the entry of the virus in resting lymphocytes by accelerating the decay of the aggregated actin as a restriction factor.

Finally, the works of Barrero-Villar et al. 2009 [10], García-Expósito et al. 2013 [14] and Yoder et al. 2008 [7] put forth the idea of active cortical actin being a factor in restricting the entry of the virus. Our model supports this hypothesis, and at the same time contributes to its understanding by specifying the phenomena by which the cortical actin impedes entry. The model also proposes that there could be actin-severing factors other than cofilin induced by the virus with importance in the entry mechanism, as recently proposed for the PDZ-adaptor protein syntenin-1 that seems to similarly regulate HIV-1 entry at a post-fusion stage [50].

Supporting Information

Figure S1 Dynamic sensitivities respecting the initial conditions of the variables.
(TIF)

Figure S2 Dynamic sensitivities respecting the parameters of the model.
(TIF)

Text S1
(DOCX)

Acknowledgments

The authors gratefully acknowledge Dr. Carlos González-Alcon for his helpful observations.

Author Contributions

Conceived and designed the experiments: GS AV-F NVT. Performed the experiments: GS. Analyzed the data: GS AV-F NVT. Contributed reagents/materials/analysis tools: GS AV-F NVT. Wrote the paper: GS NVT AV-F.

References

1. Liu Y, Belkina NV, Shaw S (2009) HIV infection of T cells: Actin-in and actin-out. Sci Signal 2: pe23.
2. Iyengar S (1998) Actin-dependent receptor colocalization required for human immunodeficiency virus entry into host cells. J Virol 72: 5251–5255.
3. Alkhatib G, Locati M, Kennedy PE, Murphy PM, Berger EA (1997) HIV-1 coreceptor activity of CCR5 and its inhibition by chemokines: independence from G protein signaling and importance of coreceptor downmodulation. Virology 234(2): 340–348;
4. Doranz BJ, Orsini MJ, Turner JD, Hoffman TL, Berson JF, et al. (1999) Identification of CXCR4 domains that support coreceptor and chemokine receptor functions. J Virol 73(4): 2752–2761
5. Gosling J, Monteclaro FS, Atchison RE, Arai H, Tsou CL, et al. (1997) Molecular uncoupling of C-C chemokine receptor 5-induced chemotaxis and signal transduction from HIV-1 coreceptor activity PNAS 94(10): 5061–5066
6. Aramori I, Ferguson SS, Bieniasz PD, Zhang J, Cullen B, et al. (1997) Molecular mechanism of desensitization of the chemokine receptor CCR-5: receptor signaling and internalization are dissociable from its role as an HIV-1 co-receptor. The EMBO J 16(15): 4606–4616
7. Yoder A, Yu D, Dong L, Iyer S, Xu X, et al. (2008) HIV envelope-CXCR4 signaling activates cofilin to overcome cortical actin restriction in resting CD4 T cells. Cell 134: 782–792.
8. Guo J, Wang W, Yu D, Wu Y (2011) Spinoculation Triggers Dynamic Actin and Cofilin Activity That Facilitates HIV-1 Infection of Transformed and Resting CD4 T Cells J Vir 85(19): 9824–9833
9. Mangeat P (1999) ERM proteins in cell adhesion and membrane dynamics. Trends Cell Biol 9: 289–289.
10. Barrero-Villar M, Cabrero JR, Gordon-Alonso M, Barroso-Gonzalez J, Alvarez-Losada S, et al. (2009) Moesin is required for HIV-1-induced CD4-CXCR4 interaction, F-actin redistribution, membrane fusion and viral infection in lymphocytes. J Cell Sci 122: 103–113.
11. Marsick BM, San Miguel-Ruiz JE, Letourneau PC (2012) Activation of Ezrin/Radixin/Moesin mediates attractive growth cone guidance through regulation of growth cone actin and adhesion receptors. The Journal of Neuroscience 32: 282–296.
12. Amieva MR (1999) Disruption of dynamic cell surface architecture of NIH3T3 fibroblasts by the N-terminal domains of moesin and ezrin: In vivo imaging with GFP fusion proteins. J Cell Sci 112 (Pt 1): 111–25.
13. Naghavi M, Valente S, Hatziioannou T, Wen K, Mott C, et al. (2007) Moesin regulates stable microtubule formation and limits retroviral infection in cultured cells. Embo j 26: 41–52.
14. García Expósito L, Ziglio S, Barroso González J, de Armas-Rillo L, Valera MS, et al. (2013) Gelsolin activity controls efficient early HIV-1 infection. Retrovirology 10: 39.
15. Jiménez-Baranda S, Gómez-Moutón C, Rojas A, Martínez-Prats L, Mira E, et al. (2007) Filamin-A regulates actin-dependent clustering of HIV receptors. Nat Cell Biol 9: 838–846.
16. Meberg P (2000) Signal-regulated ADF/cofilin activity and growth cone motility. Mol Neurobiol 21: 97–107.
17. Pan X, Baldauf H, Keppler O, Fackler O (2013) Restrictions to HIV-1 replication in resting CD4+ T lymphocytes. Cell Research 23: 876–885.
18. Gordón-Alonso M, Rocha-Perugini V, Álvarez S, Ursa A, Izquierdo-Useros N, et al. Actin-binding protein drebrin regulates HIV-1-triggered actin polymerization and viral infection. J Biol Chem 2013 Sep 27;288(39):28382–97.
19. Gordon-Alonso M, Rocha-Perugini V, Alvarez S, Moreno-Gonzalo O, Ursa A, et al. (2012) The PDZ-adaptor protein syntenin-1 regulates HIV-1 entry. Mol Biol Cell 23(12):2253–63
20. Pontow SE, Heyden NV, Wei S, Ratner L (2004) Actin cytoskeletal reorganizations and coreceptor-mediated activation of rac during human immunodeficiency virus-induced cell fusion. J Virol 78:7138–7147
21. Komano J, Miyauchi K, Matsuda Z, Yamamoto N (2004) Inhibiting the Arp2/3 complex limits infection of both intracellular mature vaccinia virus and primate lentiviruses. Mol Biol Cell 15:5197–5207

22. Vorster PJ, Guo J, Yoder A, Wang W, Zheng Y, et al. (2011) LIM Kinase 1 Modulated Cortical Actin and CXCR4 Cycling and Is Activated by HIV-1 Viral Infection. J Biol Chem 286(14): 12554–12564.
23. Xu X, Guo J, Vorster PJ, Wu Y (2012) Involvement of LIM kinase 1 in actin polarization in human CD4 T cells. Communicative & Integrative Biology 5(4): 381–383.
24. Mark S, Guo J, Wu Y (2012) The trinity of the cortical actin in the initiation of HIV-1 infection. Retrovirology 9: 45.
25. Dunia R (2013) Mathematical modeling of viral infection dynamics in spherical organs. J Math Biol 67: 1425–1455.
26. Nampala H, Luboobi LS, Mugisha JY, Obua C (2013) Mathematical modeling of liver enzyme elevation in HIV mono-infection. Math Biosci 242: 77–85.
27. Könnyû B, Sadiq SK, Turányi T, Hírmondó R, Müller B, et al. (2013) Gag-pol processing during HIV-1 virion maturation: A systems biology approach. PLoS Computational Biology 9: e1003103.
28. Phillips A (1996) Reduction of HIV concentration during acute infection: Independence from a specific immune response. Science 271: 497–499.
29. Cayota A, Vuillier F, Scott-Algara D, Dighiero G (1990) Preferential replication of HIV-1 in memory CD4+ subpopulation. Lancet 336:941
30. Wang W, Guo J, Yu D, Vorster PJ, Chen W, et al. (2012) A dichotomy in cortical actin and chemotactic actin activity between human memory and naive T cells contributes to their differential susceptibility to HIV-1 infection. J Biol Chem 287: 35455–35469
31. Permanyer M, Pauls E, Badia R, Esté JA, Ballana E (2013) The cortical actin determines different susceptibility of naïve and memory CD4+ T cells to HIV-1 cell-to-cell transmission and infection. PLoS One 8(11):e79221.
32. Cameron PU, Saleh S, Sallmann G, Solomon A, Wightman F, et al. (2010) Establishment of HIV-1 latency in resting CD4+ T cells depends on chemokine-induced changes in the actin cytoskeleton. Proc Natl Acad Sci USA 107:16934–16939
33. Spear M, Guo J, Turner A, Weifeng W, Yu D, et al. (2012) Arp2/3-Dependent Nuclear Migration in HIV-1 Infection of CD4 T Cells. Cold Spring Harbor, NY: The 2012 Retroviruses Meeting
34. Spear M, Guo J, Wu Y (2013) Novel anti-HIV therapeutics targeting chemokine receptors and actin regulatory pathways. Immunol Rev 256(1): 300–12.)
35. Spear M, Guo J, Turner A, Yu D, Wang W, et al. (2014) HIV-1 Triggers WAVE2 Phosphorylation in Primary CD4 T Cells and Macrophages, Mediating Arp2/3-dependent Nuclear Migration. J Biol Chem 289(10): 6949–6959.
36. Rasaiyaah J, Ping-Tan C, Fletcher AJ, Price AJ, Blondeau C, et al. (2013) HIV-1 evades innate immune recognition through specific cofactor recruitment. Nature 21;503(7476):402–5.
37. Roederer M, Raju PA, Mitra DK, Herzenberg LA, Herzenberg LA (1997) HIV does not replicate in naive CD4 T cells stimulated with CD3/CD28. J Clin Invest 99: 1555–1564
38. Spina CA, Prince HE, Richman DD (1997) Preferential replication of HIV-1 in the CD45RO memory cell subset of primary CD4 lymphocytes in vitro. J Clin Invest 99: 1774–1785
39. Schnittman SM, Lane HC, Greenhouse J, Justement JS, Baseler M, et al. (1990) Preferential infection of CD4+ memory T cells by human immunodeficiency virus type 1: evidence for a role in the selective T-cell functional defects observed in infected individuals. Proc Natl Acad Sci USA 87:6058–6062
40. Chomont N, El-Far M, Ancuta P, Trautmann L, Procopio FA (2009) HIV reservoir size and persistence are driven by T cell survival and homeostatic proliferation. Nat Med;15:893–900
41. Helbert MR, Walter J, L'Age J, Beverley PC (1997) HIV infection of CD45RA+ and CD45RO+ CD4+ T cells. Clin Exp Immunol 107:300–305.
42. Voit E (2000) Computational analysis of biochemical systems. A practical guide for biochemists and molecular biologists. Cambridge, UK: Cambridge University Press. 530 p.
43. Savageau MA (1976) Biochemical systems analysis: A study of function and design in molecular biology. USA: Addison-Wesley, Reading, Mass. 379 p.
44. Vera J, Bachmann J, Pfeifer AC, Becker V, Hormiga JA, et al. (2011) A systems biology approach to analyse amplification in the JAK2-STAT5 signalling pathway-6.
45. Hormiga J, González-Alcón C, Sevilla Á, Cánovas M, Torres N (2010) Quantitative analysis of the dynamic signaling pathway involved in the cAMP mediated induction of l-carnitine biosynthesis in E. coli cultures. Mol Biosyst 6: 699–710.
46. Santos GS, José Hormiga, Paula Arense, Manuel Cánovas, Néstor Torres (2012) Modelling and analysis of central metabolism operating regulatory interactions in salt stress conditions in a L-carnitine overproducing E. coli strain. Plos One 7: e34533.
47. Santos GS, Torres NV (2013) New targets for drug discovery against malaria. Plos One 8: e59968.
48. Frank PM (1978) Introduction to system sensitivity theory. New York: Academic Press.
49. Siljak DD (1969) Nonlinear system. The parameter analysis and design. New York: Wiley.
50. Burtnick L (1997) The crystal structure of plasma gelsolin: Implications for actin severing, capping, and nucleation. Cell 90: 661–670.

10. VIH – Supplementary Material

Model equations

Equations S4 and S5 show the mathematical model (see also Equations S7, in the Model equation derivation section).

Rec represents the component receptors (CD4 and CXCR4 or CCR5) while Fil, Act and Moe stand for filamin-A, F-actin and moesin, respectively.

Since the experimental data (Barrero-Villar et al. 2009; 4) used for the parameter estimation (see the Parameter estimation section) are given as amount of each component present in the cap over the total amount of the component, the model variables are expressed also in relative values. In these cases this is denoted by the subscript *r*. The additional subscript AM in the case of Act and Moe indicates that these variables are the ratio of each component in the cap over the total amount of actin and moesin. Cof_a and Cof_i represent active and inactive cofilin, repectively. Subscript *r* means here that its value is the ratio of active or inactive cofilin over to the total amount of cofilin.

The Cofilin inactivation rate depends on Cof_{ar} and is activated by the virus signaling (K_{12}·HIV·Cof_{ar}). It is thus assumed that, during the invasion, the activation of cofilin only depends on the Cof_{ir} (K_{13}·Cof_{ir}).

HIV represents the signaling intensity of the virus on the lymphocyte. It is measured as the proportion of lymphocytes that triggers the signal in response of virus. The model assumes that the HIV signaling inactivates cofilin and turn the signal off.

Process 12 in Figure 1 (K_{12}·HIV·Cof_{ar}) represents both, the inactivation of cofilin and the decrease in the intensity of HIV.

$$\frac{dRec_r}{dt} = K_1{}' \cdot Fil_r - K_1{}' \cdot Fil_r \cdot Rec_r - K_2 \cdot Rec_r$$

$$\frac{dFil_r}{dt} = K_4{}' \cdot Rec_r \cdot Act_{rAM} - K_4{}' \cdot Rec_r \cdot Act_{rAM} \cdot Fil_r + K_3 - K_3 \cdot Fil_r - K_5 \cdot Fil_r$$

$$\frac{dAct_{rAM}}{dt} = (1 - K_r) \cdot K_6' \cdot Fil_r \cdot Moe_{rAM} - K_6' \cdot Fil_r \cdot Moe_{rAM} \cdot Act_{rAM} - K_7{}' \cdot Cof_{ar} \cdot Act_{rAM} - K_8 \cdot Act_{rAM}$$

$$\frac{dMoe_{rAM}}{dt} = K_r \cdot K_9 - K_9 \cdot Moe_{rAM} + K_r \cdot K_{10}' \cdot Cof_{ir} \cdot Act_{rAM} - K_{10}{}' \cdot Cof_{ir} \cdot Act_{rAM} \cdot Moe_{rAM} - K_{11} \cdot Moe_{rAM}$$

$$\frac{dCof_{ar}}{dt} = K_{13} \cdot Cof_{ir} - K_{12} \cdot HIV \cdot Cof_{ar}$$

$$\frac{dHIV}{dt} = -K_{12} \cdot HIV \cdot Cof_{ar}$$

Equations S4

$$X_{nc} = X_t - X_c$$
$$\frac{dX_r}{dt} = \frac{1}{X_t} \cdot \frac{dX_c}{dt}$$
$$\frac{dAct_{rAM}}{dt} = \frac{Act_t}{Act_t + Mor_t} \cdot \frac{dAct_r}{dt}$$
$$\frac{dMoe_{rAM}}{dt} = \frac{Moe_t}{Act_t + Mor_t} \cdot \frac{dMoe_r}{dt}$$
$$K_r = \frac{Moe_t}{Moe_t + Act_t}$$
$$\frac{dCof_{ir}}{dt} = \frac{-dCof_{ar}}{dt}$$
$${K_1}' = K_1 \cdot Fil_t$$
$${K_4}' = K_4 \cdot \frac{1}{1 - K_r} \cdot Rec_t \cdot Act_t$$
$${K_6}' = K_6 \cdot \frac{1}{K_r} \cdot Fil_t \cdot Moe_t$$
$${K_7}' = K_7 \cdot Cof_t$$
$${K_{10}}' = K_{10} \cdot \frac{1}{1 - K_r} \cdot Cof_t \cdot Act_t$$

Equations S5

Parameter estimation

The model parameters (K_1 to K_{13} and K_r; K_r being the model parameter used to predict the ratio between total actin and total moesin) were with data from Barrero-Villar et al. 2009 (4). Data were presented as co-localization ratio of the components over the total amount in the cell (ERM proteins with actin, ERM proteins with CD4, REM proteins with CXCR4 and CD4 with CXCR4) during HIV invasion, measured at 0, 15, 30, 45 and 60 minutes after inoculation of the virus. Rec_r aggregates both CD4 and CXCR4 receptors. In this case the measurement of the co-localization of CD4 and CXCR4 was compared with the prediction of the variable Rec_r in the model. Moesin was used as a the representative component of the ERM proteins (Barrero-Villar et al. 2009; 4); thus co-localization data of actin and ERM proteins were used for comparison purposes with the prediction of the sum of the variables Moe_{rAM} and Act_{rAM} (see Figure 1).

Equation S6 shows the objective function used.

$$F_{obj} = \sqrt{\frac{\sum((D_{i,j} - M_{i,j})^2)}{N}}$$

Equation S6

In this equation $D_{i,j}$ represents the experimental data for time(i)=[0, 15, 30, 45, 60] (minutes), being j=1 the co-localization measure of CD4 and CXCR4 and j=2 the co-localization measure of actin and ERM proteins. $M_{i,j}$ represents the model prediction of the variable Rec for j=1 and the sum of Moe_{rAM} and Act_{rAM} for j=2. N is the number of elements of the matrix $D_{i,j}$.

In the process, the first stage was to find a model solution close enough in order to define the

maximum value of the objective function. Then, one hundred solutions with objective function values lower than the previous solution were chosen. Only those solutions that best predict the experimental value of the ratio of total actin and moesin (taken from confocal imaging in Barrero-Villar et al. 2009, 4) were selected.

In order to select the solutions best predicting the ratio between total actin and total moesin we randomly sampled 10 solutions from the total and determined if the confidence interval of K_r for the sample includes the experimental measure of the ratio of moesin over the total actin and moesin. Those solutions whose K_r confidence interval includes the experimental measure was primed and after 1000 samplings the solutions with the best scoring were selected. Only 12 solutions of the total of 100 were selected by this procedure that were used for the subsequent analysis (see Figure 2).

Sensitivity analysis

Figures S1 and S2 show the dynamic sensitivity values for the initial conditions and parameters, respectively.

Introducing an inactivation of cofilin process

To make the model able to simulate a resting lymphocyte we changed the model in order to represent that condition present of the resting lymphocyte which is relevant for the scope of the model, namely the mostly inactivated state of the cofilin (10). The model is initially in a steady situation, where cofilin is activated (see Figure 2), but when the HIV triggers the signaling, cofilin begins to decrease. To change the initial steady value of active cofilin, process 13, which denotes the rate of activation of cofilin, has to be decreased since this change will cause the initial steady value of active cofilin decrease. We set up the value of 55% of activated cofilin at the beginning; a value that can be obtained by decreasing the rate of process 13 down to 2% of the initial value.

Model derivation

Equations S7 show the first mathematical model presentation that results from the direct translation of the mechanistic model represented in Figure 1 to the Generalized Mass Action formalism (18).

In this representation variables not belonging to the cap are represented as the difference between total minus the amount in the cap (see Equations S8).

$$\frac{dRec_c}{dt} = K_1 \cdot Fil_c \cdot Rec_{nc} - K_2 \cdot Rec_c$$

$$\frac{dFil_c}{dt} = K_4 \cdot Rec_c \cdot Act_c \cdot Fil_{nc} + K_3 \cdot Fil_{nc} - K_5 \cdot Fil_c$$

$$\frac{dAct_c}{dt} = K_6 \cdot Fil_c \cdot Moe_c \cdot Act_{nc} - K_7 \cdot Co_{\ a} \cdot Act_c - K_8 \cdot Act_c$$

$$\frac{dMoe_c}{dt} = K_9 \cdot Moe_{nc} + K_{10} \cdot Cof_i \cdot Act_c \cdot Moe_{nc} - K_{11} \cdot Moe_c$$

$$\frac{dCof_a}{dt} = K_{13} \cdot Cof_i - K_{12} \cdot HIV \cdot Cof_a$$

$$\frac{dHIV}{dt} = -K_{12} \cdot HIV \cdot Cof_a$$

Equations S7

$$\frac{dRec_c}{dt} = K_1 \cdot Fil_c \cdot (Rec_t - Rec_c) - K_2 \cdot Rec_c$$

$$\frac{dFil_c}{dt} = K_4 \cdot Rec_c \cdot Act_c \cdot (Fil_t - Fil_c) + K_3 \cdot (Fil_t - Fil_c) - K_5 \cdot Fil_c$$

$$\frac{dAct_c}{dt} = K_6 \cdot Fil_c \cdot Moe_c \cdot (Act_t - Act_c) - K_7 \cdot Cof_a \cdot Act_c - K_8 \cdot Act_c$$

$$\frac{dMoe_c}{dt} = K_9 \cdot (Moe_t - Moe_c) + K_{10} \cdot Cof_i \cdot Act_c \cdot (Moe_t - Moe_c) - K_{11} \cdot Moe_c$$

$$\frac{dCof_a}{dt} = K_{13} \cdot Cof_i - K_{12} \cdot HIV \cdot Cof_a$$

$$\frac{dHIV}{dt} = -K_{12} \cdot HIV \cdot Cof_a$$

Equations S8

In order to represents the variables in relative values each variable is divided by the total amount of each component (Equations S9).

$$\frac{dRec_r}{dt} = K_1 \cdot \frac{Fil_t}{Fil_t} \cdot Fil_c - K_1 \cdot \frac{Fil_t}{Fil_t} \cdot Fil_c \cdot Rec_r - K_2 \cdot Rec_r$$

$$\frac{dFil_r}{dt} = K_4 \cdot \frac{Rec_t}{Rec_t} \cdot Rec_c \cdot \frac{Act_t}{Act_t} \cdot Act_c - K_4 \cdot \frac{Rec_t}{Re\ _t} \cdot Rec_c \cdot \frac{Act_t}{Act_t} \cdot Act_c \cdot Fil_r + \\ + K_3 - K_3 \cdot Fil_r - K_5 \cdot Fil_r$$

$$\frac{dAct_r}{dt} = K_6 \cdot \frac{Fil_t}{Fil_t} \cdot Fil_c \cdot \frac{Moe_t}{Moe_t} \cdot Moe_c - K_6 \cdot \frac{Fil_t}{Fil_t} \cdot Fil_c \cdot \frac{Moe_t}{Moe_t} \cdot Moe_c \cdot Act_r - \\ - K_7 \cdot \frac{Cof_t}{Cof_t} \cdot Cof_a \cdot Act_r - K_8 \cdot Act_r$$

$$\frac{dMoe_r}{dt} = K_9 \cdot -K_9 \cdot Moe_r + K_{10} \cdot \frac{Cof_t}{Cof_t} \cdot Cof_i \cdot \frac{Act_t}{Act_t} \cdot Act_c - \\ - K_{10} \cdot \frac{Cof_t}{Cof_t} \cdot Cof_i \cdot \frac{Act_t}{Act_t} \cdot Act_c \cdot Moe_r - K_{11} \cdot Moe_r$$

$$\frac{dCof_{ar}}{dt} = K_{13} \cdot Cof_{ir} - K_{12} \cdot HIV \cdot Cof_{ar}$$

$$\frac{dHIV}{dt} = -K_{12} \cdot HIV \cdot Cof_{ar}$$

Equations S9

By substitution of the variables as indicated in the Model equations paragraph we obtain Equations S10.

$$\frac{dRec_r}{dt} = K_1 \cdot Fil_t \cdot Fil_r - K_1 \cdot Fil_t \cdot Fil_r \cdot Rec_r - K_2 \cdot Rec_r$$

$$\frac{dFil_r}{dt} = K_4 \cdot Rec_t \cdot Act_t \cdot Rec_r \cdot Act_r - K_4 \cdot Rec_t \cdot Act_t \cdot Rec_r \cdot Act_r \cdot Fil_r + \\ + K_3 - K_3 \cdot Fil_r - K_5 \cdot Fil_r$$

$$\frac{dAct_r}{dt} = K_6 \cdot Fil_t \cdot Moe_t \cdot Fil_r \cdot Moe_r - K_6 \cdot Fil_t \cdot Moe_t \cdot Fil_r \cdot Moe_r \cdot Act_r - \\ - K_7 \cdot Cof_t \cdot Cof_{ar} \cdot Act_r - K_8 \cdot Act_r$$

$$\frac{dMoe_r}{dt} = K_9 - K_9 \cdot Moe_r + K_{10} \cdot Cof_t \cdot Act_t \cdot Cof_{ir} \cdot Act_r - \\ - K_{10} \cdot Cof_t \cdot Act_t \cdot Cof_{ir} \cdot Act_r \cdot Moe_r - K_{11} \cdot Moe_r$$

$$\frac{dCof_{ar}}{dt} = K_{13} \cdot Cof_{ir} - K_{12} \cdot HIV \cdot Cof_{ar}$$

$$\frac{dHIV}{dt} = -K_{12} \cdot HIV \cdot Cof_{ar}$$

Equations S10

Due to the nature of the experimental data used (4) variables Moe and Act are normalized by dividing by the summation of Moe and Act. Equation S11, S12 and S13 show the procedure followed.

$$\frac{dRec_r}{dt} = K_1 \cdot Fil_t \cdot Fil_r - K_1 \cdot Fil_t \cdot Fil_r \cdot Rec_r - K_2 \cdot Rec_r$$

$$\frac{dFil_r}{dt} = K_4 \cdot Rec_t \cdot Act_t \cdot Rec_r \cdot Act_r - K_4 \cdot Rec_t \cdot Act_t \cdot Rec_r \cdot Act_r \cdot Fil_r + \\ + K_3 - K_3 \cdot Fil_r - K_5 \cdot Fil_r$$

$$\frac{Act_t}{Act_t + Mor_t} \cdot \frac{dAct_r}{dt} = \frac{Act_t}{Act_t + Mor_t} \cdot (K_6 \cdot Fil_t \cdot Moe_t \cdot Fil_r \cdot Moe_r - \\ - K_6 \cdot Fil_t \cdot Moe_t \cdot Fil_r \cdot Moe_r \cdot Act_r - \\ - K_7 \cdot Cof_t \cdot Cof_{ar} \cdot Act_r - K_8 \cdot Act_r)$$

$$\frac{Moe_t}{Act_t + Mor_t} \cdot \frac{dMoe_r}{dt} = \frac{Moe_t}{Act_t + Mor_t} \cdot (K_9 - K_9 \cdot Moe_r + K_{10} \cdot Cof_t \cdot Act_t \cdot Cof_{ir} \cdot Act_r - \\ - K_{10} \cdot Cof_t \cdot Act_t \cdot Cof_{ir} \cdot Act_r \cdot Moe_r - K_{11} \cdot Moe_r)$$

$$\frac{dCof_{ar}}{dt} = K_{13} \cdot Cof_{ir} - K_{12} \cdot HIV \cdot Cof_{ar}$$

$$\frac{dHIV}{dt} = -K_{12} \cdot HIV \cdot Cof_{ar}$$

Equations S11

$$\frac{dRec_r}{dt} = K_1 \cdot Fil_t \cdot Fil_r - K_1 \cdot Fil_t \cdot Fil_r \cdot Rec_r - K_2 \cdot Rec_r$$

$$\frac{dFil_r}{dt} = K_4 \cdot Rec_t \cdot Act_t \cdot Rec_r \cdot \frac{Act_t + Mor_t}{Act_t} \cdot Act_{rAM} -$$

$$-K_4 \cdot Rec_t \cdot Act_t \cdot Rec_r \cdot \frac{Act_t + Mor_t}{Act_t} \cdot Act_{rAM} \cdot Fil_r + K_3 - K_3 \cdot Fil_r - K_5 \cdot Fil_r$$

$$\frac{dAct_{rAM}}{dt} = \frac{Act_t}{Act_t + Mor_t} \cdot (K_6 \cdot Fil_t \cdot Moe_t \cdot Fil_r \cdot \frac{Moe_t + Mor_t}{Act_t} \cdot Moe_{rAM} -$$

$$-K_6 \cdot Fil_t \cdot Moe_t \cdot Fil_r \cdot \frac{Moe_t + Mor_t}{Act_t} \cdot Moe_{rAM} \cdot \frac{Act_t + Mor_t}{Act_t} \cdot Act_{rAM} -$$

$$-K_7 \cdot Cof_t \cdot Cof_{ar} \cdot \frac{Act_t + Mor_t}{Act_t} \cdot Act_{rAM} - K_8 \cdot \frac{Act_t + Mor_t}{Act_t} \cdot Act_{rAM})$$

$$\frac{dMoe_{rAM}}{dt} = \frac{Moe_t}{Act_t + Mor_t} \cdot (K_9 - K_9 \cdot \frac{Moe_t + Mor_t}{Act_t} \cdot Moe_{rAM} +$$

$$+K_{10} \cdot Cof_t \cdot Act_t \cdot Cof_{ir} \cdot \frac{Act_t + Mor_t}{Act_t} \cdot Act_{rAM} -$$

$$-K_{10} \cdot Cof_t \cdot Act_t \cdot Cof_{ir} \cdot \frac{Act_t + Mor_t}{Act_t} \cdot Act_{rAM} \cdot \frac{Moe_t + Mor_t}{Act_t} \cdot Moe_{rAM} -$$

$$-K_{11} \cdot \frac{Moe_t + Mor_t}{Act_t} \cdot Moe_{rAM})$$

$$\frac{dCof_{ar}}{dt} = K_{13} \cdot Cof_{ir} - K_{12} \cdot HIV \cdot Cof_{ar}$$

$$\frac{dHIV}{dt} = -K_{12} \cdot HIV \cdot Cof_{ar}$$

Equations S12

$$\frac{dRec_r}{dt} = K_1 \cdot Fil_t \cdot Fil_r - K_1 \cdot Fil_t \cdot Fil_r \cdot Rec_r - K_2 \cdot Rec_r$$

$$\frac{dFil_r}{dt} = K_4 \cdot Rec_t \cdot Act_t \cdot Rec_r \cdot \frac{Act_t + Moe_t}{Act_t} \cdot Act_{rAM} -$$

$$-K_4 \cdot Rec_t \cdot Act_t \cdot Rec_r \cdot \frac{Act_t + Moe_t}{Act_t} \cdot Act_{rAM} \cdot Fil_r + K_3 - K_3 \cdot Fil_r - K_5 \cdot Fil_r$$

$$\frac{dAct_{rAM}}{dt} = \frac{Act_t}{Act_t + Moe_t} \cdot K_6 \cdot Fil_t \cdot Moe_t \cdot Fil_r \cdot \frac{Moe_t + Act_t}{Moe_t} \cdot Moe_{rAM} -$$

$$-K_6 \cdot Fil_t \cdot Moe_t \cdot Fil_r \cdot \frac{Moe_t + Act_t}{Moe_t} \cdot Moe_{rAM} \cdot Act_{rAM} -$$

$$-K_7 \cdot Cof_t \cdot Cof_{ar} \cdot Act_{rAM} - K_8 \cdot Act_{rAM}$$

$$\frac{dMoe_{rAM}}{dt} = \frac{Moe_t}{Act_t + Moe_t} \cdot K_9 - K_9 \cdot Moe_{rAM} +$$

$$+K_{10} \cdot Cof_t \cdot Act_t \cdot Cof_{ir} \cdot \frac{Moe_t}{Act_t + Moe_t} \cdot \frac{Act_t + Moe_t}{Act_t} \cdot Act_{rAM} -$$

$$-K_{10} \cdot Cof_t \cdot Act_t \cdot Cof_{ir} \cdot \frac{Act_t + Moe_t}{Act_t} \cdot Act_{rAM} \cdot Moe_{rAM} - K_{11} \cdot Moe_{rAM}$$

$$\frac{dCof_{ar}}{dt} = K_{13} \cdot Cof_{ir} - K_{12} \cdot HIV \cdot Cof_{ar}$$

$$\frac{dHIV}{dt} = -K_{12} \cdot HIV \cdot Cof_{ar}$$

Equations S13

K_r is a model constant representing the constant ratio value of total moesin over the summation of total moesin and actin.

$$\frac{dRec_r}{dt} = K_1 \cdot Fil_t \cdot Fil_r - K_1 \cdot Fil_t \cdot Fil_r \cdot Rec_r - K_2 \cdot Rec_r$$

$$\frac{dFil_r}{dt} = K_4 \cdot \frac{1}{1 - K_r} \cdot Rec_t \cdot Act_t \cdot Rec_r \cdot Act_{rAM} - K_4 \cdot \frac{1}{1 - K_r} \cdot Rec_t \cdot Act_t \cdot Rec_r \cdot Act_{rAM} \cdot Fil_r +$$

$$+K_3 - K_3 \cdot Fil_r - K_5 \cdot Fil_r$$

$$\frac{dAct_{rAM}}{dt} = \frac{(1 - K_r)}{K_r} \cdot K_6 \cdot Fil_t \cdot Moe_t \cdot Fil_r \cdot Moe_{rAM} -$$

$$-K_6 \cdot \frac{1}{K_r} \cdot Fil_t \cdot Moe_t \cdot Fil_r \cdot Moe_{rAM} \cdot Act_{rAM} - K_7 \cdot Cof_t \cdot Cof_{ar} \cdot Act_{rAM} - K_8 \cdot Act_{rAM}$$

$$\frac{dMoe_{rAM}}{dt} = K_r \cdot K_9 - K_9 \cdot Moe_{rAM} + \frac{K_r}{1 - K_r} \cdot K_{10} \cdot Cof_t \cdot Act_t \cdot Cof_{ir} \cdot Act_{rAM} -$$

$$-K_{10} \cdot \frac{1}{1 - K_r} \cdot Cof_t \cdot Act_t \cdot Cof_{ir} \cdot Act_{rAM} \cdot Moe_{rAM} - K_{11} \cdot Moe_{rAM}$$

$$\frac{dCof_{ar}}{dt} = K_{13} \cdot Cof_{ir} - K_{12} \cdot HIV \cdot Cof_{ar}$$

$$\frac{dHIV}{dt} = -K_{12} \cdot HIV \cdot Cof_{ar}$$

Equations S14

The total amount of each variable, that also remains constant are grouped all together in the constant (K_n).

$$\frac{dRec_r}{dt} = K_1' \cdot Fil_r - K_1' \cdot Fil_r \cdot Rec_r - K_2 \cdot Rec_r$$

$$\frac{dFil_r}{dt} = K_4' \cdot Rec_r \cdot Act_{rAM} - K_4' \cdot Rec_r \cdot Act_{rAM} \cdot Fil_r + \\ + K_3 - K_3 \cdot Fil_r - K_5 \cdot Fil_r$$

$$\frac{dAct_{rAM}}{dt} = (1 - K_r) \cdot K_6' \cdot Fil_r \cdot Moe_{rAM} - K_6' \cdot Fil_r \cdot Moe_{rAM} \cdot Act_{rAM} - \\ - K_7' \cdot Cof_{ar} \cdot Act_{rAM} - K_8 \cdot Act_{rAM}$$

$$\frac{dMoe_{rAM}}{dt} = K_r \cdot K_9 - K_9 \cdot Moe_{rAM} + K_r \cdot K_{10}' \cdot Cof_{ir} \cdot Act_{rAM} - \\ - K_{10}' \cdot Cof_{ir} \cdot Act_{rAM} \cdot Moe_{rAM} - K_{11} \cdot Moe_{rAM}$$

$$\frac{dCof_{ar}}{dt} = K_{13} \cdot Cof_{ir} - K_{12} \cdot HIV \cdot Cof_{ar}$$

$$\frac{dHIV}{dt} = -K_{12} \cdot HIV \cdot Cof_{ar}$$

Equations S15

$$X_{nc} = X_t - X_c$$

$$\frac{dX_r}{dt} = \frac{1}{X_t} \cdot \frac{dX_c}{dt}$$

$$\frac{dAct_{rAM}}{dt} = \frac{Act_t}{Act_t + Mor_t} \cdot \frac{dAct_r}{dt}$$

$$\frac{dMoe_{rAM}}{dt} = \frac{Moe_t}{Act_t + Mor_t} \cdot \frac{dMoe_r}{dt}$$

$$K_r = \frac{Moe_t}{Moe_t + Act_t}$$

$$\frac{dCof_{ir}}{dt} = \frac{-dCof_{ar}}{dt}$$

$$K_1' = K_1 \cdot Fil_t$$

$$K_4' = K_4 \cdot \frac{1}{1 - K_r} \cdot Rec_t \cdot Act_t$$

$$K_6' = K_6 \cdot \frac{1}{K_r} \cdot Fil_t \cdot Moe_t$$

$$K_7' = K_7 \cdot Cof_t$$

$$K_{10}' = K_{10} \cdot \frac{1}{1 - K_r} \cdot Cof_t \cdot Act_t$$

Equations S16

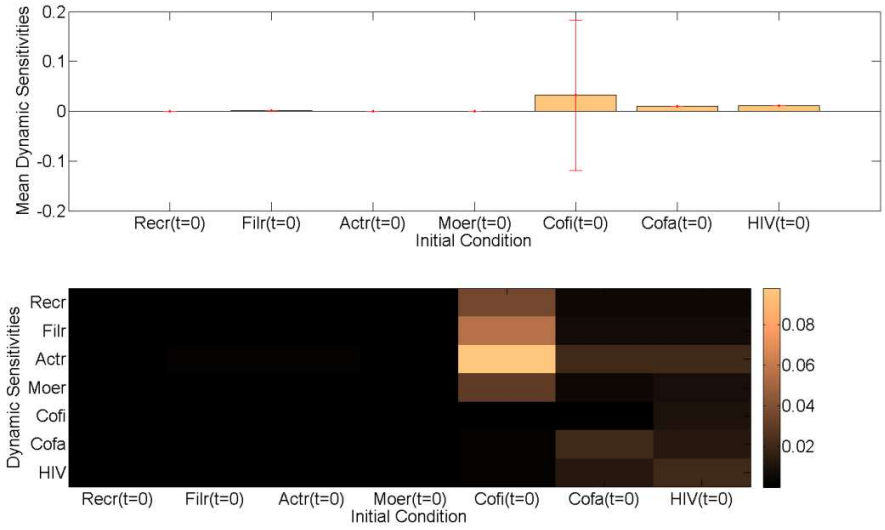

Figure S1. Dynamic sensitivities respecting the initial conditions of the variables.

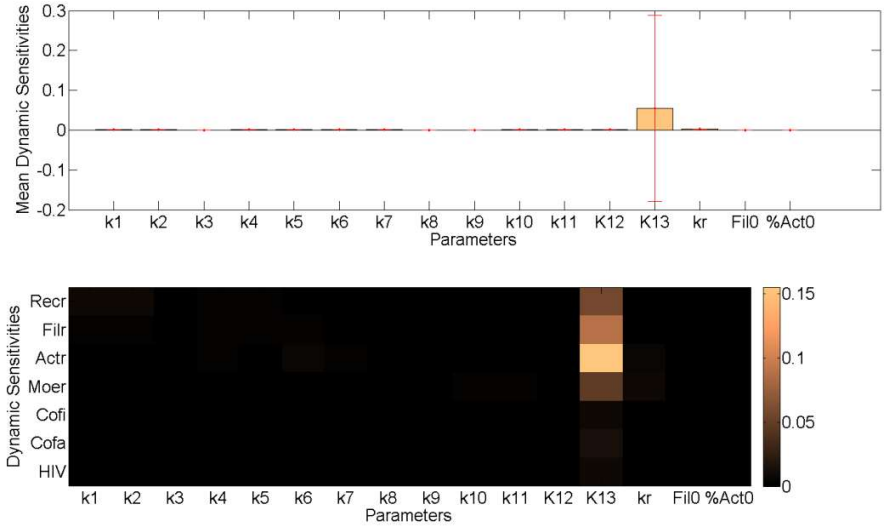

Figure S2. Dynamic sensitivities respecting the parameters of the model.

11. Alzheimer's disease - *Frontiers in Physiology*

DOI: 0.3389/fphys.2016.00090

frontiers in Physiology

ORIGINAL RESEARCH
published: 15 March 2016
doi: 10.3389/fphys.2016.00090

Lipid Raft Size and Lipid Mobility in Non-raft Domains Increase during Aging and Are Exacerbated in APP/PS1 Mice Model of Alzheimer's Disease. Predictions from an Agent-Based Mathematical Model

Guido Santos[1], *Mario Díaz*[2]* *and Néstor V. Torres*[1]*

[1] Systems Biology and Mathematical Modelling Group, Departamento de Bioquímica, Microbiología, Biología Celular y Genética, Instituto de Tecnologías Biomédicas, CIBICAN, Universidad de La Laguna, San Cristóbal de La Laguna, Spain, [2] Laboratorio de Fisiología y Biofísica de Membranas, Departamento de Biología Animal y Edafología y Geología, Facultad de Ciencias, Unidad Asociada de Investigación ULL-CSIC, Universidad de La Laguna, San Cristóbal de La Laguna, Spain

OPEN ACCESS

Edited by:
Ali Mobasheri,
University of Surrey, UK

Reviewed by:
Angel Catala,
Universidad Nacional de La Plata, Argentina
Garth L. Nicolson,
The Institute for Molecular Medicine, Inc., USA

***Correspondence:**
Mario Díaz
madiaz@ull.es;
Néstor V. Torres
ntorres@ull.edu.es

Specialty section:
This article was submitted to Membrane Physiology and Membrane Biophysics, a section of the journal Frontiers in Physiology

Received: *10 November 2015*
Accepted: *25 February 2016*
Published: *15 March 2016*

Citation:
Santos G, Díaz M and Torres NV (2016) Lipid Raft Size and Lipid Mobility in Non-raft Domains Increase during Aging and Are Exacerbated in APP/PS1 Mice Model of Alzheimer's Disease. Predictions from an Agent-Based Mathematical Model. Front. Physiol. 7:90. doi: 10.3389/fphys.2016.00090

A connection between lipid rafts and Alzheimer's disease has been studied during the last decades. Mathematical modeling approaches have recently been used to correlate the effects of lipid composition changes in the physicochemical properties of raft-like membranes. Here we propose an agent based model to assess the effect of lipid changes in lipid rafts on the evolution and progression of Alzheimer's disease using lipid profile data obtained in an established model of familial Alzheimer's disease. We have observed that lipid raft size and lipid mobility in non-raft domains are two main factors that increase during age and are accelerated in the transgenic Alzheimer's disease mouse model. The consequences of these changes are discussed in the context of neurotoxic amyloid β production. Our agent based model predicts that increasing sterols (mainly cholesterol) and long-chain polyunsaturated fatty acids (LCPUFA) (mainly DHA, docosahexaenoic acid) proportions in the membrane composition might delay the onset and progression of the disease.

Keywords: Alzheimer's disease, lipid rafts, membrane domains, lipid composition, mathematical modeling, agent based model, DHA, cholesterol

INTRODUCTION

Alzheimer's disease (AD) is the most frequent dementia worldwide, affecting more than 40 million people worldwide, with a prevalence of around 10% of the population above 65 years, which doubles every 10 years (Han and Han, 2014). AD is a degenerating irreversible disease that impairs memory and cognitive abilities and, at present, has no cure. AD occurs in two forms: the familial and the sporadic. Although the familial type is known to be associated to several well-defined genetic alterations (Tanzi, 2012; Loy et al., 2014), it does only explain <1% of AD cases currently diagnosed.

Abbreviations: η_{app}, apparent microviscosity; AD, Alzheimer's disease; APP, amyloid precursor protein; APP/PS1, double transgenic mice model of AD carrying mutated forms of APP and PSEN1; ARA, arachidonic acid; DHA, docosahexaenoic acid; DPH, 1,6-diphenyl-1,3,5-hexatriene.LCPUFA, long-chain polyunsaturated fatty acids; WT, wild-type littermates.

Conversely, in the sporadic AD, the most common neurodegenerative form (99% of all cases, Holtzman et al., 2011), the causes are largely unknown, and most evidence indicate that the genome has only a partial contribution on the onset of the disease.

One of the neuropathological hallmarks in AD is the occurrence of senile plaques in neuronal tissue, caused by the accumulation of the neurotoxic amyloid β (Aβ) proteins. Aβ peptides result from the sequential activity of two enzymes, namely β-secretase and γ-secretase (Blennow et al., 2006), which cleavage the transmembrane amyloid precursor protein (APP). According to the amyloidogenic hypothesis of AD, this is a major responsible cause of AD. Aβ peptides become pathological because the 1–40 and 1–42 fragments have a trend to oligomerize and fibrillate, and eventually to precipitate generating neurotoxic aggregates (Rushworth and Hooper, 2010; Claeysen et al., 2012; Hicks et al., 2012) designated as senile plaques. Alternatively, APP protein may be processed in a non-amyloidogenic manner by the α-secretase instead of β-secretase, which release non-amyloidogenic peptides, whose exact function in the normal brain has not been completely elucidated (Claeysen et al., 2012; Postina, 2012).

Furthermore, several recent reports have demonstrated a clear relationship between lipid rafts and amyloidogenic APP processing (reviewed in Rushworth and Hooper, 2010; Vetrivel and Thinakaran, 2010; Hicks et al., 2012). This relationship appears to be tightly linked to the lipid composition and physicochemical properties of lipid rafts (Martín et al., 2010), and is present even at the earliest stages of the disease (Fabelo et al., 2014; Díaz et al., 2015). Lipid rafts are membrane microdomains characterized by a differentiated lipid and protein composition that segregate within the plasma membrane (Brown and London, 2000; Simons and Ehehalt, 2002; Hicks et al., 2012). These chemical features, confer them some particular physicochemical properties including closer lipid packing, rather restricted lateral movement, higher viscosity, and differential thermodynamic properties, compared to the surrounding non-raft regions (Brown and London, 2000; Pike, 2006; Klymchenko and Kreder, 2014). Lipid composition of lipid rafts is the most important biochemical parameter in determining their structure and physicochemical properties (Sonnino and Prinetti, 2013). In particular, the proportion of cholesterol, a key element regarding their maintenance and stability is higher in these domains than in their surroundings. In addition, sphingolipids and saturated fatty acids are notably augmented compared to non-raft membrane domains, these contributing to the higher density, and degree of packing of lipid rafts (Simons and Ehehalt, 2002; Róg and Vattulainen, 2014). Further, long-chain polyunsaturated fatty acids (LCPUFA), including docosahexaenoic acid (DHA), and arachidonic acid (ARA) have been found to be present in lipid raft from nerve cells in the brain of both animal models and humans, yet to much lower amounts than in non-raft domains (Martín et al., 2010; Fabelo et al., 2012), but still they are essential to allow a degree of freedom required for protein-protein and lipid-protein interactions within lipid rafts.

In the context of AD, it is known that the molecules involved in the production of Aβ are segregated inside and outside lipid rafts. In particular, APP is mainly, but not exclusively, located outside the lipid rafts, while the β-secretase and γ-secretase predominantly reside inside (Rushworth and Hooper, 2010; Vetrivel and Thinakaran, 2010; Fabelo et al., 2014). These observations make lipid rafts principal actors in the study of the evolution of AD, since under non-pathological situations, APP is cut outside lipid rafts by the α-secretase and then inside by γ-secretase, while in the pathological condition, APP is sequentially cleavage inside raft domains by β- and γ-secretases (Vetrivel and Thinakaran, 2010; Hicks et al., 2012) This issue have been the subject of many studies aimed to elucidate the role of lipid rafts on the emergence of AD (Rushworth and Hooper, 2010; Zhou et al., 2014), although the precise role of lipid environment in the evolution of AD remains largely misunderstood.

One of the recent findings that pinpoint to lipid rafts as critical elements in the development of AD, has been the demonstration that lipid rafts are subjected to age-dependent changes, which has been coined as "lipid raft aging hypothesis" (Fabelo et al., 2012). Aging is known to be the main risk factor in the development of AD, and the available evidence have demonstrated that the time-course of lipid raft alterations are more pronounced and accelerated in APP/PS1 brains, a familial model of AD (Fabelo et al., 2012). Further, in line with these observations, we have recently demonstrated the presence of altered lipid rafts in human brains, even at the earliest stages of the disease (stages I/II of Braak and Braak). It has also been demonstrated that changes in lipid composition may alter the thermodynamic and physicochemical properties of lipid rafts (Müller et al., 2001; Wood et al., 2002; Diaz et al., 2012), which, on their own, can influence the evolution of AD. Interestingly, in animal models of familial AD, the induced increase in the production of Aβ provokes, in turn, changes in the observed lipid composition (Müller et al., 2001; Wood et al., 2002). Thus, it seems that the system is positively fed back to increase AD neuropathology. In this work we aim to elucidate how changes in lipid composition influence the biophysical properties of lipid rafts and non-raft domains, and how the alterations in lipid rafts might affect the rate of production of Aβ and plaque formation in the evolution of AD. How changes in lipid composition influence?

The experimental analysis of the structure, biophysical properties, dynamic behavior and composition of lipids rafts encompass many difficulties and require different, independent methodological approaches. In this regard the mathematical approach represents a valid and potentially useful alternative to the study of the physicochemical properties and dynamic behavior of lipid rafts and their relation with its composition under normal and pathological conditions. In recent years, several studies have been published using *in silico* approaches (Nicolau et al., 2006, 2007; Burrage et al., 2007; Richardson et al., 2007; Zhang et al., 2008; Herrera and Pantano, 2012; Soula et al., 2012). In some of these contributions, coarse grain models of cell membranes and lipid rafts have been reported (Marrink et al., 2008; Risselada and Marrink, 2008; Perlmutter and Sachs, 2009, 2011; Kucerka et al., 2010; Schäfer and Marrink, 2010; de Joannis et al., 2011; Risselada et al., 2011; Rosetti and Pastorino, 2011, 2012; Baoukina et al., 2012; Fischer et al., 2012; Muddana et al., 2012; Bennett and Tieleman, 2013; Davis et al., 2013; Hakobyan

and Heuer, 2013; Marrink and Tieleman, 2013; Barnoud et al., 2014). These studies have allowed unraveling the effects and roles of different types of lipids on the structure of these lipid domains, some of which were confirmed *in vitro* and verified experimentally using artificial membrane vesicles (Barenholz and Thompson, 1980; Finegold, 1993; Maulik and Shipley, 1996). However, at present, there has been no attempt to model the formation of lipid rafts and relate this to the pathogenesis of AD using real nerve cell membranes based on *in vivo* data, thereby using real nerve cell membranes. In this article, we propose a mathematical model to deal with this issue. We ask ourselves here on how the lipid composition of these domains influence the biophysical properties of lipid rafts (measured in terms of size, number, viscosity, and proportion of membrane lipid rafts) during normal aging and also along the evolution of senile plaque formation in animal models of AD. We also inquired on the effect of these biophysical changes on the emergence of AD neuropathology. Finally, based in the mathematical model predictions on the evolution of the physicochemical properties of these domains in AD, we were able to assess how changes in the lipid composition of raft and non-raft microdomains might restore membrane stability and modify AD-like pathogenic processes in an animal model of AD. Our findings lead us to sketch out potential therapies aiming to delay the pathological evolution of AD.

MATERIALS AND METHODS

Experimental Data

Isolation of Lipid Rafts and Non-raft Fractions

WT and APP/PS1 mice were sacrificed using carbon dioxide. All experimental manipulations were performed following the procedures authorized by the Ethics Committee for manipulation of laboratory animals at University of La Laguna (Spain). Frontal cortices of four animals from each age and genotype were dissected out and rapidly immersed in liquid nitrogen until membrane domains purification. Lipid raft and non-raft fractions were isolated by ultracentrifugation in sucrose gradients following the protocols described in detail in Diaz et al. (2012) and Fabelo et al. (2012). After differential centrifugation, fractions were collected from top to bottom. The first 2 mL fractions, contained the lipid rafts fractions, while the last fraction of the gradient and the pellet were collected and designated as non-raft fractions. Both fractions were routinely tested for purity in Western blot assays using different lipid raft and non-raft protein markers (i.e., anti-flotillin 1 for lipid rafts and anti-α1 subunit of the Na^+/K^+ ATPase for non-raft plasma membrane) following Fabelo et al. (2012).

Microviscosity Estimates of Lipid Rafts and Non-raft Domains

For this purpose we determined the steady-state fluorescence anisotropy of the non-polar 1,6-diphenyl-1,3,5-hexatriene (DPH) following the methodology described in detail in Diaz et al. (2012). Fluorescence polarization spectroscopy was performed using 355 nm excitation filter and 420 nm emission filter in an Appliskan multiplate reader (Thermo Scientific), equipped with appropriate polarizers. Controls containing the fluorophores alone were concurrently examined to correct for light scattering and intrinsic fluorescence. Microviscosity estimates (η) were derived from DPH steady-state anisotropy values using an adaptation of the Perrin equation (Lakowicz, 1999) for rotational depolarization of nonspherical fluorophore as described previously for DPH (de Laat et al., 1977).

Lipid Raft Lipid Composition

The lipid composition data (including lipid classes and fatty acids composition) from cortical lipid rafts, non-raft domains, and whole nerve cell membranes both in WT and APP/PS1 animals at the different ages (3, 6, 9, and 14 months) used here, have been recently published by our group (Diaz et al., 2012; Fabelo et al., 2012). Further, based on these data we have also delved into some relevant biophysical and thermodynamic properties of lipid rafts in these same genotypes and ages and reported them in Diaz et al. (2012).

Mathematical Model

According to our previous findings, the nerve cell membrane of cortical tissue in mouse and human brain has the form of an agent based model, as stated in the approaches previously presented elsewhere (Wurthner et al., 2000; Jicha and Markesbery, 2010). Here, we have considered each element representing a lipid group. Based on previous findings by our group on the involvement and importance of lipids in the development and progression of Alzheimer's disease in humans and transgenic mice models (Martín et al., 2010; Fabelo et al., 2012, 2014) we simplified the membrane lipid matrix and defined five groups of lipids: sterols (cholesterol and sterol esters); n-3 LCPUFA DHA and n-6 LCPUFA (mainly arachidonic acid, ARA); monoenoic fatty acids and saturated fatty acids. Although phospholipids in the plasma membrane are esterified by two fatty acids, we assumed that they move rather independently, which could be a reasonable assumption if there is no much segregation of fatty acids between LCPUFA-containing phospholipid (which in the brain are mainly esterifying phosphatydylethanolamine, phosphatydylserine, and phosphatidylinositol) (Farooqui et al., 2000).

The model represents a fragment of membrane semi-layer (200 × 200 units) with a torus-like topology. In this system, each lipid can interact with four neighbors (up, down, left, and right). There is a given interaction between each pair of neighboring lipids that are calculated based on the non-retarded and additive London-Van der Waals (LVW) attraction (Hamaker, 1937; Israelachvili, 2011). We can assume this type of interactions because forces between lipids within the semilayer occurs between lipid molecules which are very close to each other and because the medium is highly enriched in membrane lipids (see the recent updated review by Nicolson, 2014).

A key feature in the present agent model is the quantification of the interaction between and amongst lipid groups. In this model, each lipid is represented as the minimum cylinder that can contain it (see **Figure 1**). This approach has been proven to be useful to predict the behavior of lipids in the cell membrane

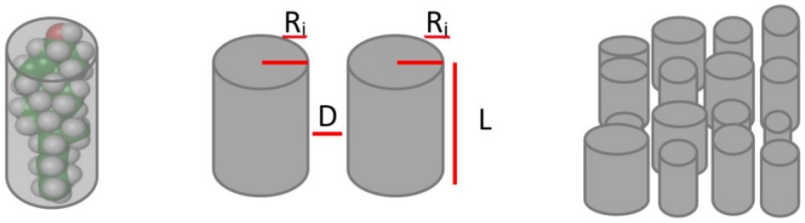

FIGURE 1 | Lipid groups representation. Lipid molecules are simplified as the cylinder that best fits their volume and then are parametrized by their radiuses (R_i, R_j), lengths (L) and mean distance between them (D). Finally they are disposed in a matrix to simulate the cell membrane.

(Kumar, 1991). Accordingly, the LVW interaction between them is given by Equation 1 (Israelachvili, 2011).

$$LVW_{i,j} = \frac{AL}{12\sqrt{2}D^{3/2}}\left(\frac{R_iR_j}{R_i + R_j}\right)^{1/2} \quad (1)$$

In this Equation, A is the Hamaker constant, with a value between 10^{-20} and 10^{-19} J (in vacuum). L represents the length of each lipid. Its magnitude (in Å) corresponds to the length of the lower interacting lipid. D is the distance between lipids (in Å) while R_i and R_j represent the radiuses (Å) of the different lipid groups. In the case of saturated fatty acids, its length and width were determined by using Equations (2) and (3) (Israelachvili, 2011):

$$length = 0.154 + 0.1265n\ nm \quad (2)$$
$$volume = 27.4 + 26.9n \cdot 10^{-3}nm^3 \quad (3)$$

where n is the number of carbons; this value being the mean number of carbons in the fatty acids in each lipid group. In the case of unsaturated fatty acids the double bonds increase the volume of the minimum cylinder, as double bonds increase the width of the fatty acids. We have calculated their width based in the number of double bonds and their physicochemical parameters (see Prediction of lipids rafts section). Using Equation 1 and the physicochemical parameters for each lipid, the matrix of interaction forces between pairs of lipids ($LVW_{i,j}$) was determined. Here, it is worth noting that these physical parameters do not represent the actual dimensions of the molecules, but describe the dimension of the cylinder which best represent the interaction of a lipid group in the context of the cell membrane.

In our model, two adjacent lipids can exchange their positions, the direction of any movement being random. Based in the values of the matrix of interaction ($LVW_{i,j}$) we were able to assign a probability of movement for each lipid group. For the calculation of this probability we took into account the force keeping each lipid in its current position, this being the sum of all forces acting on the exchanging lipids of the four surrounding molecules. In the case of sphingolipids an additional parameter is required since it is necessary to consider the interdigitation between the two membrane leaflets demonstrated for this lipid class (Maulik et al., 1986) (see later).

The above procedure provides two values of force, which are the corresponding energies that keep each lipid in its current position. In any instance switch movements will occur if both values are lower than a given threshold defined by a uniform probability distribution. This procedure lets more interchanges between pairs of lipids that have lower interacting forces in their current state. Further, each lipid-lipid interaction have a chance to switch, being the lipid to be switched selected randomly.

Model Mobility and Lipid Rafts

The proposed model was designed to predict the occurrence of lipid rafts, the influence of the membrane lipid composition on this process, the time-course of the changes associated with aging and genotype, and the potential changes in their physicochemical parameters.

We define mobility within the lipid rafts as the quotient number of switching movements observed in each lipid in a 50 times iterations set over 100. Lipids with no movement's restrictions will have 100 switching movements in average (2 movements in each iteration), so values of mobility close to one represent free moving lipids. Accordingly, a mobility value of 1 indicates that the molecule is free to move through, while values lower than 1 indicate the existence of some sort of switching restrictions. This mobility model based measurements can be easily compared with the observed membrane microviscosities measured in nerve cells from animal models, using anisotropy fluorescence spectroscopy (de Laat et al., 1977; Lakowicz, 1999). Repeated model runs showed that a mobility value of 0.36 well describes those regions that can be considered as lipid rafts. Accordingly, regions with mobility values below this threshold will be considered as lipid rafts and values above this value as non-raft regions.

We were able to estimate the model physicochemical parameters (longitude and width) for each group of the model lipids to be used in our model. For this purpose we make use of published data of the membrane lipid composition of neocortex in WT and APP/PS1 mice (Fabelo et al., 2012). Also, based on these data we determined the threshold mobility value to define lipid rafts. For this determination, we used the above indicated initial parameters values. In the case of cholesterol, the physicochemical parameters were estimated using the language of molecular structure modeling *Jmol*. These parameters, which were refined within intervals, were: (1) the dependence of lipid

width on the number of double bonds and (2) the width and length of the sterol group. First, an initial search of a 50% above and below the initial value of all parameters let us to restrict the search to intervals where lipid rafts were observed. The best solution predicting the lipid composition of lipid rafts under all conditions found in 2000 solutions was selected.

Estimation of the Number and Size of Lipid Rafts

In order to obtain a measure of the mean size and the approximate number of lipid rafts predicted by the model under each situation. Some properties in the domains must be assumed, these are: (1) Membrane domains are round-shaped, and (2) All lipid raft domains would have the same size.

These assumptions are not very far from the actual situation (see **Figure 3**). Under assumption 1, the area and the perimeter of each domain can be estimated using circle geometry functions, as follows:

$$\text{Area (A)} = \pi \cdot \text{radius}^2 \quad (4)$$

$$\text{Perimeter (P)} = 2\pi \cdot \text{radius} \quad (5)$$

On the other hand, under assumption 2, the total perimeter of raft domains as well as their total area can be obtained by counting the number of domains (n), and applying the following equations:

$$\text{Total area} = \text{area (A)} \cdot \text{n} \quad (6)$$

$$\text{Total perimeter} = \text{perimeter (P)} \cdot \text{n} \quad (7)$$

Total area and total perimeter can be calculated from data on **Figure 3**. Total area is just the number of spots on the matrix which have a mobility value lower than a previously defined threshold value. The total perimeter was calculated by summing the outcomes of differential function applied to the data of lipid raft identification matrix from left to right and from up to down. The lipid rafts identification matrix was obtained transforming the data of **Figure 3** on a matrix of the same dimension, in which a value of one is assigned when the mobility was under the defined threshold value and zero when it did not.

Once the total perimeter and total area were obtained, Equations (6) and (7) can be replaced on Equations (4) and (5), providing a system of two equations with two unknowns variables (number and radius), which can be easily solved. These number (n) and radius (r) values correspond to the estimations of the number and size of lipid raft membrane domains, respectively.

$$n = \frac{P^2}{4 \cdot \pi \cdot A} \quad (8)$$

$$r = \frac{2 \cdot A}{P} \quad (9)$$

In these equations, A and P represent the area and perimeter of the lipid rafts, respectively. Estimates of changes in surface area of non-rafts regions can be obtained by following the changes in radius size of lipid domains (r), as we are considering a piece of membrane of constant surface. Increasing values of lipid rafts size (r) result in decreasing value of surface area of non-rafts regions.

The Possibility that AD-like Pathology can be Modified

Based in the model, it was possible to propose a set of changes in the lipid composition of cell membrane microdomains which could eventually displace the parameters obtained for old transgenic APP/PS1 animals toward the values corresponding to those of young Wild-type animals.

The initial pathological condition chosen was that of 9 months old transgenic APP/PS1 mice, which corresponds to a pathological but, not irreversible condition (Diaz et al., 2012; Fabelo et al., 2012). The final, healthy condition, we wanted to move to, was that of 3 months Wild-type mice. To accomplish this, we changed in the mathematical model the composition of each lipid group on the cell membrane domains of the 9 months transgenic mice by 50% in the direction opposing the pathological change in lipid rafts from transgenic mice.

RESULTS

Insights into Lipid Raft Composition

The comparison of some observed and model-predicted membrane features are shown in **Figure 2**. **Figures 2B,C** compare the experimentally observed data and the predicted model composition for lipid rafts in WT and APP/PS1 mice (Fabelo et al., 2012), respectively. In addition, it can be seen (**Figure 2A**) the differences between the observed composition of selected groups of lipids in the whole membrane (Diaz et al., 2012) and the model-predicted composition of the lipid raft (**Figure 2C**).

Based in the model, we have also assessed the predicted membrane lipid structure in WT and APP/PS1 mice under different experimental conditions, including the changes that are found in aging animals. The results are shown in **Figure 3**.

As it can be seen, the model was able to predict some of the experimental observations. First, there was a good agreement with the observed decrease in the concentration of sterols in lipid rafts with respect to the whole nerve cell membrane. Also, the model reproduced well the observed increase of saturated fatty acids and sphingolipids within the lipid rafts. Finally, the model also showed that the composition of monoenoic fatty acids, DHA, and n-6 LCPUFA on rafts domains and total membrane followed the changes demonstrated experimentally in both Wild-type and APP/PS1 mice (Fabelo et al., 2012).

Sphingolipids are essential and characteristic components of lipid rafts, and partly responsible for the higher degree of lateral packing of lipid within these domains endowing them with a limited lateral mobility (Maulik et al., 1986). Compared with other phospholipids, i.e., phosphatidylcholine, the main structural dissimilarity is chain length in sphingomyelins, where the N-acyl group (usually highly saturated) can be up to 10 carbons longer than the sphingosine (Barenholz and Thompson, 1980). Such a chain disparity give sphingomyelins the unique ability to form both intra- and intermolecular hydrogen bonding and increases the hydrophobic interaction with other membrane components within the membrane plane, and more importantly this property enables sphingomyelins to

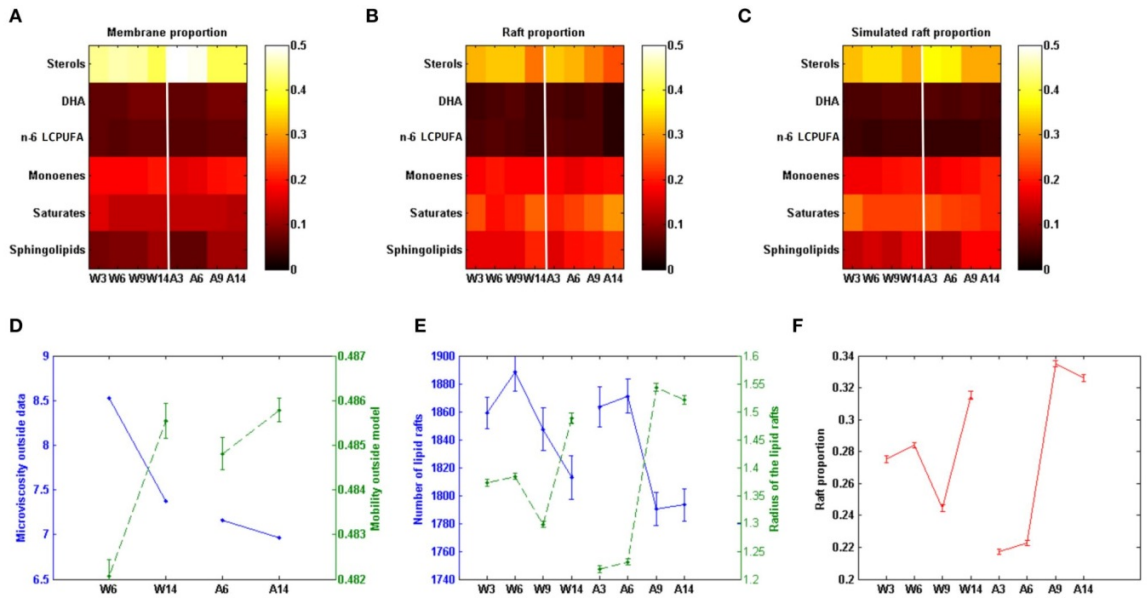

FIGURE 2 | Comparison of experimental and model predicted membrane features. (A) Lipid groups composition in cell membrane in different conditions (data on Table S1). **(B)** Lipid groups composition in lipid rafts in different conditions (data on Table S2). **(C)** Model predicted lipid rafts composition (data on Table S3). **(D)** Comparison between model based values of mobility (dashed line) and experimental values of microviscosity (continuous line) in the membrane domain (data on Table S4). **(E)** Model predicted number (continuous line) and size (dashed line, as measured by the mean radius) of lipid rafts (data on Table S5). **(F)** Model prediction rafts proportion in membrane. W3; W6; W9; W14: Wild-type mice at 3, 6, 9, and 14 months of age. A3; A6; A9; A14: APP/PS1 transgenic mice of 3, 6, 9, and 14 months of age, respectively. Vertical red lines separate Wild-type and AD induced conditions (data on Table S6). All the experimental data in this figure were taken from Fabelo et al. (2012).

participate in transbilayer hydrocarbon interdigitation (Slotte, 1999; Sonnino and Prinetti, 2010). In order to characterize and represent this feature we defined the interdigitating parameter and introduced a parameter that decrease its switching between the membrane leaflets, as most sphingomyelin is located in the external leaflets of the membrane. We found that the model predicts that the sphingolipids probability of switching is ∼10% lower than for the other lipid groups.

Lipid Shape Parameters and Van der Waals Forces

Table 1 shows the estimated parameters of the set of cylinders that better encase the membrane lipids considered in this study, these including length, width, mean intermolecular distance, and the Hamaker constant.

Other relevant parameters for the model are the interaction forces between the same lipid molecules. These interaction values were calculated as indicated by Equation 1 and are shown in **Table 2**. It can be seen that the strongest interactions occur for saturated fatty acids and sphingolipids, and the weakest for n-6 LCPUFA.

Also relevant are the interactions amongst different lipid groups (**Table 3**). In this case, the strongest interactions are observed for sphingolipids and saturated fatty acids. On the other hand, the n-6 LCPUFA group displays the lowest interaction values. Overall, these estimates indicate that lipid raft domains exhibit stronger interaction forces because their particular enrichment in sphingolipids, saturates, and sterols, which is in agreement the restricted lateral mobility and higher compressibility compared to non-raft regions, which, in turn, are depleted of sphingolipids but enriched in polyunsaturated (n-3 and n-6 LCPUFA) whose pair interacting forces are weakest. Therefore, based on the biochemical composition of the model can predict phase segregation and domain formation in nerve cell membranes.

Microviscosity Quantification in Rafts and Non-rafts Fractions Membranes

The experimentally determined values of apparent microviscosity (η_{app}) in lipid rafts and non-raft fractions (see Section Materials and Methods) are shown in **Table 4**. Microviscosity is a membrane environmental property that measures the difficulty for a probe to move in the membrane. We have used the DPH probe as a hydrophobic probe that buries within the membrane core. As it can be seen in **Table 4**, lipid rafts display higher values of η_{app} compared to non-raft fractions in all groups of animals irrespective of their genotype. However, these values tend to be higher in lipid rafts from APP/PS1 transgenic AD mice. Moreover, paralleling these observations it can be observed that in both genotypes,

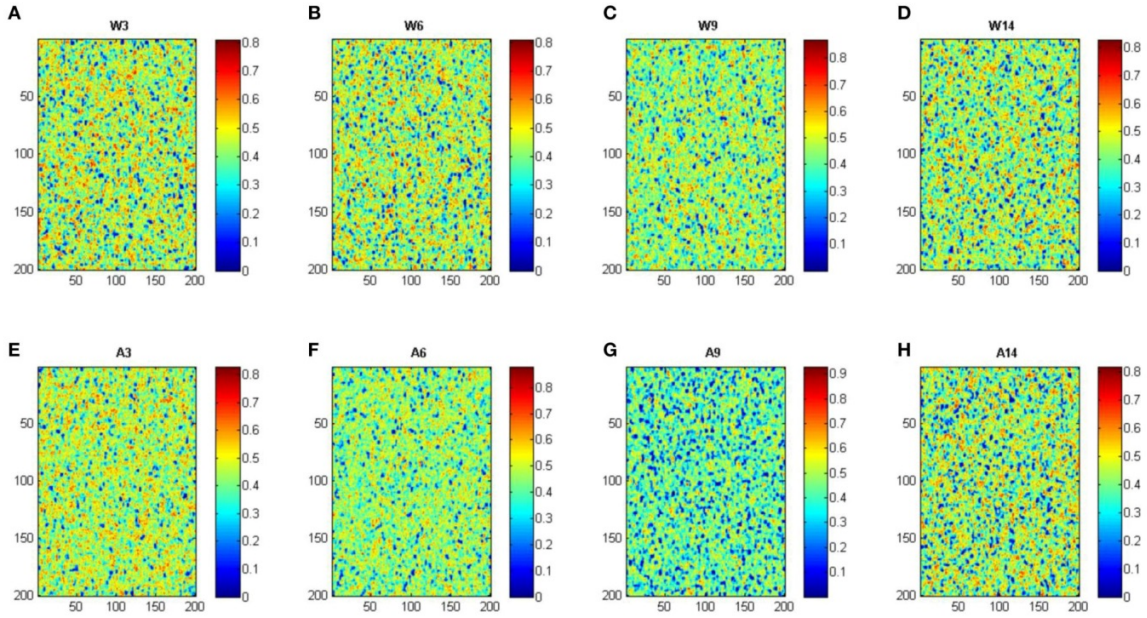

FIGURE 3 | Simulation of cell membrane lipid composition under different conditions. W, Wild-type mice; A, APP/PS1 transgenic mice; ages, 3, 6, 9, and 14 months. Color scale indicates mobility. Panels **(A–H)** corresponds to conditions: wild-type 3, 6, 9, and 14 months, APP/PS1 3, 6, 9, and 14 months, respectively.

TABLE 1 | Data based estimation (Diaz et al., 2012) of the cylinders representing the modeled lipid membrane.

	Width (radius Å)	Length (Å)
Sterols	5.94	19.99
DHA	6.74	19.01
n-6 LCPUFA	5.84	17.70
Monoenoic fatty acids	5.30	22.59
Saturated fatty acids	6.14	22.44
Sphingolipids	6.18	22.44
Intermolecular distante (Å)	1.5	
Hamaker constant	9.70×10^{-19}	

Sterols include cholesterol and sterol esters. The Hamaker constant comes from the non-retarded and additive London-Van der Waals (LVW) attraction (Hamaker, 1937; Israelachvili, 2011).

TABLE 2 | Mean force of interaction between lipid groups.

Lipid groups	Mean forces (N)
Sterols	1.05×10^{-18}
DHA	1.04×10^{-18}
n-6 LCPUFA	9.48×10^{-19}
Monoenoic fatty acids	1.08×10^{-18}
Saturated fatty acids	1.12×10^{-18}
Sphingolipids	1.12×10^{-18}

Forces are measured in Newtons (N). Sterols include cholesterol and sterol esters.

increased age leads to more viscous domains. It can also be observed that experimental extraction of cholesterol using methyl-β-cyclodextrine (MβCD) brought about a considerable reduction of η_{app} in all fractions, which was more dramatic and severe in lipid rafts, therefore reinforcing the notion that cholesterol (and sterols) and critical components particularly enriched in lipid rafts and largely responsible for their higher viscosity.

Based in our mathematical representation we can calculate a closely microviscosity related magnitude, the mobility. Mobility is also a medium property, which measures the facility of movements of molecule in the membrane. It is thus the inverse of the microviscosity. As can be seen in **Figure 2D** the model predicted mobility values correlates with the experimental microviscosity data. This constitutes *a posteriori* model verification.

Proportion, Number, and Size of Lipid Raft

Based in our model we could determine the ratio of lipid rafts/total membrane and the number and mean size of lipid rafts. Results are show in **Figures 2E,D**. **Figure 2E** it can be seen that in Wild-type mice the number of lipid rafts increase until the age of 6 months and then decrease. The observed pattern in APP/PS1 mice is different since the decrease of the number of domains after 6 months is initially sharper than in Wild-type animals and then remains stable. Regarding the mean size of lipid rafts, we find striking differences as well. Thus, in Wild-type mice, the mean radius remained constant until the age of 6 months,

TABLE 3 | Pairs mean force interactions amongst the different lipid groups measured in Newtons (N).

Forces \ Lipid	Sterols	DHA	n-6 LCPUFA	Monoenoic fatty acids	Saturates fatty acids	Sphingolipids
Sterols	1.07×10^{-18}	1.05×10^{-18}	9.45×10^{-19}	1.04×10^{-18}	1.08×10^{-18}	1.08×10^{-18}
DHA		1.09×10^{-18}	9.74×10^{-19}	1.02×10^{-18}	1.06×10^{-18}	1.06×10^{-18}
n-6 LCPUFA			9.41×10^{-19}	9.18×10^{-19}	9.53×10^{-19}	9.55×10^{-19}
Monoenoic fatty acids				1.14×10^{-18}	1.18×10^{-18}	1.18×10^{-18}
Saturated fatty acids					1.22×10^{-18}	1.23×10^{-18}
Sphingolipids						1.23×10^{-18}

Sterols include cholesterol and sterol esters.

TABLE 4 | Microviscosity values (η_{app}) of lipid rafts (LR) and non-rafts (NR) domains proved with DPH.

	W6		A6		W14		A14	
	NR	LR	NR	LR	NR	LR	NR	LR
Microviscosity app (η_{app})	0.847	1.409	0.711	1.937	0.732	1.448	0.691	1.822
Microviscosity app$_{M\beta CD}$(η_{app})	0.645	0.691	0.602	0.644	0.698	0.748	0.531	0.809
Percent reduction	−23.813	−14.825	−15.329	−42.168	−4.629	−10.206	−23.244	−22.859
Microviscosity ctrl (38°C)	8.525	14.193	7.157	19.503	7.374	14.578	6.962	18.345
Microviscosity MβCD (38°C)	3.416	7.672	3.188	9.722	3.700	6.887	2.811	12.198
APP/WT (6 months old)	83.950	137.412						
APP/WT (14 months old)					94.412	125.834		

MβCD, methyl-β-cyclodextrine.

but then decreased and lastly the size increased at 14 months. In contrast, in APP/PS1 mice, lipid rafts sizes were smaller than in the Wild-type strain in the youngest animals and then increased significantly after the age of 6 months. Moreover, the evolution of the proportion of lipid rafts on the membrane (**Figure 2F**) followed the same pattern than the domain size in both Wild-type and APP/PS1 mice. Since the proportion of raft depends on both, the raft size and number, the model thus indicates that the relevant factor here is the size. Interestingly, for both parameters, the time-course of age-related changes in the number and size of lipid rafts, appear to be accelerated in APP/PS1 mice compared to Wild-type animals.

The Possibility that AD-like Pathology can be Modified

Provided with a reliable model representation we decided to explore what sort of conditions could delay the onset of AD-related lipid alterations, as assessed by the size of lipid rafts being the variable which best correlates with raft proportion (see **Figures 2E,F**). We explored this in the 9-month APP/PS1 mice. We chose this condition because animal group is older enough to display the pathological changes measured in brain cortex raft membranes (Aso et al., 2012; Fabelo et al., 2012) but at the same time younger enough to allow a reversion of membrane lipids alterations.

Figure 4 shows the results obtained after a 50% change (increase or decrease) in each lipid group and compared with the 3 months old Wild-type mice. It can be seen that there are three lipid groups (sterols, DHA, and n-6 LCPUFA) showing a significant decrease of lipid raft size after an increase of their proportions by comparing first row (3 months Wild-type) and third row (9 months APP/PS1). The other three lipid groups (monoenoic, saturates, and sphingolipids) drive an improvement in raft size when they are reduced (first and fourth rows for WT and APP/PS1 mice, respectively).

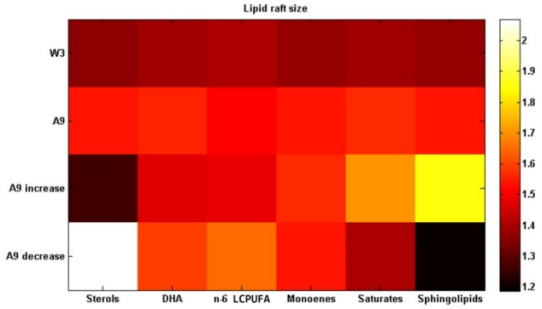

FIGURE 4 | Changing lipid composition. Lipid raft size after increasing each lipid proportion by 50% in the 9 months APP/PS1 transgenic mice (third row) or decreasing it (fourth row). First row displays the data from 3 months old Wild-type mice and second row the data from 9 months old APP/PS1 transgenic mice (data on Table S7). All the experimental data in this figure were taken from Fabelo et al. (2012).

DISCUSSION

In this work we present, the first attempt to quantify the evolution of lipid rafts in Alzheimer's disease by means an agent based mathematical model supported by *in vivo* lipid data composition of nerve cell membranes and their integrated domains, namely lipid rafts and non-raft domains in Wild-type and APP/PS1 transgenic mice at 3, 6, 9, and 14 months. As mentioned before, the original, *in vivo* data used here, derives from our previous work on the detailed analyses of the lipid composition of cortical lipid rafts and whole membrane fractions in these same genotypes and determined at the same ages considered here (Diaz et al., 2012; Fabelo et al., 2012). Moreover, some biophysical and thermodynamic consequences of lipid changes associated with aging have been experimentally determined, particularly in cortical lipid rafts from APP/PS1 animals (Diaz et al., 2012). However, at present there have no modeling attempts to modify lipid compositions and lipid domain formation *in vivo* in order to modify nerve cell membranes in the central nervous system in animal models of AD. The objective of this work was to build up a mathematical model aiming at delving into how molecular alterations in the lipid composition of these domains (raft and non-raft) influence not only their biophysical properties but also their formation and stability. To strength the significance of the predictions, the present agent based mathematical model was calibrated with the real experimental data.

As it has been shown in **Figure 2**, the model was able to predict the lipid composition of lipid rafts. Lipid rafts microdomains, defined as nanoscopic membrane regions involved in a number signaling processes, with specific lipid composition and differential physicochemical properties compared to their surrounding (non-raft) membrane domains (Brown and London, 2000; Pike, 2006), show mobility values around 30% lower than in the whole membrane or non-raft domains. The model also showed that the presence of sphingolipids provides interdigitation between the two membrane leaflets. The occurrence of this mechanism is responsible of about 10% mobility reduction of sphingolipids, which, in turn, is reinforced by its interaction with saturates and sterols (Barenholz and Thompson, 1980). In addition, since interdigitation influences lateral mobility and compressibility (Maulik et al., 1986), this observation could also explain its stability and higher lipid density within raft domains.

The evaluation of interaction forces between each lipid group and amongst distinct lipid groups (**Table 2**) show that highly unsaturated lipids (DHA and n-6 LCPUFA groups) exhibit weak interactions between them as well as with sterols, while monoenes, display intermediate interaction force values. At the other end, saturated fatty acids and sphingolipids are the lipid groups showing the strongest interactions. This graduation correlates well with the molecular structures, from the weakest interacting (corresponding to the more twisted molecules, the polyunsaturated fatty acids) to the strongest (the linear; saturated fatty acid).

In addition to this, we have observed that cholesterol strongly interacts with saturated lipids and sphingolipids, which is in agreement with the umbrella effect (Róg and Vattulainen, 2014) (see **Table 3**). Another model verification comes from the observation that DHA molecules interact more strongly amongst them than with other lipids; an observation in accordance with the role of DHA as dissociating structures in cell domains (Jicha and Markesbery, 2010) which largely contribute to phase separation within the membrane hemilayer (Shaikh et al., 2009; Sonnino and Prinetti, 2010; Georgieva et al., 2015), and likely give rise to the generation of DHA-rich domains bordering (and stabilizing) lipid rafts within nerve cell membranes (Wassall and Stillwell, 2008).

Microviscosity was experimentally determined in lipid rafts and also in non-raft regions surrounding the membrane rafts in Wild-type and AD transgenic mice at different ages (**Table 4**). The obtained values were found to correlate with the model based mobility values; being these results, at least in part, a sort of experimental model verification.

Furthermore, these observations give new insights regarding the evolution of AD, at least in this transgenic model of familial AD. Thus, we have observed that mobility outside lipid raft domains in AD mice of 6 and 14 months is greater than in Wild-type mice of the same age (**Figure 2D**). This entails that in the AD conditions lipids and proteins in non-raft regions might move more freely than in lipid rafts, which, in turn, appear to be more viscous, with lipid and protein lateral movements being more restricted in the APP/PS1 mice. In fact, experimental microviscosity values agree with the model predictions.

Based in these observations we propose a mechanism to explain whereby there is an increased production of β-amyloid in AD brain cortex. Since there is a greater molecular mobility outside lipid rafts in these conditions, the entry rate of APP into lipid rafts would be augmented and therefore the rate of amyloidogenic reactions catalyzed within the domain the by β- and γ-secretases would be expected to increase, to the detriment of APP processing in non-raft domains by the α-secretase. This trend increase with aging in WT and APP/PS1 brains, but in AD mice it is of higher magnitude. Since WT mice do not exhibit senile plaques and very low levels of amyloid peptides throughout their lifespan (Aso et al., 2012), there should exist a lipid alteration threshold (probably determined by the level of DHA depletion) above which lipid mobility around lipid rafts would favor the incorporation of APP into lipid rafts. We thus suggest that the increased molecular mobility in non-raft domains is a condition that exacerbates during aging and plays a central role in the observed increase of amyloid β-production in AD patients. In agreement, we have recently demonstrated in human brains that the accumulation of APP and β-secretase in lipid raft is a determinant factor in amyloidogenic APP processing, and that this is an early event in the development of the disease (Fabelo et al., 2014). Also in line with our hypothesis, Das et al. (2013) have demonstrated that convergence of APP and BACE-1 within lipid rafts via an endocytic-dependent pathway triggers the increase of β-secretase cleavage activity, which eventually favors the generation of senile plaques. In addition, the aberrant organization of lipid rafts predicted here in AD brains might be related to the disarrangement of degradative

autophagic-lysosomal pathway of β-amyloid peptides observed in AD (Zhou et al., 2014), which, in turn, would facilitate its accumulation.

We have been able also to predict the time-course of age-associated changes in the number, mean size and proportion of lipid raft domains both in Wild-type and APP/PS1 mice (shown in **Figures 2E,F**). In both genotypes, the number of rafts decreases with aging, but in APP/PS1 mice this occurs earlier and more abruptly, which is in agreement with previous experimental data. However, the good correlation between rafts proportion and raft sizes indicates that the determinant factor to explain the surface increase of rafts is the increase in radius, not its number. Regarding lipid raft sizes and proportion there is an opposite trend with respect to the number of rafts, since the mean radius and proportion increase with age. But, again, the change is sharper in APP/PS1 mice. These results point to the fact that, since we should expect to find a bigger area in the cell membrane as lipid rafts in older individuals, there would exist an increased amount of lipid rafts-associated signaling molecules interacting and likely higher molecular activity in these cases, as suggested by Marin et al. (2013). This situation leads to an unbalanced physiological condition that can be cause and, at the same time, consequence of the aging process. We suggest that homeostatic mechanisms should be operating to control the lipid rafts proportion (in terms of size and number). Perhaps, the reduction of lipid rafts proportion observed in Wild-type mice between 6 and 9 months might be a cellular response to these mechanisms, which appear disrupted in APP/PS1 mice. In the AD mice model the situation becomes somewhat extreme: the increase in rafts proportion occurs earlier and are exacerbated compared to WT. This prediction supports the hypothesis of accelerated "lipid raft aging" that we have previously postulated for this same transgenic mice model of AD (Fabelo et al., 2012). Furthermore, raft proportion in 3 months-old AD mice was predicted to be smaller than in Wild-type animals at the same age. Since in these mice, β-amyloid is produced since the first months of age (Aso et al., 2012), it is suggested that this is an early effect on homeostatic mechanisms controlling the size and proportion of these microdomains. The increase in lipid domains observed later may well reflect the disarrangement of this controlling mechanism. In the same vein as the production of β-amyloid occurs inside lipid rafts, any increase of the raft area during aging would increase the accumulation of all components of amyloidogenic machinery, eventually leading to increased production of β-amyloid. We propose that the increased proportion of lipid rafts is one of the consequences of aging, and that this trend is accelerated in AD patients, which can positively feedback the production of β-amyloid. Interestingly, the prediction that lipid rafts sizes increase prematurely might be extrapolated to human AD patients at early stages of the disease, where not only alterations in the lipid matrix and biophysical properties occur (Díaz et al., 2015), but also the accumulation of APP and γ- and β-secretases as well as their association are increased (Fabelo et al., 2014).

What sort of changes in the lipid matrix could delay or prevent these age-related events? As we stated in the last paragraph, the parameter of domains which best correlates aging and AD evolution is the domain size. This measure was used here as an indicator of the restoring, by comparing for each lipid species the original situation with the situation after modifying one lipid group each time. Taking as reference of the healthy state the 3 month-old Wild-type mice, and the pathological condition to be restored that of the 9 month-old AD mice, we explored different scenarios and found out that the best strategies to partially restore a healthy condition were either, increasing the amount of sterols (mainly cholesterol), DHA, and n-6 LCPUFA or decreasing monoenoic, saturates, and sphingolipids, separately. **Figure 4** displays some of these results. It is interesting to note that the healthy effects of the DHA intake on the evolution of AD has been already stablished by a number of epidemiological studies (Jicha and Markesbery, 2010), which constitutes an additional, *a posteriori*, model validation. The other strategy was increasing sterols in lipid rafts. However, the role of cholesterol in the onset and progression of AD remains controversial (Ledesma and Dotti, 2005; Martins et al., 2009; Gamba et al., 2012; Martín et al., 2014) and most studies has not yet been proved to have a positive effect on AD. In fact, most epidemiological and experimental studies on cholesterol have shown a negative effect on AD progression (Martins et al., 2009; Gamba et al., 2012; Maulik et al., 2013). The controversy about the role of cholesterol in AD remains unsolved, however, we have recently postulated a reconciling hypothesis according to which it is the balance between cholesterol and DHA in lipid raft (which affect membrane viscosity of opposite ways), rather than their individual contents, what mostly affect the physicochemical and thermodynamic properties of these domains, eventually impacting the rate of amyloidogenic processing of APP (Díaz et al., 2015).

CONCLUSIONS

The mathematical, agent based model, presented here is able to provide a quantitative assessment of the effect of lipid rafts alterations on some aspects of the progression of AD in relation to the progress of aging. The model was based on previous experimental data of lipid composition and biophysical analyses in whole membrane and lipid domains obtained from Wild-type mice and in a familial model of AD at different ages.

The outcomes indicate that changes in the proportion of lipid rafts (and lipid rafts radius) occur naturally along aging and that this process is accelerated in AD mice, which can positively feedback the production of β-amyloid. We suggest that the mechanisms controlling the domain size are critical in AD evolution. Also, we found increased lipid mobility in non-raft domains associated with aging; this phenomena being even greater in AD. We speculate that both factors, i.e., larger raft domains and higher non-raft lipid mobility would favor amyloidogenic machinery to increase β-amyloid production.

Based on our findings we propose to claim about the importance of sterols and LCPUFA present in the cell membrane domains on the progression of AD and on the potential benefits of these lipid species in delaying the onset of AD.

AUTHOR CONTRIBUTIONS

GS and NT designed the agent-based model. MD performed experminental work. GS, NT, and MD prepared, discussed, and wrote the manuscript.

ACKNOWLEDGMENTS

This work was funded by research grants from BIO2014-54411-C2-2-R and SAF2014-52582-R from Ministerio de Economía y Competitividad (MINECO, Spain). GSR acknowledges the support of Obra Social La Caixa-Fundación CajaCanarias that granted him a Posgraduate Fellowship at the Universidad de La Laguna.

SUPPLEMENTARY MATERIAL

The Supplementary Material for this article can be found online at: http://journal.frontiersin.org/article/10.3389/fphys.2016.00090

REFERENCES

Aso, E., Lomoio, S., López-González, I., Joda, L., Carmona, M., Fernández-Yagüe, N., et al. (2012). Amyloid generation and dysfunctional immunoproteasome activation with disease progression in animal model of familial Alzheimer's disease. *Brain Pathol.* 22, 636–653. doi: 10.1111/j.1750-3639.2011.00560.x

Baoukina, S., Mendez-Villuendas, E., and Tieleman, D. P. (2012). Molecular view of phase coexistence in lipid monolayers. *J. Am. Chem. Soc.* 134, 17543–17553. doi: 10.1021/ja304792p

Barenholz, Y., and Thompson, T. E. (1980). Sphingomyelins in bilayers and biological membranes. *Biochim. Biophys. Acta* 604, 129–158.

Barnoud, J., Rossi, G., Marrink, S. J., and Monticelli, L. (2014). Hydrophobic compounds reshape membrane domains. *PLoS Comput. Biol.* 10:e1003873. doi: 10.1371/journal.pcbi.1003873

Bennett, W. F. D., and Tieleman, D. P. (2013). Computer simulations of lipid membrane domains. *Biochim. Biophys. Acta* 1828, 1765–1776. doi: 10.1016/j.bbamem.2013.03.004

Blennow, K., de Leon, M. J., and Zetterberg, H. (2006). Alzheimer's disease. *Lancet* 368, 387–403. doi: 10.1016/S0140-6736(06)69113-7

Brown, D. A., and London, E. (2000). Structure and function of sphingolipid- and cholesterol-rich membrane rafts. *J. Biol. Chem.* 275, 17221–17224. doi: 10.1074/jbc.R000005200

Burrage, K., Hancock, J., Leier, A., and Nicolau, D. V. (2007). Modelling and simulation techniques for membrane biology. *Brief. Bioinformatics* 8, 234–244. doi: 10.1093/bib/bbm033

Claeysen, S., Cochet, M., Donneger, R., Dumuis, A., Bockaert, J., and Giannoni, P. (2012). Alzheimer culprits: cellular crossroads and interplay. *Cell. Signal.* 24, 1831–1840. doi: 10.1016/j.cellsig.2012.05.008

Das, U., Scott, D. A., Ganguly, A., Koo, E. H., Tang, Y., and Roy, S. (2013). Activity-induced convergence of APP and BACE-1 in acidic microdomains via an endocytosis-dependent pathway. *Neuron* 79, 447–460. doi: 10.1016/j.neuron.2013.05.035

Davis, R. S., Sunil Kumar, P. B., Sperotto, M. M., and Laradji, M. (2013). Predictions of phase separation in three-component lipid membranes by the MARTINI force field. *J. Phys. Chem. B* 117, 4072–4080. doi: 10.1021/jp4000686

de Joannis, J., Coppock, P. S., Yin, F., Mori, M., Zamorano, A., and Kindt, J. T. (2011). Atomistic simulation of cholesterol effects on miscibility of saturated and unsaturated phospholipids: implications for liquid-ordered/liquid-disordered phase coexistence. *J. Am. Chem. Soc.* 133, 3625–3634. doi: 10.1021/ja110425s

de Laat, S. W., van der Saag, P. T., and Shinitzky, M. (1977). Microviscosity modulation during the cell cycle of neuroblastoma cells. *Proc. Natl. Acad. Sci. U.S.A.* 74, 4458–4461. doi: 10.1073/pnas.74.10.4458

Díaz, M., Fabelo, N., Martín, V., Ferrer, I., Gómez, T., and Marín, R. (2015). Biophysical alterations in lipid rafts from human cerebral cortex associate with increased BACE1/AβPP interaction in early stages of Alzheimer's disease. *J. Alzheimers Dis* 43, 1185–1198. doi: 10.3233/JAD-141146

Diaz, M. L., Fabelo, N., and Marín, R. (2012). Genotype-induced changes in biophysical properties of frontal cortex lipid raft from APP/PS1 transgenic mice. *Front. Physiol.* 3:454. doi: 10.3389/fphys.2012.00454

Fabelo, N., Martín, V., Marín, R., Moreno, D., Ferrer, I., and Díaz, M. (2014). Altered lipid composition in cortical lipid rafts occurs at early stages of sporadic Alzheimer's disease and facilitates APP/BACE1 interactions. *Neurobiol. Aging* 35, 1801–1812. doi: 10.1016/j.neurobiolaging.2014.02.005

Fabelo, N., Martín, V., Santpere, G., Aso, E., Ferrer, I., and Díaz, M. (2012). Evidence for premature 'Lipid raft aging' in APP/PS1 double transgenic mice, a familial model of Alzheimer's disease. *J. Neuropathol. Exp. Neurol.* 71, 858–881. doi: 10.1097/NEN.0b013e31826be03c

Farooqui, A. A., Horrocks, L. A., and Farooqui, T. (2000). Glycerophospholipids in brain: their metabolism, incorporation into membranes, functions, and involvement in neurological disorders. *Chem. Phys. Lipids* 106, 1–29. doi: 10.1016/S0009-3084(00)00128-6

Finegold, L. (1993). *Cholesterol in Membrane Models*. Boca Ratón, FL: CRC Press.

Fischer, T., Risselada, H. J., and Vink, R. L. C. (2012). Membrane lateral structure: the influence of immobilized particles on domain size. *Phys. Chem. Chem. Phys.* 14, 14500–14508. doi: 10.1039/c2cp41417a

Gamba, P., Testa, G., Sottero, B., Gargiulo, S., Poli, G., and Leonarduzzi, G. (2012). The link between altered cholesterol metabolism and Alzheimer's disease. *Ann. N.Y. Acad. Sci.* 1259, 54–64. doi: 10.1111/j.1749-6632.2012.06513.x

Georgieva, R., Chachaty, C., Hazarosova, R., Tessier, C., Nuss, P., Momchilova, A., et al. (2015). Docosahexaenoic acid promotes micron scale liquid-ordered domains. A comparison study of docosahexaenoic versus oleic acid containing phosphatidylcholine in raft-like mixtures. *Biochim. Biophys. Acta* 1848, 1424–1435. doi: 10.1016/j.bbamem.2015.02.027

Hakobyan, D., and Heuer, A. (2013). Phase separation in a lipid/cholesterol system: comparison of coarse-grained and united-atom simulations. *J. Phys. Chem. B* 117, 3841–3851. doi: 10.1021/jp312245y

Hamaker, H. C. (1937). The London-Van der Waals attraction between spherical particles. *Physica* 10, 1058–1072. doi: 10.1016/s0031-8914(37)80203-7

Han, J.-Y., and Han, S.-H. (2014). Primary prevention of Alzheimer's disease: is it an attainable goal? *J. Korean Med. Sci.* 29, 886–892. doi: 10.3346/jkms.2014.29.7.886

Herrera, F. E., and Pantano, S. (2012). Structure and dynamics of nano-sized raft-like domains on the plasma membrane. *J. Chem. Phys.* 136:015103. doi: 10.1063/1.3672704

Hicks, D. A., Nalivaeva, N. N., and Turner, A. J. (2012). Lipid rafts and Alzheimer's disease: protein-lipid interactions and perturbation of signaling. *Front. Physiol.* 3:189. doi: 10.3389/fphys.2012.00189

Holtzman, D. M., John, C. M., and Goate, A. (2011). Alzheimer's disease: the challenge of the second century. *Sci. Trans. Med.* 3, 77sr1. doi: 10.1126/scitranslmed.3002369

Israelachvili, J. N. (2011). *Intermolecular and Surface Forces, 3rd Edn.* London: Academic Press.

Jicha, G. A., and Markesbery, W. R. (2010). Omega-3 fatty acids: potential role in the management of early Alzheimer's disease. *Clin. Interv. Aging* 5, 45–61. doi: 10.2147/CIA.S5231

Klymchenko, A. S., and Kreder, R. (2014). Fluorescent probes for lipid rafts: from model membranes to living cells. *Chem. Biol.* 21, 97–113. doi: 10.1016/j.chembiol.2013.11.009

Kucerka, N., Marquardt, D., Harroun, T. A., Nieh, M.-P., Wassall, S. R., de Jong, D. H., et al. (2010). Cholesterol in bilayers with PUFA chains: doping with DMPC or POPC results in sterol reorientation and membrane-domain formation. *Biochemistry* 49, 7485–7493. doi: 10.1021/bi100891z

Kumar, V. V. (1991). Complementary molecular shapes and additivity of the packing parameter of lipids. *Proc. Natl. Acad. Sci. U.S.A.* 88, 444–448. doi: 10.1073/pnas.88.2.444

Lakowicz, J. R. (1999). *Principles of Fluorescence Spectroscopy*. New York, NY: Kluwer Academic/Plenum Publisher.

Ledesma, M. D., and Dotti, C. G. (2005). The conflicting role of brain cholesterol in Alzheimer's disease: lessons from the brain plasminogen system. *Biochem. Soc. Symp.* 72, 129–138. doi: 10.1042/bss0720129

Loy, C. T., Schofield, P. R., Turner, A. M., and Kwok, J. B. J. (2014). Genetics of dementia. *Lancet* 383, 828–840. doi: 10.1016/S0140-6736(13)60630-3

Marin, R., Rojo, J. A., Fabelo, N., Fernandez, C. E., and Diaz, M. (2013). Lipid raft disarrangement as a result of neuropathological progresses: a novel strategy for early diagnosis? *Neuroscience* 245, 26–39. doi: 10.1016/j.neuroscience.2013.04.025

Marrink, S. J., and Tieleman, D. P. (2013). Perspective on the Martini model. *Chem. Soc. Rev.* 42, 6801–6822. doi: 10.1039/c3cs60093a

Marrink, S. J., de Vries, A. H., Harroun, T. A., Katsaras, J., and Wassall, S. R. (2008). Cholesterol shows preference for the interior of polyunsaturated lipid membranes. *J. Am. Chem. Soc.* 130, 10–11. doi: 10.1021/ja076641c

Martín, M. G., Pfrieger, F., and Dotti, C. G. (2014). Cholesterol in brain disease: sometimes determinant and frequently implicated. *EMBO Rep.* 15, 1036–1052. doi: 10.15252/embr.201439225

Martín, V., Fabelo, N., Santpere, G., Puig, B., Marín, R., Ferrer, I., et al. (2010). Lipid alterations in lipid rafts from Alzheimer's disease human brain cortex. *J. Alzheimers Dis.* 19, 489–502. doi: 10.3233/JAD-2010-1242

Martins, I. J., Berger, T., Sharman, M. J., Verdile, G., Fuller, S. J., and Martins, R. N. (2009). Cholesterol metabolism and transport in the pathogenesis of Alzheimer's disease. *J. Neurochem.* 111, 1275–1308. doi: 10.1111/j.1471-4159.2009.06408.x

Maulik, M., Westaway, D., Jhamandas, J. H., and Kar, S. (2013). Role of cholesterol in APP metabolism and its significance in Alzheimer's disease pathogenesis. *Mol. Neurobiol.* 47, 37–63. doi: 10.1007/s12035-012-8337-y

Maulik, P. R., and Shipley, G. G. (1996). Interactions of N-stearoyl sphingomyelin with cholesterol and dipalmitoylphosphatidylcholine in bilayer membranes. *Biophys. J.* 70, 2256–2265. doi: 10.1016/S0006-3495(96)79791-6

Maulik, P. R., Atkinson, D., and Shipley, G. G. (1986). X-ray scattering of vesicles of N-acyl sphingomyelins. Determination of bilayer thickness. *Biophys. J.* 50, 1071–1077. doi: 10.1016/S0006-3495(86)83551-2

Muddana, H. S., Chiang, H. H., and Butler, P. J. (2012). Tuning membrane phase separation using nonlipid amphiphiles. *Biophys. J.* 102, 489–497. doi: 10.1016/j.bpj.2011.12.033

Müller, W. E., Kirsch, C., and Eckert, G. P. (2001). Membrane-disordering effects of beta-amyloid peptides. *Biochem. Soc. Trans.* 29(Pt 4), 617–623. doi: 10.1042/bst0290617

Nicolau, D. V. Jr., Burrage, K., Parton, R. G., and Hancock, J. F. (2006). Identifying optimal lipid raft characteristics required to promote nanoscale protein-protein interactions on the plasma membrane. *Mol. Cell. Biol.* 26, 313–323. doi: 10.1128/MCB.26.1.313-323.2006

Nicolau, D. V. Jr., Hancock, J. F., and Burrage, K. (2007). Sources of anomalous diffusion on cell membranes: a Monte Carlo study. *Biophys. J.* 92, 1975–1987. doi: 10.1529/biophysj.105.076869

Nicolson, G. L. (2014). The Fluid-mosaic model of membrane structure: still relevant to understanding the structure, function and dynamics of biological membranes after more than 40 years. *Biochim. Biophys. Acta* 1838, 1451–1466. doi: 10.1016/j.bbamem.2013.10.019

Perlmutter, J. D., and Sachs, J. N. (2009). Inhibiting lateral domain formation in lipid bilayers: simulations of alternative steroid headgroup chemistries. *J. Am. Chem. Soc.* 131, 16362–16363. doi: 10.1021/ja9079258

Perlmutter, J. D., and Sachs, J. N. (2011). Interleaflet interaction and asymmetry in phase separated lipid bilayers: molecular dynamics simulations. *J. Am. Chem. Soc.* 133, 6563–6577. doi: 10.1021/ja106626r

Pike, L. J. (2006). Rafts defined: a report on the Keystone symposium on lipid rafts and cell function. *J. Lipid Res.* 47, 1597–1598. doi: 10.1194/jlr.E600002-JLR200

Postina, R. (2012). Activation of α-secretase cleavage. *J. Neurochem.* 120(Suppl. 1), 46–54. doi: 10.1111/j.1471-4159.2011.07459.x

Richardson, G., Cummings, L. J., Harris, H. J., and O'Shea, P. (2007). Toward a mathematical model of the assembly and disassembly of membrane microdomains: comparison with experimental models. *Biophys. J.* 92, 4145–4156. doi: 10.1529/biophysj.106.090233

Risselada, H. J., and Marrink, S. J. (2008). The molecular face of lipid rafts in model membranes. *Proc. Natl. Acad. Sci. U.S.A.* 105, 17367–17372. doi: 10.1073/pnas.0807527105

Risselada, H. J., Marrink, S. J., and Müller, M. (2011). Curvature-dependent elastic properties of liquid-ordered domains result in inverted domain sorting on uniaxially compressed vesicles. *Phys. Rev. Lett.* 106:148102. doi: 10.1103/physrevlett.106.148102

Róg, T., and Vattulainen, I. (2014). Cholesterol, sphingolipids, and glycolipids: what do we know about their role in raft-like membranes? *Chem. Phys. Lipids* 184, 82–104. doi: 10.1016/j.chemphyslip.2014.10.004

Rosetti, C., and Pastorino, C. (2011). Polyunsaturated and saturated phospholipids in mixed bilayers: a study from the molecular scale to the lateral lipid organization. *J. Phys. Chem. B* 115, 1002–1013. doi: 10.1021/jp1082888

Rosetti, C., and Pastorino, C. (2012). Comparison of ternary bilayer mixtures with asymmetric or symmetric unsaturated phosphatidylcholine lipids by coarse grained molecular dynamics simulations. *J. Phys. Chem. B* 116, 3525–3537. doi: 10.1021/jp212406u

Rushworth, J. V., and Hooper, N. M. (2010). Lipid rafts: linking alzheimer's amyloid-β production, aggregation, and toxicity at neuronal membranes. *Int. J. Alzheimers Dis.* 2011:603052. doi: 10.4061/2011/603052

Schäfer, L. V., and Marrink, S. J. (2010). Partitioning of lipids at domain boundaries in model membranes. *Biophys. J.* 99, L91–L93. doi: 10.1016/j.bpj.2010.08.072

Shaikh, S. R., Rockett, B. D., Salameh, M., and Carraway, K. (2009). Docosahexaenoic acid modifies the clustering and size of lipid rafts and the lateral organization and surface expression of MHC class I of EL4 cells. *J. Nutr.* 139, 1632–1639. doi: 10.3945/jn.109.108720

Simons, K., and Ehehalt, R. (2002). Cholesterol, lipid rafts, and disease. *J. Clin. Invest.* 110, 597–603. doi: 10.1172/JCI0216390

Slotte, J. P. (1999). Sphingomyelin-cholesterol interactions in biological and model membranes. *Chem. Phys. Lipids* 102, 13–27. doi: 10.1016/S0009-3084(99)00071-7

Sonnino, S., and Prinetti, A. (2010). Lipids and membrane lateral organization. *Front. Physiol.* 1:153. doi: 10.3389/fphys.2010.00153

Sonnino, S., and Prinetti, A. (2013). Membrane domains and the 'lipid raft' concept. *Curr. Med. Chem.* 20, 4–21. doi: 10.2174/0929867311320010003

Soula, H. A., Coulon, A., and Beslon, G. (2012). Membrane microdomains emergence through non-homogeneous diffusion. *BMC Biophys.* 5:6. doi: 10.1186/2046-1682-5-6

Tanzi, R. E. (2012). The genetics of Alzheimer disease. *Cold Spring Harb. Perspect. Med.* 2:a006296. doi: 10.1101/cshperspect.a006296

Vetrivel, K. S., and Thinakaran, G. (2010). Membrane rafts in Alzheimer's disease beta-amyloid production. *Biochim. Biophys. Acta* 1801, 860–867. doi: 10.1016/j.bbalip.2010.03.007

Wassall, S. R., and Stillwell, W. (2008). Docosahexaenoic acid domains: the ultimate non-raft membrane domain. *Chem. Phys. Lipids* 153, 57–63. doi: 10.1016/j.chemphyslip.2008.02.010

Wood, W. G., Schroeder, F., Igbavboa, U., Avdulov, N. A., and Chochina, S. V. (2002). Brain membrane cholesterol domains, aging and amyloid beta-peptides. *Neurobiol. Aging* 23, 685–694. doi: 10.1016/S0197-4580(02)00018-0

Wurthner, J. U., Mukhopadhyay, A. K., and Peimann, C. J. (2000). A cellular automaton model of cellular signal transduction.

Comput. Biol. Med. 30, 1–21. doi: 10.1016/S0010-4825(99)00020-7

Zhang, J., Steinberg, S. L., Wilson, B. S., Oliver, J. M., and Williams, L. R. (2008). Markov random field modeling of the spatial distribution of proteins on cell membranes. *Bull. Math. Biol.* 70, 297–321. doi: 10.1007/s11538-007-9259-0

Zhou, X., Yang, C., Liu, Y., Li, P., Yang, H., Dai, J., et al. (2014). Lipid rafts participate in aberrant degradative autophagic-lysosomal pathway of amyloid-beta peptide in Alzheimer's disease. *Neural Regen. Res.* 9, 92–100. doi: 10.4103/1673-5374.125335

Conflict of Interest Statement: The authors declare that the research was conducted in the absence of any commercial or financial relationships that could be construed as a potential conflict of interest.

12. Alzheimer's disease – Supplementary Material

Table S1. Data of Figure 2A.

Membrane proportion data	W3	W6	W9	W14	A3	A6	A9	A14
Sterols	0.44	0.46	0.45	0.41	0.5	0.49	0.41	0.41
DHA	0.07	0.07	0.08	0.08	0.07	0.07	0.08	0.08
n-6 LCPUFA	0.07	0.06	0.07	0.07	0.06	0.06	0.07	0.07
Monoenes	0.18	0.18	0.18	0.2	0.16	0.17	0.19	0.2
Saturates	0.16	0.14	0.14	0.14	0.14	0.14	0.14	0.13
Sphingolipids	0.08	0.09	0.09	0.11	0.07	0.07	0.11	0.11

Table S2. Data of Figure 2B.

Raft proportion data	W3	W6	W9	W14	A3	A6	A9	A14
Sterols	0.32	0.33	0.33	0.27	0.33	0.32	0.28	0.24
DHA	0.04	0.05	0.06	0.04	0.05	0.04	0.05	0.03
n-6 LCPUFA	0.05	0.06	0.05	0.04	0.06	0.05	0.05	0.03
Monoenes	0.18	0.2	0.18	0.18	0.18	0.17	0.18	0.19
Saturates	0.24	0.19	0.21	0.25	0.21	0.23	0.25	0.29
Sphingolipids	0.17	0.17	0.17	0.21	0.16	0.19	0.2	0.22

Table S3. Data of Figure 2C.

Predicted proportion data	W3	W6	W9	W14	A3	A6	A9	A14
Sterols	0.3272	0.3444	0.3515	0.3057	0.3691	0.3660	0.3059	0.3070
DHA	0.0480	0.0516	0.0570	0.0571	0.0547	0.0533	0.0555	0.0534
n-6 LCPUFA	0.0431	0.0371	0.0392	0.0421	0.0381	0.0383	0.0382	0.0432
Monoenes	0.1788	0.1797	0.1917	0.2002	0.1646	0.1815	0.1946	0.2099
Saturates	0.2669	0.2333	0.2275	0.2282	0.2433	0.2341	0.2214	0.2036
Sphingolipids	0.1360	0.1539	0.1331	0.1667	0.1302	0.1268	0.1843	0.1829

Table S4. Data of Figure 2D.

	Microviscosity outside data	Mobility outside model	Mobility outside model (s.d.)
W6	8.5250	0.4821	0.0004
W14	7.3740	0.4855	0.0004

A6	7.1570	0.4848	0.0004
A14	6.9620	0.4858	0.0003

Table S5. Data of Figure 2E.

	Number of lipd rafts	Number of lipd rafts (s.d.)	Radius of the lipid rafts	Radius of the lipid rafts (s.d.)
W3	1,859.0311	11.1610	1.3727	0.0065
W6	1,888.3124	13.6461	1.3841	0.0051
W9	1,847.2337	15.3095	1.2984	0.0062
W14	1,812.7992	15.8212	1.4885	0.0091
A3	1,863.4189	14.1870	1.2182	0.0058
A6	1,871.0945	12.0621	1.2309	0.0057
A9	1,790.2199	11.7272	1.5437	0.0076
A14	1,793.1793	11.3204	1.5215	0.0082

Table S6. Data of Figure 2F.

	Raft proportion	Raft proportion (s.d.)
W3	0.2751	0.0021
W6	0.2841	0.0018
W9	0.2445	0.0022
W14	0.3153	0.0023
A3	0.2172	0.0015
A6	0.2226	0.0015
A9	0.3350	0.0018
A14	0.3260	0.0023

Table S7. Data of Figure 4.

Lipid raft size	Sterols	DHA	n-6 LCPUFA	Monoenes	Saturates	Sphingolipids
W3	1.3860	1.3763	1.3746	1.3736	1.3890	1.3921
A9	1.5197	1.5376	1.5526	1.5527	1.5466	1.5776
A9 increase	1.2649	1.4564	1.4649	1.5563	1.6963	1.8425
A9 decrease	2.0282	1.6409	1.6078	1.4991	1.3824	1.2015

13. Immunotherapy against melanoma – *Scientific Reports*

DOI: 10.1038/srep24967

SCIENTIFIC REPORTS

OPEN

Received: 19 November 2015
Accepted: 08 April 2016
Published: 26 April 2016

Model-based genotype-phenotype mapping used to investigate gene signatures of immune sensitivity and resistance in melanoma micrometastasis

Guido Santos[1,2,3], Svetoslav Nikolov[1,4,5], Xin Lai[1,2], Martin Eberhardt[1,2], Florian S. Dreyer[1,2], Sushmita Paul[1,2], Gerold Schuler[2] & Julio Vera[1,2]

In this paper, we combine kinetic modelling and patient gene expression data analysis to elucidate biological mechanisms by which melanoma becomes resistant to the immune system and to immunotherapy. To this end, we systematically perturbed the parameters in a kinetic model and performed a mathematical analysis of their impact, thereby obtaining signatures associated with the emergence of phenotypes of melanoma immune sensitivity and resistance. Our phenotypic signatures were compared with published clinical data on pretreatment tumor gene expression in patients subjected to immunotherapy against metastatic melanoma. To this end, the differentially expressed genes were annotated with standard gene ontology terms and aggregated into metagenes. Our method sheds light on putative mechanisms by which melanoma may develop immunoresistance. Precisely, our results and the clinical data point to the existence of a signature of intermediate expression levels for genes related to antigen presentation that constitutes an intriguing resistance mechanism, whereby micrometastases are able to minimize the combined anti-tumor activity of complementary responses mediated by cytotoxic T cells and natural killer cells, respectively. Finally, we computationally explored the efficacy of cytokines used as low-dose co-adjuvants for the therapeutic anticancer vaccine to overcome tumor immunoresistance.

In many solid cancer types, the interaction between the tumor and the immune system is a key element governing critical steps in the tumor progression path[1]; its deep understanding is necessary to design efficient anticancer immunotherapies. In recent times, a number of published works suggest the use of a systemic approach combining quantitative experimental data and mathematical modeling to dissect the tumor-immune system interaction[2,3]. However, most of these modelling efforts focus on representing and simulating cell-to-cell processes and do not consider the intracellular networks controlling immune and tumor cells, thereby losing the chance to integrate and analyze omics data on the molecular events underlying the tumor-immunity interaction and the immune-based therapies.

The immune system is by definition multi-scale because it involves complex biochemical networks that regulate cell fate across cell boundaries[4], and also because immune cells communicate with each other by direct contact or through secretion of local or systemic signals[3,6–8]. Moreover, immune cells and cancer cells interact, and these interactions are affected by the tumor microenvironment. The complex nature of this tumor-immunity-microenvironment interaction favors and sometimes requires a systemic approach in its analysis[2].

[1]Laboratory of Systems Tumor Immunology, Friedrich-Alexander University of Erlangen-Nuremberg, Germany. [2]Department of Dermatology and Erlangen University Hospital and Faculty of Medicine, Friedrich-Alexander University of Erlangen-Nuremberg, Germany. [3]Systems Biology and Mathematical Modelling Group, University of La Laguna, Spain. [4]Institute of Mechanics, Bulgarian Academy of Science, Sofia, Bulgaria. [5]University of Transport, Sofia, Bulgaria. Correspondence and requests for materials should be addressed to J.V. (email: julio.vera-gonzalez@uk-erlangen.de)

A systemic approach is able to combine quantitative experimental data, mathematical modeling and other methods from computational biology [7]. In recent literature, several contributions have made use of this approach to dissect the tumor-immunity interaction[9,10]. The interplay between the tumor, the immune system and different types of therapies has been modelled in the last decade[5,6,8,11], including a study that employed model simulations and patient data to predict the optimal timing and dosage for a therapeutic anticancer vaccination[12]. Although these models in some cases incorporate detailed descriptions of the underlying cell-to-cell communication, they do not take into account the intracellular networks governing immune or tumor cells. Thus, these models by design cannot take advantage of the large amount of omics data produced nowadays to provide molecular-level insights into immunotherapies and their assessment or re-engineering[2]. One option to overcome these limitations is to perform a model-based genotype-phenotype mapping in which model parameters are associated to gene ontology terms[13]. When trying to reconcile simulation results with experimental and clinical data, aggregation of the differentially expressed genes into metagenes will provide a means to connect omics data with model predictions. This is the approach we propose and explore in this paper.

High-throughput data can be combined with mathematical modelling to assess the efficacy of anticancer therapies. For example, Hector *et al.*[14] quantified apoptosis-regulating proteins in samples of colorectal carcinomas (stage II and III) and normal colonic tissue, and simulated apoptosis signaling to predict the efficacy of apoptosis-inducing therapeutics. Systems approaches have also been used for patient-data-based assessment of experimental immunotherapies. For example, Ulloa-Montoya *et al.*[15] analyzed biopsy samples from metastatic melanoma patients and identified a pretreatment gene expression signature that can be used to predict the response to immunotherapy.

In this paper we set up and characterized a kinetic model accounting for the interaction of the immune system with melanoma micrometastases as well as for the role of an immunotherapy in controlling and depleting them. It is important to highlight that the work will be focused on the simulation of distributed micrometastases instead of the dynamics of primary melanoma tumors. Here, the immunotherapy refers to treatments stimulating the adaptive immune response, like therapeutic vaccines which are based on melanoma antigens, or patient monocyte-derived dendritic cells loaded with antigens from primary tumor cells[16].

We combined mathematical analysis, systematic model simulations and statistical techniques to generate phenotypic signatures accounting for melanoma sensitivity and resistance to the inherent immune response and immunotherapy. In the context of this study, the term inherent immune response refers to the patient's natural immune reactions without any artificial stimulus, while the immunotherapy refers to treatments like dendritic-cell or melanoma antigen vaccination. The phenotypic signatures were compared with metagene signatures derived from clinical data. The comparison not only confirmed the correlation of model predictions with clinical data, but it also allowed the mechanistic interpretation of the clinically derived metagene signatures underlying various biological processes. Furthermore, improvements in the therapeutic anticancer vaccination were proposed based on the model analysis.

Taken together, our results highlight that mathematical models are useful tools for the assessment of tumor immunogenicity, and also that high-throughput data can be employed to detect key genes involved in the tumor-immune system interaction.

Materials and Methods

Overview of the methodology. The presented method makes use of mathematical modeling to a) infer biological mechanisms explaining gene expression signatures obtained from clinical data and b) propose simulation result -based improvements in existing therapies. The workflow used was as follows (see Fig. 1 for a graphical illustration):

1. A mathematical model describing the biological system under investigation is derived and characterized using published data, and, when possible, model-driven experiments[17];
2. The model parameters are systematically perturbed and simulations are performed for relevant biomedical scenarios;
3. According to the resulting simulated biological behavior, the model parameter sets are classified into groups. A statistical analysis of the model parameter sets extracted from those groups is used to obtain phenotypic signatures (e.g., patterns in the perturbed model parameter sets for each defined group);
4. Subsequently, clustering analysis is performed to obtain fine-grained signatures of subpopulations within each group. The features of these signatures are linked to the (de)regulation of given biological processes defined in the mathematical model;
5. Mathematical analysis is used to further investigate and define the gene signatures;
6. The genes in clinical signatures are annotated and grouped into metagenes. These metagenes represent genes with a similar gene ontology annotation in terms of the biochemical processes described in the model;
7. The clinical signatures are aggregated using the described metagenes;
8. Phenotypic signatures from the model are compared to metagene signatures from clinical data. Agreement between them allows a biological interpretation of the clinical signatures based on the identification of disrupted or deregulated biological processes. The derivation and calculation of the metagenes is presented in *Gene annotation* and *Metagene grouping* sections;
9. Analysis of additional simulation results are used to propose therapy improvements which must be validated in further experimental and clinical setups.

In the following, the different elements of the procedure are discussed in detail.

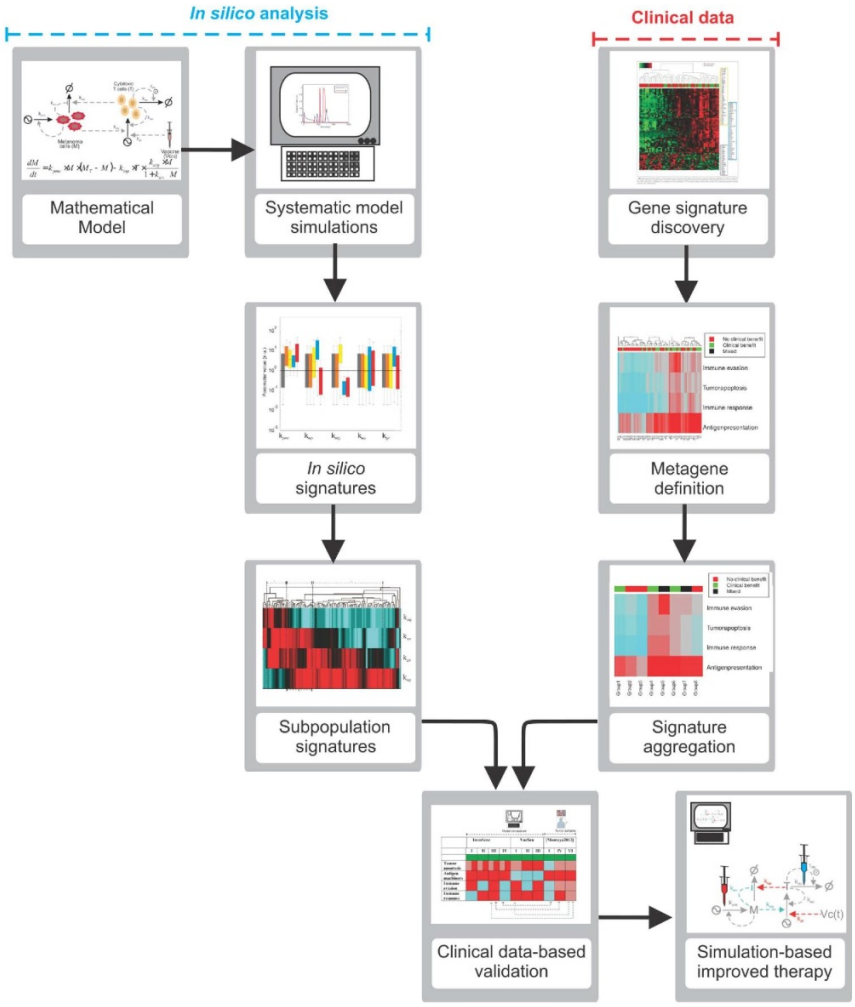

Figure 1. Workflow of the study. Our goal was to generate phenotypic signatures and to compare them with signatures derived from patient data.

Mathematical model derivation. We used published knowledge and preexisting mathematical models describing the interaction between the tumor and the immune system to derive a new simplified kinetic model based on nonlinear ordinary differential equations with time delay[5,6,18] (Fig. 2). The model reflects the dynamics of cytotoxic T cells and tumor cells during the growth of melanoma micrometastases, as well as some features associated with the inherent and immunotherapy-induced immune response. It has the following structure:

$$\frac{dT}{dt} = k_{apc} \cdot \left(1 + k_{gir} \cdot V_C(t)\right) \cdot \frac{\left[k_{atg} \cdot M + V_C(t)\right]^{g_1}}{k_{tapc}^{g_1} + \left[k_{atg} \cdot M + V_C(t)\right]^{g_1}} + k_{atc} \cdot T \cdot \frac{\left(k_{atg} \cdot M\right)^{g_2}}{k_{tatc}^{g_2} + \left(k_{atg} \cdot M\right)^{g_2}} - k_{dtc}[T^3 + k_x \cdot T^{0.1} \cdot T(t - \tau_{dtc})^{0.9}] \quad [1]$$

$$\frac{dM}{dt} = k_{pmc} \cdot M \cdot (M_T - M) - k_{iap} \cdot T \cdot \frac{k_{atg} \cdot M}{1 + k_{iev} \cdot M} - k_{ink} \cdot M \cdot \frac{(HLA^{-1})^{nk}}{(k_{nkc})^{nk} + (HLA^{-1})^{nk}} \quad [2]$$

where T accounts for the population of cytotoxic T cells and M for the population of melanoma cells that compose a micrometastasis. In case of cytotoxic T cells, Equation [1] includes the first term accounting for the activation of

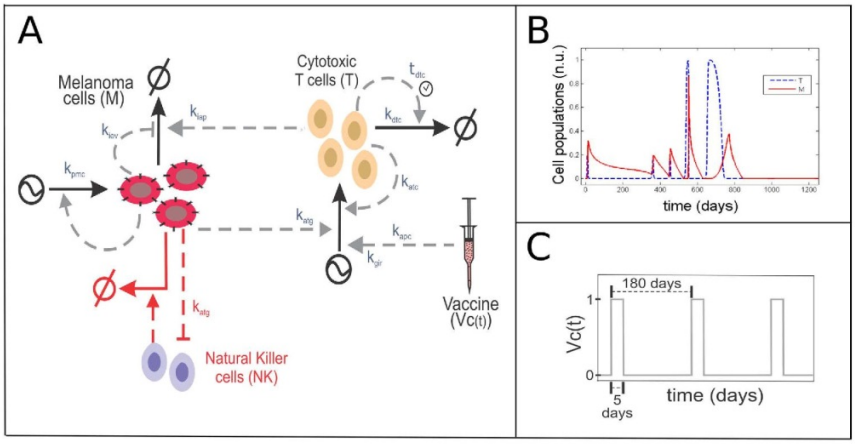

Figure 2. (**A**) Sketch representing the structure of the mathematical model derived to represent the interaction between a melanoma micrometastasis and the natural or therapy-mediated immune response. Parameters: k_{pmc} – tumor proliferation rate; k_{iap} – antitumor cytotoxic efficiency; k_{atg} – antigen presentation efficiency; k_{iev} – immune evasion efficiency; k_{gir} – global immune response efficiency; k_{dtc} – depletion rate of activated cytotoxic T cells (fixed value) k_{apc} – inherent immune response; t*dtc* – time delay; (**B**) The model can be used to simulate the kinetics of cytotoxic T cells (*T*) in a time-dependent manner and the growth of melanoma cells (*M*) under the corresponding immune stress ($T(0) = 0$; $M(0) = 0.00081$; nominal values for the model parameters). (**C**) Sketch of the immune therapy simulation used as described in Material and Methods section.

cytotoxic T cells by antigen-presenting cells as a result of a) the inherent immune response (k_{apc}) or b) an immunotherapy, for example dendritic cell or antigen vaccination. The immunotherapy-mediated activation of naïve T cells is represented by a time-dependent input variable, $V_c(t)$ (for details, see "Simulation of vaccine administration" below). An additional feature associated with the immunotherapy is the ability to promote a global unspecific immune response, which amplifies the process of cytotoxic cell activation (k_{gir}).The efficacy of the cytotoxic T cell activation process is dependent on the amount of antigens (k_{atg}) presented by tumor cells (*M*) and follows a saturation dynamics represented by a Hill function with a Michaelis-Menten like parameter (k_{tapc})[13] with exponent g_1. The equation also includes a term accounting for the self-expansion of activated cytotoxic T cells upon interaction with tumor cells (k_{atc}) which follows a Hill function, with the corresponding Michaelis-Menten like parameter (k_{tatc}) with exponent g_2, and is proportional to the amount of antigens (k_{atg}) produced by the tumor cells (*M*). Finally, the equation includes a summand accounting for a biphasic depletion of activated cytotoxic T cells (k_{dtc}). In this term, we included a fast third-order depletion term together with a slower, time-delayed one which accounts for the small fraction of activated cytotoxic T cells that have a longer lifespan (and represent memory T cells in a phenomenological fashion; for time delay estimation and previous kinetic model see[19]). By using this structure for the T cell depletion rate, our model is able to reproduce the basic features of the short-term and memory cytotoxic T cells dynamics with a single differential equation (Supp. Fig. S1).

For the melanoma cells, Equation [2], the first rate term includes a logistic equation accounting for the self-limiting growth of the melanoma cell population (k_{pmc}): we introduced this rate term under the assumption that the melanoma cells in the micrometastasis have not yet broken the blood vessel barrier and therefore achieve a maximum size represented by M_T[20]. In addition, the model includes a term accounting for the T cell and NKC-mediated killing of melanoma cells on the second and third term respectively ($k_{ink} \approx 0.02 \cdot k_{iap}$). In our model, the strength of this process is proportional to the level of antigen presentation (k_{atg}) of the tumor cells *M*. In addition, we also consider the possibility that the melanoma cells could evolve an immune evasion strategy, thereby reducing the efficiency of T cell-mediated recognition and killing (k_{iev}). The final Hill kinetics term, which features the Michaelis like constant k_{nkc} and the exponent g_{nk}, accounts for the activation of natural killer cells (NKCs) by tumor cells that exhibit low levels of human leukocyte antigen (*HLA*) complexes on the cell surface, and for the ability of activated NKCs to target the tumor cells for killing. *HLA* accounts for the plasma membrane levels of *HLA* complexes, which is assimilated for simplicity into the model parameter k_{atg} ($HLA \approx k_{atg}$). This model can be used to simulate the evolution of specific cytotoxic T cell (*T*) populations in a time dependent manner and the behavior of melanoma cells (*M*) under distinct immune-related scenarios (Fig. 2B).

We point out that the derived kinetic model features a combination of mass-action, Hill kinetics and power-law terms, a strategy previously used to model complex regulatory processes in simplified model equations[13,21,22]. The values of the rate parameters were assigned by surveying published information. For example, the half-life of cytotoxic T cells was used to characterize k_{dtc}. Also, k_{tapc} and g_1 were estimated to induce a sigmoidal APC (antigen presenting cell)-mediated cytotoxic T cell response within the interval of feasible values of the model variables. Alternatively, we reduced some parameters by normalization (e.g., normalizing the expression level of melanoma antigen presentation such that it is equal to 1 in the nominal version of the model). Model parameter values and further explanations are provided in Supplementary Table S1.

Model simulations. To search for phenotypic signatures accounting for sensitivity or resistance of melanoma cells to inherent and immunotherapy-supported immune responses, we randomly perturbed the values of biologically relevant model parameters using the Latin hypercube sampling method in the logarithmic space. The parameters chosen account for tumor cell proliferation, antigen presentation, efficiency of T cell-mediated killing of melanoma cells, tumor immune escape, and the intensity of systemic immune responses induced by the immunotherapy (respectively k_{pmc}, k_{atg}, k_{iap}, k_{iev}, and k_{gir}). The parameter k_{pmc} was perturbed in the interval [1, 5]. The upper bound corresponds to with a duplication time of approx. 12 hours for an nominal population M = 0.3. The lower bound was fixed to 1: preliminary simulations indicated that values of k_{pmc} below initial value did not satisfy the conditions for tumor growth. The parameters k_{atg}, k_{iap}, k_{iev}, and k_{gir} account for a rather complex aggregation of biological parameters and therefore they were perturbed in the wider interval [0.02 50]. Thereby, we generated 10^4 solutions, each one with a distinct set of parameter values. For each combination, we performed simulations in three scenarios relevant for describing the interaction between the tumor micrometastasis and the immune system: **scenario 1)** non-immunogenic tumor growth conditions ($M(0) = 0.00081$, which represents an initiating tumor cell cluster of 30 cells, $T(0) = 0$, no pre-existing T cell response, $k_{apc} = 0$, $V_c(t) = 0$); **scenario 2)** inherent antitumor immune response ($M(0) = 0.00081$, $T(0) = 0$, $k_{apc} = 0.04$, $V_c(t) = 0$); and **scenario 3)** immunotherapy-supported (vaccine) antitumor immune response ($M(0) = 0.00081$, $T(0) = 0$, $k_{apc} = 0.04$, $V_c(t) = F_{vac}(t)$). Based on exploratory clinical results (data not shown), vaccine administration was simulated by introducing a step-like time-dependent function $F_{vac}(t)$ simulated during six subsequent periods of 180 days, with the following structure: $F_{vac}(t) = 1$ *if* $0 < t < 5$; $F_{vac}(t) = 0$ *if* $5 < t < 180$ (see Fig. 2C).

We investigated phenotypic signatures providing resistance to inherent and vaccine-mediated immune responses by simulating the response of the model to the described scenarios. According to the simulation results, the model parameter combinations were classified into the following biologically relevant groups:

(a) **Tumor**: parameter combinations for which the melanoma cell population is bigger than 90% of the maximum tumor population size ($M > 0.9$ n.u.) after 30 days of non-immunogenic tumor growth conditions (see scenario 1 above). The subsequent groups (b–d) are subclasses of this group;
(b) **Immune-sensitive**: parameter combinations that generate a growing melanoma micrometastasis in scenario 1, but they are depleted or controlled by the inherent immune response in scenario 2 ($M < 0.05$ n.u. 1500 days after starting of the wild-type immune response);
(c) **Vaccine-sensitive**: parameter combinations that generate a growing melanoma micrometastasis in scenario 1, are resistant to the inherent immune response in scenario 2, and are depleted or controlled by the immunotherapy-mediated immune response in scenario 3 ($M < 0.05$ n.u. 1500 days after starting the immunotherapy treatment);
(d) **Vaccine-resistant**: parameter combinations that generate a growing melanoma micrometastasis in scenario 1 and are resistant to both the inherent (scenario 2) and immunotherapy-supported (scenario 3) immune response.

With the criteria chosen, groups b, c, and d do not overlap because our intention was to define "extreme cases", in a way clear phenotypic signatures could be found. Thus, we are able to unambiguously assign each solution to one of the groups above. It could be possible to find solutions that do not belong to any of the groups defined, and that may account for intermediate cases (not found in our current results). In this case, the subset of non-allocated solutions maybe further analysed independently.

Determining phenotypic subpopulation signatures. In order to investigate the potential existence of subpopulations of solutions with a clear-cut distinction in the values of the model parameters, the solutions belonging to each population were examined using hierarchical clustering analysis. The dendrogram and heat map of the solutions were obtained in MATLAB 2014 using the function '*clustergram*' which performs hierarchical clustering with the Euclidean distance metric, average linkage and optimal leaf ordering by clustering first along the columns[23]. For visualizing the heat map, we used a customized color map (red for high values and cyan for low values). In the heat map, we classified the solutions in subpopulations that: a) are as large as possible, b) correspond to a division (cluster) in the dendrogram, and c) at least 75 % of the solutions have similar color codes for each model parameter (i.e., the cluster must predominantly be either red or cyan for each model parameter).

Gene annotation. The 84 genes identified in Ulloa-Montoya *et al.*[15] were manually annotated with emphasis on classifying them into one of the following categories according to their established role in the immune response: 1) antigen presentation machinery, 2) immune-mediated tumor apoptosis/cytotoxic T cell-mediated killing of tumor cells, 3) tumor immune evasion mechanisms, 4) general immune response and 5) none/unknown. Gene annotation was carried out using the information contained in Ensembl and UniProt databases. In case that the gene function was not or only partially described in context of the phenotypes in question, we searched literature for complementing its annotation using NCBI's MEDLINE database. The results of the gene annotation procedure can be found in Supplementary Figure S3.

Metagene definition and estimation. The metagenes defined here represent the averaged expression of the genes that belong to categories 1–4 as defined above. Hierarchical clustering with complete linkage and Euclidean distance was performed on the patient samples using the heatmap.2 function of the gplots package in R. Both margin clusters of the generated heat map had a consistent pattern. These two clusters were used for further analysis. The genes present in the heat map were further assigned to one of the four immune-related metagenes (s. above) and the metagene expression values estimated by taking the arithmetic average of the corresponding genes. Interestingly, we obtained similar values using both arithmetic and geometric mean.

Comparison between *in silico* and patient signatures. In order to make possible a comparison, the solutions from the *in silico* clusters were log10-transformed and normalized to the interval [−1, 1]. For every cluster, we calculated the average value for each parameter. The average values for the metagenes in the patient clusters of clinical and no clinical benefit were also log10-transformed and normalized to the interval [−1, 1]. We created a matrix by merging *in silico* clusters for vaccine resistant and the two patient signatures and performed hierarchical clustering using the MATLAB 2014 function 'clustergram', which performs hierarchical clustering with the Euclidean distance metric, average linkage and optimal leaf ordering by clustering first along the columns. Next, for every *in silico* cluster we calculated the Euclidean distance between its average (X) and the average for the patient clusters (X_{Nbn} and X_{Bn}, for non-benefit and benefit respectively) using the following equations:

$$\text{Distance to non-benefit patient cluster: } D(X_{Nbn}, X) = \sqrt{\sum_{i=1}^{4}(X_{Nbn}^{i} - X^{i})^2}$$

$$\text{Distance to benefit patient cluster: } D(X_{B}n, X) = \sqrt{\sum_{i=1}^{4}(X_{Bn}^{i} - X^{i})^2}$$

We followed a similar procedure for *in silico* vaccine sensitive clusters. In this case, we also merged into the matrix two representative clusters from the *in silico* immune sensitive solutions.

Computing of solutions and analysis. Computational simulations and data analysis were performed using MATLAB 2014 running on a Dell Precision T7600 with 2 Intel Xeon E5-2687W 3.1 GHz processors and 64 GB RAM. The computing time for the 10^4 simulations was in the order of hours.

Results

A kinetic model of the interaction between melanoma micrometastasis and the immune system.

To investigate the interactions of the tumor with the immune system in the context of melanoma micrometastases and immunotherapy, we set up, characterized and analyzed a kinetic model in nonlinear ordinary differential equations (see Fig. 2). To construct the model, we used published data and mathematical models on the interaction between the tumor and the immune system[5,6,18,24]. The model accounts for the interaction between the local immune system and tumor cells during the growth of melanoma micrometastases. In the model, the variable M accounts for the population size of melanoma cells, while T accounts for the local population size of specific cytotoxic T cells. The latter one is used as a surrogate for an efficient antitumor response of the adaptive immune system.

Our model for the dynamics of cytotoxic T cells contains terms representing a) the activation of naïve T cells by antigen-presenting cells from the inherent immune system (k_{atg}); b) the self-expansion of activated cytotoxic T cells upon detection of tumor cells (k_{atc}) and c) the depletion of active cytotoxic T cells (k_{dtc}). In addition, the model includes a term for the immunotherapy-mediated activation of naïve T cells, here represented by the time-dependent input model variable $V_c(t)$. In our model, the strength of the activation process is modulated by a model parameter (k_{gir}). This parameter accounts for the patient-to-patient variability of the therapy to promote a systemic immune response which amplifies the process of cytotoxic cell activation[15].

Our model for melanoma cell dynamics contains equations accounting for: a) the growth of the tumor cell population in micrometastases (k_{pmc}); b) killing of melanoma cells by cytotoxic T cells (k_{iap}); and c) biological functions attributed to the antigen presentation machinery by linking its downregulation to the activation of natural killer cells (k_{atg}). In our model, the cytotoxicity of T cells depends positively on the amount of specific antigens presented by the tumor cells, and negatively on the ability of the tumor cells to evade immune response. Both aspects are represented by the tunable parameters k_{atg} and k_{iev} (see respectively Parmiani, G. *et al.*[25] and Umansky, V. & Sevko, A.[26]).

To answer the question which parameter ranges confer immunoresistance to the micrometastasis, we used systematic model simulations to identify regulatory patterns in the tumor-immunity interaction.

Detection of phenotypic signatures providing immune resistance in melanoma. Recent experimental and clinical data have shown that metastatic melanoma has the ability to evade immunotherapies that are based on antibodies and therapeutic anticancer vaccination[15,27,28]. In order to detect putative phenotypic signatures promoting immunoresistance of melanoma micrometastases, we generated a set of 10^4 model parameter configurations through random systematic perturbation. Parameter sensitivity analysis was performed on the solutions to ensure robustness of the simulations (see Figure S4). The solutions of the model parameter combinations were grouped in the following biologically relevant groups (see Fig. 3A and Material and Methods section Detection of phenotypic signatures): i) tumor, those for which the melanoma cell population shows fast growth; ii) immune-sensitive, those combinations for which the inherent immune system can eliminate melanoma micrometastasis; iii) vaccine-sensitive, parameter combinations for which immunotherapy results in effective killing of melanoma cells that were resistant to the inherent immunity; and iv) vaccine-resistant, those model parameter values for which melanoma micrometastasis are resistant to both inherent immunity and to immunotherapy. Fig. 3B–D show model simulations for the scenarios 2 (red) and 3 (blue) in a sample of ten solutions for the groups immune-sensitive, vaccine-sensitive and vaccine-resistant.

According to our simulations, vaccine-sensitivity micrometastases can cope with low T cell-mediated cytotoxicity against tumor cells (k_{iap}) due to the high levels of tumor antigen expression and presentation (k_{atg}) (see Fig. 3A). The results also suggest that the micrometastases, although they express low levels of tumor antigens (k_{atg}), could be sensitive to immunotherapy in case the therapy induces a high systemic immune response and if there is an efficient T cell-mediated cytotoxicity (k_{iap}) (see Fig. 3A). In the case of vaccine-resistant solutions, the genotypic-phenotypic constitution of the tumor in combination with features of the patient's immune system

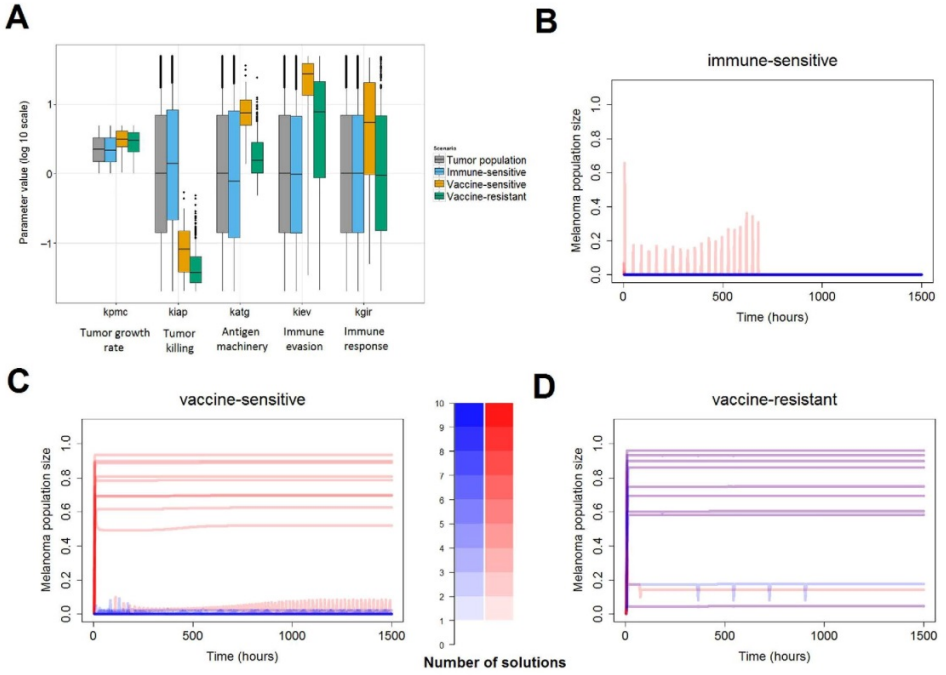

Figure 3. Simulation-result-based detection of signatures responsible for immune resistance or immune sensitivity in melanoma. (**A**) Phenotypic signatures obtained for the four sets of solutions (randomly generated set of parameters). In each boxplot the inner horizontal line is the median, the lower and upper edges are the 25th and 75th percentiles, respectively, and the whiskers extend to the most extreme data points. The ordinate axis origin in the plot accounts for the values in the nominal immune sensitive signature (that is, the model with all the parameters as table S1). Outliers are denoted as dots. See text or caption of Fig. 2 for parameter definitions. (**B–D**) Random sample of 10 solutions from each of the groups immune-sensitive, vaccine-sensitive, and vaccine-resistant, respectively. Red lines correspond to simulation scenario 2 and blue ones to simulation scenario 3. Color bar indicates the number of solutions on overlapping regions.

permits micrometastases to become and remain resistant to both the inherent response and the immunotherapy. Our simulations indicate that lower levels of tumor antigen expression (k_{atg}) in combination with a weak T cell-mediated cytotoxicity (k_{iap}) can render micrometastases refractory to anticancer immunotherapy (see Fig. 3A).

Elucidation of finer phenotypic signatures using data clustering techniques. The previous analysis gave us a rough classification for the model populations. For example, the vaccine-sensitive group extends still across most of the available parameter space accounting for the strength of the immunotherapy-mediated systemic immune response (k_{gir}, Fig. 3A). This revealed the need for additional data analysis techniques to extract subpopulations with a clearer distinction of parameter values. To this end, the solutions belonging to each population were clustered using hierarchical clustering and visualized using heat maps (Fig. 4; see Material and Methods for details). The heat maps were scrutinized to detect finer subpopulations. We here further discuss the results for the vaccine-sensitive and vaccine-resistant solutions, while the analysis of the immune-sensitive solutions is included in the Supplementary Material.

In case of the vaccine-sensitive population, we detected three subpopulations of solutions displaying distinct phenotypic signatures (Fig. 4A,B; subpopulations a, b and c, highlighted with dendrogram lines in grey, blue and orange, respectively). All of them had inefficient T cell-mediated killing of melanoma and high tumor antigen expression and presentation in common (i.e., the value of k_{iap} is low, and the value of k_{atg} is high). The differences resulted in two groups:

group a) low values of immune evasion (k_{iev}) with high values of immune response (k_{gir}), so a micrometastasis without evasion mechanisms cannot survive in a context of high antigen presentation and vaccination;

group b/c) solutions with high values of immune evasion (k_{iev}), either high or low values of immune response (k_{gir}), so high antigen presentation in combination with immunotherapy is enough to counteract the immune evasion mechanisms of the micrometastases. For the purpose of better visualization of the results, every subpopulation is shown connected to a customized illustration of the mathematical model in which the parameters and their associated biological process are colored according to their observed value (Fig. 4A). This allows an understanding of the mechanisms modulating the interactions of the tumor with the immune system in each subpopulation.

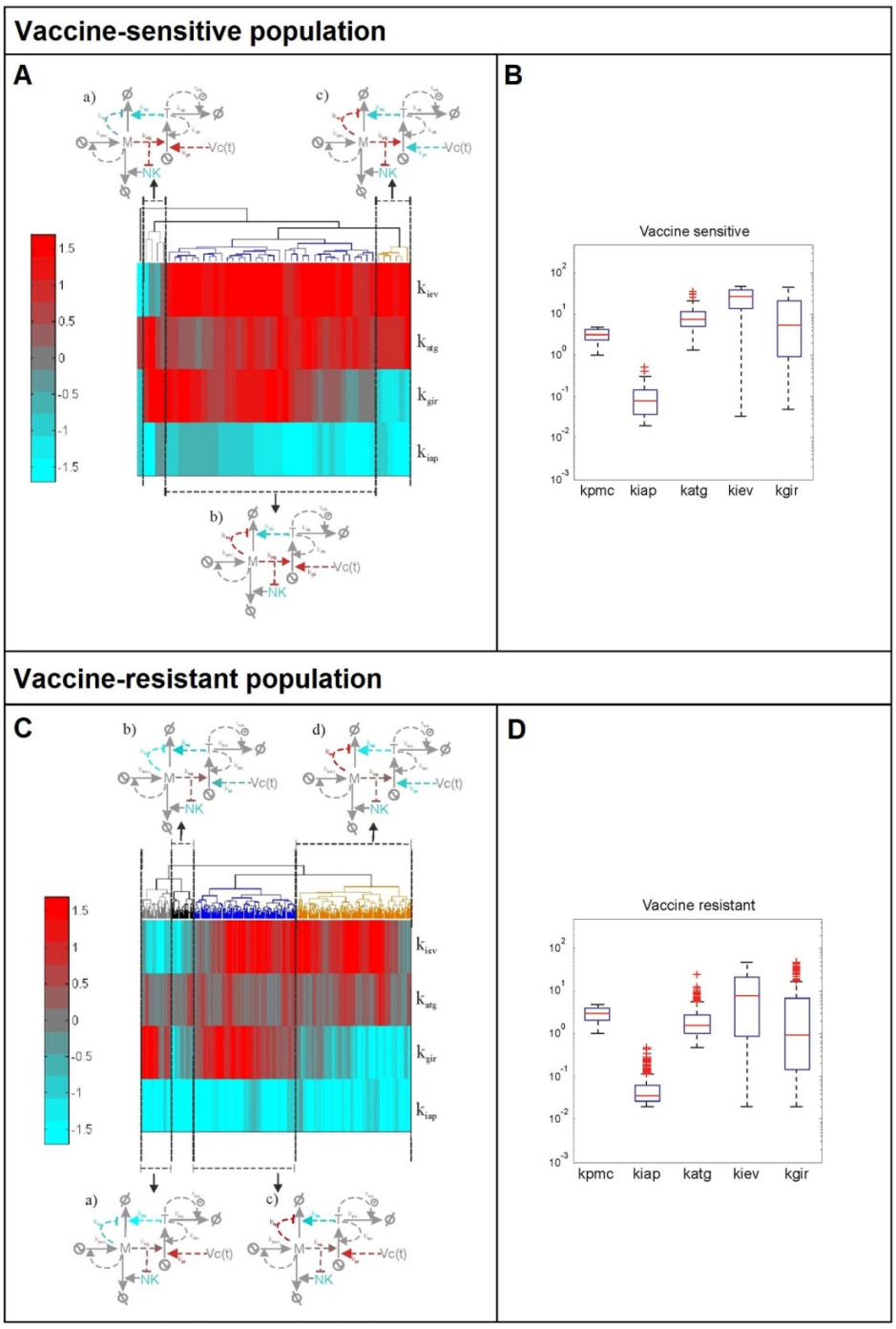

Figure 4. Phenotypic signatures for the subpopulations of vaccine-sensitive (top) and vaccine-resistant (bottom) solutions. Log10 of the nominal parameters in Supplementary Table 1 value is shown (**A,C**). Hierarchical clustering of the solutions in each population with dendrograms and sketches of the regulatory pattern they elicit (**B,D**). Original overall phenotypic signature for each population of solutions.

In case of the vaccine-resistant solutions we obtained four subpopulations (Fig. 4C,D; subpopulations a, b, c and d, highlighted with dendrogram lines in grey, black, blue and orange, respectively). Our analysis revealed

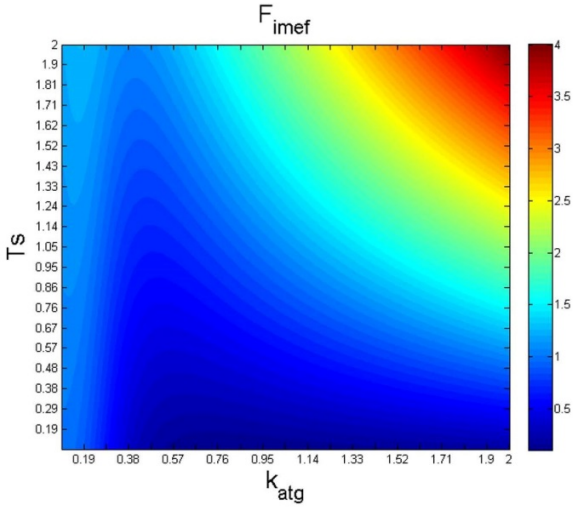

Figure 5. Graphical visualization of the parameter dependency of Equation [3]. The value of the F_{imef} (showed in the colorbar) is plotted against values of T_s and k_{atg} (ordinates and abscissas axis ordinate and abscissa, respectively) F_{imef} corresponds to the term between brackets in Equation [3].

multiple phenotypic signatures, all of them having intermediate levels of antigen presentation in common (k_{atg}):

group a/b) solutions with either high or low values of immune response (k_{gir}), low values of immune evasion (k_{iev}) and T cell-mediated killing of melanoma (k_{iap}), meaning that even micrometastases without evasion mechanisms can survive in a context of low cytotoxic effect of T cells and intermediate levels of antigen presentation machinery even under immunotherapy;

group c/d) solutions with high value of immune evasion (k_{iev}) with either high or low values of immune response (k_{gir}) and low values of T cell-mediated killing of melanoma (k_{iap}), so the micrometastases survive with high immune evasion mechanisms in the context of intermediate levels of antigen presentation even under immunotherapy.

Taken together, our detailed analysis indicates that each of the three classes (vaccine-sensitive, vaccine-resistant and immune-sensitive, last one presented in Supp. Mat.) can arise through multiple phenotypic signatures.

Interpretation of phenotypic signatures by mathematical model analysis. In order to further understand the phenotypic signatures, the model was examined to determine the relationship between the parameter values that promote sustained, immunoresistant tumor growth. The condition for tumor resistance and maintenance is the presence of a minimal amount of persistent melanoma cells (existence of a non-zero steady state of M and instability on $M = 0$, see Supp. Mat.). Because the equation for T is highly non-linear, a complete definition of the steady state cannot be obtained; instead, we will examine the dynamic behavior of the melanoma cells while the T cell population size remains transiently stable.

Equation [3] represents the parameter dependency that is mathematically defining the condition for a sustained tumor growth (see Supplementary Material for derivation). It considers the relation between the following parameters: the tumor growth rate (k_{pmc}), strength of the T cell mediated killing of melanoma cells (k_{iap}), the level of specific antigens presented by the tumor cells (k_{atg}), the steady amount of T cells (T_s), the Hill exponent (g_{nk}) and kinetic parameter of the NKC interaction (k_{nkc}):

$$k_{pmc} > k_{iap} \cdot \left(\frac{k_{atg}^{-g_{nk}}}{k_{nkc}^{g_{nk}} + k_{atg}^{-g_{nk}}} + k_{atg} \cdot T_s \right) \quad [3]$$

The right part of the inequality can be interpreted as the ability of the patient's immune system, whether by itself or after therapy, to efficiently counteract micrometastasis growth. Our analysis indicates that when this function is lower than the tumor growth rate (k_{pmc}), the tumor resists the anticancer immunotherapy. In Fig. 5, the factor F_{imef} is equal to $\left(\frac{k_{atg}^{-g_{nk}}}{k_{nkc}^{g_{nk}} + k_{atg}^{-g_{nk}}} + k_{atg} \cdot T_s \right)$ and accounts for the efficiency of the immune response. Next, for simplicity we considered only the effect of k_{atg} (level of antigen presentation by the tumor cells) and T_s on the values of F_{imef} (Fig. 5). The minimum values for F_{imef} (the blue region in Fig. 5) are reached under intermediate values of k_{atg} and low values of T_s. This blue region corresponds to solutions in which the efficiency of the immune response should be lower than the tumor growth rate (k_{pmc}), so the micrometastasis can resist the immune therapy. This region in which the micrometastasis resists the anticancer immunotherapy can be escaped when the

strength of T cell-mediated killing of melanoma cells (k_{iap}) increases, thereby restoring the competence of the patient's immune system to counteract the tumor. As it was to be expected, for low values of T_s, the range in which F_{imef} has minimum values widens and the patient's immune system remains unable to suppress tumor growth for a larger region of k_{atg} values.

In summary, the model-derived analysis indicates that patients who are not competent to eliminate the micrometastasis even in the presence of vaccination (as these results do not depend on the vaccine parameters) are those with a signature of a) low steady-state levels of T cells, which cannot be rescued even by high amounts of antigens presented by the tumor cells (k_{atg}) or b) high levels of T cells with an intermediate level of antigen presentation (k_{atg}). Furthermore, the benefit of the immune response is proportional to the strength of the T cell-mediated killing of melanoma cells (k_{iap}) and inversely correlated with the tumor growth rate (k_{pmc}). These results are consistent with the numerical analysis of vaccine resistance (Fig. 4C, four signatures present intermediate levels of k_{atg} and low levels of k_{iap}). Furthermore, the equation [3] shows the different combination of parameter values favor tumor cells in vaccine resistance.

Comparison of mathematical model predictions with molecular data. To test our model predictions, we retrieved data from a recently published paper in which biopsy samples of metastatic-melanoma patients were analyzed to define a pretreatment gene expression signature for the prediction of the response to an anticancer immunotherapy[15]. To compare the data with our model predictions, the 84 genes in Ulloa-Montoya *et al.*[15] were manually annotated and classified into one of the following categories according to their potential role in interactions of the immune system with the tumor: 1) antigen presentation machinery (corresponding to parameter k_{atg}), 2) immune-mediated tumor apoptosis/cytotoxic T cell mediated killing of tumor cells (corresponding to parameter k_{iap}), 3) tumor immune evasion mechanisms (corresponding to parameter k_{iev}), 4) immune response (corresponding to parameter k_{gir}) and 5) none/unknown (see Material and Methods, and Supp. Mat. Table S3). For the categories with productive annotation (1–4), we averaged the expression values of the assigned genes in each patient to come up with one metagene per category. We then aggregated the average relative expression values for these metagenes in clusters of patients with and without clinical benefit (Fig. 6, see also SM figure S3). In order to make possible a comparison, the solutions from the *in silico* and the patient clusters were log10 transformed, normalized and averaged following the procedure explained in Material and methods. We displayed side-by-side the *in silico* phenotypic vaccine-resistant and vaccine-sensitive signatures to make a comparison with the patient groups[15] and employed hierarchical clustering to generate a heat map grouping *in silico* and patient signatures together (see Material and Methods). As seen in the heat map (Fig. 6), in case of resistant solutions the agreement between the non benefit patient cluster (Nbn) and the *in silico* cluster b is good and is further supported by the small Euclidean distance (highligthed in red). In addition both solutions are qualitatively similar, that is metagenes and parameters keep the same trend of up/down regulation. We notice that, in case of vaccine-resistant solutions, the hierarchical clustering puts aside the benefit patient cluster (Bn). In case of sensitive solutions, none of the three *in silico* clusters conserves the same trend in the up/down regulation of all the parameters compared to the Bn cluster. To further extend our analysis we merged two representative clusters from the *in silico* immune sensitive solutions (a_{is}, accounting for immune sensitive solution solutions of high antigen presenting machinery and b_{is} accounting for solutions with low antigen presenting machinery; see Figure S2). Our analysis indicates that cluster a_{is} is similar to the Bn patient cluster. We notice that the hierarchical clustering puts aside the Nbn cluster, clustered together with the b_{is}.

Taken together, pairing the phenotypic signatures with those derived from patient data offers a possible means for understanding the biological mechanisms behind the stratification of patients into groups with and without clinical benefit. We think the procedure described can have an application when stratifying patients for therapy or when redesigning immunotherapies.

Model-predicted co-adjuvants to therapeutic vaccine. We next looked for a way to capitalize on the *in silico* phenotypic signatures obtained in this study. As adjuvant therapies have been proposed and studied in anticancer vaccinations[29,30], we speculated that extension of the model to account for co-adjuvants might provide insights on how to improve the vaccine efficacy in less immunocompetent patients. Based on published results, we decided to explore the combination of immunotherapy with cytokines IL-2 and IFN-α used as co-adjuvants. In our model, we assumed that IL-2 can alter the cytotoxic effect of T cells and T cell proliferation (k_{iap} and k_{atc}, respectively), while IFN-α increases the presentation of antigens via upregulation of HLAs (k_{atg}). We display simulations of the vaccine-resistant set of solutions either under immunotherapy alone, or in combination with IL-2, IFN-α or both cytokines (Fig. 7). For the treatment with IL-2, the parameters related to T cell proliferation (k_{atc}) and the cytotoxic effect of T cells (k_{iap}) were increased by a factor of 10. For the treatment with INF-α, the parameter for the presentation of antigens (k_{atg}) was increased by a factor of 15. The therapy was simulated during the first 30 days. Afterwards, the simulation was run until day 100. It can be seen that only the combination of both co-adjuvants in conjunction with the immunotherapy is able to deplete the micrometastasis in the high majority of the vaccine-resistant solutions (Fig. 7B,C compared to Fig. 7D).

There is experimental evidence of the benefits of IL-2 or IFN-α supplementation, whether as monotherapy or combined with DC vaccine[29–33]. Concerning targeted cytostatic therapies, a cytostatic drug (cetuximab) in combination with vaccination against epidermal growth factor receptor has been shown to be efficacious[34]. Our analysis suggests an improvement of the DC vaccine therapy through the co-administration of both cytokines in patients who do not respond to the vaccine alone, together with targeted cytostatic drugs (reduce k_{pmc}). However, this is an outcome of our modelling exercise and therefore it would in any case require extensive experimental validation.

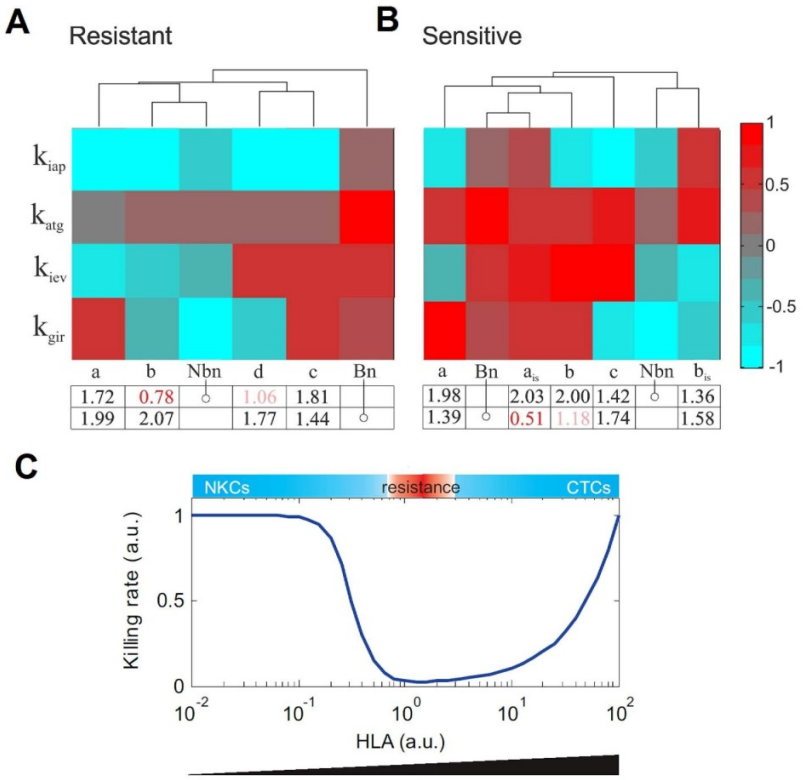

Figure 6. Comparison between the model-based phenotypic signatures and the pretreatment gene expression signature. (**A**) Vaccine-resistant signatures vs. patient clusters. Columns named a, b, c and d correspond to the *in silico* signatures, while columns named Nbn and Bn correspond to the patient clusters without and with clinical benefit, respectively. The phenotypic signatures were clustered using hierarchical clustering (see Material and methods for further details). The table below the heat map displays the Euclidian distances between the average of the *in silico* signatures and the average of the benefit and non-benefit patient clusters. (**B**) Vaccine-sensitive signatures vs. patient clusters. For the purpose of further analysis and discussion, we also included two representative clusters from the in silico immune-sensitive solutions (named a_{is} and b_{is}) (**C**) Our analysis revealed the need for a tight balance in antigen presentation in the tumor. The total rate of melanoma cell killing (ordinate) was computed and displayed for different expression values of antigen presentation proteins (k_{atg}, abscissa HLA). The total killing rate includes both the contributions of NK and cytotoxic T cells. $k_{atg} \in [0.01\ 100]$; $M = 1$; $T = 1$, nominal values for other model parameters.

Discussion

In this paper, we set up and characterized a kinetic model accounting for the interactions of a tumor with the immune system in the context of melanoma micrometastases. The model reflects the interplay between the inherent immune response, the micrometastases and the anticancer immunotherapies stimulating the adaptive immune response against the tumor. Although the model builds on and is able to mimic many basic features of the tumor-immunity interaction, it is far from being a complete description of the system. Modifications that can improve the model are: a) a more detailed description of the local interactions between the micrometastasis and the immune system, including additional key immune cell populations, cytokines and growth factors which can mediate immune responses and immunosuppression (see models containing this feature in Robertson-Tessi, M. *et al.*[18] and de Pillis, L. G. *et al.*[6]); and b) a more precise description of the dynamics associated with immunotherapies[11,35], or the addition of clinical data sets[12]. Moreover, the critical signaling and transcriptional pathways controlling the regulation of key phenotypic features in the tumor-immunity interaction could be modelled in detail, providing means for defining more precise gene signatures and hence more accurate model predictions[13]. In line with this, it will be interesting to improve the resolution of the pathways controlling the antigen-mediated dendritic-cell activation and their role in optimizing anticancer vaccination[36]. The model can be expanded to provide more accurate, clinically relevant predictions in accordance with the obtained results. However, the aim of the present work was not to generate a comprehensive model of the interactions of the tumor with the immune system in a melanoma micrometastasis, but to present, describe and illustrate with a case study a methodology that is able to 1) generate phenotypic signatures of the tumor-immunity interaction using kinetic model

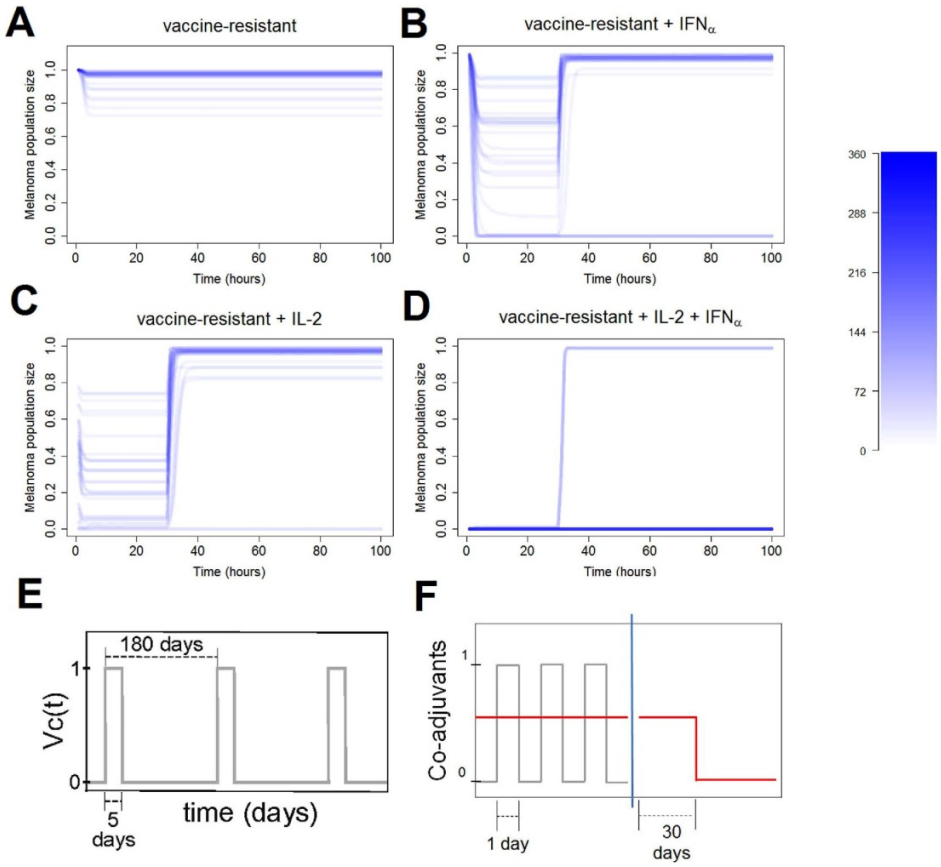

Figure 7. Numerical simulation of the co-adjuvant (IL-2 and IFN-α) therapy. (**A**) A time profile for the vaccine-resistant solutions. (**B**) IFN-α co-adjuvant therapy applied to the solutions from A for 30 days from initial condition. (**C**) IL-2 co-adjuvant therapy applied to the solutions from A for 30 days from initial condition. (**D**) Both co-adjuvants applied in combination to the solutions froms A for 30 days from initial condition. Color bar indicates the number of solutions on overlapping regions. (**E**) Sketch of the immune therapy simulation. (**F**) Sketch of the co-adjuvant therapy simulation (IL-2 and IFN-α), red line is a simplification of the actual dynamics of co-adjuvant therapy, representing the mean value.

simulations and mathematical analysis; 2) to compare *in silico* gene signatures with patient data; and 3) to propose model-based co-adjuvants for existing immunotherapies.

We combined systematic model simulations, statistical techniques and mathematical analysis to generate phenotypic signatures accounting for the sensitivity or resistance of melanoma micrometastases to the inherent immune response of individual patients and to the application of immunotherapies. We recently used a similar method to obtain and validate gene signatures of chemoresistance in malignant melanoma[13], but to the best of our knowledge similar approaches have not been used in the context of interactions of the tumor with the immune system and the assessment of anticancer immunotherapies.

The obtained phenotypic signatures were compared to published data on pretreatment gene expression signatures able to predict the response to immunotherapy in melanoma[15]. To this end, the gene signatures derived from clinical data sets were aggregated by defining and using metagenes which match the features of the biological mechanisms investigated and the mathematical model constructed. This provides a strategy to compare clinical data model predictions, which we think can be applied to other case studies for the assessment of anticancer therapies. Through our analysis, phenotypic signatures identified from model simulations are in agreement with those obtained from patient data sets, but our results also show the existence of additional more fine-grained signatures that can promote immune sensitivity or resistance. This comparison provides support for the interpretation of the predictive signatures obtained in reference 15. Concerning vaccine-resistant signatures, our results and the clinical data indicate that patient immuno-resistant signatures share intermediate (rather than low) expression levels for the genes related to antigen presentation. Our simulations suggest that this tight balance in the expression levels of these genes constitutes a resistance mechanism through which metastatic melanoma cells minimize the effect of immune responses mediated by cytotoxic T cells and natural killer cells, respectively

(Fig. 6C). Concerning vaccine-sensitive results, our analysis preferentially grouped the patients with clinical benefit together with an *in silico* signature corresponding to a cluster of immune-sensitive solutions displaying high levels for all the parameters sampled (Figure S2, the cluster a_{is}). These results are consistent with previously experimental observations from several cancer immunotherapy trials, in which immunotherapies proved to work in immunocompetent individuals[37].

Based on the phenotypic signatures, we computationally analyzed the effect of cytokines used as co-adjuvants and proposed potential treatment improvements, in any case require further *in vitro*/*in vivo* experimental validation. The development of a more detailed mathematical model could help improving the predictive and explanatory capabilities of the obtained phenotypic signatures, and hopefully suggest more detailed adjuvant strategies to improve the efficacy of the therapy in patients with a resistant signature. A possible extension of the model could be an adaptation to include the effect of the recently approved immune checkpoint inhibitors[38] (e.g. anti-CTLA4 and anti-PD1 antibodies) in combination with cellular-based immunotherapies like dendritic cell vaccination.

In the literature, some methodologies have been described to generate regulatory network patterns in the context of biomedicine and biotechnology, which are based on the use of systematic parameter sampling in kinetic model simulations[39–41]. The distinctive features of our methodology are that a) it puts primary emphasis on the detailed definition of the biological scenarios that are simulated and analyzed; and b) we design the model in a way that makes the generated phenotypic signatures comparable with high-throughput data. The ultimate goal of our method is to integrate high-throughput data analysis with model simulations in for the assessment of cancer immunotherapies. Moreover, we think that it will be useful to other immune-related diseases, including infectious ones.

References

1. Vesely, M. D., Kershaw, M. H., Schreiber, R. D. & Smyth, M. J. Natural innate and adaptive immunity to cancer. *Annu. Rev. Immunol.* **29,** 235–271 (2011).
2. Gupta, S. K. *et al.* Personalized cancer immunotherapy using Systems Medicine approaches. *Brief. Bioinform.* bbv046 doi: 10.1093/bib/bbv046 (2015).
3. Vera, J., Gupta, S. K., Wolkenhauer, O. & Schuler, G. In *Cancer Immunology* (ed. Rezaei, N.) 429–449 (Springer Berlin Heidelberg, 2015). at http://link.springer.com/chapter/10.1007/978-3-662-44006-3_23.
4. Eberhardt, M. *et al.* Third-Kind Encounters in Biomedicine: Immunology Meets Mathematics and Informatics to Become Quantitative and Predictive. *Methods Mol. Biol. Clifton NJ* **1386,** 135–179 (2016).
5. Letellier, C., Denis, F. & Aguirre, L. A. What can be learned from a chaotic cancer model? *J. Theor. Biol.* **322,** 7–16 (2013).
6. de Pillis, L. G., Radunskaya, A. E. & Wiseman, C. L. A validated mathematical model of cell-mediated immune response to tumor growth. *Cancer Res.* **65,** 7950–7958 (2005).
7. Wolkenhauer, O. *et al.* Systems biologists seek fuller integration of systems biology approaches in new cancer research programs. *Cancer Res.* **70,** 12–13 (2010).
8. Bianca, C., Chiacchio, F., Pappalardo, F. & Pennisi, M. Mathematical modeling of the immune system recognition to mammary carcinoma antigen. *BMC Bioinformatics* **13,** S21 (2012).
9. López, A. G., Seoane, J. M. & Sanjuán, M. A. F. A validated mathematical model of tumor growth including tumor-host interaction, cell-mediated immune response and chemotherapy. *Bull. Math. Biol.* **76,** 2884–2906 (2014).
10. Tabatabai, M. A., Eby, W. M., Singh, K. P. & Bae, S. T model of growth and its application in systems of tumor-immune dynamics. *Math. Biosci. Eng. MBE* **10,** 925–938 (2013).
11. Kim, P. S. & Lee, P. P. Modeling protective anti-tumor immunity via preventative cancer vaccines using a hybrid agent-based and delay differential equation approach. *Plos Comput. Biol.* **8,** e1002742 (2012).
12. Kogan, Y., Halevi-Tobias, K., Elishmereni, M., Vuk-Pavlović, S. & Agur, Z. Reconsidering the paradigm of cancer immunotherapy by computationally aided real-time personalization. *Cancer Res.* **72,** 2218–2227 (2012).
13. Vera, J. *et al.* Kinetic Modeling-Based Detection of Genetic Signatures that Provide Chemoresistance via the E2F1-p73/DNp73-miR-205 Network. *Cancer Res.* doi: 10.1158/0008-5472.CAN-12-4095 (2013).
14. Hector, S. *et al.* Clinical application of a systems model of apoptosis execution for the prediction of colorectal cancer therapy responses and personalisation of therapy. *Gut* **61,** 725–733 (2012).
15. Ulloa-Montoya, F. *et al.* Predictive Gene Signature in MAGE-A3 Antigen-Specific Cancer Immunotherapy. *J. Clin. Oncol.* **31,** 2388–2395 (2013).
16. Schuler, G., Schuler-Thurner, B. & Steinman, R. M. The use of dendritic cells in cancer immunotherapy. *Curr. Opin. Immunol.* **15,** 138–147 (2003).
17. Vera, J. *et al.* Investigating dynamics of inhibitory and feedback loops in ERK signalling using power-law models. *Mol. Biosyst.* **6,** 2174–2191 (2010).
18. Robertson-Tessi, M., El-Kareh, A. & Goriely, A. A mathematical model of tumor-immune interactions. *J. Theor. Biol.* **294,** 56–73 (2012).
19. De Boer, R. J. & Perelson, A. S. Quantifying T lymphocyte turnover. *J. Theor. Biol.* **327,** 45–87 (2013).
20. Gatenby, R. A. & Gillies, R. J. A microenvironmental model of carcinogenesis. *Nat. Rev. Cancer* **8,** 56–61 (2008).
21. Lai, X., Nikolov, S., Wolkenhauer, O. & Vera, J. A multi-level model accounting for the effects of JAK2-STAT5 signal modulation in erythropoiesis. *Comput. Biol. Chem.* **33,** 312–324 (2009).
22. Vera, J., Balsa-Canto, E., Wellstead, P., Banga, J. R. & Wolkenhauer, O. Power-law models of signal transduction pathways. *Cell. Signal.* **19,** 1531–1541 (2007).
23. Bar-Joseph, Z., Gifford, D. K. & Jaakkola, T. S. Fast optimal leaf ordering for hierarchical clustering. *Bioinforma. Oxf. Engl.* **17** Suppl 1, S22–29 (2001).
24. De Pillis, L. G. & Radunskaya, A. The dynamics of an optimally controlled tumor model: A case study. *Math. Comput. Model.* **37,** 1221–1244 (2003).
25. Parmiani, G. *et al.* Immunotherapy of melanoma. *Semin. Cancer Biol.* **13,** 391–400 (2003).
26. Umansky, V. & Sevko, A. Melanoma-induced immunosuppression and its neutralization. *Semin. Cancer Biol.* **22,** 319–326 (2012).
27. Gajewski, T. F., Schreiber, H. & Fu, Y.-X. Innate and adaptive immune cells in the tumor microenvironment. *Nat. Immunol.* **14,** 1014–1022 (2013).
28. Dong, H. *et al.* Tumor-associated B7-H1 promotes T-cell apoptosis: A potential mechanism of immune evasion. *Nat. Med.* **8,** 793–800 (2002).
29. Kirkwood, J. M. *et al.* Interferon alfa-2b adjuvant therapy of high-risk resected cutaneous melanoma: the Eastern Cooperative Oncology Group Trial EST 1684. *J. Clin. Oncol. Off. J. Am. Soc. Clin. Oncol.* **14,** 7–17 (1996).

30. Shimizu, K., Fields, R. C., Giedlin, M. & Mulé, J. J. Systemic administration of interleukin 2 enhances the therapeutic efficacy of dendritic cell-based tumor vaccines. *Proc. Natl. Acad. Sci. USA.* **96,** 2268–2273 (1999).
31. Atkins, M. B. *et al.* High-dose recombinant interleukin 2 therapy for patients with metastatic melanoma: analysis of 270 patients treated between 1985 and 1993. *J. Clin. Oncol. Off. J. Am. Soc. Clin. Oncol.* **17,** 2105–2116 (1999).
32. Fyfe, G. *et al.* Results of treatment of 255 patients with metastatic renal cell carcinoma who received high-dose recombinant interleukin-2 therapy. *J. Clin. Oncol. Off. J. Am. Soc. Clin. Oncol.* **13,** 688–696 (1995).
33. Motzer, R. J., Bacik, J., Murphy, B. A., Russo, P. & Mazumdar, M. Interferon-alfa as a comparative treatment for clinical trials of new therapies against advanced renal cell carcinoma. *J. Clin. Oncol. Off. J. Am. Soc. Clin. Oncol.* **20,** 289–296 (2002).
34. Vanneman, M. & Dranoff, G. Combining immunotherapy and targeted therapies in cancer treatment. *Nat. Rev. Cancer* **12,** 237–251 (2012).
35. Radunskaya, A., de Pillis, L. & Gallegos, A. A model of dendritic cell therapy for melanoma. *Mol. Cell. Oncol.* **3,** 56 (2013).
36. Pfeiffer, I. A. *et al.* Triggering of NF-κB in cytokine-matured human DCs generates superior DCs for T-cell priming in cancer immunotherapy. *Eur. J. Immunol.* **44,** 3413–3428 (2014).
37. Gray, A., Raff, A. B., Chiriva-Internati, M., Chen, S.-Y. & Kast, W. M. A paradigm shift in therapeutic vaccination of cancer patients: the need to apply therapeutic vaccination strategies in the preventive setting. *Immunol. Rev.* **222,** 316–327 (2008).
38. Lipson, E. J. & Drake, C. G. Ipilimumab: an anti-CTLA-4 antibody for metastatic melanoma. *Clin. Cancer Res. Off. J. Am. Assoc. Cancer Res.* **17,** 6958–6962 (2011).
39. Alves, R. & Savageau, M. A. Extending the method of mathematically controlled comparison to include numerical comparisons. *Bioinforma. Oxf. Engl.* **16,** 786–798 (2000).
40. Savageau, M. A. & Fasani, R. A. Qualitatively distinct phenotypes in the design space of biochemical systems. *FEBS Lett.* **583,** 3914–3922 (2009).
41. Savageau, M. A., Coelho, P. M. B. M., Fasani, R. A., Tolla, D. A. & Salvador, A. Phenotypes and tolerances in the design space of biochemical systems. *Proc. Natl. Acad. Sci. USA.* **106,** 6435–6440 (2009).

Acknowledgements

This work was supported by the German Federal Ministry of Education and Research (BMBF) as part of the projects e:Bio SysMet [0316171 to JV] e:Bio MelEVIR [031L0073A to JV] and e:Med CAPSYS [01ZX1304F to JV]. Julio Vera is funded by the Erlangen University Hospital (ELAN funds, 14-07-22-1-Vera-González and direct Faculty support) and the German Research Foundation (DFG) through the project the GRK-1660 (JV) and the SFB-643 (to Gerold Schuler). The authors thank Alexander Steinkasserer (University Hospital Erlangen) for constructive comments.

Author Contributions

The original idea was developed by J.V. and S.N. Mathematical model construction and analysis were performed by J.V. and G.S.R. (Guido Santos-Rosales). Statistical analysis was performed by J.V., G.S.R., M.E., X.L. and S.P. Further biological data were collected, curated and processed by F.S.D. and S.P. Biological interpretation of the results was done by J.V. and G.S.R. All the authors drafted the manuscript.

Additional Information

Supplementary information accompanies this paper at http://www.nature.com/srep

Competing financial interests: The authors declare no competing financial interests.

How to cite this article: Santos, G. *et al.* Model-based genotype-phenotype mapping used to investigate gene signatures of immune sensitivity and resistance in melanoma micrometastasis. *Sci. Rep.* **6**, 24967; doi: 10.1038/srep24967 (2016).

14. Immunotherapy against melanoma – Supplementary Material

Derivation of analytic gene signature

For a persistent tumor, the existence of a stable non-zero solution of melanoma cell number (M) and instability on its zero solution are prerequisites. First we test the stability of the zero solution. As the steady state for both variables cannot be analytically obtained because of the high non-linearity of the T cell equation (T), we will analyze the dynamic behavior of melanoma cells while maintaining T constant (T_s). Under this assumption, the stability of the zero solution of melanoma cells (S.1.1) can be analyzed as the partial derivative of the zero steady state respecting changes on melanoma cells, under the restrictions (S1.2), i.e.

$$\frac{dM}{dt} = k_{pmc}.M.\left(M_T - M\right) - k_{iap}.T.\frac{k_{atg}.M}{1+k_{iev}.M} - k_{iap}.M.\frac{\left(HLA^{-1}\right)^{g_{nk}}}{\left(k_{nkc}\right)^{g_{nk}} + \left(HLA^{-1}\right)^{g_{nk}}} \tag{S1.1}$$

$$M_T = 1,\ T = T_s,\ HLA = k_{atg} \tag{S1.2}$$

$$\left.\frac{\partial\left(dM/dt\right)}{\partial M}\right|_{M=0} = k_{pmc} - \frac{k_{iap}.k_{atg}^{-g_{nk}}}{k_{nkc}^{g_{nk}} + k_{atg}^{-g_{nk}}} - k_{iap}.k_{atg}.T_s \tag{S1.3}$$

According to (35), the steady state at $M = 0$ is unstable if equation (S1.3) is greater than zero. In (S1.4) and (S1.5) are given these conditions for the instability of the zero solution, i.e.

$$k_{pmc} - \frac{k_{iap}.k_{atg}^{-g_{nk}}}{k_{nkc}^{g_{nk}} + k_{atg}^{-g_{nk}}} - k_{iap}.k_{atg}.T_s > 0, \tag{S1.4}$$

$$k_{pmc} > k_{iap}.\left(\frac{k_{atg}^{-g_{nk}}}{k_{nkc}^{g_{nk}} + k_{atg}^{-g_{nk}}} + k_{atg}.T_s\right). \tag{S1.5}$$

Now we will consider the conditions for the existence of stable solutions for M different from zero. First, as values of M are bounded between 0 and Mt, the solutions for M have to be either oscillating or steady for all initial values between these magnitudes. On the other hand, under the assumption that T remains constant, M cannot oscillate, as the restriction reduces the model to

only one variable, so the only possibility for *M* under these conditions is to reach a stable steady state. We are going to consider the solutions which satisfy equation (S1.5), so there is no stable zero solution and, under our reasoning, there must be at least one steady positive solution for *M*. This will be proven now. We solve equation S1.1 under the restrictions (S1.2) and (S2.1)

$$\frac{dM}{dt} = 0\,. \tag{S2.1}$$

Thus, we obtain equation (S2.2), i.e.

$$k_{pmc}.M.(1-M) - k_{iap}.T_s.\frac{k_{atg}.M}{1+k_{iev}.M} - k_{iap}.M.\frac{k_{atg}^{-g_{nk}}}{k_{nkc}^{g_{nk}} + k_{atg}^{-g_{nk}}} = 0. \tag{S2.2}$$

This equation can be solved analytically, and we obtain three different solutions, one of them is the zero solution, which is going to be instable under assumption (S1.5). Of solutions $\overline{M}_{2,3}$,at least one must be positive for all values of the parameters satisfying S2.2.

$$\overline{M}_1 = 0, \tag{S3.1}$$

$$\overline{M}_{2,3} = \frac{k_{pmc}.k_{iev} - k_{pmc} - A \pm \sqrt{\left(k_{pmc}.k_{iev} - k_{pmc} - A\right)^2 + 4k_{pmc}.k_{iev}\left(A - k_{iap}.k_{atg}.T_s\right)}}{2.k_{pmc}.k_{iev}} \tag{S3.2}$$

where $A = \dfrac{k_{iap}.k_{iev}.k_{atg}^{-g_{nk}}}{k_{nkc}^{g_{nk}} + k_{atg}^{-g_{nk}}}$.

Applying condition (S1.5) for (S3.2) makes the right term inside the root positive. Because the left term in the root is equal to the one in front of the root before squaring, the root itself will have a higher value than the term in front of it. That means that the sign of the solutions will be the sign of the root term. In this condition, there is going to be one positive and one negative solution, so there is at least one positive solution that will always exist when the zero steady solution is instable.

Summing up, when equation (S1.5) is satisfied, at least one positive solution for *M* exists and the zero steady solution will be instable.

Figure S1. Biphasic depletion of active cytotoxic T cells

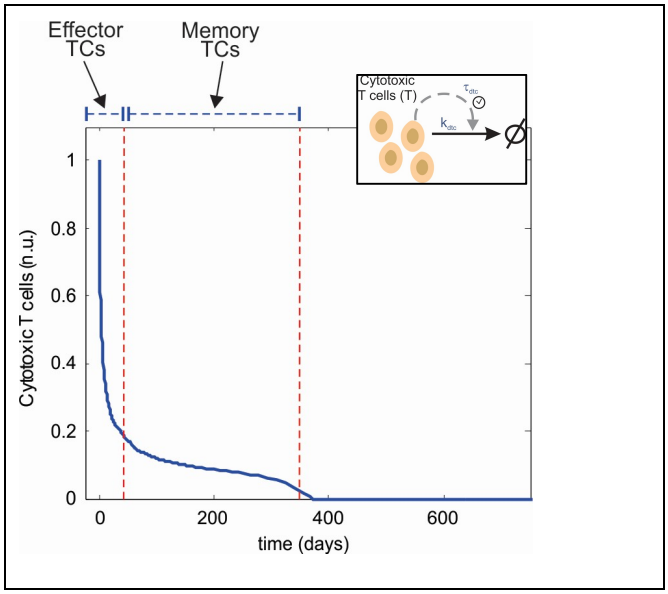

Figure S1. Biphasic depletion of active cytotoxic T cells. Upon the introduction of a slower, time-delayed T cell depletion term, our model can account for a small fraction of activated cytotoxic T cells (approx. 10 %) that have a longer lifespan and act as a phenomenological representation of memory T cells [19]. (*T(0)=1; M(0)= 0*; nominal values for the model parameters).

Table S1. Model parameter definition and values

Parameter	Description of associated process	Nominal Value	Reference and Comments
k_{apc}	APC-mediated initiation of cytotoxic T cell response	0.04 day^{-1}	PMID:9182685
k_{gir}	Vaccine mediated global immune response	1 a.u.	Normalized
k_{atg}	Expression of melanoma specific antigen	1 a.u.	Normalized
k_{tapc}	Threshold APC-mediated initiation of cytotoxic T cell response	0.2605 a.u.	Fitted to normalization†
g_1	Hill-coefficient DC-mediated initiation of cytotoxic T cell response	2.784	Fitted to normalization†
k_{atc}	Expansion of active cytotoxic T cells	2.0791 day^{-1}	PMID:14530309
k_{tatc}	Threshold expansion of active cytotoxic T cells	0.2605 a.u.	Fitted to normalization£
g_2	Hill-coefficient expansion of active cytotoxic T cells	2.784	Fitted to normalization£
k_{dtc}	Main (linear) depletion of effector cytotoxic T cells	0.3466 day^{-1}	PMID:14530309
k_x	Fraction of memory T cells	0.1 a.u	PMID:14530309
τ_{dtc}	Half-life of memory T cells	500 days	PMID:14530309
k_{pmc}	Proliferation of melanoma cells	0.5545 day^{-1}	PMID:20406486
k_{iap}	Cytotoxic T cell-mediated melanoma cell apoptosis	5.4931 day^{-1}	PMID: 15725959
M_T	Maximum size of micrometastasis	1 a.u.	Normalized¥
k_{iev}	Melanoma-elicited immune evasion mechanism	1	Normalized
M_0	Initial condition melanoma micrometastasis	0.00081 a.u.	Normalized¥
g_{nk}	Hill exponent for NKC interaction	3.9913	Fitted to normalization†
k_{nkc}	Kinetic parameter for NKC interaction	3.1623	Fitted to normalization†

Notes to the table: †.The values of Hill equation coefficients were calculated such that the APC-mediated initiation of cytotoxic T cell response reaches 95 % of the saturation value for a tumor population size of 75 % of the maximum micrometastasis size and normal expression level of melanoma specific antigens. A similar assumption was used to calculate£. ¥. PMID:12794026, PMID:16968875, PMC:2922988

Figure S2. *In silico* signatures for immune-sensitive subpopulations from the model. A. Hierarchical clustering of the solutions in each population, with dendrograms. **B.** Original overall phenotypic signature for the each population of solutions.

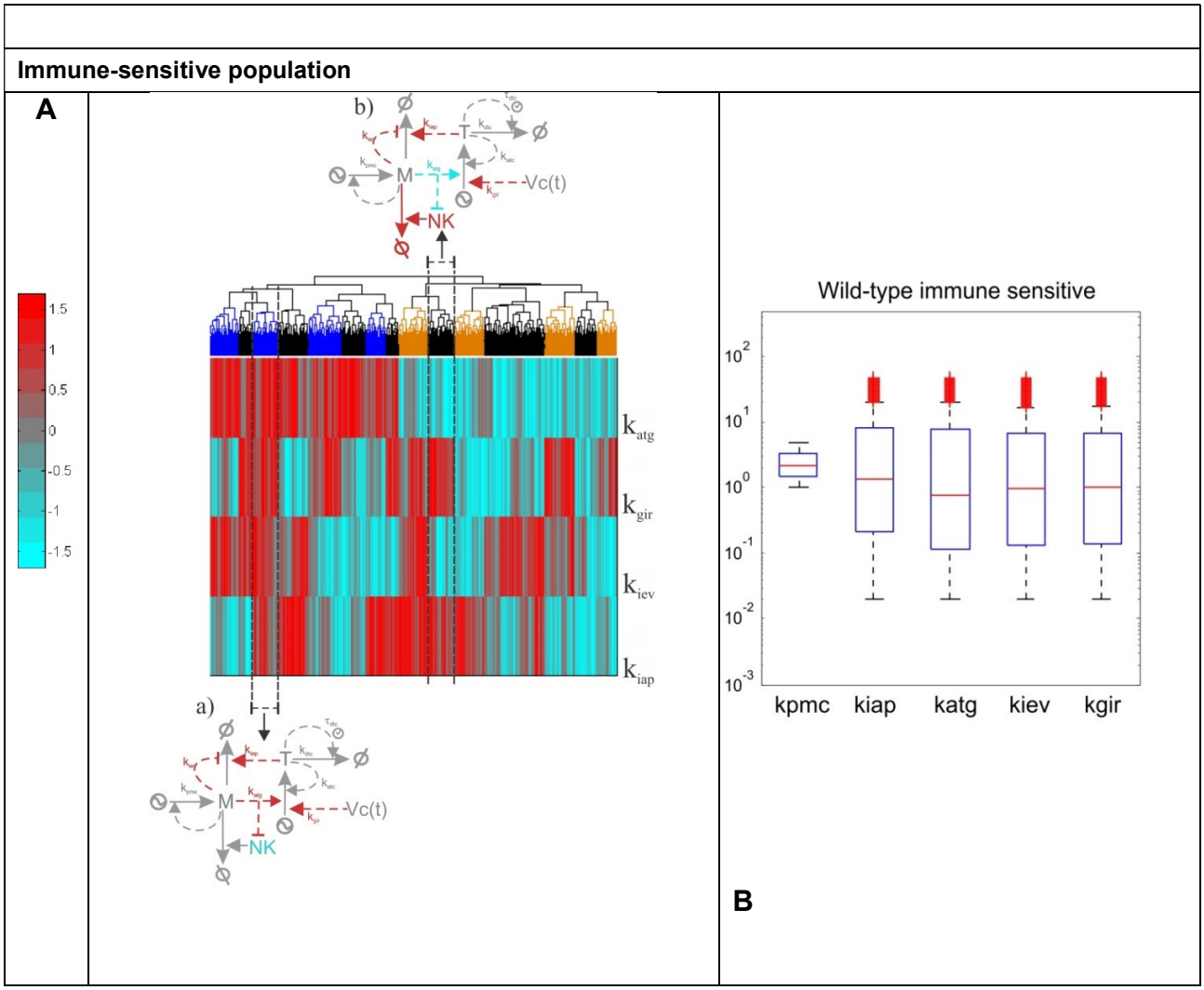

Figure S3. Grouping of patient data into clusters of clinical benefit vs. no clinical benefit.

Original patient clustering	Clustering after gene and patient aggregation

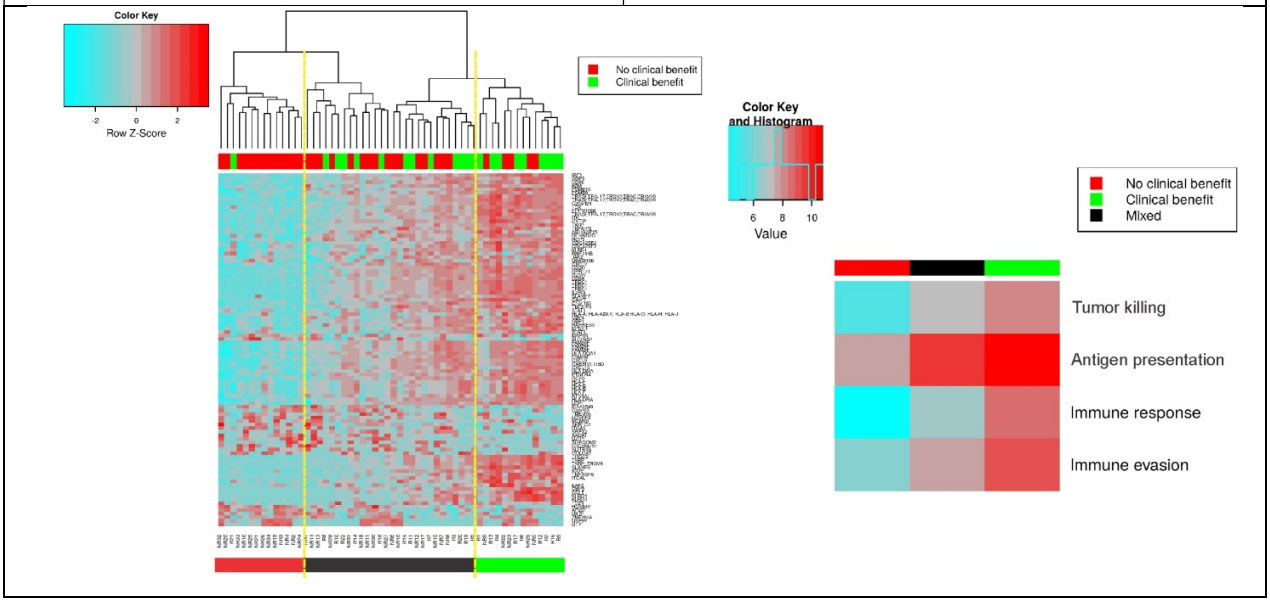

Figure S4. Sensitivity analysis for the four groups of solutions: tumor, immune-sensitive, vaccine-sensitive and vaccine-resistant. The sensitivities are calculated dynamically, they measure the ratio of the log change in the integral of the simulation of the variables over the log change in the parameters. The panels show histograms for the mean value of parameter sensitivities of each solution. The vast majority of the solutions have a mean value of sensitivity less than one, which means that changes in parameters affects very little to the dynamical behavior of the solutions.

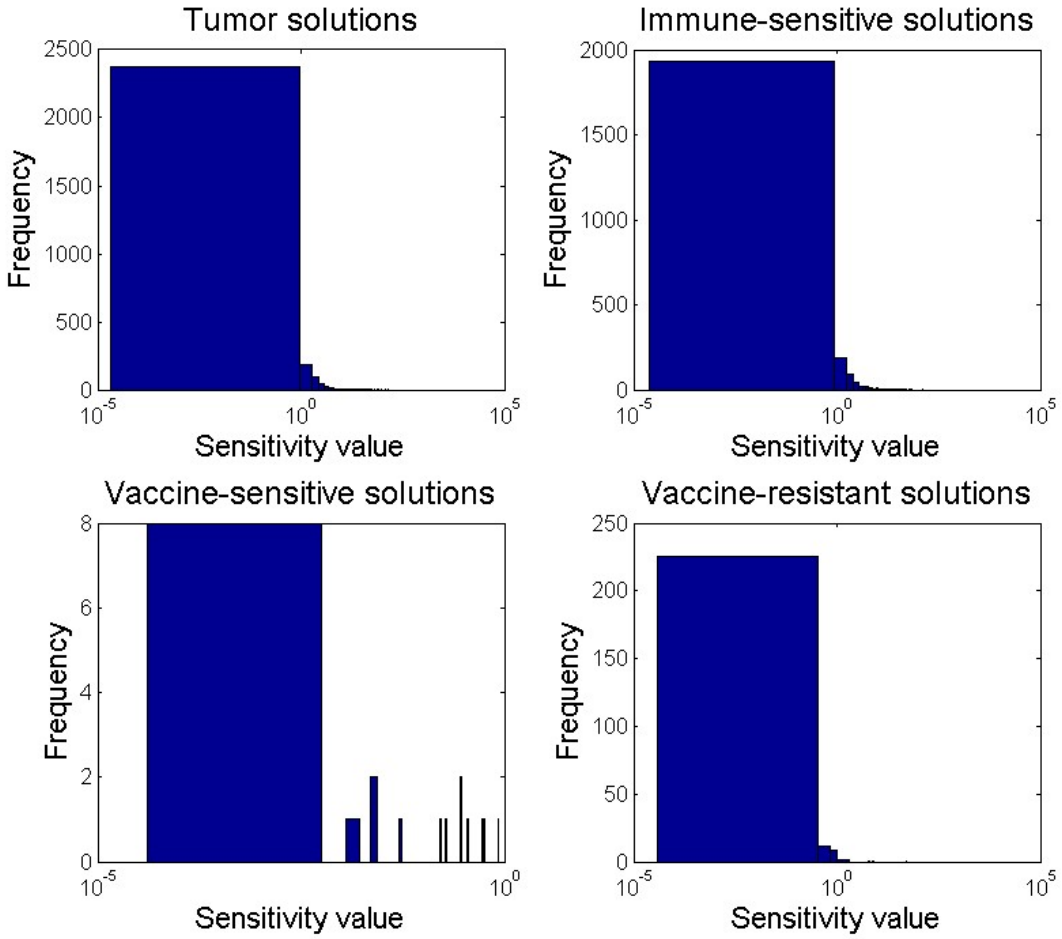

Table S2. Numerical data of the Figure 7 in the text. Data are normalized between 0 and 1.

Resistant	a	b	Nbn	d	c	Bn
k_{iap}	-0.97	-1.00	-0.50	-0.89	-0.91	0.30
k_{atg}	0.05	0.11	0.20	0.17	0.17	1.00
k_{iev}	-0.71	-0.54	-0.30	0.63	0.61	0.50
k_{gir}	0.60	-0.42	-1.00	-0.59	0.53	0.50

Sensitive	a	Bn	a_{is}	b	c	Nbn	b_{is}
k_{iap}	-0.65	0.30	0.41	-0.74	-0.83	-0.50	0.53
k_{atg}	0.60	1.00	0.54	0.55	0.66	0.20	0.66
k_{iev}	-0.33	0.50	0.67	0.93	1.00	-0.30	-0.70
k_{gir}	0.93	0.50	0.48	0.53	-0.76	-1.00	-0.47

15. General results and discussion

Mathematical modelling has been applied to biomedical problems during the last and present century, but it has increased the interest in the last two decades. The main procedures in the formalization and analysis of mathematical models in biosciences are discussed in the first article of the present collection. Any mathematical approach in biosciences can be categorized into three different stages: i) conceptualization of the biological system, ii) mathematical formalization and iii) optimization and system management from the analysis.

As an example of the application of systems biology to biomedical problems it is reviewed in the next section a collection of articles in which it has been used mathematical models in the topic of malaria-host interactions. Malaria research has a strong connection with mathematical models in biology because epidemiological models were proposed by Sir Ronald Ross for the study of the life cycle of this disease. It also was one of the first mathematical modelling exercises in biosciences. Following the history of modelling approaches in malaria is a representative way to analyze the evolution of mathematical modelling in biosciences.

Four mathematical modelling approaches in biosciences have been developed for this present work. These models previously presented focused on different diseases and the methodology and characteristics of the models are different, but they have in common the systemic approach and the quantitative and dynamical analysis of the diseases. The first work about malaria used an ODE mathematical model on the power-law formalism; this gives many parameters to be calibrated in the model but more power to predict non-linear dynamics of the relationship between the parasite and the host. To deal with many parameters it was needed to use many data from bibliography and also a lot of verification with new data to be sure that the prediction of the model is biologically accurate. The model of HIV infection was also based on ODE equations, but the formalism used was mass action. In this case it was more appropriate assuming linear relationship between velocities and the concentration of the molecules. Since the linear assumption cannot be realistic in many biological situations, it is a key point providing a very good verification of the model, so we can be sure about the linear assumption in the interesting conditions for the objective proposed. For the model of Alzheimer's disease it was used a different mathematical framework, instead of being formulated by an equation based model it was used an agent based model. The reason to have chosen that is because the main hypothesis for the cause of the disease is focused on the cell membrane of the neurons. It is assumed that there is a relationship between the lipid dynamics in the membrane and the production of β-amyloid, but it is not an easy way to formalize what the specific mechanism behind is. By contrast, they are known the interactions between lipids in the membrane which explain the mobility and fluidity. This kind of situation is optimal for applying agents based models; in this case the agents are the lipids interacting in the membrane. Finally, a simple mathematical model was made using ODE equations; it was used a mix of formalism between mass action and Hill equation. In this case it was a starting exercise to find promising improvements of immunotherapy against melanoma using mathematical analysis.

The objective of the malaria work was to propose new targets on which to focus the antimalarial drug search. The advantage of using mathematical modelling is that the therapeutic strategies are based on a model which integrates a lot of information coming from different studies and also because it considers the dynamical relationship between the parasite and the host. It was included the amount of red blood cells of the patient, the parasitemia as the amount of erythrocytes infected by two different phases of the parasite (asexual and sexual phase) and also it was considered an element which represents the state of activation of the immune system. The model was calibrated using data from bibliography, specifically measures of parasitemia, the red blood cells count and the concentration of immunoglobulin IgG1 in mice infected with malaria during time. In order to verify the model it was used new experimental data taken in different condition. First, to validate the use of the model in humans it was compared the long term dynamics (more than 200 days) of the model with the long term evolution of patients with malaria without any treatment. The model reproduces the damped oscillations in parasitemia and the delay in the peaks between both species of the parasite in the bloodstream. Then new data taken in different conditions was collected, it was measured the first peak of parasitemia in monkeys with malaria with and without vaccination. The vaccination was simulated in the model increasing the initial condition of the immune variable of the model. The model was able to reproduce the decrease and the delay of the first peak of parasitemia when the vaccine was given. Finally, to analyze the validity of the model after applying a treatment, experimental data taken from mice with malaria was used, two different formats of treatment were applied: i) an injection and ii) a slow releasing drug vesicle. The parasitemia observed on mice was different depending on the way the drug was applied. The model was modified to consider these treatments and the predictions of the model were very accurate comparing them with the experimental data. Based on the model it was proposed a set of four single targets for drug searching and one additional combination of two simultaneously modifications which could serve as a strategy to give two drugs instead of only one. The best strategy was decreasing the invasion of erythrocytes by the parasites. Another strategy consist on killing the asexual phase of the parasite which is also a current treatment used in malaria. Other proposals were killing the sexual phase of the parasites, increasing the transformation of the asexual phase into the sexual one and decreasing the activation of the immune system promoted only by the sexual phase. The combined strategy was decreasing the activation of the immune system promoted only by the sexual phase and increasing the clearance of erythrocytes from the bloodstream simultaneously.

The work on HIV infection was focused on the invasion of T4 lymphocytes by HIV, which is a key part of the process, as the virus reproduce inside them. The objective was to understand the relative importance of the molecular pathways activated during the viral entry and pointing to interesting molecular targets for designing drugs which can prevent the invasion of T4 lymphocytes by the virus. The model considered many pathways of interacting molecules which are known to play a role during the invasion: i) the activation of moesin, which joins the actin filaments to the invasion point of the membrane; ii) the activation of filamin, joining actin filaments to the CD4 receptor in which the virus triggers the signal; iii) action of gelsolin, which cuts actin filaments into smaller pieces; iv) cofilin inactivation, so stopping its actin severing activity. The final result of the modification of these pathways by the HIV is producing an accumulation of actin filaments and other molecules at the point of viral contact in the membrane, called cap. This structure facilitates the opening of a pore through which the virus can enter in the cell. The cap is a dynamic structure built by changes in a complex network of molecule interactions. Because of that it is necessary to integrate the information in a quantitative model which considers the time dimension to understand the relative importance of each pathway in the process. For the calibration of the model it was used experimental data *in vitro* of HIV invading lymphocytes. This data contains dynamical quantification of the clustering of CD4 receptors, moesin and actin in the point of invasion. The model was able to reproduce the clustering dynamics observed *in*

vitro. Due to the lack of data the model was subjected to many verification exercises. First, the response of the model after changing (increasing and decreasing) the total amount of moesin was compared with experimental modifications of this protein *in vitro*. The model prediction of the behavior of the experiment was accurate. Then data from another experiment was used, the amount of gelsolin was increased and decreased in the lymphocytes and it was simulated in the model. The prediction of the model fitted the data when it was assumed that gelsolin had a positive effect on the construction of the cap, this is interesting because it points to a potential benefit on inhibiting gelsolin to prevent the invasion of HIV. It was also experimentally analyzed the decrease in filamin and compared with the model prediction of this reduction, and the model was able to reproduce the effect of that on the infectivity. Finally, increasing the severing of the actin filaments introducing the effector Lat-A on the cells affects the infectivity of the virus. The change in infectivity after different doses of Lat-A was verified by the model simulating these different doses. Based on the model it was established that the main factors to reduce the invasion of the lymphocytes by HIV is decreasing the cap structure and extending the time to release the cap after the pore is formed. As it was mentioned, the cap is a dynamical structure and its physiology can only be understood in a dynamical way. Long before the first contact of the virus with the immune cell the cap has to be formed with a minimal amount of actin filaments to facilitate the tensional forces to open the pore. But, as the virus has to enter inside, the cap structure has to be cleared just before the pore is open. Increasing the amount of the actin severing molecule cofilin has been observed to affect the production of the cap, so our model proposes that even inhibiting its actin severing activity it can decrease the invasion ability of the virus because it could extend the time to clear the cap structure allowing the entry through the pore.

The study of Alzheimer's disease was focused on the lateral movements of the lipids in the cell membrane of neurons. In the cell membrane there exist lipid domains with differential physical characteristics and composition from the rest of the membrane, they are called lipid rafts. Inside lipid rafts the lateral movement is lower than outside. The relationship of lipid rafts with the disease is that inside these domains it is produced the aberrant peptide β-amyloid. The objective of the work is finding a correlation between the changes of the physical properties of the lipid rafts and the evolution of the disease. The model of Alzheimer's disease was built using agent based modelling; this mathematical framework defines a set of elements which interact in a defined landscape following a set of rules. All lipids were aggregated into six groups attending to the common molecular structure: i) sterols; ii) docosahexaenoic acid (DHA); iii) n-6 long chain polyunsaturated fatty acids; iv) monoenes; v) saturates fatty acids; vi) sphingolipids. The landscape of interaction is a lattice organized by rows and columns; the elements (lipid groups) were located in the lattice and they could interact with their four neighbours. The probability of one lipid interchanging its position with one neighbour is inversely proportional to the force by which it is detained in its position. This force comes from the sum of the forces of pairwise interactions with the other three neighbours, and each pair force depends on the molecular structure of the groups. This molecular structure was initially given by averaging the width and the length of the lipids inside each group using a molecular visualization program (*Jmol*), so each group was fitted to a cylinder with a width and a length similar to the elements of the corresponding group. As this characterization of the molecular structure using cylinders is a gross approximation it was made a refinement of the structural parameters for the cylinders using experimental measurements of the lipid compositions of the cell membrane and of the isolated lipid rafts. These experimental measurements of the lipid composition were made in mice of 3, 6, 9 and 14 months of two groups: i) wild type (WT); ii) Alzheimer's disease induced mice model (AD). The initial assigned width and length was slightly changed in order to predict the lipid composition of lipid rafts after giving to the model the lipid composition of the whole cell membrane. The model reproduced the experimental lipid composition in all conditions. Then, the model was verified using experimental data taken *a posteriori*, first the lateral mobility of the

lipids outside lipid rafts was predicted on four different conditions: i) 6 months WT; ii) 14 months WT; iii) 6 months AD; iv) 14 months AD. The experimental microviscosity (as an experimental measurement of lateral movement) was measured in these four conditions. The changes in microviscosity observed in the experiments through the different conditions were the same than the ones predicted by the model. The model predicted that the increase in the lipid rafts size and in the lateral mobility outside these domains are the main factors which correlate with the disease evolution. In order to find dietary treatment strategies, the condition of 3 months WT in the model was assumed to be the healthy situation of the membrane and the 9 months AD condition is considered as a pathological but reversible condition. The proportion of each lipid group on the membrane was systematically increased and decreased to follow the effect on the lipid raft composition of the 9 months AD condition respecting the lipid rafts composition of the 3 months condition. Increasing the proportion of sterols or DHA was promising dietary strategies to revert the physical modification on the lipid rafts during the Alzheimer's disease evolution.

Finally, a mathematical model using ODE equations was proposed to simulate the interaction between melanoma cells and the immune response of the patients. Immunotherapy is a very recent strategy to treat cancer, and specifically in melanoma. Additional improvements on the therapy are needed to make it effective in patients in whom it is not working. Mathematical analysis on the proposed model was made to unravel the hidden mechanisms of tumor cells resistance to immunotherapy. First, based in the known mechanisms of interaction between tumor cells and the immune system, it is proposed a simple mathematical model. It considers the T cell activation and proliferation in response to tumor cells, the response promoted by the immunotherapy, the T cell inactivation and memory cell long term action, the tumor cell growth, the tumor cell death by T cells and NK cells and the immune evasion mechanisms of the tumor. The results of the mathematical analysis of the model give a gene signature for the tumor resistance. This gene signature is a relationship between the parameters of the models that explains the tumor cell resistance to the therapy. This gene signature proposes that intermediate levels of antigen presentation machinery and low amounts of T cells in the patients are hallmarks that can explain the melanoma tumor resistance. Numerical analysis based on this signature points to potential improvements on the immunotherapy against melanoma in resistant patients. Increasing T cell amount and T cell activity against melanoma cells using IL-2 and increasing the presentation of tumor cell antigens by INF-α is the best strategy to combine with vaccine immunotherapy. These co-adjuvant therapies have been individually proved in previously studies, but the combined strategy is, under our knowledge, to be proven.

16. Conclusions

Mathematical modelling in biosciences

i) The theoretical principles of mathematical modelling are available since the XVII century, but only in the last century it was possible to apply them to actual problems in biology.
ii) The new paradigm of systems biology proposes a new way to analyse the biological systems, integrating many elements in a single framework and considering the dynamics of the processes.

Review of mathematical models in malaria

iii) Mathematical modelling of malaria-host interactions has increased the knowledge of the disease and it has been used to propose potential molecular targets for the design of new therapies.
iv) The interaction between the malaria parasite and the immune system elements of the host has been clarified using mathematical approaches, it is highlighted the non-linear, dynamical and complex nature of these interactions.

Malaria

v) The best therapeutic strategy predicted by the mathematical model of malaria is impeding the invasion of erythrocytes by the parasite; this option is being evaluated in current antimalarial drug searching protocols.
vi) Another interesting target to reduce the infectivity of the disease is focusing on killing the sexual phase of the parasite. This strategy is currently used in the effective antimalarial drugs.
vii) One new target never evaluated to find new efficient drugs, which could replace the current ones when they lose efficacy, is increasing the transformation of the asexual phase into its sexual phase.
viii) One last unique target on which to focus the search of drugs is decreasing the activation of the immune system by the sexual phase of the parasite. This strategy is not only a never evaluated target, but it is also interesting to potentially decrease the emergence of resistance by the parasite, as it does not affect directly the parasite.
ix) One combination of two targets which would increase the efficacy of the therapy is decreasing the activation of the immune system by the sexual phase of the parasite and increasing the clearance of red blood cells by the organism.

VIH

x) The virulence factors which increase the invasion of lymphocytes by HIV are a strong actin structure at the invasion point and a fast clearance of this structure just after the pore is formed.

xi) Gelsolin is a molecule which increases the infectivity by favouring the formation of the actin structure; even though it is a severing factor. It is an interesting target in which focus on the search of drugs to cure HIV.
xii) Although cofilin is a severing factor which completely destroys actin filaments and it has been proved that increasing cofilin the actin structure is destabilized, cofilin inactivation can also be an interesting target against HIV as doing it would delay the clearance of the actin structure which impedes the entry of the virus.

Alzheimer's disease

xiii) A lipid grouping into six categories: sterols, DHA, n-6 long chain polyunsaturated fatty acids, monoenes, saturates and sphingolipids; is able to predict the observed lipid domains in the membrane.
xiv) Increasing the lateral mobility outside the lipid domains and increasing the size of the lipid domains are the main membrane factors which explain the evolution of Alzheimer's disease.
xv) These membrane factors are observed in healthy individuals during aging, and Alzheimer's disease makes these factors occurring before in time.
xvi) Increasing the amount of sterols and DHA composition in the cell membrane of neurons are the best dietary strategies to delay the evolution of the Alzheimer's disease.

Immunotherapy against melanoma

xvii) Intermediate level of antigen presentation on dendritic cells is a hallmark of melanoma patients presenting resistance against immunotherapy.
xviii) Cytokine co-adjuvation therapies for patients resistant to immunotherapy could improve the outcome of the therapy; based on the model it is proposed increasing the antigen presentation together with increasing the proliferation of lymphocytes combined with immunotherapy and cytostatic chemotherapy.

Common conclusions

xix) Mathematical modelling is an approach which let us integrate spread information about relevant diseases improving the knowledge about the physiology of these diseases.
xx) Looking for new targets for drug development can be accelerated by proposing targets based on the entire system physiology of the disease by mathematical modelling approaches.